Working together to grow
libraries in developing countries

www.elsevier.com | www.bookaid.org | www.sabre.org

ELSEVIER   BOOK AID
            International   Sabre Foundation

CONTRIBUTORS

Numbers in parentheses indicate the page on which the authors' contributions begins.

Abderrahmane Amgoune (1)
Laboratoire Hétérochimie Fondamentale Appliquée, Université de Toulouse, UPS, CNRS, Toulouse, France

Ghenwa Bouhadir (1)
Laboratoire Hétérochimie Fondamentale Appliquée, Université de Toulouse, UPS, CNRS, Toulouse, France

Didier Bourissou (1)
Laboratoire Hétérochimie Fondamentale Appliquée, Université de Toulouse, UPS, CNRS, Toulouse, France

Ian R. Crossley (109)
Department of Chemistry, University of Sussex, Falmer, Brighton, UK

1

Phosphine-Boranes and Related Ambiphilic Compounds: Synthesis, Structure, and Coordination to Transition Metals

Ghenwa Bouhadir, Abderrahmane Amgoune and
Didier Bourissou*

Laboratoire Hétérochimie Fondamentale Appliquée, Université de Toulouse, UPS, CNRS, Toulouse, France

*Corresponding author.
E-mail address: dbouriss@chimie.ups-tlse.fr

I. INTRODUCTION

Ambiphilic derivatives, also called amphoteric derivatives, are polyfunctional compounds combining Lewis bases and Lewis acids (Figure 1). Such donor–acceptor compounds typically combine group 15 and 13 elements featuring, respectively, a lone pair of electrons and a vacant orbital. Among the possible combinations, phosphine-boranes (PB) clearly occupy a forefront position.

To the best of our knowledge, the first such derivatives were reported in the 1960s. Relatively few studies were reported during the following four decades, but the last few years have witnessed a spectacular renaissance with the discovery of an increasing variety of interesting properties. This includes the interplay of PBs with a variety of chemical compounds (from small molecules to metal-ligand fragments), but also the ambiphilic compounds in their own right. Indeed, PBs featuring π-conjugated linkers have been investigated as electro-optical and electronic materials.[1] Following the pioneering work of D. W. Stephan et al.,[2] the interaction of PBs with small molecules has attracted increasing interest. This concerns: (i) the activation and transfer of reputed inert molecules such as H_2;[3] (ii) the stabilization of putative intermediates in phosphine-promoted reactions;[4] and (iii) the formation of photoisomerizable heterodienes.[5] In addition, PBs and related ambiphilic compounds have been shown to be versatile ligands for
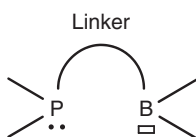

Figure 1 Generic structure of phosphine-boranes.

transition metals.[6,7] Here, the phosphine moieties are used as anchors to introduce Lewis acids in close proximity to metal centers, thereby facilitating the participation of the Lewis acids in the coordination.

In this review, the synthesis and structure of PBs are presented, followed by their coordination to transition metals and the properties of the ensuing complexes. The related ambiphilic derivatives combining phosphines with other Lewis acid moieties (heavier group 13 or group 14 elements) are also discussed.

II. SYNTHESIS

In this section, the PBs and related ambiphilic compounds prepared to date are presented. Phosphino-boranes $R_2PBR'_2$ are not considered and the ambiphilic compounds incorporating heavier group 13 elements are included only when their coordination properties have been investigated. The various synthetic strategies used to assemble these bifunctional compounds are successively discussed: ionic-type (salt elimination) couplings, hydrofunctionalization reactions, and finally condensation processes. Unless otherwise stated, the compounds presented here typically adopt monomeric *open* structures. The structural aspects related to the formation of intra- or intermolecular donor–acceptor interactions between the antagonist sites will be thoroughly discussed in the following section.

A. Ionic coupling (salt elimination) and related reactions

In this section, the preparation of ambiphilic derivatives via ionic coupling (salt elimination) and related reactions is presented, following the nature of the linker between the donor and acceptor sites: (1) one atom spacers (NR, CH_2); (2) rigid, two-to-four atom spacers (ethynyl, phenylene, ethenyl); (3) flexible, three atom spacers (benzyl); and (4) aryl-E-aryl spacers (E = S, O, ethynyl). For the ionic coupling reactions, the group 15 element (corresponding to the future donor site) is most often included as the nucleophilic partner, while the group 13 element (corresponding to the future acceptor site) is included in the electrophilic partner. However, the reverse situation has also been described, albeit rarely, using nucleophilic boron-containing reagents.

1. Ambiphilic compounds featuring one atom spacers
In 1966, Clemens reported one of the very first syntheses of ambiphilic derivatives, namely the phosphine-alanes **1a,b**, by aminolysis of triethylaluminium with the corresponding amino-phosphines Ph_2PNHR (Scheme 1).[8] Compounds **1a,b** were obtained in good to excellent yields, and characterized by IR, ^{31}P and ^{1}H NMR spectroscopy as well as

elemental analysis. A trimeric (respectively monomeric) structure was proposed for **1a** (resp. **1b**).

About 15 years later, Labinger and Miller extended the scope of phosphine-alanes to **1c–f** by deprotonation of amino-phosphines followed

1a R = *i*-Pr, n = 3 (87%)
1b R = *t*-Bu, n = 1 (96%)
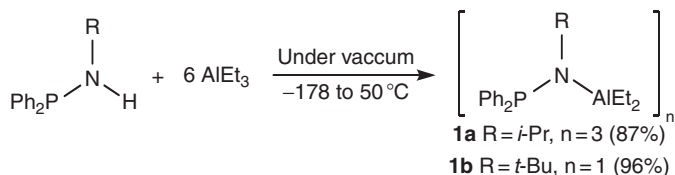
Scheme 1

by electrophilic trapping with chloro-alanes (Scheme 2).[9,10] The substitution pattern was chosen to minimize self-aggregation via intermolecular P–Al interactions, and the new compounds were characterized by multinuclear NMR spectroscopy. No further information regarding the structure of **1b**, which was described as a trimer when obtained by aminolysis, was reported.

Karsch described in 1985 the preparation of the related methylene-bridged phosphine-alane **2** by coupling Me_2PCH_2Li and Me_2AlCl

1a R = *i*-Pr, R′ = Ph, R′′ = Et
1b R = *t*-Bu, R′ = Ph, R′′ = Et
1c R = *t*-Bu, R′ = Ph, R′′ = Me
1d R = *t*-Bu, R′ = R′′ = Ph
1e R = R′ = Ph, R′′ = Et
1f R = *t*-Bu, R′ = Me, R′′ = Et
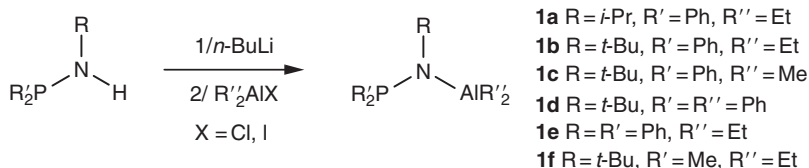
Scheme 2

(Scheme 3).[11] Compound **2** was isolated in 93% yield by sublimation and characterized by elemental analysis, IR, and multinuclear NMR spectroscopy. Its head-to-tail dimeric structure was unambiguously established by X-ray diffraction analysis (see Section III).

The corresponding PB **3a** had been reported as early as in 1972,[12] by coupling dimethylphosphine and dimethylchloromethylborane under

2(93%)

Scheme 3

thermally forcing conditions (100 °C, neat) (Scheme 4). Here also, mass spectrometry and NMR spectroscopic data supported a dimeric structure.

More recently, several groups prepared related methylene-bridged PBs by reacting R_2PCH_2Li derivatives (R = Me, Ph, t-Bu) with chloro-boranes

Scheme 4

(Scheme 5). In 1997, Braunschweig reported the monomeric diamino-substituted compound **3b**.[13] All attempts to introduce methoxy groups or chlorine atoms at boron by exchange reactions with MeOH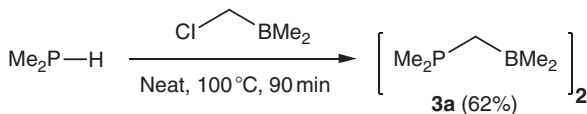 or BCl_3 failed. Using i-Pr_2NBHCl as the electrophilic partner, Alcaraz and Sabo-Etienne recently prepared the related derivative **3c** featuring a single amino group and a B–H bond.[14] The same strategy was exploited by Peters to introduce two phosphino buttresses at boron. Upon addition of two equivalents of t-Bu_2PCH_2Li to $PhBCl_2$, the diphosphine-borane (DPB) **4** was readily prepared.[15]

2. Ambiphilic compounds featuring rigid, two-to-four atom spacers
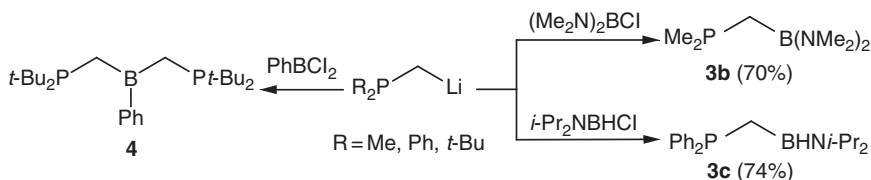
Scheme 5

a. Ethynyl-bridged ambiphilic derivatives   In 1993, Marder prepared the ethynyl-bridged PB **5a** by treating successively the diphenyl(ethynyl) phosphine with n-BuLi and Mes_2BF (Scheme 6).[16] Compound **5a** was fully characterized in solution by UV, IR, multinuclear NMR spectroscopy, and in the solid state by X-ray diffraction. There is only weak, if any, π-interaction between the phosphorus lone pair and the ethynyl bridge, as apparent from the strongly pyramidalized environment around P (ΣP_α = 307.8°), and the rather long PC(ethynyl) bond. In line with the negligible degree of charge transfer in the ground-state structure of **5a**, the nonlinear
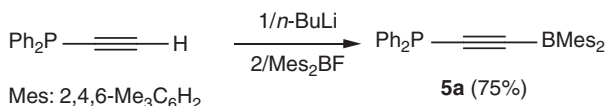
Scheme 6

optical measurements gave a small first molecular hyperpolarizability β of 3.3 × 10^{-30} esu.

Taking advantage of the ability of "frustrated" Lewis pairs to activate the terminal C-H bond of alkynes,[17] Stephan reported in 2010 the preparation of a strongly polarized PB **5b** related to **5a** (Scheme 7).[18] Reaction of di-*t*-butyl(ethynyl)phosphine with $(C_6F_5)_2BCl$ first afforded the key zwitterionic intermediate **6**. Here, π-coordination of the alkyne to $(C_6F_5)_2BCl$ is likely to enhance the acidic character of the terminal C–H bond and induce the C–P migration of the hydrogen atom. Chlorine to hydrogen exchange at boron was then achieved with an excess of Me_2SiHCl to give **6'**. Finally, the proton at phosphorus and hydride at boron were removed concomitantly by the frustrated Lewis pair *t*-Bu$_3$P/B(C$_6$F$_5$)$_3$. The ^{31}P and ^{19}F NMR data for the PB **5b** are consistent with a monomeric structure.
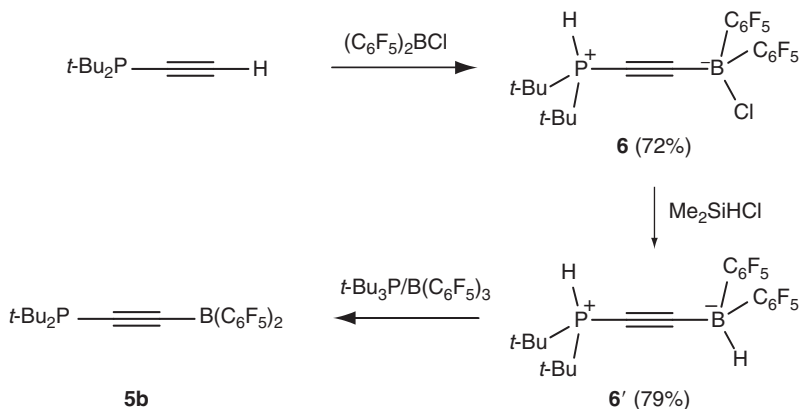
Scheme 7

b. Phenylene-bridged ambiphilic derivatives   The preparation of ambiphilic derivatives featuring *ortho*-phenylene spacers will now be described. The incorporation of an *ortho*-phenylene spacer between phosphine and borane moieties was first reported by Balueva in 1991[19] by metallation of (2-bromophenyl)diphenylphosphine with *n*-BuLi followed by electrophilic trapping with *n*-Bu$_2$BCl (Scheme 8). The phosphino-borane **7a**
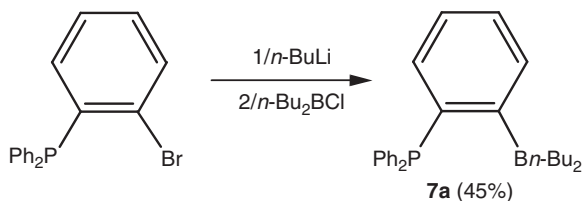
Scheme 8

was obtained in low yield (4.5%) and was characterized by elemental analysis, mass spectrometry, ^{1}H and ^{31}P NMR spectroscopy.

In 2006, we initiated a research program aimed at exploring the coordination properties of ambiphilic derivatives toward transition metals, and became particularly interested in mono-, di-, and triphosphine-boranes featuring *ortho*-phenylene spacers. The bromine–lithium–boron exchange strategy starting from (2-bromophenyl)phosphines was extended to a variety of monophosphine-boranes (MPB) **7b–e** (Scheme 9).[5,20–22] All compounds (except **7c** that proved extremely moisture and temperature sensitive) were obtained in good yields and fully characterized by mass spectrometry and multinuclear NMR spectroscopy. Derivatives **7b** and **7e** adopt monomeric structures without intramolecular P–B interactions, while the *closed* form is favored for the BPh$_2$ and BFlu (BFlu = 9-borafluorenyl) compounds **7c** and **7d**. The same strategy was also used to prepare DPB. Starting from (2-bromophenyl)diisopropylphosphine and dichlorophenylborane, derivative **8a** was obtained in 70% yield and fully characterized by multinuclear NMR, high-resolution mass spectrometry, and X-ray diffraction analysis.[22–24] ^{31}P and ^{11}B NMR experiments performed both in solution at variable temperatures and in the solid state revealed that the *open* and *closed* structures (with and without intramolecular P–B interaction) are in equilibrium in solution. The related DPB **8b** featuring phenyl substituents at phosphorus was
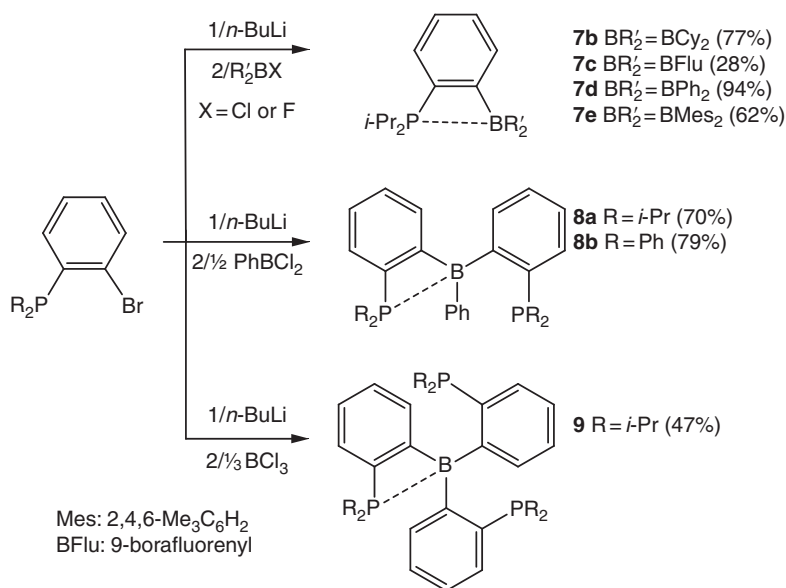
Scheme 9

obtained in 79% yield by the same procedure.[25] The triphosphine-borane (TPB) **9** related to **8a** was prepared using BCl_3 as the electrophilic partner.[24] Here also, the spectroscopic data indicated the coexistence of the *open* and *closed* forms in solution.

In order to assess the influence of the nature of the Lewis acid on the coordination properties of ambiphilic derivatives, we have recently prepared related compounds with heavier group 13 elements. Bromine–lithium–aluminium exchange using $AlCl_3$ afforded the diphosphine-alane **10** (Scheme 10).[26] The extreme sensitivity of **10** has precluded its structural characterization, but the ^{31}P and ^{27}Al NMR data, combined with DFT calculations, supported a pentacoordinate environment around the aluminum center as the result of intramolecular donor–acceptor interactions with the two phosphorus atoms (see Section III). Using ½ or ⅓ equivalent of $GaCl_3$ as the electrophilic partner, the di- and triphosphine-gallanes **11** and **12** were also prepared using $GaCl_3$.[27] So far, all attempts to isolate these derivatives failed due to exchange processes at gallium and/or decomposition reactions, but their *in situ* coordination to AuCl afforded stable complexes (see Sections IV.C and D).
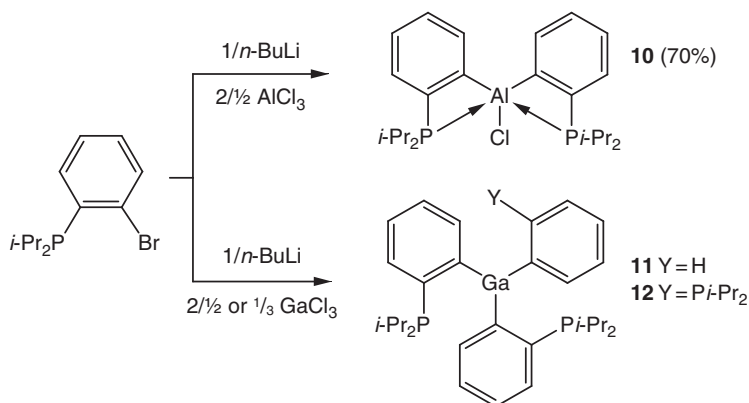
Scheme 10

Within the framework of the investigation on hetero-π-conjugated molecules, Kawashima described in 2005 the PB compounds featuring two *ortho*-phenylene linkers between the phosphorus and boron atoms, namely dibenzophosphaborins.[28–30] Double lithiation of bis(o-bromophenyl)phosphines and subsequent cyclization with $MesB(OMe)_2$ allowed efficient access to compounds **13a** and **13b** (Scheme 11). According to the X-ray diffraction analysis carried out on **13a**, the phosphaborin ring significantly deviates from planarity and the phosphorus is in a strongly

pyramidalized environment ($\Sigma P_\alpha = 306.9°$). This indicates negligible delocalization of the phosphorus lone pair into the π-system, by analogy with that observed in the ethynyl-bridged PB **5a**. The UV–vis absorption data ($\lambda_{max} \sim 380$ nm), combined with computational results (NBO analysis and TD-DFT calculations), indicated electronic excitation associated with intramolecular charge transfer from the phosphorus lone pair to the boron vacant orbital.

Mes: $2,4,6\text{-}Me_3C_6H_2$

13a R = Ph (80%)
13b R = Mes (62%)

Scheme 11

Aldridge recently extended the variety of *ortho*-aryl spacers preparing the 1-phosphino-2-boryl-ferrocene **15** (Scheme 12).[31] The key step is the conversion of 1,1′-dibromoferrocene into the 1,2-bromo-dimesitylboryl-ferrrocene **14** (the monolithiated ferrocene readily isomerizes in the presence of tmp = 2,2,6,6-tetramethylpiperidine). The ionic coupling of the two fragments was performed via an unconventional ''reverse'' approach. Taking advantage of the two sterically protecting mesityl groups at boron, **14** was metallated and Ph_2PCl was used as electrophile. Compound **15** was isolated as a racemic mixture in 70% yield, and its monomeric *open* structure was unambiguously substantiated by multinuclear NMR, UV–vis, and X-ray diffraction analysis.

tmp: 2,2,6,6-tetramethylpiperidine
Mes: $2,4,6\text{-}Me_3C_6H_2$
tmeda: $Me_2NCH_2CH_2NMe_2$

14   **15** (70%)

Scheme 12

PBs featuring *para*-phenylene spacers have also been prepared. Marder reported the synthesis of derivative **16a** (related to the ethynyl-bridged compound **5a**) by bromine–lithium–boron exchange

(Scheme 13).[16] The presence of the BMes$_2$ group induces a moderate downfield shift of the ^{31}P NMR signal (by 2–3 ppm), suggesting only weak, if any, electron transfer from phosphorus to boron. Consistently, the UV–vis absorption band for **16a** ($\lambda_{max} \sim 332$ nm) is blue shifted compared with that of the related NB system (354 nm).


Mes: 2,4,6-Me$_3$C$_6$H$_2$
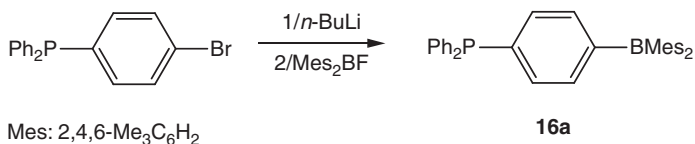
Scheme 13

In his pioneering contribution to the metal-free activation of H$_2$ by frustrated Lewis pairs,[3] Stephan described in 2006 an alternative route to *para*-phenylene-bridged PBs.[2] Compound **16b** featuring a highly electrophilic boron center was obtained from B(C$_6$F$_5$)$_3$ and Mes$_2$PH (Scheme 14). The secondary phosphine is too sterically demanding to attack at boron and instead effects nucleophilic aromatic substitution at one *para* position. After C–B migration of the fluorine atom, the zwitterionic phosphonium-

16b R = Mes (75%)
16c R = t-Bu (75%)

Mes: 2,4,6-Me$_3$C$_6$H$_2$
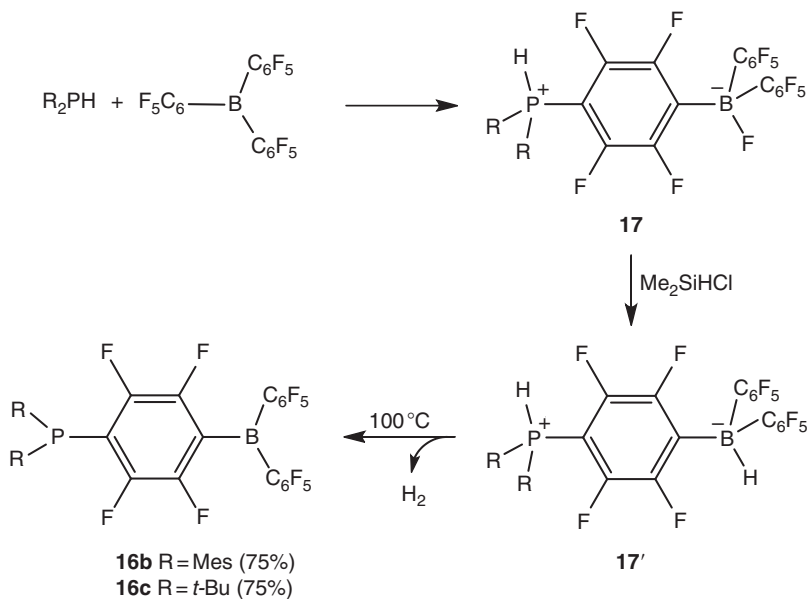
Scheme 14

borate **17** was obtained (75% yield). Fluoride/hydride exchange at boron was then achieved with dimethylchlorosilane Me$_2$SiHCl in near quantitative yield. Most remarkably, heating the phosphonium-borate **17**′ above 100 °C induced a stoichiometric elimination of H$_2$. PB **16b** was thereby obtained in 75% yield. Its structure has been unambiguously supported by multinuclear NMR (^{1}H, ^{13}C, ^{11}B, ^{31}P, ^{19}F) spectroscopy and elemental analysis as well as X-ray diffraction study of its THF adduct. The intense red-orange color of **16b** ($\lambda_{max} \sim 445$ nm in hexanes) contrasts with the colorless character of the phosphonium-borates **17**′ and PB **16a**, and most likely indicates some internal charge transfer from phosphorus to boron. The related PB **16c** featuring *t*-Bu groups at phosphorus can be obtained following the same strategy,[32] or advantageously by direct coupling of *t*-Bu$_2$PSiMe$_3$ and B(C$_6$F$_5$)$_3$.[33]

Their interest in multistep redox systems featuring crowded triarylphosphines prompted Sasaki and Yoshifuji to prepare PBs **16d** and **20** featuring tetramethyl *para*-phenylene and trimethyl *meta*-phenylene linkers, respectively (Scheme 15).[34] The ''reverse'' approach involving the metallation of the boryl-bromo-benzenes **18** and **19** was used. Derivatives **16d** and **20**, isolated in moderate yields (∼25%) after column chromatography, were characterized by multinuclear NMR (^{1}H, ^{13}C, ^{31}P, ^{11}B) and HRMS analysis. As expected, the cyclic voltammograms of **16d** and **20** display a reversible oxidation wave and a quasi-reversible reduction wave associated with the phosphine and borane moieties, respectively. Apparently, large redox potential differences (∼3 V) prevent significant interaction between the two antagonist sites in both cases. However, some

Mes: 2,4,6-Me$_3$C$_6$H$_2$
Tip: 2,4,6-*i*-Pr$_3$C$_6$H$_2$
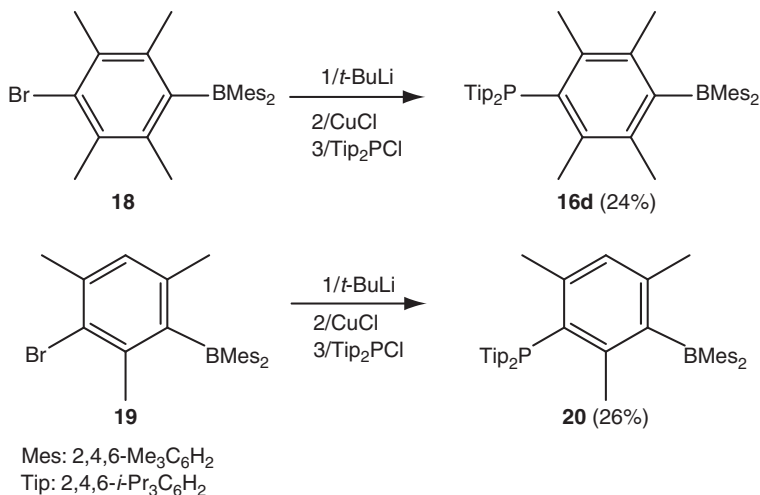
Scheme 15

differences between the *para* and *meta* derivatives were noticed in the UV–vis spectra (λ_{max} = 385 and 324 nm for **16d** vs. λ_{max} = 330 nm for **20**). Along with a slight downfield shift of the ^{31}P NMR resonance (from δ = −42 ppm for **16d** to δ = −47 ppm for **20**), this was attributed to the existence of some charge transfer in the *para* compound **16d**, with contribution from the corresponding quinoid-type structure in the excited state.

c. Ethenyl-bridged ambiphilic derivatives   Ambiphilic compounds featuring phosphine and borane, or alane, moieties in 1,2-positions of a C=C double bond have been investigated early on. Here, a completely different synthetic strategy was used, namely the coupling of alkynyl-borates with chlorophosphines in a reaction that is accompanied by the 1,2-shift of an organic group from boron to the adjacent carbon center (Scheme 16). Remarkably, the reaction proceeds with complete stereoselectivity (the nucleophilic attack of C_β toward phosphorus occurs in the position *anti* to the B–C_α migration), affording exclusively the Z isomers (that are related to the *ortho*-phenylene-bridged systems).
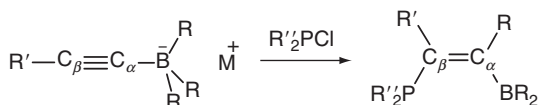
Scheme 16

This process was first illustrated by Binger and Köster in 1974 (Scheme 17).[35] Taking advantage of the readily available alkynyl-borates **21** (obtained by addition of alkynyl lithium or sodium compounds to triorganylboranes),[36] the PBs **22a–d** were prepared in good to excellent yields. During their investigation of the stereoselectivity of this
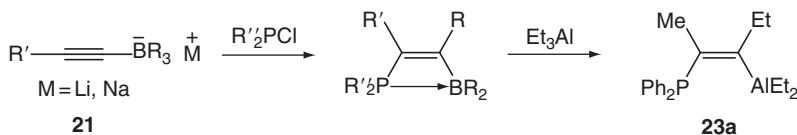

22a R = Et, R′ = Me, R′′ = Ph (88%)
22b R = R′ = Me, R′′ = Ph (71%)
22c R = R′′ = Et, R′ = Me (91%)
22d R = Et, R′ = Me, R′′ = C$_6$H$_{11}$ (91%)
22e R = R′′ = Ph, R′ = Me$_3$Si (66%)
22f R = Et, R′ = Me$_3$Si, R′′ = Ph (87%)
22g R = *n*-Bu, R′ = R′′ = Ph
22h R = R′ = R′′ = Ph
22i R = R′ = R′′ = Me

Scheme 17

transformation, Hagelee and Köster reported the preparation of related PBs **22e** and **22f** derived from trimethylsilylalkynylborates.[37] Later on, the scope of such ethenyl-bridged compounds was extended to **22g** and **22h** by Balueva, Nikonov, and Erastov[38–40] and to the permethylated derivative **22i** by Grobe.[41] Interestingly, reaction of **22a** with triethylaluminum afforded the corresponding phosphine-alane **23a** by B–Al transmetallation.[35] Taken together, the NMR, cryoscopic, and dipole moment data support closed monomeric structures for the PBs **22a–i**. This was unambiguously established crystallographically for **22e**[37] and **22g**[40] (see Section III).

Another synthetic route was also used to prepare the perphenyl PB **22h** (Scheme 18).[42] The boratacyclopropene precursor **24** is readily prepared by irradiating $NaBPh_4$ in the presence of diphenylacetylene. Compound **24** behaves as a synthetic equivalent of the corresponding alkynylborate $(PhC≡CBPh_3)^-$ and reacts with chlorodiphenylphosphine to give **22h**. Here also, the reaction proceeds with complete stereoselectivity and affords exclusively the Z isomer.
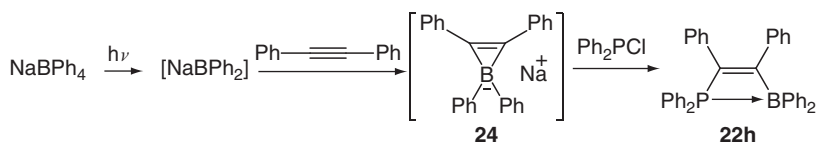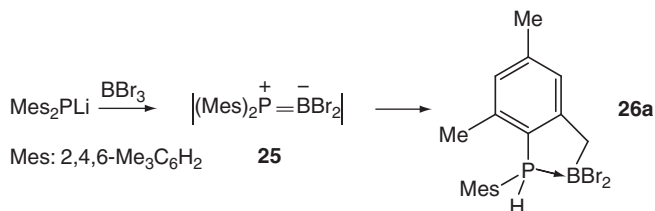

Scheme 18

3. Ambiphilic compounds featuring benzyl spacers

The following subsection considers PBs featuring 2-benzyl spacers. Both conceivable arrangements (the phosphine or the borane moiety in benzylic position) have been demonstrated experimentally.

Aiming at preparing a phosphino-borane $R_2PBR'_2$ with PB double-bond character,[43] Karsch reacted the lithium phosphide $LiPMes_2$ with tribromoborane (Scheme 19).[44] Instead of the desired compound **25**, they isolated the PB **26a** that results formally from the 1,2-addition of a C-H bond of a mesityl group across the PB double bond of **25**. The ^{31}P and

Scheme 19

^{11}B NMR data for **26a** support the presence of a strong intramolecular P–B interaction leading to a five-membered ring.

Using the bromine–lithium–boron exchange strategy, Müller and Lachmann reported in 1993 a series of MPB, DPB, and TPB **27–29** (Scheme 20).[45] All of these compounds were isolated by crystallization and characterized by IR, multinuclear NMR (^{1}H, ^{13}C, ^{31}P, and [11]B), and elemental analysis. The presence of P–B interactions was spectroscopically apparent and monomeric closed structures were authenticated crystallographically for **27** and **28** (see Section III).
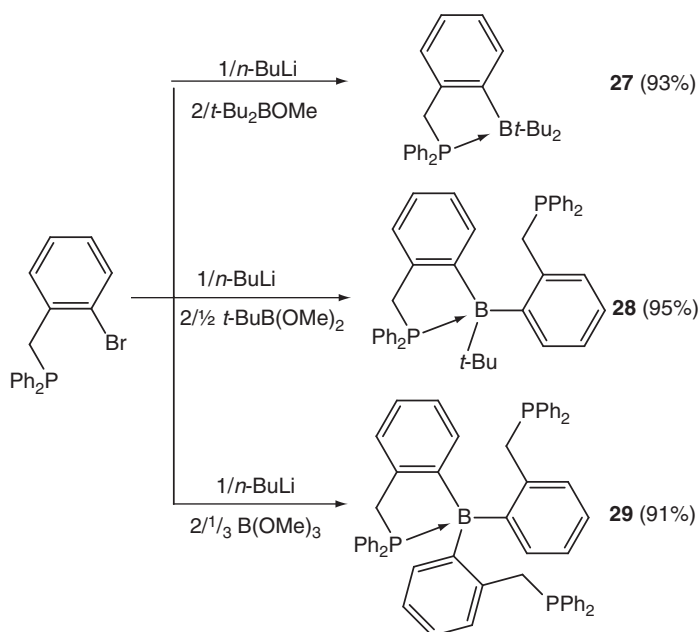
Scheme 20

Braunschweig reported in 1997 the preparation of related PBs **26b–e** in which the relative positions of the phosphine and borane moieties on the benzyl spacer are exchanged compared to compound **27** (Scheme 21).[46] Derivative **26b** was first prepared by deprotonation of $Ph_2P(o\text{-}C_6H_4)CH_3$ with n-BuLi/tmeda (tetramethylethylene diamine) and subsequent reaction with $(Me_2N)_2BCl$. Treatment of **26b** with MeOH induced NMe_2/OMe exchange at boron, leading to the methyl boronic ester **26c**. The related hydrogen substituted compound **26d** was obtained by reducing **26c** with $LiAlH_4$, while the dichloro derivative **26e** was prepared by treatment of **26b** by BCl_3. Compounds **26b–e** were isolated in good to high yields by

crystallization and characterized by multinuclear NMR spectroscopy, mass spectrometry, and elemental analysis. According to the ^{31}P and ^{11}B NMR data, **26b** and **26c** adopt monomeric *open* structures, while **26d** and **26e** feature intramolecular P–B interactions (*closed* form).
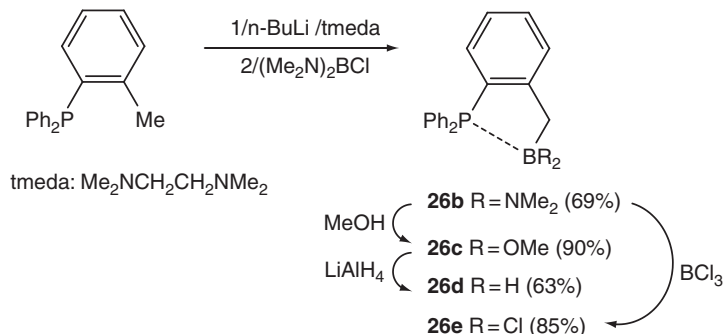
Scheme 21

## 4. Ambiphilic compounds featuring aryl-E-aryl spacers (E = S, O, ethynyl)

A few aryl-E-aryl spacers have also been used to connect phosphine and borane sites. Emslie first described the synthesis of the rigid thioxanthene derivative **32** featuring the two antagonist groups in 4 and 5 positions (Scheme 22).[47] Compound **32** was prepared in five steps from the commercially available thioxanthone **30**. The key 4,5-dibromo thioxanthene intermediate **31** was obtained by reacting **30** with AlMe$_3$, followed by double Friedel–Crafts alkylation and bromination of the 4 and 5 positions. The phosphine and borane moieties were then introduced by two successive lithiation/electrophilic trapping sequences, using Ph$_2$PCl and then Ph$_2$BBr as electrophilic partners. The high solubility of **32** prevented its direct purification, but the corresponding acetonitrile adduct could be
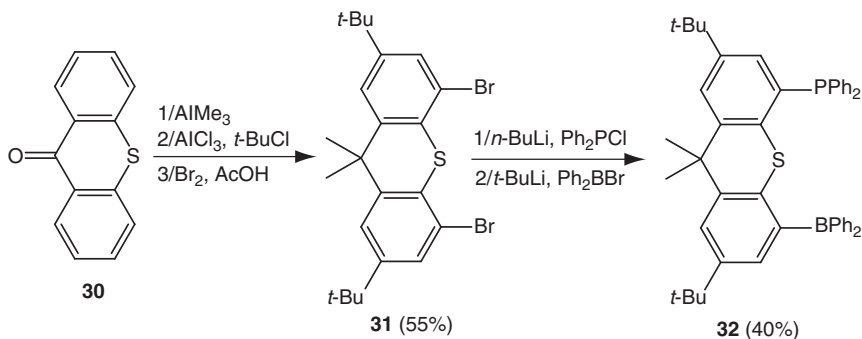
Scheme 22

easily formed, precipitated, and converted back to the base-free species **32** under dynamic vacuum.

With the aim to extend the structural variety of PBs to flexible systems, we reported in 2007 the synthesis and characterization of the related compound **36** featuring a diphenyl ether tether (Scheme 23).[48] Starting from the readily available 2-bromo-2′-iododiphenylether **33**, the bromo-phosphine **34** was first prepared by halogen/lithium/phosphorus exchange using *n*-BuLi and Ph$_2$PCl. The subsequent bromine/lithium/ boron exchange was complicated by the tendency of the transient lithiated phosphine to undergo cyclization leading to **35**. But this unde-sirable process could be prevented by changing the solvent from tetrahy-drofuran to toluene. The desired PB **36**, obtained in 55% yield, was characterized by multinuclear NMR (^{1}H, ^{13}C, ^{31}P, and ^{11}B), mass spec-trometry, and X-ray diffraction.

Mes: 2,4,6-Me$_3$C$_6$H$_2$
tmeda: Me$_2$NCH$_2$CH$_2$NMe$_2$
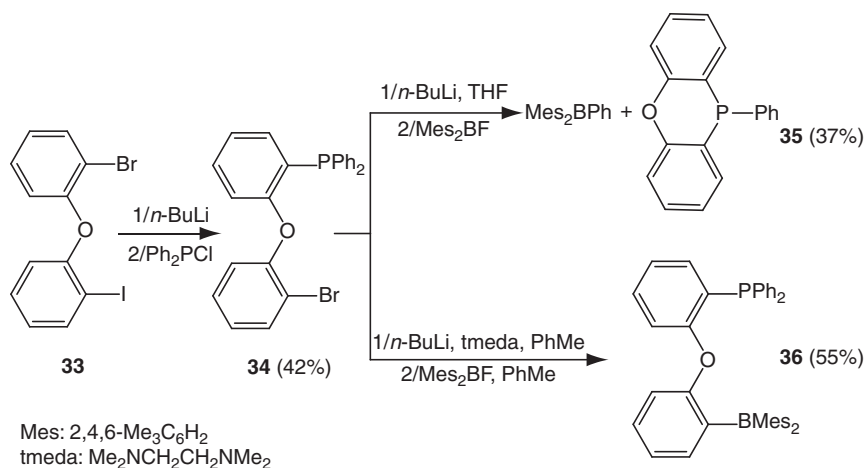
Scheme 23

His interest in ladder π-conjugated molecules prompted Yamaguchi to investigate PBs **38** featuring diphenylacetylene backbones (Scheme 24).[49] The two antagonist sites were successively introduced by lithiation/elec-trophilic trapping of bis(2-bromophenyl)acetylene. But in contrast with the preparation of compounds **32** and **36**, the borane moiety was intro-duced first, and various phosphine groups (PPh$_2$, PCy$_2$, and P*t*-Bu$_2$) were then installed (''reverse'' approach). Compounds **38a–c** were isolated in 31–59% yields and characterized by multinuclear NMR, HRMS, and UV–vis analyses. Compound **38a** adopts a monomeric *open* form, whereas

the doubly cyclized form, a stilbene-bridged phosphonium-borate, is preferred for derivatives **38b** and **38c**. DFT calculations on model compounds (featuring Ph or Me at phosphorus and Ph at boron) indicated that the two forms are close in energy ($\Delta H \sim 10$ kcal/mol), and the cyclization is most likely favored by the higher nucleophilicity of the dialkylphosphine vs. diphenylphosphine groups.
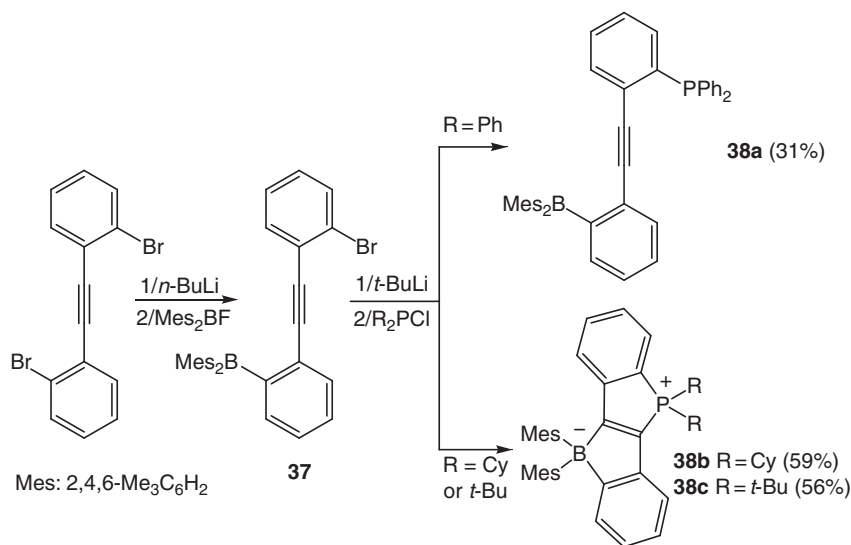
Scheme 24

B. Hydrofunctionalization

To date, the hydrofunctionalization route has mainly been used to prepare PBs. Both conceivable strategies, namely the hydroboration of unsaturated phosphines and the hydrophosphination of unsaturated boranes have been reported (Scheme 25). With dialkyl and diarylboranes, the reactions proceed spontaneously under mild conditions, while the addition of boronates $HB(OR)_2$ is catalyzed by a titanium complex, and the
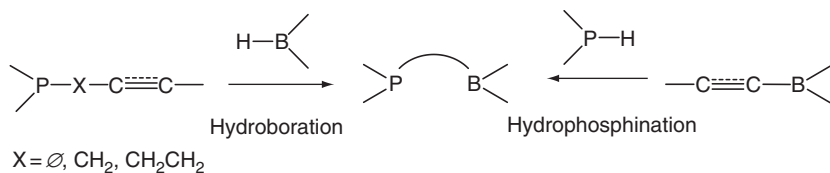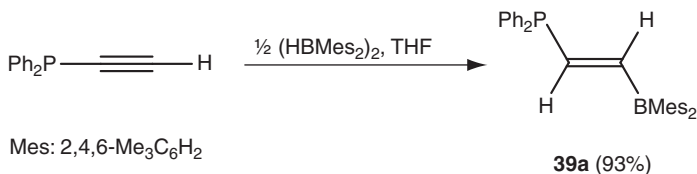

Scheme 25

reaction of secondary phosphines to vinyl-boranes is promoted by radical initiators. The additions of B–H/P–H bonds occur usually with complete stereoselectivity (*syn*-addition) and regioselectivity (with the heteroelement being introduced at the least hindered position of the π-system). The preparation of PBs by hydroboration of α-alkynyl-, α-alkenyl-, and ω-alkenyl-phosphines will be successively presented. The few examples of hydrophosphination of unsaturated boranes will then be discussed.

1. Hydroboration of α-alkynyl-phosphines

Marder reported in the early 1990s the reaction of dimesitylborane with the diphenyl(ethynyl)phosphine (Scheme 26).[16,50] Only monohydroboration was observed, and the reaction occurred with complete regio- and stereoselectivity. The *E* isomer of the alkenyl-bridged PB **39a** was thereby obtained in 93% yield as an air-stable solid. Compound **39a** was characterized by multinuclear NMR (^{1}H, ^{13}C, ^{31}P) and UV–vis spectroscopy as well as singlecrystal X-ray diffraction analysis. In the solid state, the valence plane around the three-coordinate boron atom is rotated by 17° with respect to the C=C double bond, the phosphorus atom remains in a strongly pyramidalized environment ($\Sigma P_\alpha = 307.8°$), and the lone pair at phosphorus is almost perpendicular to the P–CH=CH–B plane. As for the related ethynyl-bridged derivative **5a**, no significant charge transfer occurs from P to B in the groundstate structure of **39a**, and accordingly, the first molecular hyperpolarizability β measured for **39a** is very small (2.6×10^{-30} esu).
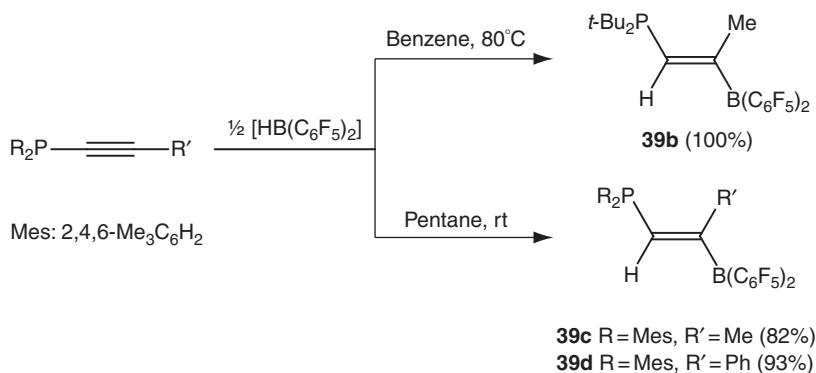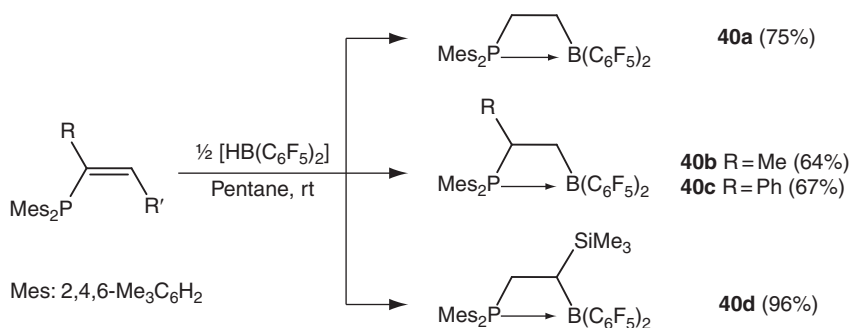

Mes: 2,4,6-Me$_3$C$_6$H$_2$

39a (93%)

Scheme 26

In 2008, Erker extended this methodology to the hydroboration of internal alkynyl-phosphines. Using Piers' borane HB(C$_6$F$_5$)$_2$, the PBs **39b–d** featuring *E*-CH=C(R) linkers were isolated in excellent yields (Scheme 27).[51] Compounds **39b–d** have been characterized by multinuclear NMR (^{1}H, ^{13}C, ^{31}P, ^{11}B), UV–vis, and elemental analyses.
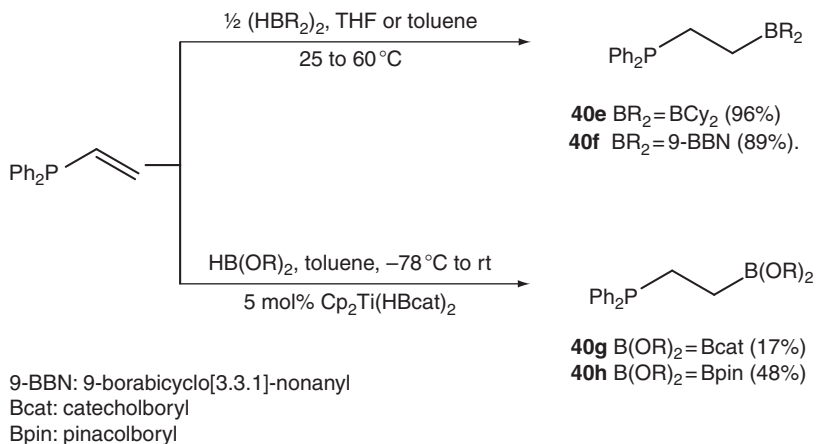
2. Hydroboration of α-alkenyl-phosphines

In the framework of Frustrated Lewis Pairs, Erker also investigated the hydroboration of α-alkenyl-phosphines with HB(C$_6$F$_5$)$_2$.[52,53] Starting from dimesityl(vinyl)phosphine, the CH$_2$CH$_2$-bridged PB **40a** was first

R_2P————————R' ½ [HB(C_6F_5)_2]

Benzene, 80°C →

$t\text{-Bu}_2P$ Me

H $B(C_6F_5)_2$

39b (100%)

Mes: 2,4,6-Me_3C_6H_2

Pentane, rt →

R_2P R'

H $B(C_6F_5)_2$

39c R = Mes, R′ = Me (82%)
39d R = Mes, R′ = Ph (93%)

Scheme 27

prepared (Scheme 28).[52] The ^{31}P and ^{11}B NMR data support a four-membered ring structure, as a result of intramolecular P–B interaction (see Section III). PBs **40b–d** featuring substituted ethano bridges were then prepared by hydroboration of the corresponding alkenyl-phosphines (Scheme 28).[53] Here also, the reactions occurred with complete regioselectivity, the boron atom being exclusively installed at the carbon in the position β to phosphorus.

R

Mes_2P R'   ½ [HB(C_6F_5)_2]
          Pentane, rt

Mes_2P————→ B(C_6F_5)_2   **40a** (75%)

R

Mes_2P————→ B(C_6F_5)_2   **40b** R = Me (64%)
                          40c R = Ph (67%)

SiMe_3

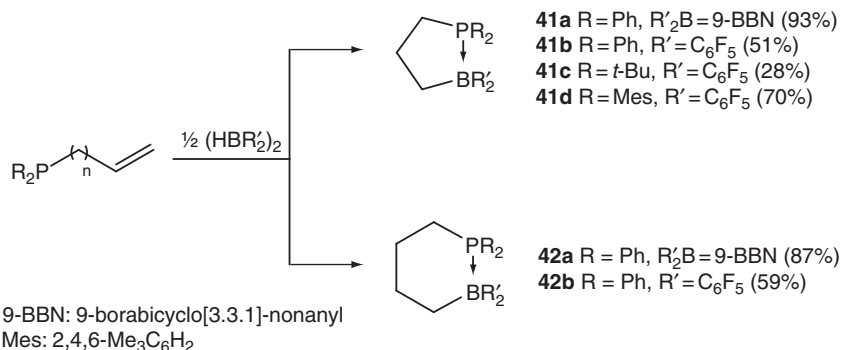Mes_2P————→ B(C_6F_5)_2   **40d** (96%)

Mes: 2,4,6-Me_3C_6H_2

Scheme 28

Simultaneously with Tilley, we studied the hydroboration of diphenyl (vinyl)phosphine with dialkylboranes (Scheme 29).[54,55] The reactions can be conducted in toluene as well as THF, and required a slightly elevated temperature for 9-H-BBN (60 °C) compared to Cy_2BH (room temperature). PBs **40e** and **40f** were obtained in near quantitative yields as extremely hygroscopic white solids. The P–B adducts [(vinyl)Ph_2P–BHR_2] are likely intermediates in these hydroboration reactions. The ^{31}P and ^{11}B NMR data substantiate monomeric *open* structures for both **40e** and **40f** in solution.

9-BBN: 9-borabicyclo[3.3.1]-nonanyl
Bcat: catecholboryl
Bpin: pinacolboryl

Scheme 29

The variety of C_2-bridged PBs was further extended by Muhoro via hydroboration of diphenyl(vinyl)phosphine with catechol- and pinacol-boranes (Scheme 29).[56] To compensate for the low Lewis acidity of these boronates, the hydroboration reactions were carried out in the presence of 5 mol% of titanocene bis(catecholborane) as catalyst. The desired products **40g** and **40h** were obtained with complete *anti*-Markovnikov selectivity. The spectroscopic data and the crystallographic study performed on **40h** showed the expected monomeric *open* structure.

3. Hydroboration of ω-alkenyl-phosphines

PBs featuring propylene and butylene spacers were also prepared by hydroboration of ω-alkenyl-phosphines. Schmidbaur treated the allyl- and 3-butenyl-diphenylphosphines with 9-H-BBN (9-borabicyclono-nane) in boiling tetrahydrofuran (Scheme 30).[57] Compounds **41a** and **42a** were isolated as colorless crystals in high yields, and readily identified by the means of multinuclear NMR spectroscopy, mass spectrometry, and elemental analysis. Unconstrained five- and six-membered ring structures resulting from intramolecular P–B interactions were authenticated crystallographically. More recently, Erker performed similar reactions with Pier's borane $HB(C_6F_5)_2$ (Scheme 30).[53,58] The PBs **41b–d** and **42b** were obtained in 28–70% isolated yields and X-ray diffraction studies systematically revealed monomeric *closed* structures (see Section III).

41a R = Ph, R'$_2$B = 9-BBN (93%)
41b R = Ph, R' = C$_6$F$_5$ (51%)
41c R = t-Bu, R' = C$_6$F$_5$ (28%)
41d R = Mes, R' = C$_6$F$_5$ (70%)

42a R = Ph, R'$_2$B = 9-BBN (87%)
42b R = Ph, R' = C$_6$F$_5$ (59%)

9-BBN: 9-borabicyclo[3.3.1]-nonanyl
Mes: 2,4,6-Me$_3$C$_6$H$_2$

Scheme 30

4. Hydrophosphination of vinyl-boranes

Although much less developed than the hydroboration of unsaturated phosphines, the hydrophosphination of unsaturated boranes also proved an efficient route to PBs. As early as in 1965, Braun had reported the reaction of Et$_2$PH with vinyl-boronate **43** affording the *anti*-Markovnikov adduct **44** (Scheme 31).[59] The reaction is promoted by azobis(isobutyronitrile) serving as a radical initiator, and requires only 2 h in refluxing petroleum ether. Following the same strategy, Grobe prepared some 40 years later the TPB **46** starting from the trimethylamine adduct of tris (vinyl)borane **45** (Scheme 31).[42] The addition of Me$_2$PH can be promoted

44 (60%)

46 (61%)

48 (68%)

AIBN: azobis(isobutyronitrile)
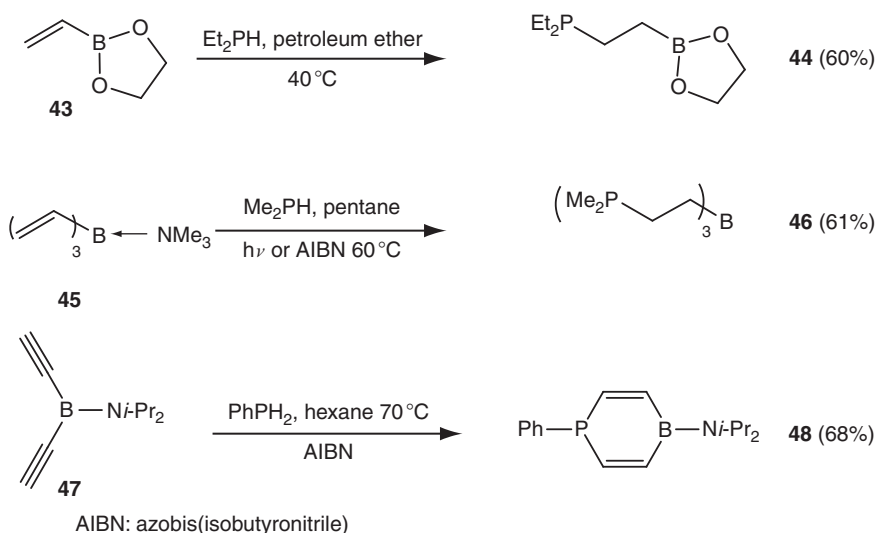
Scheme 31

photochemically or thermally. Compound **46** was isolated in 61% yield, and its propensity to engage into both intra- and intermolecular P–B interactions was supported by ^{31}P and ^{11}B NMR spectroscopic data. Recently, the AIBN-catalyzed hydrophosphination route was nicely extended by Ashe to the double addition of PhPH$_2$ to the bis(alkynyl)borane **47** (Scheme 30).[60] The ensuing phosphaborin **48** was isolated in 68% yield and fully characterized. As for the related systems (dibenzophosphaborins **13a** and **13b** and the alkenyl-bridged PB **39**), the molecular structure of **48** indicates negligible delocalization of the phosphorus lone pair into the π-system: the phosphorus atom remains in a strongly pyramidalized environment ($\Sigma P_\alpha = 306°$), and the Lewis acidity of boron is strongly attenuated by π-donation from the amino group (BN distance $=1.407(3)$ Å).

C. Condensation reactions with boronic acids

Phosphine-boronates featuring rigid backbones have been accessed by condensing adequately functionalized phosphines and boronic acids. This strategy was first developed by Kagan[61] and Jacobsen[62] who independently reported the synthesis of the tartrate-derived boraDIOP compounds **50** (Scheme 32). The key precursor **49** was readily obtained by acidic hydrolysis of the diphosphine (*R,R*)-DIOP (DIOP = 2,3-*O*-isopropylidene-2,3-dihydroxy-1,4-bis(diphenylphosphino)butane). Upon reaction with PhB(OH)$_2$ or PhBCl$_2$, the phosphine-boronate **50a** was isolated in

50a R = H (85%)
50b R = Cl (88%)
**50c** R = CF$_3$ (79%)
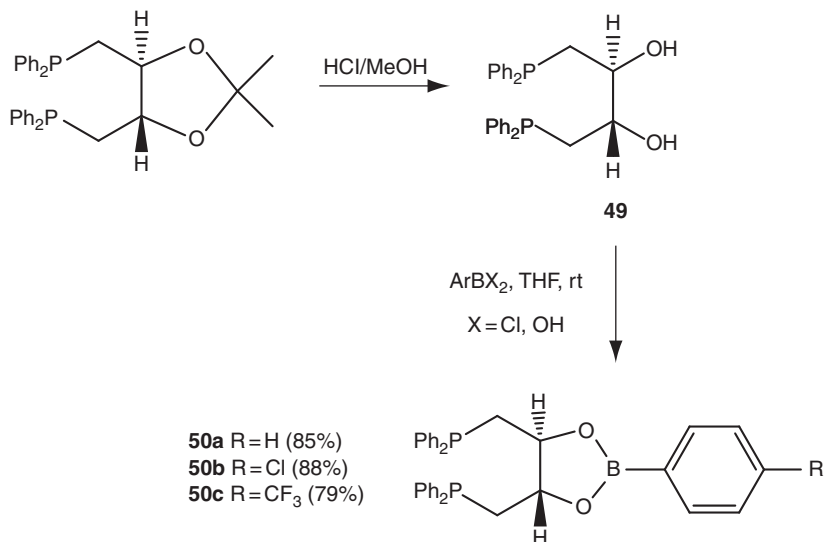
Scheme 32

~85% yield. The structure of **50a** was supported by multinuclear NMR spectroscopy, mass spectrometry, and elemental analysis. In order to finely tune the acidity of the boron center, the related derivatives **50b** and **50c** were prepared by condensing **49** with *p*-substituted arylboronic acids.

Following the same strategy, Landis prepared the 1,1′-ferrocenyldiphosphines **53a–c** featuring pendant benzoxaborolidine moieties (Scheme 33).[63] Reaction of 2-aminophenol with the ferrocene precursor **51** afforded **52** which was subsequently coupled with various boronic acids to give compounds **53a–c** in good yields. Monomeric *open* structures were supported by ^{31}P NMR spectroscopy and crystallography for **53a**.

51

52

53a R = Me (76%)
53b R = Ph (80%)
53c R = *p*-ClC$_6$H$_4$ (71%)
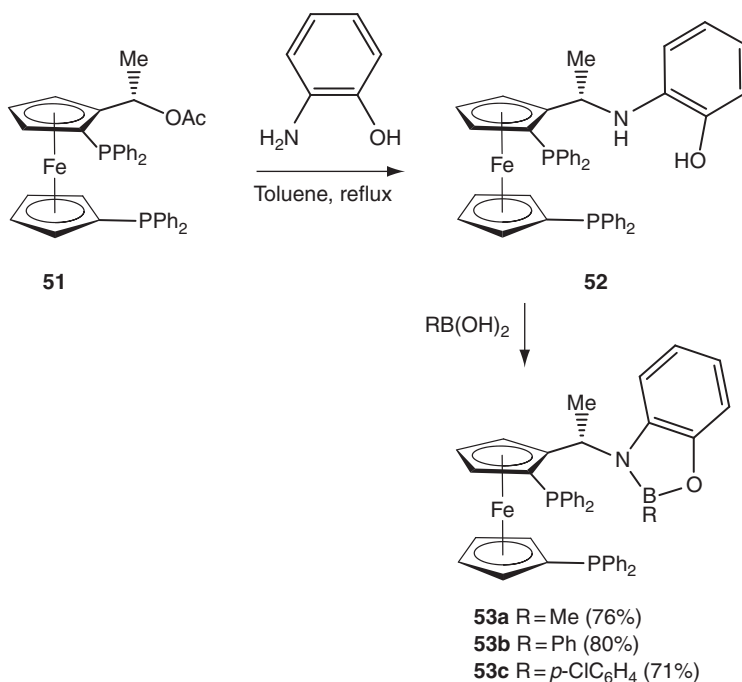
Scheme 33

In 1994, Balueva described the preparation of the phosphine-boronate **55** featuring a 1,3,2-dioxaborinane skeleton (Scheme 34). Diphenylphosphine spontaneously adds to the racemic aldol **54** and the ensuing intermediate is condensed *in situ* with phenylboronic acid. The resulting phosphine-boronate **55** was isolated as a 3:1 mixture of *cis/trans* diastereomers in 32% overall yield.[64]
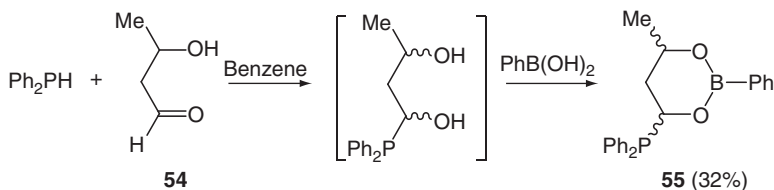
Scheme 34

Lastly, the condensation of phosphine **56** with phenylboronic acid afforded the salicylic acid-derived compound **57** (Scheme 35).[65] Following the same strategy, Gudat *et al.* recently prepared derivative **59** combining a phosphine group and a benzo 1,3,2-dioxaborol moiety (Scheme 35).[66] Compounds **57** and **59**, both obtained in quantitative yields, were characterized by multinuclear NMR spectroscopy, mass spectrometry, and elemental analysis.
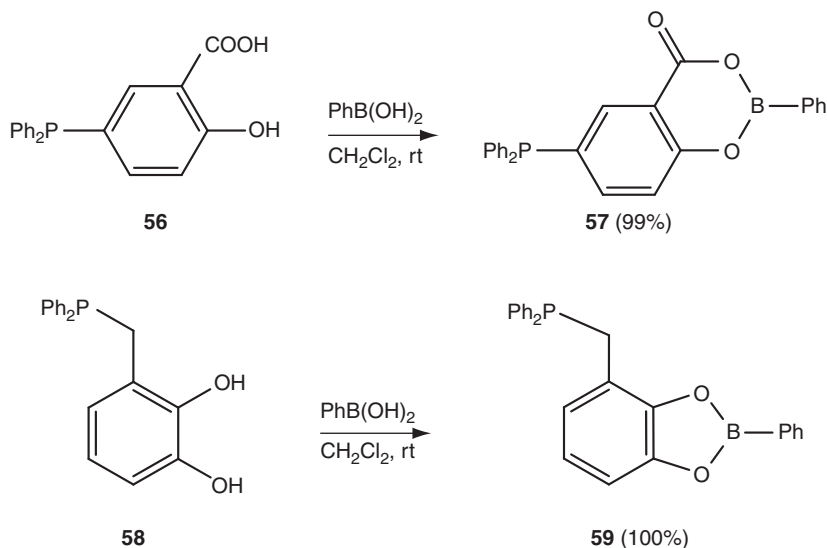
Scheme 35

III. STRUCTURE

A. General considerations

As illustrated in the previous section, a broad variety of ambiphilic compounds have been prepared by varying the different components of the PB framework (linker, substituents at phosphorus and boron).
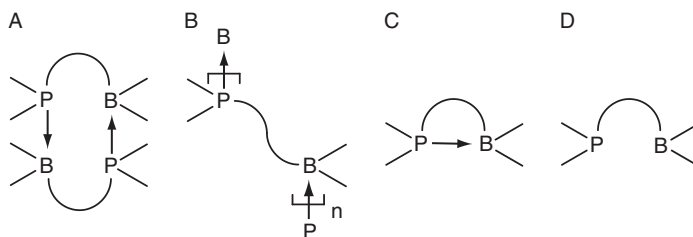
Figure 2 Schematic representation of the possible structures of phosphine-boranes.

The nature of the spacer is of utmost importance as it dictates the relative position of the antagonist sites, and thus the propensity to form donor–acceptor P–B interactions. In this respect, four different situations **A–D** can be envisaged (Figure 2), and all of them have been evidenced experimentally. Intermolecular P–B interactions can lead to head-to-tail dimers (**A**) or polymeric chains (**B**). To prevent aggregation, sterically demanding substituents are typically introduced at phosphorus and/or boron. Depending on the presence, or not, of intramolecular P–B interaction, the ensuing monomeric PBs can exist either in *closed* (**C**) or *open* (**D**) form. The dichotomy between the *closed* and *open* forms **C** and **D** is reminiscent of the adducts susceptible to form upon combining Lewis acids and Lewis bases, and the spectacular achievements reported recently with sterically frustrated Lewis pairs[3] have clearly reinforced the interest in PBs.

To probe the presence of P–B interactions and identify the ground-state structure of PBs, several analytical techniques are particularly suitable. NMR spectroscopy is undoubtedly the most informative technique, routine ^{31}P ($I = 1/2$) and ^{11}B ($I = 3/2$) NMR experiments allowing the precise assessment of the environments of both atoms. Typically, the formation of P–B interaction is accompanied by a low-field shift of the ^{31}P NMR signal, while the ^{11}B NMR signal is shifted upfield to appear in the typical range for tetracoordinate boron atoms (δ from -25 to $+20$ ppm). Another diagnostic feature for the existence of a P–B interaction is the presence of a coupling constant J_{PB} (whose magnitude can vary from 40 to 140 Hz), although it is not systematically observed. Cryoscopic/ebullioscopic measurements and mass spectrometry have also proved useful to estimate the degree of association (monomeric vs. dimeric) of PBs. When single crystals of suitable quality can be obtained, X-ray diffraction studies provide interesting geometric data. Here, the most relevant parameters are the PB distance and the geometry around boron. P–B interactions are typically associated with contacts of 2.0–2.2 Å (the sum of covalent radii[67] = 1.91 Å, and the sum of van der Waals radii[68] = 4.14 Å). The pyramidalization of the boron environment, as

estimated from the sum of bond angles around boron (excluding P), is another conspicuous feature of P–B interactions.

The presence, or absence, of P–B interactions within PBs can be unambiguously ascertained by the means of these analytical data, but their magnitude can hardly be quantified experimentally, excepted when dynamic phenomena related to the formation/cleavage of the P–B interaction are observed. As shown recently for *ortho*-phenylene and ethenyl-bridged systems, DFT calculations offer a convenient way to estimate the strength of P–B interactions. Indeed, not only the ground-state structure can be optimized computationally, so that the different forms can be compared on geometric, spectroscopic, as well as energetic grounds.

In this section, the structural features of PBs and related compounds are discussed following the nature of the organic linker. Special attention is focused on the factors that govern the presence, or not, of P–B interactions.

B. Ambiphilic ligands featuring C_1–C_4 alkyl spacers

Depending on the electronic properties of the boron substituents, C_1-bridged PBs have been shown to form either dimeric or monomeric *open* structures (Figure 3). The short methylene bridge disfavors intramolecular P–B interactions that would lead to strained three-membered rings. A dimeric structure resulting from head-to-tail P–B interactions has been ascribed to the permethyl derivative **3a**[12] on the basis of (i) the upfield ^{11}B NMR chemical shift ($\delta = 19$ ppm); (ii) significant phosphorus-boron coupling ($J_{PB} = 55.4$ Hz); and (iii) mass spectrometry. In contrast, compounds **3b**[13] and **3c**[14] were shown to adopt monomeric structures by ^{31}P and ^{11}B NMR spectroscopy. In this case, π-donation from nitrogen to boron reduces the Lewis acidity of the borane, and thereby disfavors P–B interactions.

The structural identity of **3a** was subsequently confirmed by complete characterization of the corresponding phosphine-alane **2** (Figure 4).[11] In solution, the downfield shift of the ^{31}P NMR signal combined with the ^{27}Al NMR chemical shift found in the typical range for tetracoordinate
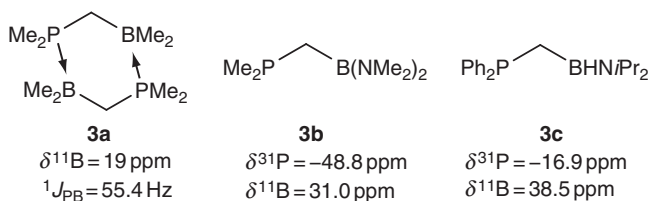

Figure 3 ^{31}P and ^{11}B NMR data for the methylene-bridged phosphine-boranes **3a–c**.
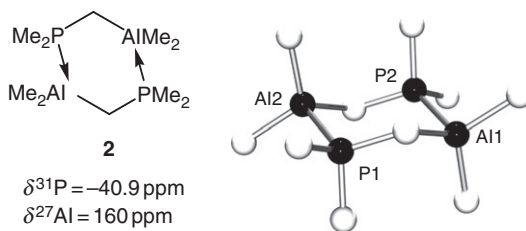
Figure 4 ^{31}P and ^{27}Al NMR data and molecular structure of the methylene-bridged phosphine-alane **2**.
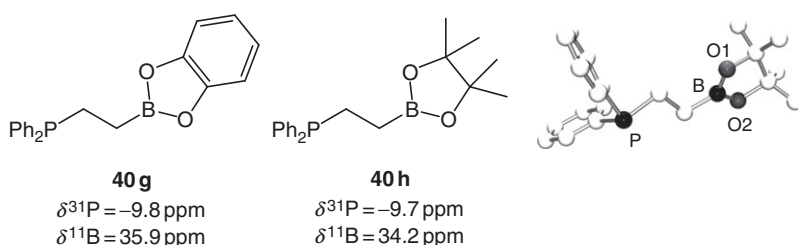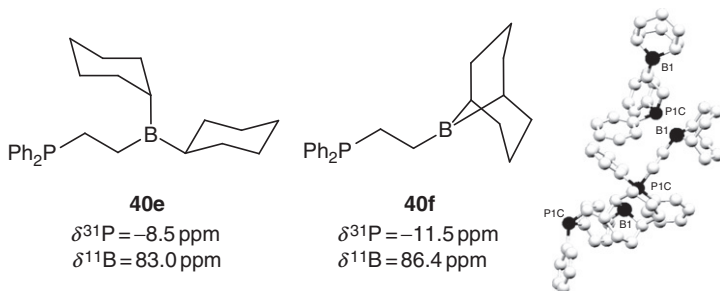

Figure 5 ^{31}P and ^{11}B NMR data for the ethenyl-bridged phosphine-boranes **40g** and **40h** and molecular structure of **40h**.
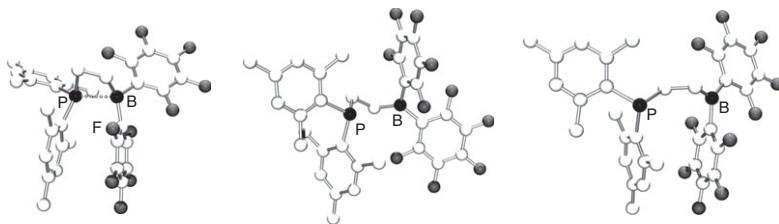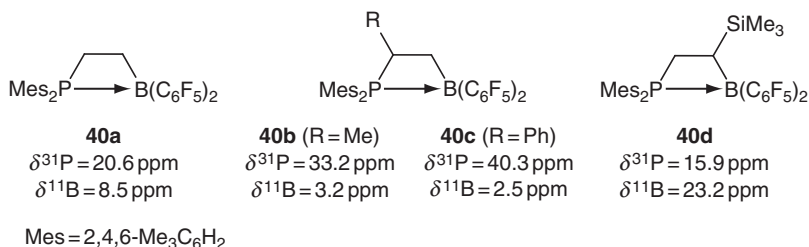
aluminum species suggest the presence of P–Al interactions. Consistently, X-ray diffraction analysis revealed a centrosymmetric head-to-tail dimeric structure. The six-membered (PCAl)$_2$ heterocycle adopts a chair conformation, the P–Al distance is short (2.451(2) Å) and the aluminum environment is noticeably pyramidalized (ΣAl$_\alpha$ = 343.4°).

An even broader structural variety has been evidenced for ethylene-bridged PBs. As for methylene-bridged systems, the presence of π-donating substituents at boron (such as catechol or pinacol) prevents intramolecular P–B interaction and leads to linear monomeric structures (compounds **40g** and **40h**).[56] This is clearly apparent in solution from the ^{31}P and ^{11}B NMR data, and was further confirmed crystallographically for **40h** (Figure 5). The environment around boron remains trigonal planar and the *anti* arrangement of the PCH$_2$CH$_2$B skeleton maintains the *distal* phosphorus and boron atoms far away from each other (4.231(2) Å).

The situation is less clear-cut when the boron atom bears two alkyl groups as in compounds **40e** and **40f**.[54,55] Although the NMR data at room temperature are found in the region of three-coordinate phosphorus and boron centers, low-temperature experiments showed a broadening of both the ^{31}P and ^{11}B signals, suggesting some P–B interaction. The X-ray diffraction analysis carried out on **40f**[54] did not reveal a cyclic structure

but rather a polymeric framework of infinite PCH$_2$CH$_2$B chains (Figure 6). The intermolecular P–B interactions are characterized by a short P–B distance (2.056(2) Å) and a strongly pyramidalized environment around boron ($\Sigma B_\alpha = 332.2°$).

Another conceivable structure, namely a monomeric four-membered ring, was observed when electron-withdrawing C$_6$F$_5$ substituents were introduced at boron to increase its Lewis acidity (compounds **40a–d**).[52,53] The presence of intramolecular P–B interaction was unambiguously substantiated by ^{31}P and ^{11}B NMR data (Figure 7). So far, the lack of suitable single crystals prevented structural characterization, but DFT calculations

40e
$\delta^{31}P = -8.5$ ppm
$\delta^{11}B = 83.0$ ppm

40f
$\delta^{31}P = -11.5$ ppm
$\delta^{11}B = 86.4$ ppm

Figure 6 ^{31}P and ^{11}B NMR data for the ethylene-bridged phosphine-boranes **40e** and **40f** and molecular structure of **40f**.

40a
$\delta^{31}P = 20.6$ ppm
$\delta^{11}B = 8.5$ ppm

40b (R = Me)
$\delta^{31}P = 33.2$ ppm
$\delta^{11}B = 3.2$ ppm

40c (R = Ph)
$\delta^{31}P = 40.3$ ppm
$\delta^{11}B = 2.5$ ppm

40d
$\delta^{31}P = 15.9$ ppm
$\delta^{11}B = 23.2$ ppm

Mes = 2,4,6-Me$_3$C$_6$H$_2$

Figure 7 ^{31}P and ^{11}B NMR data for the C$_2$-bridged phosphine-boranes **40a–d** (top). DFT-optimized structures for **40a** (bottom): *closed* form (left) benefiting from π-stacking stabilization, *open gauche* (middle) and *antiperiplanar* (right) forms.

predicted a monomeric *closed* ground-state structure for **40a** (computed P–B distance = 2.21 Å). Notably, one mesityl group at phosphorus and one pentafluorophenyl group at boron are arranged close to parallel at an average distance of 3.45 Å. The ensuing donor–acceptor π–π stacking contributes to counterbalance the strain associated with the formation of the four-membered ring. In addition, the weakness of the P–B interaction in **40a** was substantiated by the localization of two local minima associated with *open* forms (*gauche* and *antiperiplanar* conformations), which are both only 7 kcal/mol higher in energy than the *closed* form. In contrast to *o*-C_6H_4-bridged systems **7** (*vide infra*), only the *closed* form could be detected spectroscopically, but the introduction of an element of central chirality at the C_2-bridge (derivatives **40b–d**) provided a means to indirectly probe the cleavage of the P–B interaction.[53] Indeed, this process induces a change of the boron environment (from tetrahedral to trigonal planar), and thus affects the symmetry of the $B(C_6F_5)_2$ groups. Accordingly, the single set of ^{19}F NMR signals observed at high temperature (as a result of fast ring-opening/ring-closing of the four-membered ring framework) was found to decoalesce upon lowering the temperature. The activation barriers corresponding to the ring-opening process were estimated by line shape analyses and found to be very similar for the three compounds **40b–d** (11.7–12.6 kcal/mol at 280–303 K).

The formation of P–B interactions has also been discussed for the related TPB derivative **46** (Figure 8).[42] The structure of **46** could not be determined unequivocally, but the ^{31}P and ^{11}B NMR data suggested the presence of both inter- and intramolecular P–B interactions.

PBs incorporating C_3 and C_4 alkyl bridges have been shown to readily form intramolecular P–B interactions, leading to unstrained five- and six-membered rings (Figure 9). The monomeric *closed* structures of **41a**, **41d**, and **42a** were supported by diagnostic ^{31}P and ^{11}B NMR chemical shifts in solution, and short P–B distances (2.02–2.10 Å) in the solid state.[53,57]
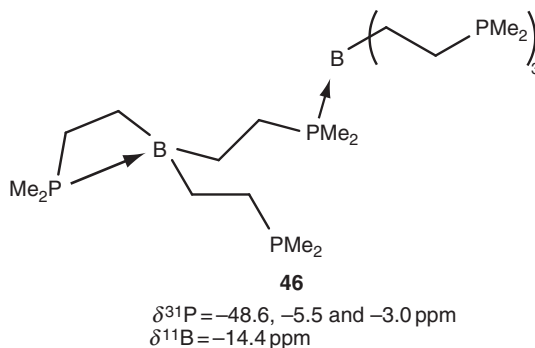

46

$\delta^{31}P = -48.6, -5.5$ and -3.0 ppm
$\delta^{11}B = -14.4$ ppm

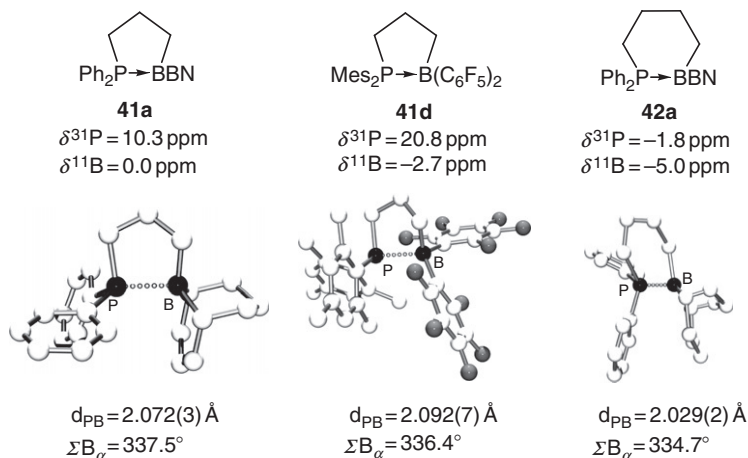**Figure 8** ^{31}P and ^{11}B NMR data for the triphosphine-borane **46**.

Figure 9 ^{31}P and ^{11}B NMR data and molecular structures for the C$_3$- and C$_4$-bridged phosphine-boranes **41a**, **41d**, and **42a**.

The P–B bond length determined crystallographically for the (CH$_2$)$_3$-bridged compound **41d** (2.092(7) Å) is noticeably shorter than that predicted computationally for the related (CH$_2$)$_2$-bridged system **40a** (2.21 Å). This further substantiates the influence of ring strain on the magnitude of intramolecular P–B interactions.

Alkyl spacers thus offer the opportunity to finely tune the interplay between the antagonist sites of ambiphilic compounds. The proximity of the phosphine and borane moieties, and thus the possible formation of intramolecular P–B interaction depend on the number of carbon atoms present in the backbone and on the Lewis acidity of the borane. Conformational considerations may also play an important role as for the ethylene-bridged systems.

C. Ambiphilic ligands featuring *ortho*-phenylene spacers

Phenylene linkers induce much higher rigidity and intramolecular P–B interactions can only occur within *ortho*-substituted derivatives. Varying the substituents at boron, we showed that both the *open* and *closed* forms of *ortho*-phenylene-bridged PBs can be observed (Figure 10). Sterically demanding groups, such as mesityl or cyclohexyl, prevent the formation of intramolecular P–B interactions, as shown by ^{31}P and ^{11}B NMR spectroscopy for compounds **7b** and **7e**.[20,22] In contrast, compounds **7c** and **7d** featuring more accessible and Lewis acidic boron centers adopt four-membered ring structures.[20,21] The corresponding ^{31}P NMR resonance signals are shifted to low field by about 20–25 ppm while the ^{11}B NMR
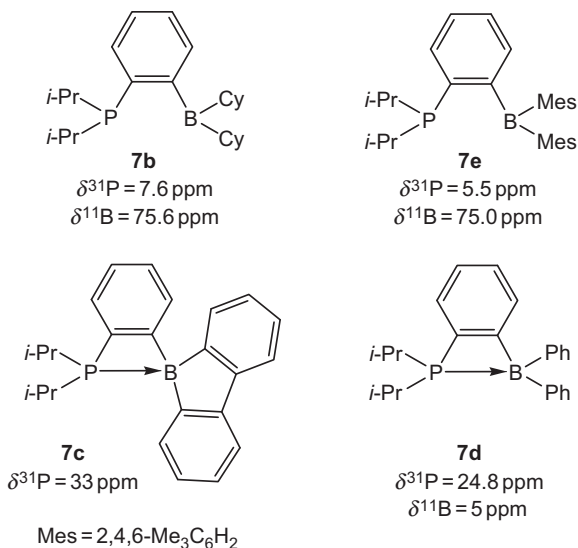
Figure 10 ^{31}P and ^{11}B NMR data for the *ortho*-phenylene bridged phosphine-boranes **7b–e**.

signal for **7d** ($\delta = 5$ ppm) appears in the typical range for tetracoordinate boron atoms.

In order to estimate the energy difference between the *open* and *closed* forms, DFT calculations were performed on the model compound **7c*** (with Me substituents on phosphorus instead of *i*-Pr groups) and on the real molecule **7d**. The optimized structures for the *closed* forms feature short P–B distances (2.13 Å for **7c***, 2.19 Å for **7d**) and pyramidalized boron environments ($\Sigma B_\alpha = 349.8°$ for **7c***, 350.1° for **7d**) (Figure 11). The corresponding *open* forms are located slightly higher in energy (5.7 kcal/mol for **7c***, 1.5 kcal/mol for **7d**). The assignment of the *closed* forms as the ground-state structures of **7c** and **7d** is further supported by the comparison of the NMR data observed experimentally with those predicted computationally in the presence, or not, of P–B interaction.

Inherently, the *ortho*-phenylene spacer induces only a weak energy difference between the *closed* and *open* forms, but the ground-state structure of all MPB **7b–d** was found to be well-defined, with or without P–B interaction. A different situation was observed for the related DPB **8a** and TPB **9**.[24] The corresponding ^{11}B NMR signals ($\delta = 43.1$ ppm for **8a** and 50.1 ppm for **9**) are in between those of triarylboranes ($\sim$70 ppm) and tetracoordinate derivatives thereof ($\sim$0 ppm), suggesting a rapid equilibrium in solution between the *open* and *closed* forms (Figure 12). This hypothesis was further corroborated by low-temperature NMR experiments and DFT calculations. The minima associated with the *open* and *closed* forms were found to be almost isoenergetic ($\Delta G < 3$ kcal/mol at 25 °C).

$\Sigma B_{\alpha} = 358.4°$ $\Sigma B_{\alpha} = 350.1°$

$\delta^{31}P = 16.5\,ppm$ $\delta^{31}P = 31\,ppm$
$\delta^{11}B = 62\,ppm$ $\delta^{11}B = 10\,ppm$

$d_{PB} = 3.064\,Å$ $d_{PB} = 2.195\,Å$
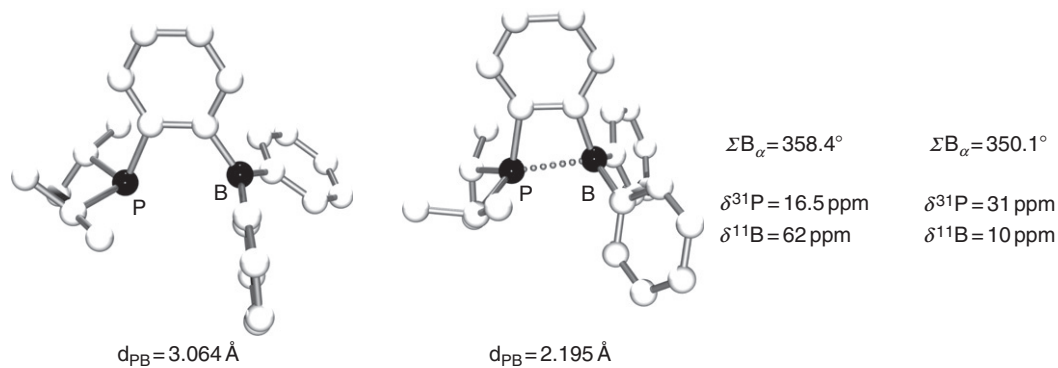
Figure 11 DFT-optimized structures for the *open* (left) and *closed* (right) forms of **7d** with selected geometric and NMR data.

8a (R = H)   **9** (R = P*i*-Pr$_2$)

$\delta^{31}P = 11.0\,\text{ppm}$ $\delta^{31}P = 4.9\,\text{ppm}$

$\delta^{11}B = 43.1\,\text{ppm}$ $\delta^{11}B = 50.1\,\text{ppm}$
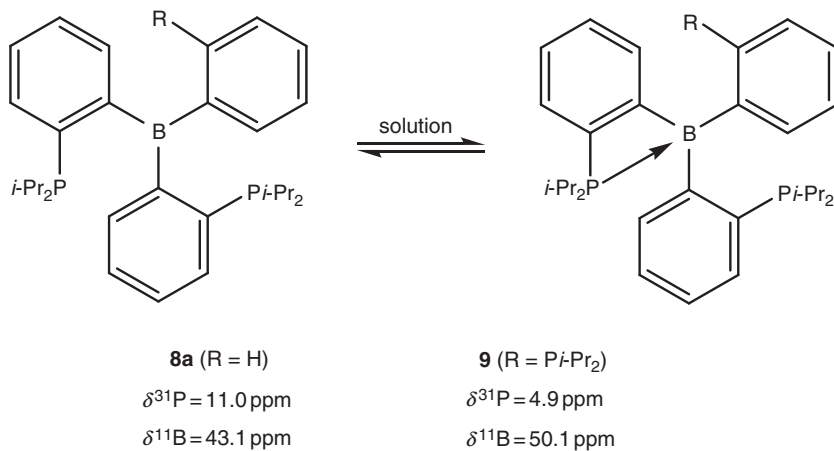
Figure 12 ^{31}P and ^{11}B NMR data for the diphosphine-borane **8a** and triphosphine-borane **9**.

$d_{PB} = 2.993(3)\,\text{Å}$ $d_{P1B} = 2.154(3)\,\text{Å}$

$\Sigma B_\alpha = 359.9°$ $\Sigma B_\alpha = 348.9°$

$\delta^{11}B = 71\,\text{ppm}$ $\delta^{11}B = 13\,\text{ppm}$
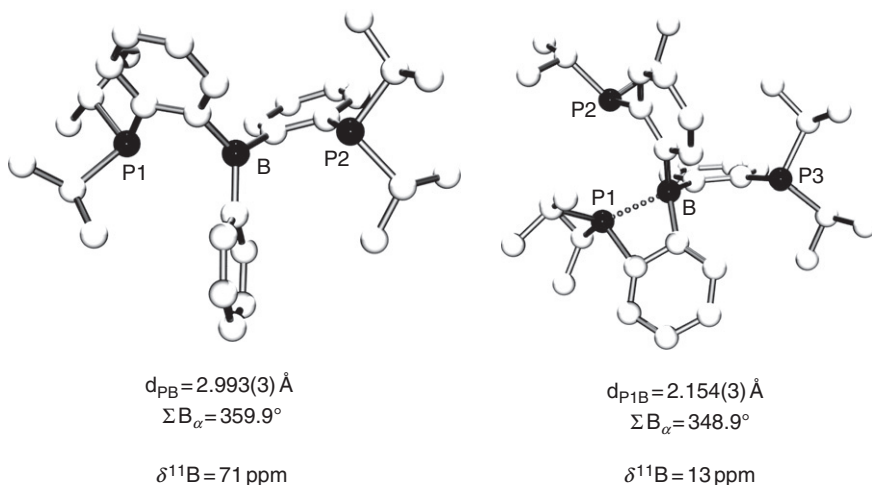
Figure 13   Molecular structures of the diphosphine-borane **8a** (*open* form, left) and triphosphine-borane **9** (*closed* form, right) with selected geometric and spectroscopic data.

In addition, the ^{11}B NMR experiments carried out on powder samples suggested that the two compounds adopt different structures in the solid state: $\delta\,^{11}B = 71\,\text{ppm}$ supported the *open* form for the DPB **8a**, while $\delta\,^{11}B = 13$ ppm argued in favor of the *closed* form for the TPB **9**. This dichotomy was unambiguously confirmed by X-ray diffraction studies (Figure 13).
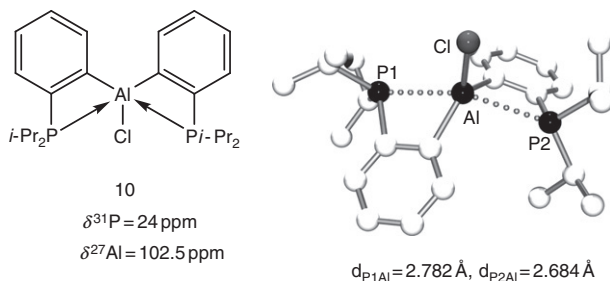
Figure 14   Optimized ground-state structure of **10** with selected geometric and NMR data.

The presence of an intramolecular P–B interaction in **9** is clearly indicated by the short P–B distance (2.154(3) Å) and the pyramidalization of the boron environment ($\Sigma B_\alpha = 348.9°$). In contrast, the two P–B distances are long in **8a** (2.993(3) Å) and the boron adopts a trigonal planar geometry ($\Sigma B_\alpha = 359.9°$).

The corresponding diphosphine-alane **10** proved too sensitive to be fully characterized, but the presence of P–Al interactions was unambiguously substantiated spectroscopically:[26] the ^{31}P NMR chemical shift for **10** ($\delta = 24$ ppm) is very similar to those of the *closed* PBs **7c,d**, while the ^{27}Al NMR signal ($\delta = 102.5$ ppm) appears in the same range as that of Al(C_6H_4-*o*-CH_2NMe_2)$_2$Cl (δ ^{27}Al $= 96$ ppm), a pentacoordinate aluminum derivative featuring two intramolecular N–Al contacts. DFT calculations carried out on the real compound **10** support a trigonal-bipyramidal environment around aluminum (PAlP $= 154.1°$ and the sum of bond angles in the equatorial plane equals $359.8°$) as a result of weak, slightly dissymmetric contacts with both phosphorus atoms ($d_{PAl} = 2.684$ and 2.782 Å) (Figure 14). The related structures featuring one or no intramolecular P–Al interaction were found 10 and 28 kcal/mol higher in energy, respectively.

With the *ortho*-phenylene linker, the formation of intramolecular P–B interaction is quasi-thermoneutral. As a consequence, the corresponding PBs retain their ambiphilic character whatever their ground-state structure (*open*, *closed*, or equilibrium between the two forms), and thus coordinate to transition metals with participation of both antagonist sites (see Section IV).

D. Ambiphilic ligands featuring benzyl spacers

More flexible systems are obtained with benzyl spacers due to free rotation around the CH_2–aryl bond. The formation of intramolecular P–B interactions is also more favorable since it leads to unstrained five-membered ring structures. Accordingly, monomeric *closed* structures were authenticated spectroscopically for compounds **26a**,[44] **26d**, and **26e**[46] (Figure 15).
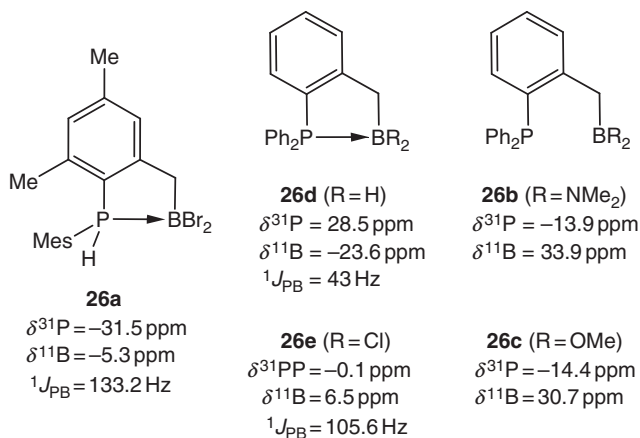
Figure 15 ^{31}P and ^{11}B NMR data for the benzyl-bridged phosphine-boranes **26a–e**.

Most indicative are the ^{11}B NMR resonance signals found in the typical range for tetracoordinate boron centers (δ varies from –23.6 to 6.5 ppm), and the significant $^1J_{PB}$ coupling constants (43–133 Hz). As for the CH$_2$ and (CH$_2$)$_2$-bridged systems, the introduction of strongly π-donating dimethylamino and methoxy substituents at boron (compounds **26b** and **26c**) was shown to prevent the intramolecular P–B interaction by decreasing the electrophilicity of boron. Consistently, the ^{11}B NMR signals for compounds **26b** and **26c** are shifted downfield ($\delta \sim 32$ ppm), while the ^{31}P NMR signals are shifted upfield ($\delta \sim -14$ ppm).

The series of MPB, DPB, and TPB **27–29** further substantiates the propensity of the benzyl spacer to favor the *closed* form (Figure 16).[45] The spectroscopic ^{31}P and ^{11}B NMR data are diagnostic of P–B interactions, while X-ray diffraction studies performed on **27** and **28** revealed short P–B distances (2.11–2.13 Å) and significantly pyramidalized environments around boron ($\Sigma B_\alpha = 343$–$347°$). In addition, low-temperature ^{31}P NMR experiments indicated rather fast exchange of the two phosphorus atoms for the DPB **28** (activation barrier < 10 kcal/mol), but in contrast to that observed for the *ortho*-phenylene-bridged system **8a**,[24] no indication of a tricoordinate boron center associated with the monomeric *open* structure was apparent in the ^{11}B NMR spectrum.

E. Ambiphilic ligands featuring *cis*-alkenyl spacers

As presented in Section II, several PBs featuring unsaturated C$_2$ linkers (–C≡C–, *trans* or *cis* –CR=CR′–) have been prepared. Here, only the structure of the *cis*-alkenyl bridged systems **22** will be discussed since these are the only systems prone to forming intramolecular P–B

27
$\delta^{31}P = 17.5\,ppm$
$\delta^{11}B = 12.2\,ppm$

28
$\delta^{31}P = 3.3\,ppm$
$\delta^{11}B = 10.9\,ppm$

29
$\delta^{31}P = -2.5\,ppm$
$\delta^{11}B = -13.4\,ppm$

$Ar = o\text{-}(Ph_2PCH_2)C_6H_4$

$d_{PB} = 2.108\,\text{Å}$ $d_{P1B} = 2.130\,\text{Å}$
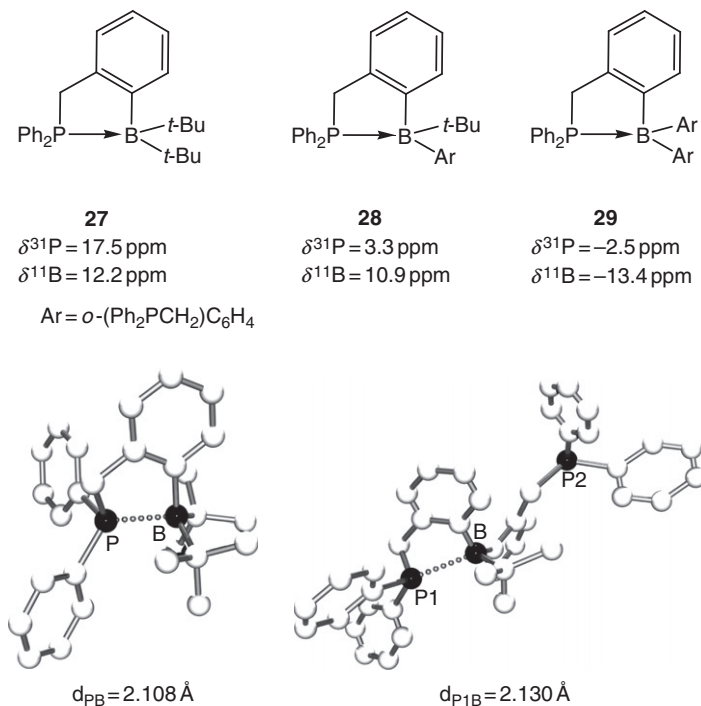
Figure 16 ^{31}P and ^{11}B NMR data for the benzyl-bridged phosphine-boranes **27–29** (top). Molecular structures of **27** (left) and **28** (right).

interactions. Monomeric structures were supported by cryoscopic/ebullioscopic measurements for PBs **22a–d,h**[35,39,69] and by mass spectrometry for **22g**.[40] Whatever the substitution pattern at phosphorus and boron (Me, Et, Bu, Cy, and Ph), the ^{11}B NMR signal appears in the typical range for tetracoordinate boron atoms (δ varies from –22 to 12.5 ppm), indicating the presence of P–B interactions. Consistently, the dipole moment measured for **22g** in benzene (4.7 D) significantly exceeds that computed for the *open* structure (1.8 D), but is in good agreement with that predicted for the *closed* form (3.5 D).[70] The monomeric *closed* structures of **22e**[37] and **22g**[40] were unambiguously authenticated by X-ray diffraction analyses (Figure 17). The observed P–B distances (2.10 Å) are very similar to those observed in the *ortho*-phenylene-bridged systems.

IV. COORDINATION

The four coordination modes **E–H** (Figure 18) have been substantiated spectroscopically and structurally for PBs and related ambiphilic ligands. They differ in the participation of the Lewis acid moiety that may remain
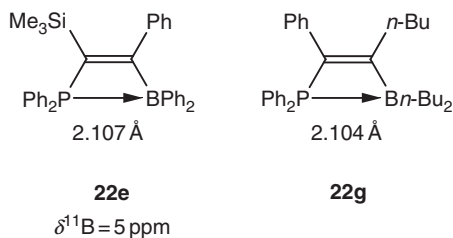
Figure 17 Key geometric and NMR data for the alkenyl-bridged phosphine-boranes **22e** and **22g**.
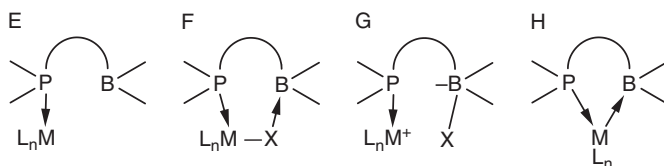
Figure 18 Schematic representation of the coordination modes **A–D** for phosphine-boranes.

pendant (mode **E**), or interact with a coligand (bridging mode **F**), leading ultimately to zwitterionic complexes (mode **G**). Alternatively, the Lewis acid may interact with the metal itself as a σ-acceptor ligand (mode **H**). These four bonding situations will be presented in this section and when possible, the factors dictating the preferred coordination mode will be discussed.

A. Complexes featuring a pendant borane

The simplest bonding situation conceivable upon coordination of an ambiphilic ligand to a transition metal is that involving the sole coordination of the Lewis base moiety, the Lewis acid fragment remaining pendant. Several examples of such complexes have been described in the recent years, most frequently upon coordination of preformed ambiphilic ligands.

In the early 1990s, Kagan[61] and Jacobsen[62] independently reported the synthesis of rhodium, platinum, and palladium complexes featuring tartrate-derived boraDIOP ligands **50**. They both sought the same objective of preparing chiral ligands presenting dual functionality, with two donor groups coordinating the metal center and a remote Lewis acid site that might be involved in substrate anchoring. In this perspective, Kagan prepared and spectroscopically characterized the cationic Rh complex **60**

(Figure 19). In the mean time, Jacobsen reported a series of Rh, Pd, and Pt complexes (**60′**, **61**, **62**). It is most likely that the rigid skeleton of these boraDIOP ligands geometrically prevents the participation of the Lewis acid to the coordination. This hypothesis has not been unambiguously confirmed by ^{11}B NMR or X-ray diffraction data, but indirectly supported by the negligible variation of the ^{31}P NMR chemical shifts of complexes **61** and **62** when varying the aryl substituent at boron.

Interestingly, the propensity of the boron atom to engage in secondary interactions was also examined by Jacobsen. The interaction of the rhodium complex **60′** with a model substrate, namely 5-hexen-1-amine, was monitored by ^{1}H NMR spectroscopy.[62] The stronger upfield shifts of the alkene resonances compared to those observed upon coordination of the same substrate to the related boron-free salt [Rh(cod)(DIOP)][ClO$_4$] (cod = cycloocta-1,5-diene) were attributed to a cooperative behavior of the boron and metal centers of **60′** that concomitantly interact with the nitrogen atom and alkene moiety, respectively (Figure 20).

Subsequently, Landis studied the coordination of the ferrocene-based diphosphine-benzoxaborolidine ligands **53** with the aim of supporting secondary interactions between the pendant Lewis acid and an external Lewis base.[63] Stable platinum complexes **63a–c** were formed by reacting

60 X = PF$_6$
60′ X = ClO$_4$

61 M = Pd   **62** M = Pt

a R = H
b R = Cl
c R = CF$_3$
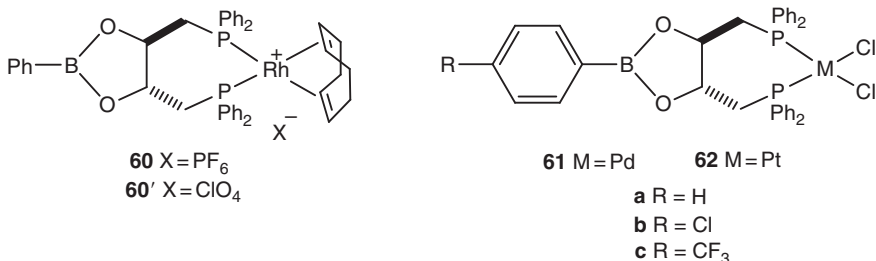
Figure 19 Complexes deriving from the boraDIOP ligands **50**.
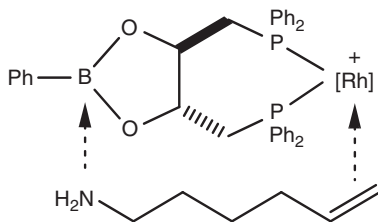
Figure 20 Proposed participation of the pendant borane moiety in the interaction of **60′** with 5-hexen-1-amine.

ligands **53a–c** with [PtMe₂(cod)] (Scheme 36). The coordination of the phosphines was apparent from the downfield shift of ^{31}P NMR resonances and from the presence of $^1J_{PPt}$ coupling patterns. Ligand **53a** was also treated with [Rh(nbd)₂][OTf] (nbd = norbornadiene, OTf = trifluoromethane-sulfonate) to yield complex **64a**. It is most likely that the weakly Lewis acidic benzoxaborolidine unit does not participate in coordination to these complexes, although it has not been substantiated unequivocally by NMR spectroscopy or X-ray diffraction.

53a R = Me
53b R = Ph
53c R = p-C₆H₄Cl

63 [M] = PtMe₂
a R = Me
b R = Ph
c R = p-C₆H₄Cl
64a R = Me,
[M] = [Rh(nbd)₂⁺, TfO⁻]
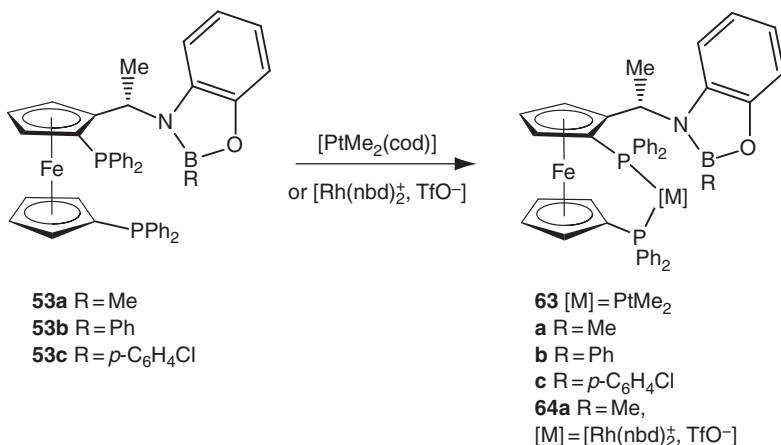
Scheme 36

Recently, Gudat reported the synthesis of the PB ligand **59** incorporating a remote, weakly acidic boronic ester, and studied its interactions toward both palladium precursors and nitrogen-containing Lewis bases.[66] The PB **59** was treated with [PdCl₂(cod)] to give the corresponding complex **65** (Scheme 37). The ^{31}P NMR spectroscopic data revealed the formation of *cis*- and *trans*-isomers in a 20/80 ratio, and as expected from the remote position of the boron atom within the
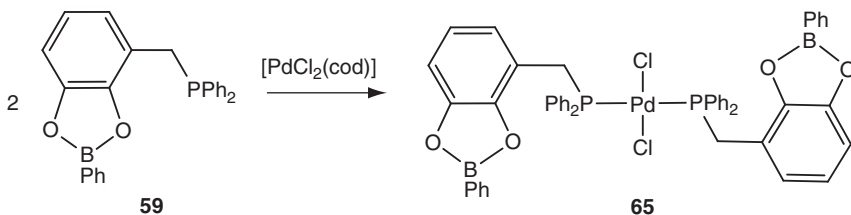
Scheme 37
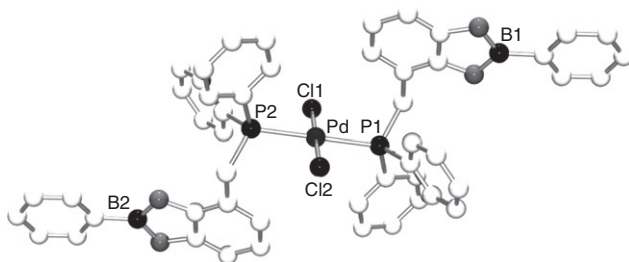
Figure 21 Molecular structure of *trans*-**65**.

rigid aryl backbone, the ^{11}B NMR resonance signal (δ ^{11}B = 29 ppm) appeared in the typical range for tricoordinate boronic esters. The structure of *trans*-**65** was further confirmed by a single-crystal X-ray diffraction study (Figure 21). In accordance with the spectroscopic data, the boron atoms display trigonal planar geometries and remain pendant, available for coordinating external Lewis bases.

The ability of the boron atom of **59** to engage in a donor–acceptor interaction was illustrated with DMAP and DABCO (DABCO = diazabicyclo-[2.2.2]-octane) that readily formed the corresponding Lewis adducts. Interestingly, a similar behavior was retained after coordination of the phosphorus atom to palladium. The formation of the Lewis base adducts **66a** and **66b** of complex **65** (Scheme 38) was supported by solid-state ^{31}P and ^{11}B CP/MAS–NMR spectroscopy (δ ^{11}B = 5–6 ppm), although the occurrence of decomposition and/or dissociation processes impeded spectroscopic characterization in solution and recrystallization to obtain X-ray quality crystals. Compounds **66a** and **66b** substantiate the ability of ambiphilic compounds to engage concomitantly into the coordination of donor and acceptor moieties. Such a dual behavior opens interesting perspectives for the preparation of metallo-polymers and multimetallic complexes.

66a N-Do = DMAP
66b N-Do = DABCO
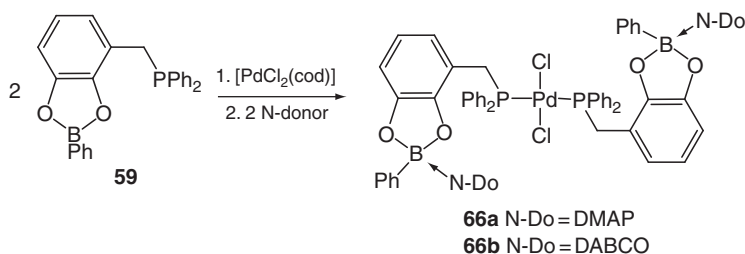
Scheme 38

In 1997, Braunschweig described the synthesis and coordination properties of the MPB **3b**.[13] Cr, Fe, and Mn complexes were prepared and isolated as highly volatile compounds upon displacement of a CO ligand (Scheme 39). Here, both the short methylene backbone and the π-donating amino groups at boron preclude the interaction of the borane moiety with the metal center. Complexes **67a–c** have been characterized in solution by multinuclear NMR spectroscopy: upon coordination, the ^{31}P NMR resonance signals are shifted downfield by $\sim$100 ppm, while the ^{11}B NMR signals remain unchanged, indicating that the phosphorus, but not the boron atom, participates to the coordination. In addition, the carbonyl stretching frequencies (IR) for complexes **67a–c** are very similar to those of the related boron-free PMe$_3$ complexes, which further supports the absence of interaction between the boron and the metal center. Interestingly, the propensity of the borane moiety for further reactivity was illustrated by substitution reactions at the boron center of complexes **67a** and **67b**. As an example, amino groups at boron were succesfully exchanged for methoxy groups upon addition of an excess of methanol to give **68a** and **68b** (Scheme 39).

67a ML$_n$ = Cr(CO)$_5$
67b ML$_n$ = Fe(CO)$_4$
67c ML$_n$ = (MeC$_5$H$_4$)Mn(CO)$_2$
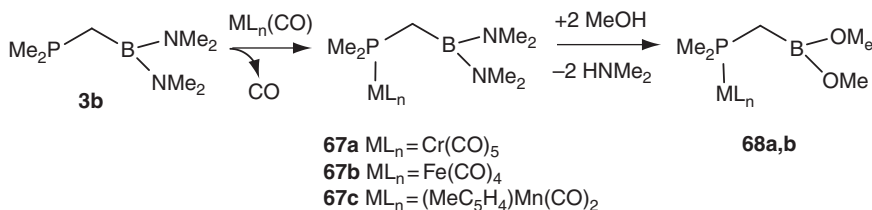
Scheme 39

The reactivity of the iron complex **68b** toward oxidative addition was studied with triphenylsilane HSiPh$_3$ under irradiation. The resulting silyl complex **69b** was isolated and fully characterized both in solution and in the solid state. The small coupling constant between the phosphorus and hydrogen atoms bonded to iron ($^2J_{PH}$ = 29.8 Hz) indicated a *cis* relationship. The X-ray structure of **69b** confirmed this arrangement, and showed a distorted octahedral geometry around iron with a quasi-linear P–Fe–Si arrangement (173.0°). The trigonal planar geometry around the boron atom combined with the long B···Fe and B···H distances (3.646 and 4.582 Å, respectively) indicated that the Lewis acid site does not interact with either the metal center or the hydrogen atom (Scheme 40).

The B-pendant coordination mode was also evidenced by Emslie upon treating the rigid PB **32** with [Pd$_2$(dvds)$_3$] (dvds = 1,3-divinyltetramethyl-disiloxane) or [Pt(cod)$_2$]/dvds (Scheme 41).[71] The ^{31}P and ^{11}B NMR data

Scheme 40

dvds: 1,3-divinyltetramethyldisiloxane
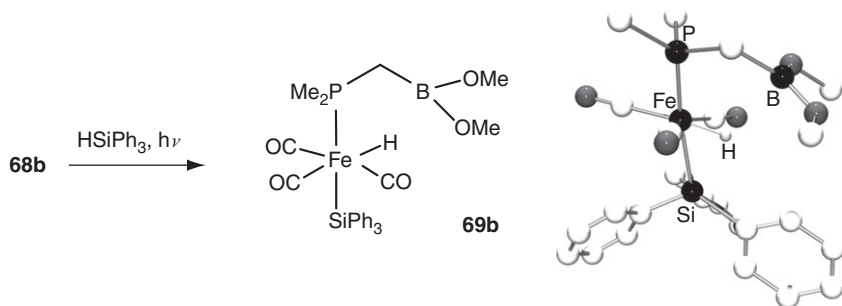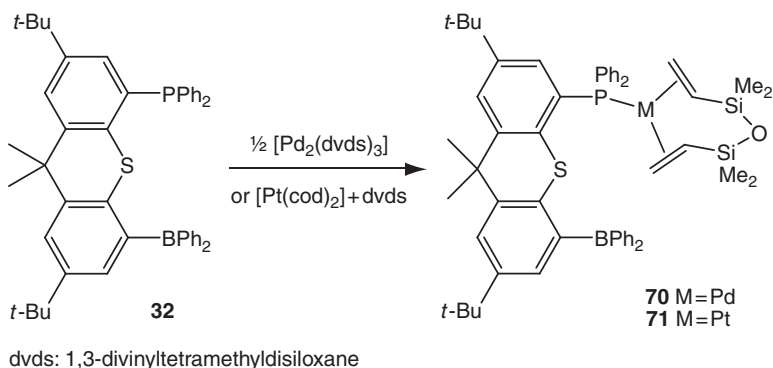
Scheme 41

of the ensuing complexes **70** and **71** (δ ^{31}P $= 23.7$ ppm and δ ^{11}B $= 74$ ppm for **70**; δ ^{31}P $= 21.1$ ppm and δ ^{11}B $= 74$ ppm for **71**) indicated the coordination of the phosphine to the metal center and the pendant character of the borane.

The structure of **70** was established by X-ray diffraction analysis (Figure 22). The palladium center is only coordinated by the phosphorus atom of **32** (the sulfur atom remains pendant) and the dvds coligand (η^2: η^2 fashion), resulting in a slightly distorted trigonal planar geometry around the metal. The rigid thioxanthene linker maintains the boron atom remote from the coordination sphere of the metal.

In our group, we have been interested in PBs featuring the rigid *o*-phenylene spacer that maintains the two antagonist sites in proximity while preventing strong intramolecular P–B interaction (see Section III). Coordination mode **E** was illustrated experimentally and studied theoretically with the PB ligand **7e** featuring sterically demanding mesityl groups at boron.[22] The corresponding palladium complex **72** was readily prepared by cleavage of the chloro bridge of the precursor [Pd(μ-Cl)(allyl)]$_2$ (Scheme 42). The coordination of the phosphine and the pendant
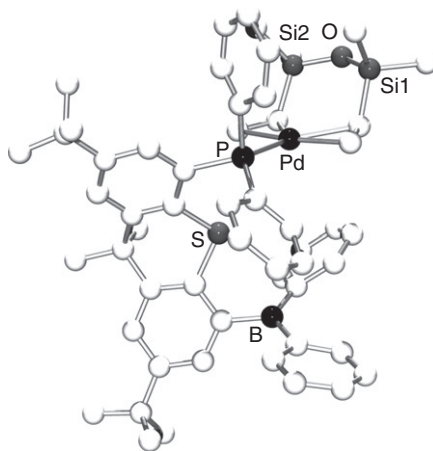
Figure 22 Molecular structure of **70**.

character of the borane were unambiguously established by ^{31}P and ^{11}B NMR spectroscopy (δ ^{31}P = 50.8 ppm and δ ^{11}B = 73 ppm for complex **72**, vs. ^{31}P = 5.5 ppm and δ ^{11}B = 76 ppm for the free ligand **7e**). An X-ray diffraction study further corroborated this coordination mode. The trigonal planar geometry around the boron center and the long B$\cdots$Pd (3.850 Å) and B$\cdots$Cl (4.381 Å) distances indicate the absence of interaction between the boron atom and the metal fragment. In line with these experimental observations, only one energy minimum associated with the pendant borane form was located computationally on the potential energy surface of a model complex **72*** (with Me instead of *i*-Pr substituents at phosphorus).
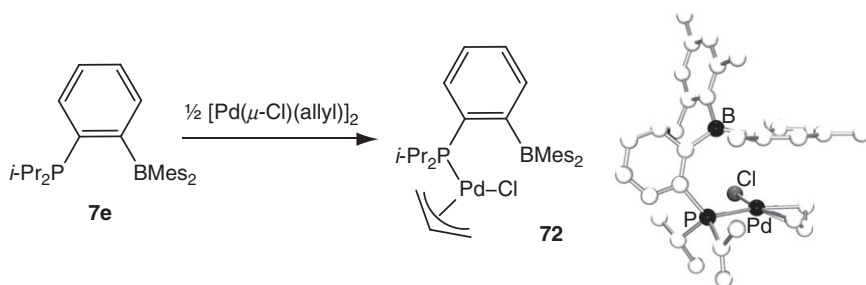
Scheme 42

The B-pendant coordination mode was also encountered in the CuCl complex deriving from the *i*Pr$_2$P-*o*-(C$_6$H$_4$)-BCy$_2$ ligand **7b** (Scheme 43).[21]

The structure of **73** was substantiated spectroscopically (δ ^{11}B $= 82.5$ ppm) and confirmed crystallographically. A centrosymmetric chloro-bridged dimeric structure with tricoordinate copper centers was observed. The pendant character of the borane is apparent from the rather long the B$\cdots$Cu (3.05 Å) and B$\cdots$Cl (4.06 Å) distances associated with a trigonal planar geometry around boron. Compared to related mononuclear palladium and rhodium complexes (see Section IV.B), the presence of the chloro-bridge disfavors the formation of Cl–B interactions (coordination mode **F**) in **73**.
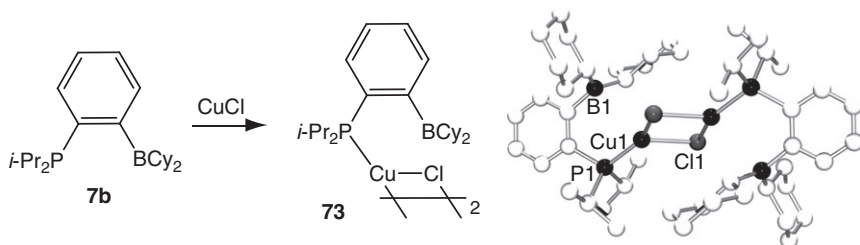
Scheme 43

The sole coordination of the phosphine sites has also been observed with PBs featuring the flexible $(CH_2)_2$ linker. The coordination of ligands **40e** and **40f** to the [Ru(p-cymene)Cl$_2$] fragment affords complexes **74a** and **74b** (Scheme 44). Despite the modest steric hindrance around boron, neither Cl–B (coordination mode **F**) nor Ru–B (coordination mode **H**) interaction was found. Coordination mode **E** was established spectroscopically (δ^{11}B $= 82$ and 87 ppm for **74a** and **74b**, respectively) and confirmed crystallographically.[55]
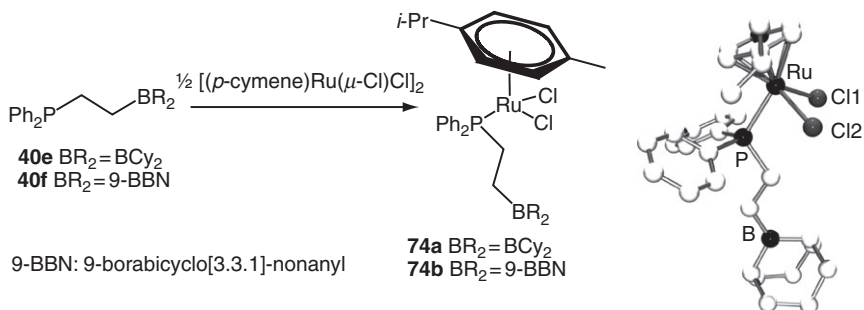
Scheme 44

The rhenium complex **76** related to **74b** was also prepared recently by Labinger and Bercaw using another synthetic strategy.[72] In this case, the pendant borane moieties were introduced by hydroboration of unsaturated phosphines in the coordination sphere of the metal. The cationic rhenium complex **75** featuring two diphenyl(vinyl)phosphines was readily converted into the corresponding bis(phosphine-borane) complex **76** (Scheme 45). The coordination mode of **76** was substantiated spectroscopically ($\delta\ ^{11}B = 87.7$ ppm) and crystallographically.
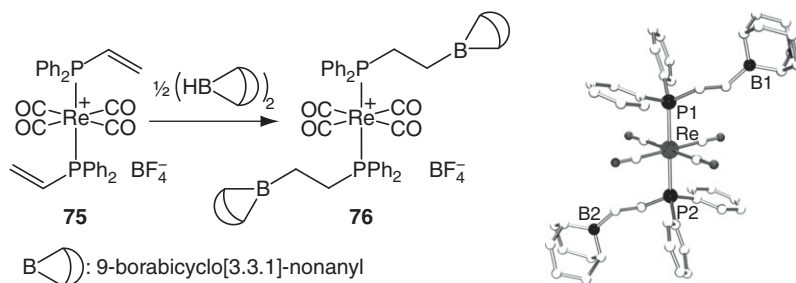
Scheme 45

Hereafter are described the few complexes featuring pendant borane moieties that have been obtained as rearranged- or side-products starting from phosphine-borates.

Tilley first reported such a pathway, in the frame of the investigation of zwitterionic complexes featuring TPB ligands for the activation of X–H bonds (X = H or Si).[73] Upon heating at 80 °C in toluene, the rhodium complex **77** was found to rearrange into the neutral DPB complex **78** (Scheme 46). The migration of the (i-Pr$_2$PCH$_2$) fragment from boron to rhodium is reversible, and complex **77** was recovered upon cooling the temperature to 20 °C. Complex **78** could be isolated from **77**, by trapping the liberated trimethylphosphine with BPh$_3$. Alternatively, it can be prepared by reacting the anionic TPB ligand **79** with a rhodium precursor featuring labile coligands such as [Rh$_2$(μ-Cl)$_2$(C$_2$H$_4$)$_4$]. The rearrangement of **77** into **78** is accompanied by a large downfield shift of the ^{11}B NMR resonance (from –16.2 to 74.9 ppm), suggesting the absence of interaction between the borane and metal fragments in **78**.

This was unambiguously confirmed by an X-ray diffraction study (Figure 23): the boron atom is in a trigonal planar environment and remains far away from the metal center (the B···Rh distance corresponds to 3.83 Å).

Similarly, Peters studied the coordination of the DPB ligand **80** to CuCl.[15] Along with the desired anionic complex **81**, a small amount (<15%) of the neutral DPB Cu(I) complex **82** was obtained, as the result of the cleavage of a boron-aryl bond (Scheme 47). In order to get complete spectroscopic data, an
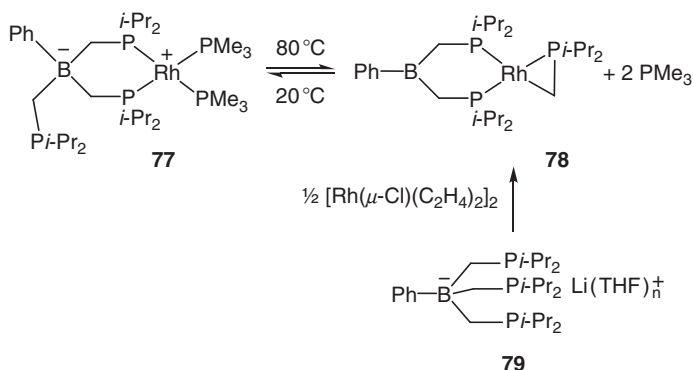
Scheme 46
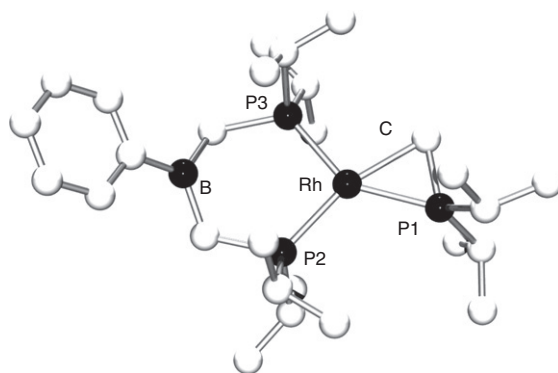
Figure 23   Molecular structure of **78**.

analogous complex **82′** was synthesized independently from the preformed ligand [PhB(CH$_2$Pt-Bu$_2$)$_2$] **4**. The ^{31}P ($\delta = 23.1$ ppm) and ^{11}B NMR ($\delta = 75.2$ ppm) data for **82′** are consistent with the coordination of the two phosphorus atoms without participation of the boron atom.
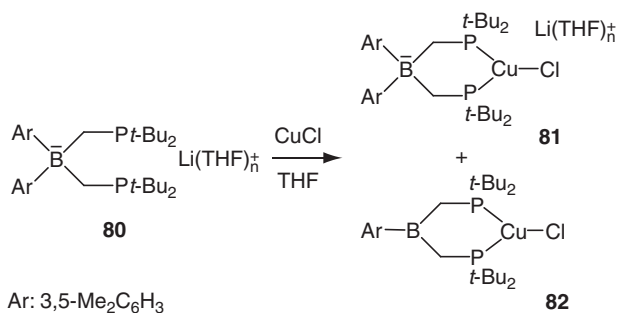
Scheme 47
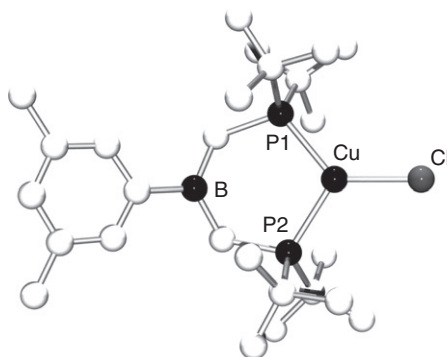
Figure 24   Molecular structure of **82**.

In addition, an X-ray diffraction analysis was performed on **82** (Figure 24) revealing a very similar situation to that encountered in the related Rh complex **78**: the trigonal planar geometry around the boron atom and the long B$\cdots$Cu distance (3.64 Å) indicate that the borane moiety also remains pendant in this case. In both complexes **78** and **82**, the participation of the Lewis acid in the coordination is prevented geometrically by the combination of short CH_2 linkers and strong chelating effect of the two phosphine buttresses.

In summary, an increasing variety of complexes illustrate the ability of ambiphilic ligands to coordination to transition metals by the sole Lewis base moiety. Typically, the participation of the Lewis acid into the coordination is prevented electronically (π-donating substituents reducing the Lewis acidity) and/or geometrically (linkers maintaining the Lewis acid in remote position or sterically demanding substituents reducing the accessibility to the Lewis acid). These examples demonstrate that it is possible to introduce a pendant Lewis acid in the second-coordination sphere of a metal. This available functionality opens interesting perspectives (such as substrate anchoring in catalytic processes), and further developments in this area will probably require the incorporation of more electron-deficient moieties.

B. Complexes featuring X- or L-Lewis acid interactions

The ability of ambiphilic ligands to bridge M–X or M–L fragments (coordination mode **F** resulting from the concomitant coordination of the donor site to the metal and interaction of the Lewis acid with a coligand) has also been demonstrated experimentally. Such bridging coordination remains rare, and most of the known examples involve PB ligands.[74]

The first example was reported by Baker and Marder in 1995.[75] The monohydride $[MH(PMe_3)(\eta^2\text{-}CH_2PMe_2)]$ complexes **83** (M = Ru)

and **84** (M = Os) were found to readily react with thexylborane {[BH (CMe$_2$CHMe$_2$)(μ-H)]$_2$} and 9-H-BBN (9-borabicyclo[3.3.l]nonane, [B (C$_8$H$_{14}$)(μ-H)]$_2$) to afford the ruthena- and osma-heterocycles **85–86a,b** (Scheme 48). These reactions formally proceed by insertion of a B-H bond of the borane into the M-C bond of the highly reactive MPC three-membered ring of **83/84**.

9-BBN: 9-borabicyclo[3.3.1]-nonanyl
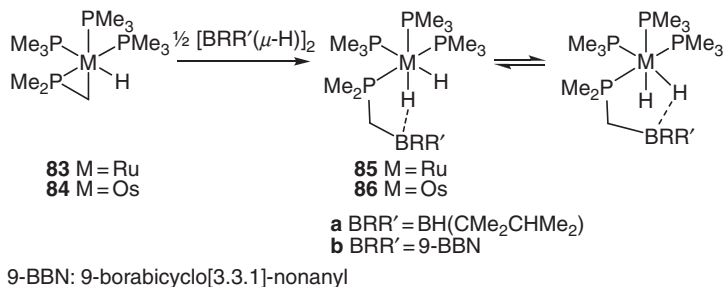
Scheme 48

The ruthena- and osma-heterocycles **85–86a,b** were characterized by multinuclear NMR spectroscopy. The ^{11}B NMR chemical shifts (δ from −12 to 1 ppm) fall in the typical range for tetracoordinate boron atoms, suggesting the presence of some residual interaction between the H and B atoms. According to variable temperature ^{1}H NMR experiments, all complexes display fluxional character due to the swinging of the borane between the two M–H bonds. The molecular structures of **85b** (Figure 25) and **86b**, as deduced from X-ray diffraction analyses, showed pseudo-octahedral environment around the metal centers, with meridional PMe$_3$ ligands and a *cis* arrangement of the two hydrides. The phosphorus atom of the PB moiety is coordinated to the metal center and the boron atom is bound to one of the hydride moieties (BH distances of 1.37–1.43 Å and pseudo-tetrahedral geometries around the boron atoms). The M–P–CH$_2$–B–H five-membered rings of complexes **85–86a,b** can thus be regarded as the result of the bridging coordination of ambiphilic Me$_2$PCH$_2$BR$_2$ ligands across Ru–H or Os–H bonds.

Subsequently, a few examples of bridging coordination of M–X and M–L fragments were reported with preformed PBs. We investigated via a combined experimental/theoretical approach the ability of the ambiphilic ligand *i*-Pr$_2$P-*o*-(C$_6$H$_4$)-BCy$_2$ **7b** to engage in bridging P–M–Cl–B interactions.[22] First, the Pd complex **87** was prepared by reacting **7b** with the dimeric precursor [Pd$_2$(μ-Cl)$_2$(allyl)$_2$] (Scheme 49). The downfield shift of the ^{31}P NMR resonance (from 7.6 to 39.2 ppm) unambiguously established the coordination of the phosphorus to the palladium center. The ^{11}B NMR signal for **87** (δ = 47 ppm) is significantly shielded compared to
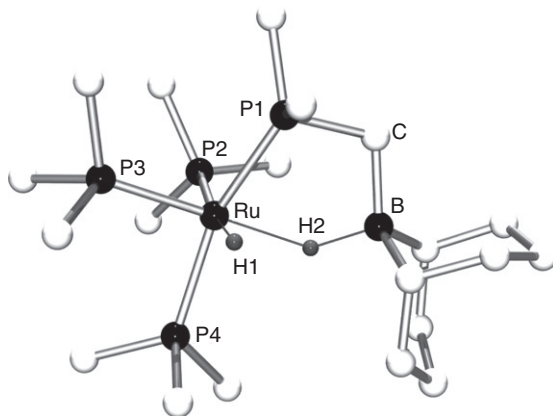
Figure 25 Molecular structure of **85b**.

that of the free ligand **7b** ($\delta = 76$ ppm), but appears at noticeably higher frequency than that expected for a strong Cl–B interaction ($\delta \sim 20$ ppm). This led us to assume that the bridging and B-pendant coordination modes coexist in solution, a hypothesis that was further supported by DFT calculations.
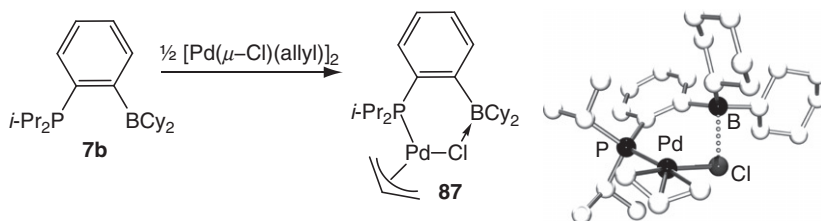
Scheme 49

According to X-ray diffraction data, in the solid-state complex **87** adopts a six-membered metallacyclic structure, as the result of P–Pd–Cl–B bridging coordination. The interaction of the borane moiety with the chlorine atom is apparent from the short Cl–B distance (2.165(2) Å) and the pyramidalization of the boron environment ($\Sigma B_\alpha = 349.1°$). The bridging coordination of the Pd–Cl bond by the PB **7b** contrasts with the B-pendant coordination mode adopted by complex **72**, deriving from the related ligand **7e** featuring mesityl groups at boron (see Section IV.A). This illustrates the role of steric factors in the participation, or not, of the Lewis acid in the coordination assembly.

The ability of Cl–B interactions to persist upon chemical transformations in the coordination sphere of the metal was then explored.[22]

Accordingly, complex **87** was treated with an excess of HCl to give the isolated dimeric, chloro-bridged complex **88** (Scheme 50). The X-ray diffraction study (Figure 26) revealed that the **7b** ligand retained its bridging coordination across the Pd–Cl bond, although the substantially longer Cl–B distance (2.334(7) Å) and less pyramidalized environment around boron ($\Sigma B_\alpha = 353.1°$) suggest some weakening of the Cl–B interaction. The ''Pd$_2$(μ–Cl)$_2$'' bridge was then cleaved by addition of one equivalent of PPh$_3$ to afford the heteroleptic mononuclear complex **89**. The two phosphines occupy *trans* positions around the Pd center, and one of the chloride ligands interacts with the boron atom. The solid-state ^{11}B NMR chemical shift (22 ppm) is diagnostic of a strong Cl–B interaction, something that was further confirmed crystallographically (Cl–B distance = 2.109(1) Å, $\Sigma B_\alpha = 343.5°$). The coordination of the basic PPh$_3$ ligand induces a substantial strengthening of the Cl–B interaction, but the Pd–Cl bond is not elongated upon coordination to the Lewis acid (Pd–Cl–B = 2.280(1) Å vs. Pd–Cl = 2.304(1) Å in **89**).
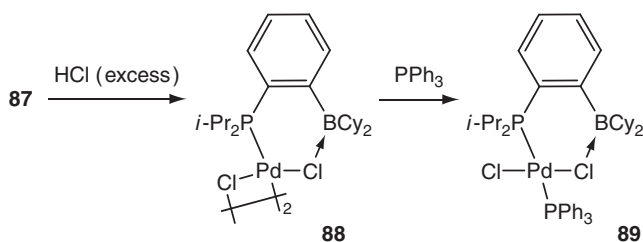
Scheme 50
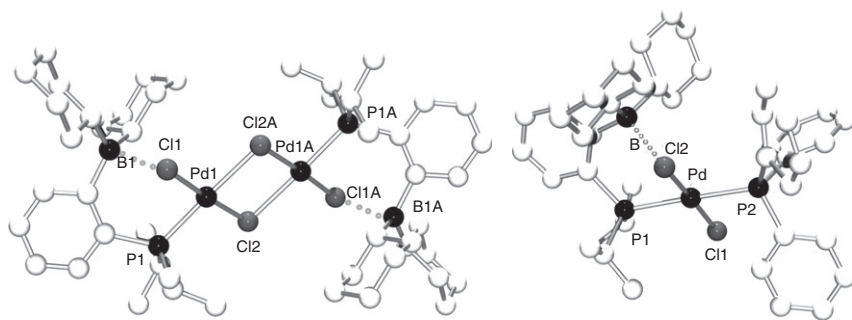
Figure 26   Molecular structures of **88** (left) and **89** (right).

In order to gain more insight into the magnitude of Cl–B interactions, DFT calculations were carried out on model complexes **87*** and **89*** bearing Me instead of *i*-Pr substituents at the phosphorus atoms.[22]
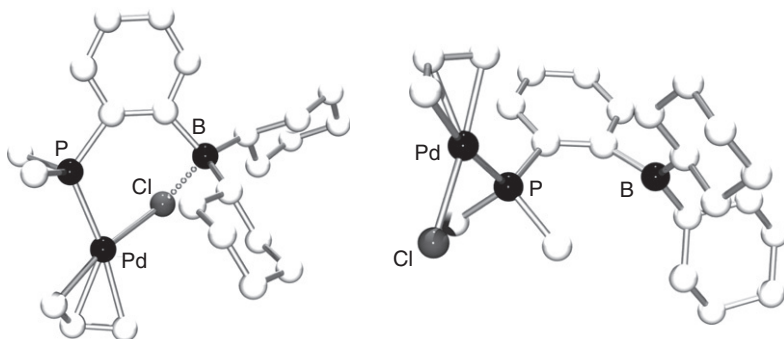
Figure 27   Optimized structures of the Pd(μ-Cl)B-bridging (left) and B-pendant (right) forms of complex **87***.

The key geometric features of the optimized Pd–Cl bridging structures were found to nicely match those determined experimentally, and the presence of rather strong Cl–B interactions was substantiated by Natural Bond Orbital (NBO) analyses. For both complexes, rotation around the P–Pd bond allowed the location of another minimum devoid of any Cl–B interaction (B-pendant form, coordination mode **E**) (Figure 27). The two forms lie very close in energy ($\Delta G_{298} = 3$–5 kcal), in agreement with the coexistence of the two coordination modes in solution.

Finally, the generality of this bonding situation was illustrated by preparing the rhodium complex **90** upon treatment of **7b** with the [Rh(μ-Cl)(nbd)]$_2$ precursor (Scheme 51).[22] The bridging coordination of the PB ligand across the Rh–Cl bond was supported both experimentally (NMR spectroscopy and X-ray diffraction) and theoretically.
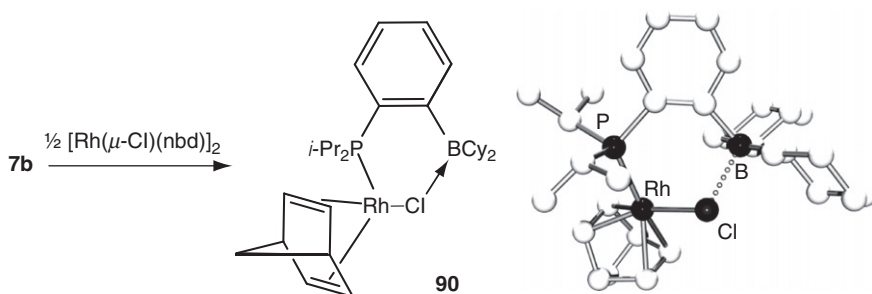
Scheme 51

Emslie also reported the ability of the related rigid phosphine–thioether–borane ligand **32** (referred to as PSB) to engage in bridging P–M–Cl–B interaction upon coordination to rhodium and palladium precursors (Scheme 52).[71,76]
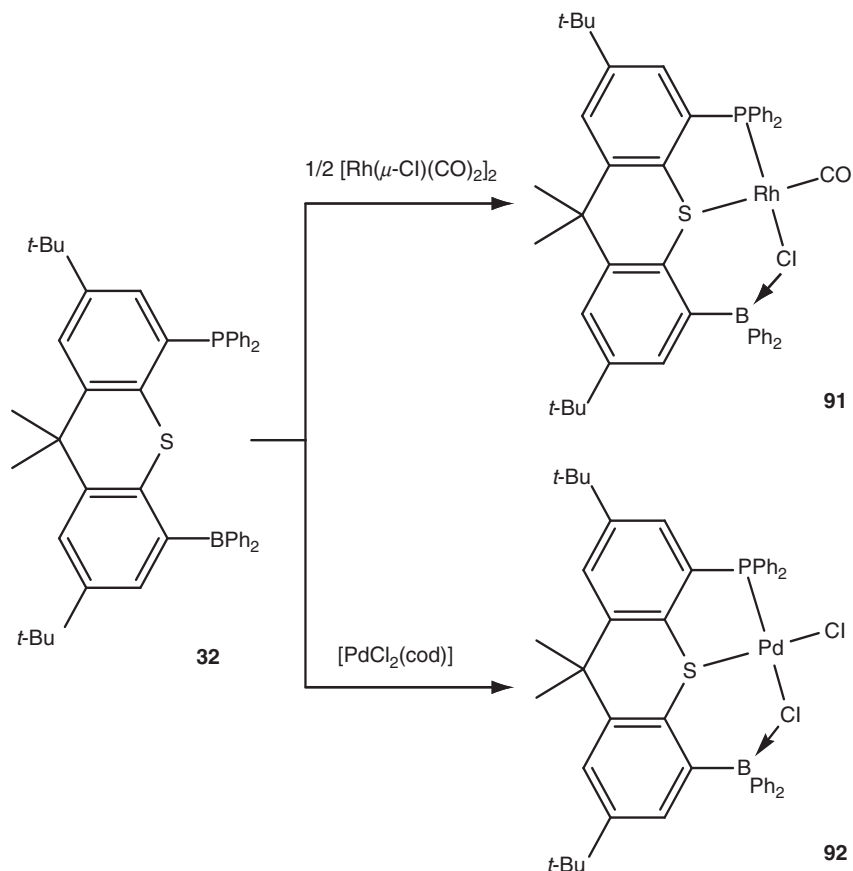
Scheme 52

The ^{31}P NMR chemical shift ($\delta = 64$ ppm) and the strong ^{11}B NMR upfield shift ($\delta = 11.5$ ppm vs. 69 ppm for free ligand) of complex **91**, resulting from the reaction of **32** with [Rh$_2$(μ-Cl)$_2$(CO)$_4$], strongly suggested the participation of both the phosphorus and boron atoms to the coordination. The solid-state structure of **91** (Figure 28) revealed the coordination of the phosphorus and sulfur atoms to a square-planar rhodium center while the boron is involved in a bridging Rh-Cl–B interaction. The interaction of the borane moiety with the chlorine atom is indicated by the short Cl–B distance (1.99 (9) Å) and the strong pyramidalization of the boron environment ($\Sigma B_\alpha = 325.5°$).

Later on, the related complex [PdCl(μ-Cl)(PSB)] **92** was shown by NMR spectroscopy (^{31}P $\delta = 58$ ppm, ^{11}B $\delta = 13$ ppm) to feature a similar P–Pd–Cl–B bridging interaction.[71] The addition of magnesium or zinc
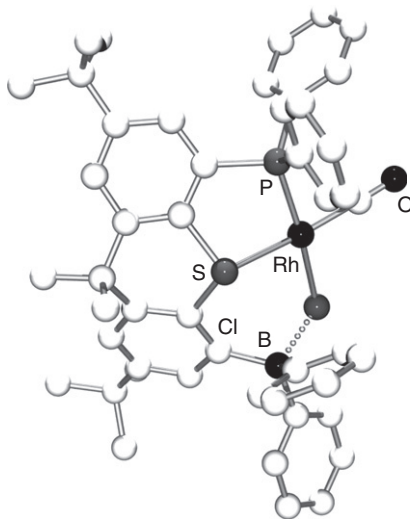
Figure 28   Molecular structure of **91**.

powder to complex **92** led to the dimeric Pd(I) complex **93** (Scheme 53), that has been characterized spectroscopically and structurally (Figure 29). The retention of the Cl–B interaction was apparent from the ^{11}B NMR chemical shift ($\delta = 2$ ppm), the short B–Cl distance (1.981(8) Å), and the pyramidalization of the boron environment ($\Sigma B_\alpha = 336.1°$).
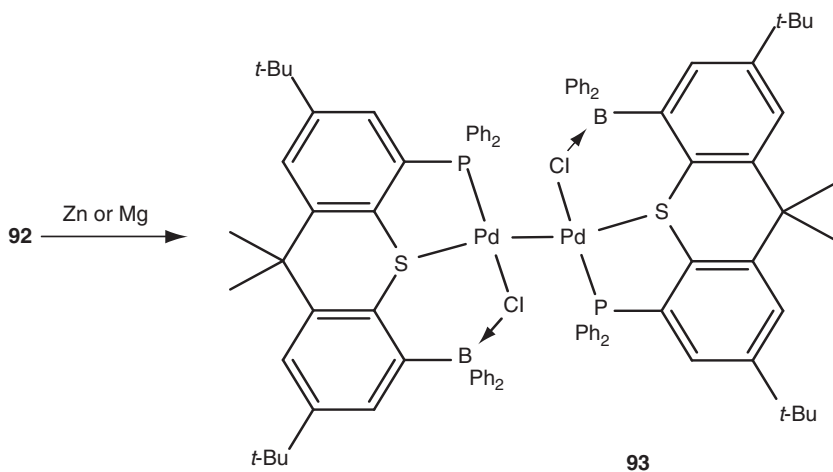
Scheme 53
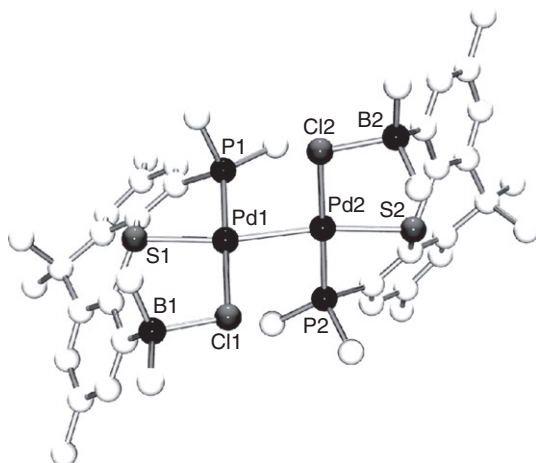
Figure 29 Molecular structure of **93**.

All of the examples described till now illustrate the propensity of PB ligands to engage in bridging coordination across M–X bonds. By reacting the phosphino-thioether-borane **32** with [Pd$_2$(dba)$_3$] (dba = dibenzylideneacetone) (Scheme 54), Emslie substantiated that ambiphilic ligands can also bridge ML fragments.[47] ^{11}B NMR spectroscopy ($\delta = 5.3$ ppm) indicated the participation of the Lewis acid in the coordination, and the molecular structure of **94** was established by X-ray diffraction analysis (Figure 30). Both the phosphorus and sulfur atoms of the ligand **32** are coordinated to the Pd center, as well as three carbon atoms of the dba fragment. In addition, the boron atom strongly interacts with the oxygen atom of the dba coligand, as shown by the short O–B distance (1.537(4) Å) and the pseudo-tetrahedral environment around boron ($\Sigma B_\alpha = 349.1°$). The dba fragment is strongly distorted by its concomitant interaction with the palladium and boron centers, and overall, complex **94** is best described by the zwitterionic Pd(II) η^3-boratoxypentadienyl structure **94a** rather than the corresponding Pd(0) alkene form **94b**. This bonding situation markedly contrasts with that encountered upon coordination of strong Lewis acids such as B(C$_6$F$_5$)$_3$ to [Pd(PPh$_3$)$_2$(η^2-PhHC=CHC(O)R)] and most probably results from the geometric constraints imposed by the rigid structure of the ambiphilic ligand.

The bridging coordination of M–X and M–L fragments by ambiphilic ligands, as described in this section, open interesting perspectives in catalysis. Complex **94** nicely illustrates the possibility to cooperatively activate functionalized π-systems by concomitant coordination to a metal center and a Lewis acid. In addition, and in line with what is typically encountered upon activation of metal complexes with Lewis
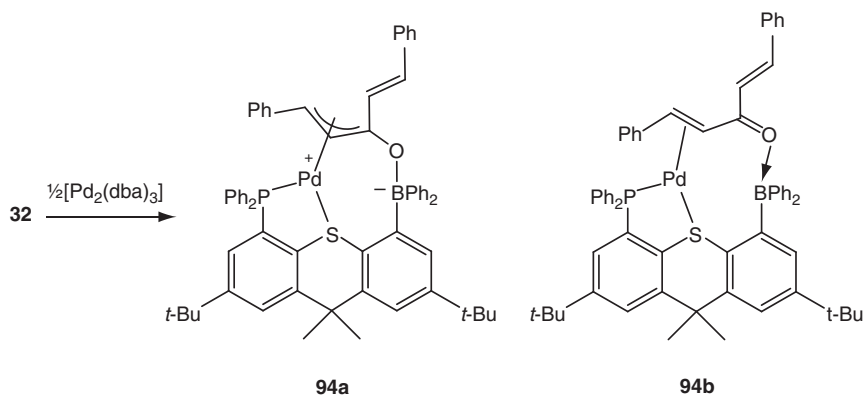
Scheme 54
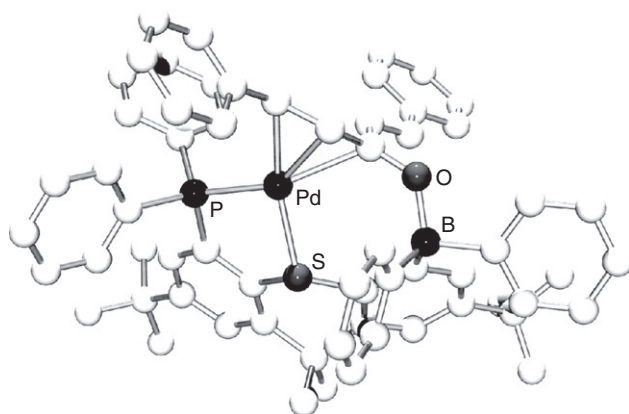
Figure 30   Molecular structure of **94**.

acids cocatalysts, the bridging coordination of M–X bonds represents a preliminary stage in their intramolecular activation, leading ultimately to zwitterionic complexes. This situation will be discussed in the following section (coordination mode **G**).

C. Zwitterionic complexes

Zwitterionic complexes combining a cationic metal center and an anionic ligand have attracted increasing interest over the past few years in catalysis. Representative examples concern the polymerization of olefins, as

well as their hydrogenation and functionalization. Zwitterionic complexes are usually prepared either by the derivatization of a coordinated ligand with a borane, or by coordination of a borate-containing ligand to a cationic metal fragment. The ability of ambiphilic ligands to activate M–X bonds (X = halogen or alkyl group) opens another route, and a few zwitterionic complexes have indeed been generated recently following this strategy.

This type of internal activation of a M–X bond was first proposed in 2004 by Fontaine and Zargarian upon combining the ambiphilic ligand (Me_2P-CH_2AlMe_2)$_2$ **2** and the nickel complex [Ni(1-MeInd)(PPh$_3$)Me].[77] In the presence of an excess of NEt$_3$, this system was found to catalyze the dehydrogenative oligomerization of PhSiH$_3$ with much higher activity and selectivity than [Ni(1-MeInd)(PPh$_3$)Me]/AlMe$_3$ (see Section V.C). This peculiar behavior was presumed to arise from the formation of the zwitterionic species **95**. The presence of the phosphine tether is likely to support the Me transfer from nickel to aluminum (Figure 31), but the addition of a Lewis base is required to split the dimeric structure of the ambiphilic ligand. So far, the key intermediates **95** could not be characterized, *in situ* spectroscopic monitoring being complicated by the concomitant presence of (Me_2P-CH_2AlMe_2)$_2$, [Ni(1-MeInd)(PPh$_3$)Me], and NEt$_3$.

The coordination properties of this phosphine-alane were further investigated by Fontaine *et al.* toward the rhodium(III) precursor [RhCp*Me$_2$(DMSO)] (Cp*=pentamethylcyclopentadienyl, DMSO = dimethylsulfoxide).[78] According to the spectroscopic data, the DMSO molecule is retained in the corresponding complex **96**, most probably by interaction of its oxygen atom with the pendant alane moiety (Scheme 55). Trimethylaluminium was added to **96** to trap DMSO and generate complex **97** related to **96**. But the competition between the external and
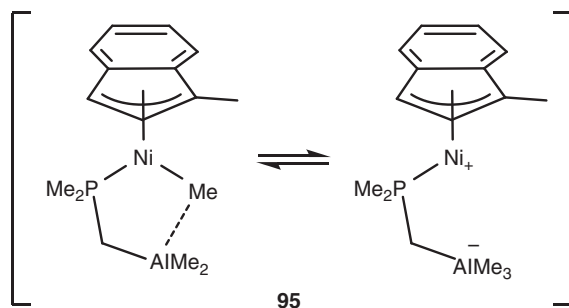
Figure 31 Postulated mechanism for the methyl transfer between Al and Ni.

pendant Lewis acid led to a dynamic system that again prevented the characterization of the putative zwitterionic complex **97**. However, fast exchange between the Me groups at aluminium and rhodium was unambiguously demonstrated by variable-temperature and spin-saturation transfer NMR experiments, in agreement with reversible, internal ionization of the Rh–Me bond by the alane moiety. Moreover, the successive addition of AlMe$_3$ and PMe$_3$ to **96** allowed for the spectroscopic characterization of the zwitterionic phosphine adduct **98**.
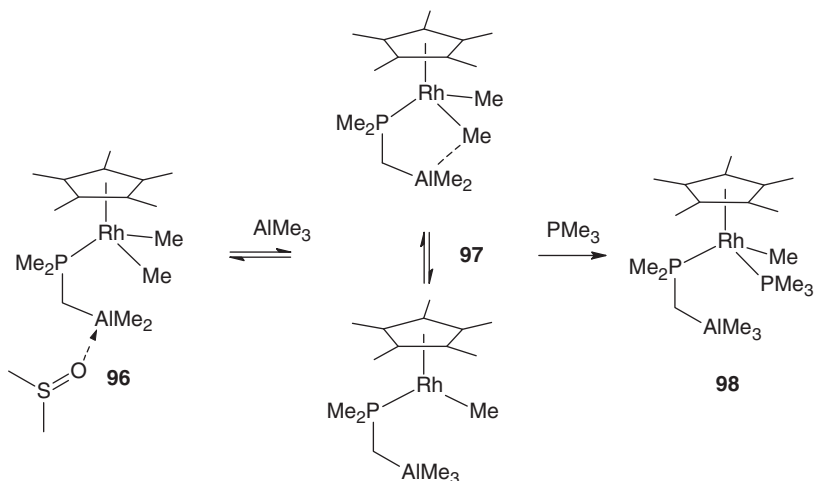
Scheme 55

The isolation and structural characterization of the zwitterionic complex **99** upon heating the reaction mixture of **96** and AlMe$_3$ to 90 °C provided another further support for the formation of **97** (Scheme 56). A plausible mechanism to account for the formation of **99** involves (i) the trapping of **97** by another molecule of Me$_2$PCH$_2$AlMe$_2$ and (ii) intramolecular transfer of the nucleophilic (Me$_2$PCH$_2$) fragment to the alane moiety with release of AlMe$_3$. A similar process had also been observed in the nickel series, and the zwitterionic complex [Ni(1-MeInd)(Me$_2$PCH$_2$AlMe$_2$CH$_2$PMe$_2$)] related to **99** was structurally authenticated as well.

Recently, direct evidence for the ionization of M–X bonds was reported upon coordination of PB and diphosphine-alane ligands. Tilley obtained the zwitterionic nickel complexes **100a** and **100b** by treating the CH$_2$CH$_2$-bridged ligands **40e** and **40f** with [NiMe$_2$(dmpe)] (dmpe = 1,2-bis(dimethylphosphino)ethane) (Scheme 57).[54] The phosphorus atom of
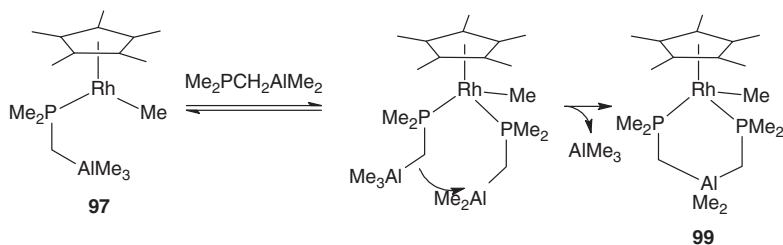
Scheme 56

the ambiphilic ligand coordinates to the metal center, while the borane moiety abstracts a methyl group at nickel, leading formally to the insertion of the P–B ligand into a Ni–Me bond of the precursor. The transfer of a methyl group from nickel to boron was clearly apparent from the multinuclear NMR data: the ^{11}B NMR resonance signals for **100a** and **100b** ($\delta \sim -15$ ppm) fall in the typical range for tetraalkylborates, and two distinct signals are observed for the methyl groups in the ^{1}H and ^{13}C NMR spectra. The solid-state structure of **100a** was confirmed by a single-crystal X-ray diffraction analysis (Figure 32). The nickel center retains its square-planar geometry, and the methyl group at boron does not exhibit any residual interaction with the nickel center. The addition of a second equivalent of the ambiphilic ligand did not result in abstraction of the second methyl group at nickel. However, using $B(C_6F_5)_3$ as a strong, external Lewis acid, the methyl group at boron was quantitatively transferred to afford the ion pair complex **101a**, according to ^{11}B NMR spectroscopy ($\delta = 82.1$ ppm for the pendant BCy$_2$ group and -14.4 ppm for the borate counteranion $[MeB(C_6F_5)_3]^-$).

In the mean time, we explored the coordination of the diphosphine-alane **10** toward AuCl and obtained thereby the zwitterionic complex **102**

100a BR$_2$=BCy$_2$
100b BR$_2$=9-BBN

9-BBN: 9-borabicyclo[3.3.1]-nonanyl

101a
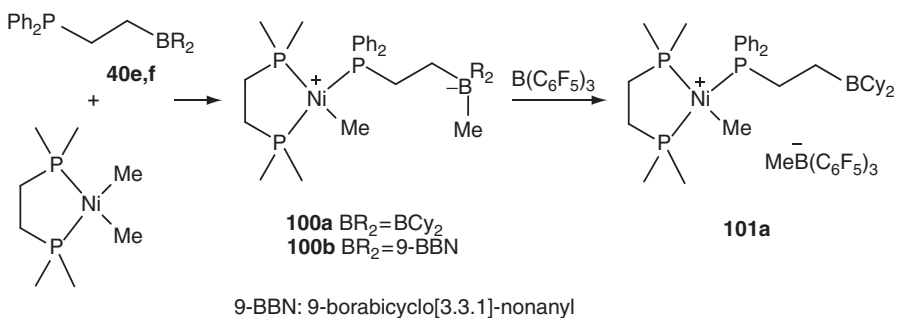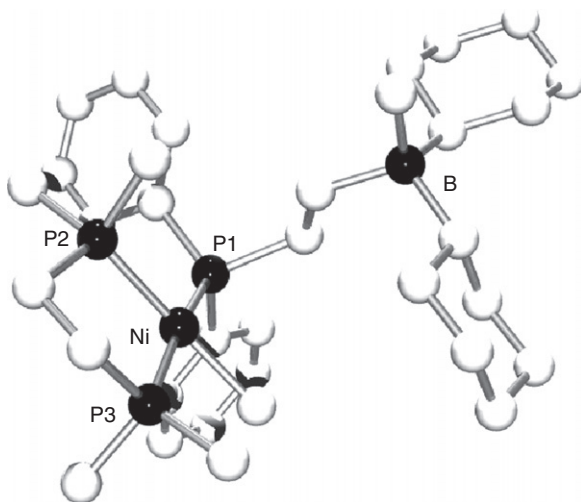
Scheme 57

Figure 32   Molecular structure of **100a**.

(Scheme 58).[26] This situation markedly contrasts with that previously observed with related DPB complexes that were found to adopt coordi-nation mode **H** with Au–B interaction (see Section IV.D). The complete transfer of the chlorine atom from gold to aluminium was established crystallographically. Indeed, the solid-state structure of complex **102** (Figure 33) showed a quasi-linear dicoordinate gold center, a tetrahedral environment around aluminium and long Cl···Au distances (>3.048 Å), ruling out any significant Al–Cl–Au bridging interaction. DFT calcula-tions were carried out on the real system. The zwitterionic form was found as the ground-state structure of complex **102**, the corresponding neutral form featuring Au–Al interaction lying about 8 kcal/mol higher in energy. According to NBO analyses, aluminium was predicted to form weaker Au–E interactions than boron. Combined with the higher affinity of the chloride anion for alanes vs. boranes, this most likely explains the preference of complex **102** for internal Au–Cl ionization vs. Au–Al interaction.

Recently, we investigated the related gold complexes deriving from the diphosphine-gallane **11** and triphosphine-gallane **12**.[27] The solid-state structure of complex **103** (Figure 34) very much resembles that of the corresponding diphosphine-alane complex **102**, but here, the zwitterionic and neutral forms **103$_{ZI}$** and **103$_N$** (Scheme 59) were shown spectroscopi-cally to coexist and interconvert in solution. Interestingly, the presence of a third phosphine buttress at gallium was found to inhibit the transfer of the
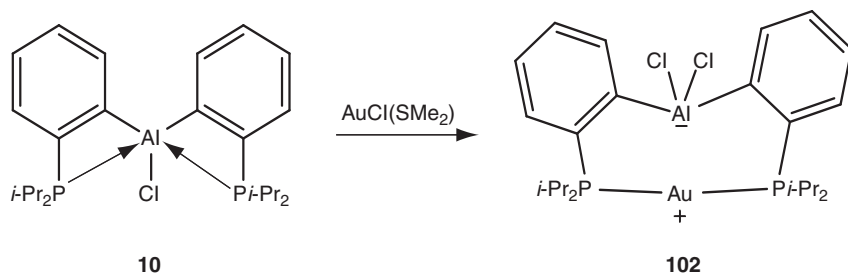
Scheme 58
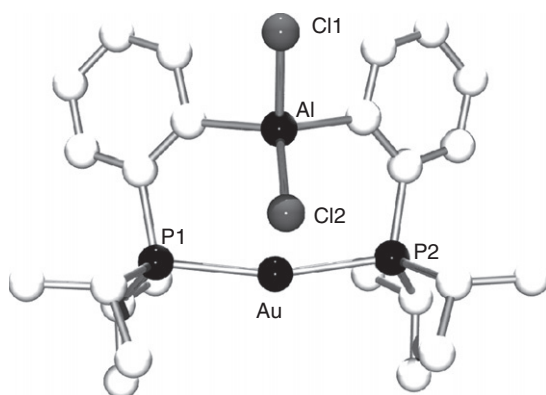
Figure 33   Molecular structure of **102**.
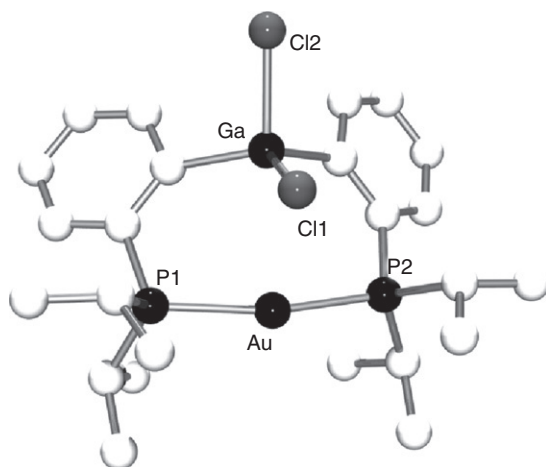
Figure 34   Molecular structure of **103$_{ZI}$**.

chloride between the metal and the Lewis acid centers, so that the two coordination isomers **104$_{ZI}$** and **104$_N$** deriving from **12** (Scheme 60) became separable and they were both structurally characterized (see Section IV.D).
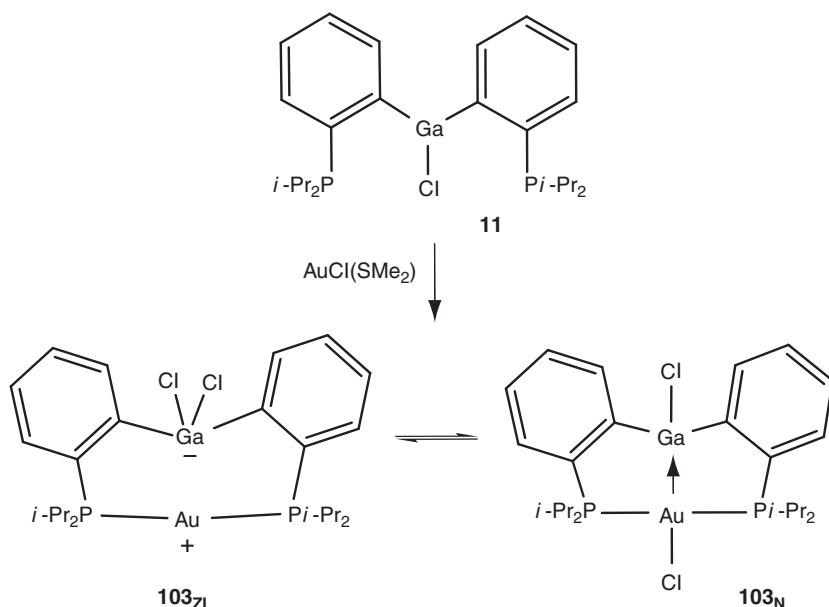

Scheme 59

D. Bridging coordination L−M−Z

The fourth conceivable coordination mode **H** involves direct metal–Lewis acid interactions supported by phosphine coordination. The ability of Lewis acids to act as σ-acceptor ligands was recognized early on, and referred to as Z-type ligands.[79,80] Here, the transition metal is forced to behave as a Lewis base and to engage into dative M–Lewis acid interaction (Figure 35).

σ-Acceptor, Z-type ligands remain considerably much less developed than their σ-donor, L- or X-type counterparts, but significant advances have been achieved in the last decade. In particular, transition metal complexes of boranes, long considered only as putative chemical curiosities,[81,82] have recently been authenticated unambiguously. The first solid-state structure was reported in 1999 by Hill for a cage complex of type **I** (with [M] = Ru(CO)(PPh$_3$)] (Figure 36).[83] Hydrido borates featuring three imidazolyl-2-thione moieties were then shown to be quite general precursors, and metal boratranes of type **I** were prepared with all group 8–10 metals.[84] Complex **II**,[84,85] deriving from a dihydrido-bis
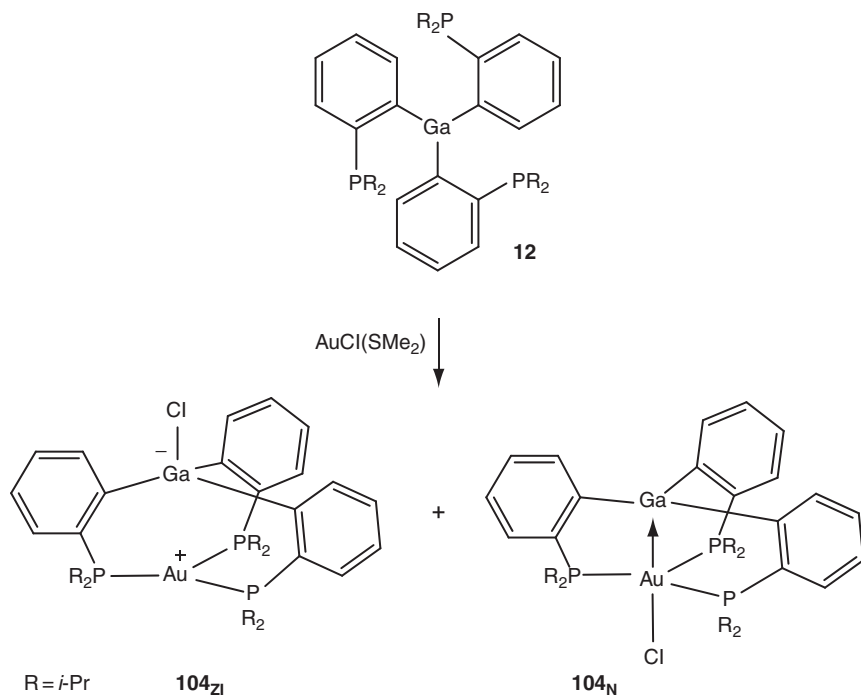
Scheme 60
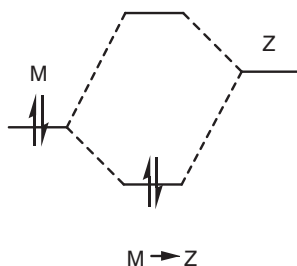
Figure 35 Schematic representation of the two-center, two-electron interaction between transition metals and Z-type ligands.

(imidazolyl)borate, illustrated that the M–B interaction may be supported by only two donor buttresses. Other heterocyclic units such as 1,2,4-triazolyl-thione,[86,87] 2-mercapto-pyridine,[88,89] and 7-aza-indole[90,91] have also been recently incorporated, leading to an increasing variety of complexes (**III–VII**) featuring M–B interactions. All of these complexes are obtained by activation of a B–H bond of a hydrido borate precursor. This process may occur spontaneously or upon chemical oxidation, and
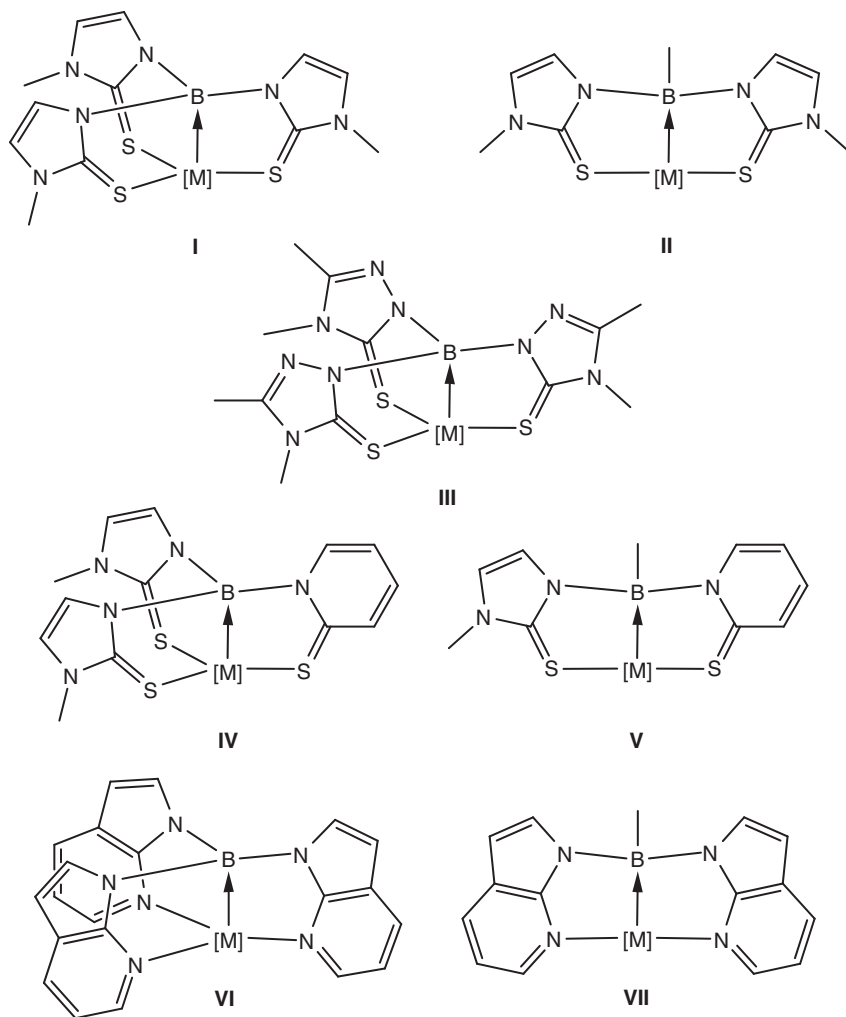
Figure 36 Schematic representation of the metal–borane complexes obtained from hydrido borates.

key intermediates related to the hydride transfer between the boron and metal centers have been eventually characterized spectroscopically and/or crystallographically.[84,86,91]

Over the past few years, the coordination of preformed ambiphilic ligands, especially PBs, has been shown to afford straightforward access to complexes featuring metal–Lewis acid interactions. As discussed hereafter, this approach has allowed the significant extension of the scope of M–Z interactions, and to gain better understanding of their bonding situation.

Attempts to support metal–borane interactions with phosphine buttresses were reported by Grobe as early as in the 1990s. Upon reaction of the ethen-diyl-bridged PB **22i** with [Rh$_2$(μ–Cl)$_2$(CO)$_4$], complex **105** was obtained by cleavage of the chloro bridges and displacement of one CO coligand at rhodium (Scheme 61).[92] Some decrease of the electron density at rhodium was suggested by the shift to higher frequency of the ν(CO) band (from 1955 cm^{-1} for the borane-free complex *trans*-[RhCl(CO){PMe$_2$(vinyl)$_2$}$_2$] to 1970 cm^{-1} in **105**). However, the X-ray diffraction analysis performed recently[42] revealed long RhB distances (2.94(3)–2.97(4) Å). These values are shorter than the sum of van der Waals radii (3.80 Å), but exceed the sum of covalent radii (2.26 Å) by about 30%, suggesting negligible, if any, Rh–B interaction. Consistently, the environment around boron is only marginally pyramidalized (ΣB$_\alpha$ = 356.3–357.6°).
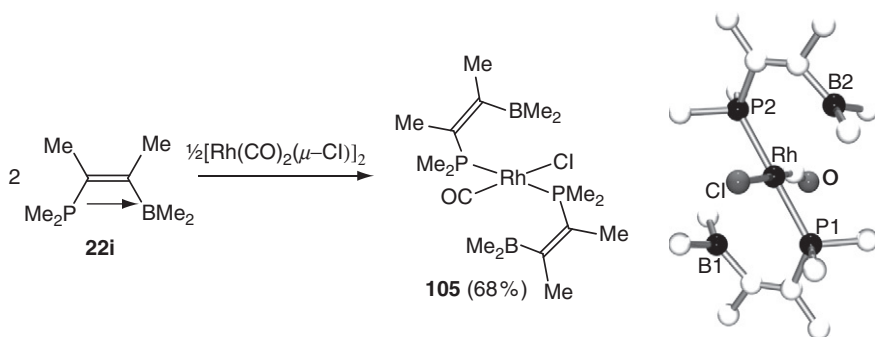
Scheme 61

Grobe has also investigated the reaction of the TPB **46** with [Pd(PPh$_3$)$_4$] with the aim of obtaining a metal boratrane related to the cage complexes of type **I**.[42] No such complex could be unambiguously authenticated spectroscopically, but DFT calculations carried out on compounds **106** and **107** (Figure 37) suggested the possible existence of relatively short Pd⋯B contacts, and thus substantial Pd–B interactions, especially in the absence of phosphine coligand in the position *trans* to the Lewis acid.

In the mid 2000s, we initiated a comprehensive study of the coordination properties of *ortho*-phenylene bridged PBs. The DPB **8a** was found to react with half an equivalent of [Rh$_2$(μ–Cl)$_2$(nbd)$_2$] in dichloromethane at room temperature (Scheme 62).[23] The yellow complex **108** that formed spontaneously was collected (92% yield) and analyzed spectroscopically. The ^{1}H, ^{13}C, and ^{31}P NMR data substantiated the displacement of the labile nbd ligands at rhodium by the phosphine moieties. In addition, the mass spectrum indicated a dimeric structure of general formula [Rh$_2$(μ–Cl)$_2$(DPB$_2$] and the ^{11}B NMR resonance signal observed at
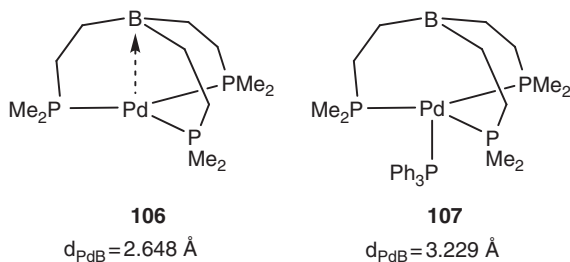
Figure 37 Optimized structures of the cage complexes deriving from the triphosphine-borane **46**.

43.1 ppm (shifted to high field by about 30 ppm compared to that of triarylboranes) suggested a tetracoordinate environment around boron. The molecular structure of **108** was definitively authenticated by X-ray diffraction analysis (Figure 38). Complex **108** adopts a centrosymmetric chloro-bridged structure, each rhodium center being surrounded by two phosphorus (*cis* arrangement, PRhP = 98.5°) and two chlorine atoms. The DPB ligand is folded so that the boron atom comes close to the rhodium center, almost perpendicular to the square coordination plane. The RhB distance (2.306(3) Å) only marginally exceeds the sum of covalent radii (2.26 Å) and the boron environment is strongly pyramidalized ($\Sigma B_\alpha = 338.8°$), clearly indicating the presence of a Rh–B interaction.
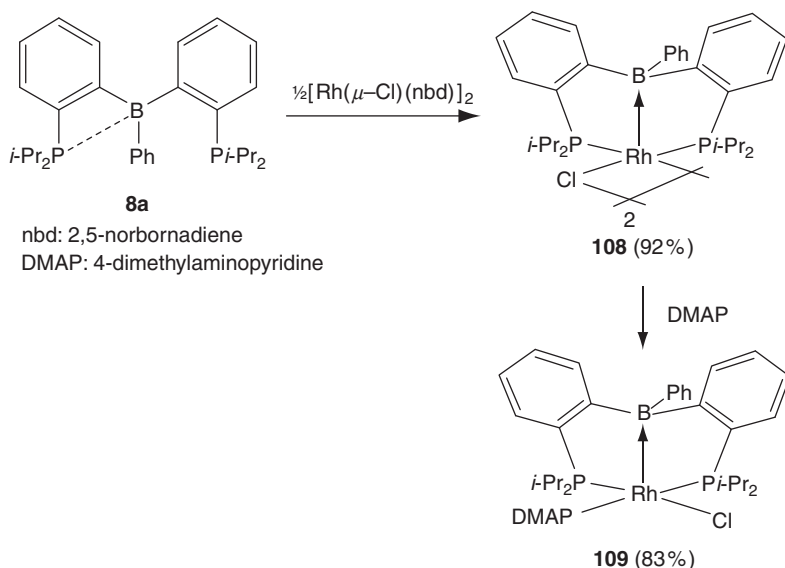
Scheme 62
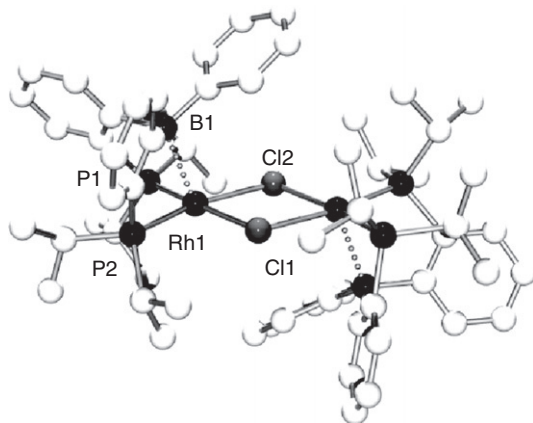
Figure 38   Molecular structure of **108**.

At this stage, the magnitude of the Rh–B interaction was qualitatively assessed by reacting **108** with an excess of DMAP. As deduced from spectroscopic and crystallographic data, the Lewis base split the chloro bridge but not the Rh–B interaction. The geometric features of the ensuing mononuclear complex **109** (RhB distance = 2.295(5) Å, $\Sigma B_\alpha = 340.3°$) are very similar to those of **108**. Further insight into the nature of the Rh–B interaction was gained by DFT calculations performed for the model mononuclear complex **109*** (the *i*-Pr groups at P were replaced by Me groups, and the Me groups at N were replaced by hydrogen atoms). The frontier molecular orbitals (Figure 39) are consistent with a two-center, two-electron bonding interaction between the occupied d_{z^2} orbital at rhodium and the vacant 2p orbital at boron. This description was further confirmed by a NBO analysis. A natural localized molecular orbital (NLMO) was found to account for the Rh–B bonding interaction, with a major contribution from the $d_{z^2}(Rh)$ orbital (80.4%) and delocalization
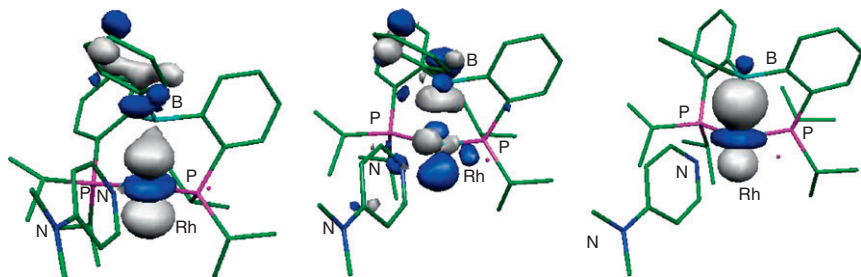
Figure 39   Molecular plots of the HOMO (left), LUMO (middle) and NLMO (right) associated with the Rh–B interaction in **109***.

tails from a slightly hybridized 2p(B) orbital (16.8%). The NBO delocalization energy associated with the Rh–B interaction amounts to 85.6 kcal/mol. The square-pyramidal complexes **108** and **109** provided the first evidence that M–B interactions are accessible by coordination of preformed ambiphilic ligands and exist even in the absence of σ-donor ligands in *trans* position.

In order to estimate the effect of the borane coordination on the electron density at Rh, the carbonyl complex **110** related to **108** and **109** was then prepared.[93] The cleavage of the chloro bridge of **108** with carbon monoxide and the reaction of the DPB **8a** with [Rh(μ–Cl)(CO)$_2$]$_2$ both afforded complex **110** in good yield as a 8:2 mixture of two diastereomers (Scheme 63). The molecular structure of **110** was unambiguously determined by multinuclear NMR spectroscopy and X-ray diffraction analysis. The two diastereomeric forms correspond to the two possible arrangements of the phenyl ring at boron, with respect to the CO and Cl coligands at rhodium (the major diastereomer is that with CO in position *syn* to the phenyl ring). As in **108** and **109**, the rhodium center is located in a square-pyramidal environment, but the two phosphines span *trans* sites (PRhP = 169°), demonstrating that the DPB ligand can accommodate both *cis* and *trans* coordination. The boron atom occupies the pseudo-axial position. Compared to complexes **108** and **109**, the RhB distance (2.374 (3) Å) is a little longer and the pyramidalization around boron (ΣB$_\alpha$= 342.6°) is somewhat less pronounced in **110a/b**. Along with the slight downfield shift of the ^{11}B NMR resonance signal (from 19–20 ppm in **108** and **109** to 26.7 ppm in **110a/b**), this indicates a slightly weaker Rh–B interaction in **110a/b**. This is consistent with the π-accepting character of the CO coligand that decreases the electron density at Rh. The electron-withdrawing effect of the borane moiety was then assessed by measuring the infrared carbonyl stretching frequency of **110a/b**. Compared to the borane-free complex *trans*-[RhCl(CO)(*i*-Pr$_2$PPh)$_2$], the ν(CO) band for **110a/b** (2001.8 cm^{-1}) is shifted by about 35 cm^{-1} to higher frequency, indicating that the Rh–B interaction withdraws a significant amount of electron density from rhodium.
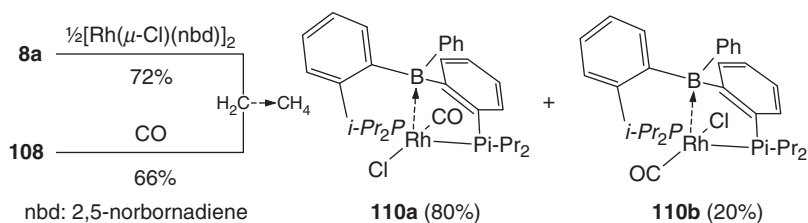
Scheme 63

With the aim of exploring the influence of the metal on the magnitude of the M–B interaction, valence isoelectronic [PtCl$_2$(DPB)] and [PdCl$_2$(DPB)] complexes were also prepared via the reactions of **8a** with the corresponding precursors [MCl$_2$(cod)] (Scheme 64).[93] The ^{31}P NMR data indicated in both cases *cis* coordination of the two phosphines, while the ^{11}B NMR resonance signals observed at 42.8 ppm (**111**) and 47.0 ppm (**112**) suggested weaker M–B interactions than those encountered in the related rhodium complexes. This trend was confirmed both crystallographically (Figure 40) and computationally (Table 1). The most prominent geometric features are the progressive increase of the M–B distance (from 2.30–2.37 Å in the Rh complexes **108**, **109**, and **110a/b** to 2.429(3) Å in the Pt complex **111** and 2.650(3) Å in the Pd complex **112**) and concomitantly, the progressive planarization of the boron environment (with ΣB_α increasing from ∼340° with Rh to 346.6° with Pt, and 354.9° with Pd). The progressive weakening of the M–B interaction from Rh to Pt, and Pd was further corroborated by DFT calculations. The NBO delocalization energies associated with the Pt–B and Pd–B interactions in **111** and **112** (49.6 and 13.6 kcal/mol, respectively) are significantly lower than that computed for **109***. The corresponding NLMO is more and more centered on the d$_{z^2}$(M) orbital (87.5% for Pt and 93.1% for Pd) with decreasing contribution of the 2p(B) orbital (10.3% for Pt and 5.5% for Pd). Thus, the M–B interaction is weakened with decreasing the intrinsic basicity of the metal [Rh(I) > Pt(II) > Pd(II)]. The magnitude of the ensuing geometric releases is unexpectedly large (given the presumed rigidity of the DPB ligand), indicating afterward that the strong Rh–B interactions observed in complexes **108** and **109** are supported, but not imposed, by the two phosphine buttresses.

cod: 1,5–cyclooctadiene
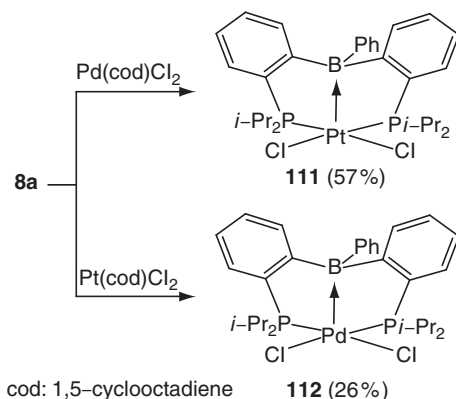
Scheme 64
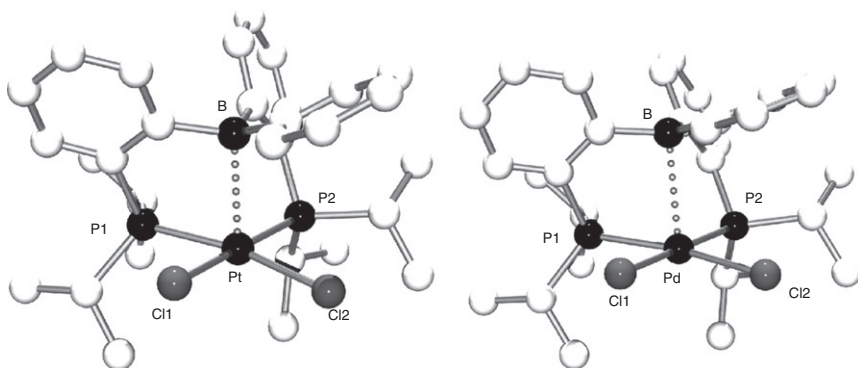
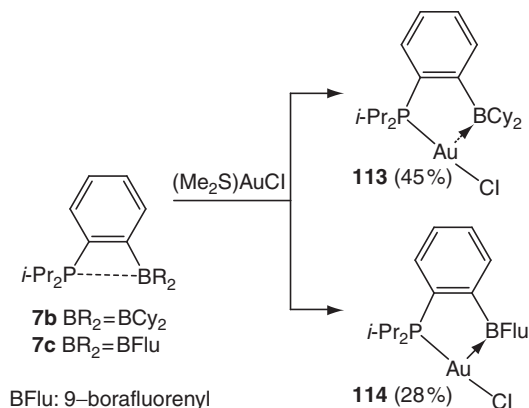**Figure 40**   Molecular structures of **111** (left) and **112** (right).

Table 1   Geometric data (bond lengths in Å and bond angles in °) determined experimentally and NBO data predicted computationally for complexes **110a∕b**, **111**, and **112**

	110a,b	111	112
M–B	2.374(3)	2.429(3)	2.650(3)
av M–P	2.330(1)	2.294(2)	2.302(2)
av PMB	85.5(2)	81.6(2)	79.0(2)
PMP	168.9(1)	99.4(1)	99.5(1)
ΣB_α	342.6	346.6	354.9
ΔE^a	46.4/46.8	49.6	13.6
% M^b	84.6/83.4	87.5	93.1
% B^b	10.8/11.3	10.3	5.5

[a]NBO stabilizing energy associated with the M–B interaction, in kcal/mol.
[b]Percentage of the donor and acceptor NBO in the corresponding NLMO.

At this stage, we wondered if such M–B interactions could be supported by a single phosphine buttress. In this perspective, we investigated the coordination of MPB **7b** and **7c** to the gold fragment AuCl. The linear geometry of (LAuCl) complexes was anticipated to prevent the bridging coordination of the M–Cl, as observed in related square-planar Pd and Rh complexes of MPB (see Section IV.B). Complexes **113** (R = Cy) and **114** (BR$_2$ = BFlu = 9-borafluorenyl) were readily obtained by displacement of the labile SMe$_2$ ligand from [AuCl(SMe$_2$)] (Scheme 65).[20]

Scheme 65
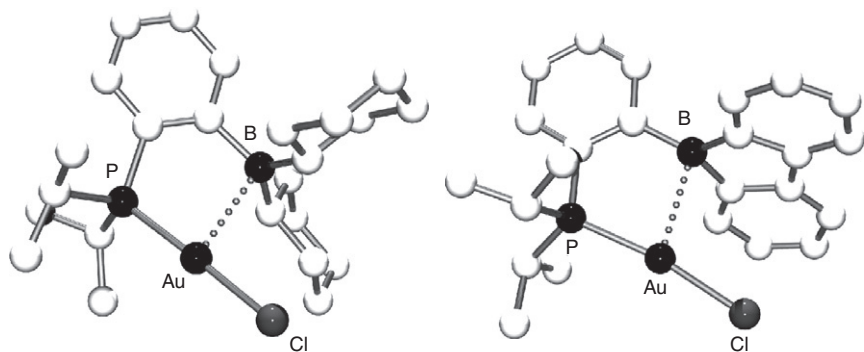
Figure 41 Molecular structures of **113** (left) and **114** (right).

Both complexes were characterized by X-ray diffraction analyses (Figure 41). The Au···B distance in **113** (2.903(6) Å) exceeds the sum of the covalent radii (2.20 Å) by about 20%, but remains significantly lower than the sum of the van der Waals radii (~3.7 Å). Replacement of the BCy$_2$ group by the more electrophilic and less sterically demanding 9-borafluorenyl moiety induces a significant shortening of the Au···B distance (2.663(8) Å in **114**), combined with a slight pyramidalization of the boron environment (ΣB$_\alpha$ decreases from 358.6° in **113**, to 355.8° in **114**). Along with the high-field shift of the ^{11}B NMR resonance signal (from 75 ppm for **113** to 55 ppm for **114**), this supports the presence of a Au–B interaction of increasing strength from **113** to **114**. DFT calculations further confirmed these conclusions. The NBO delocalization energies associated with the Au–B interactions increase from 4.6 kcal/mol for **113** to

12.8 kcal/mol for **114**. In addition, Natural Population Analyses (NPA) revealed some transfer of electron density from the metal to the σ-acceptor ligand. The charge at gold increases from 0.25 in the boron-free complex [AuCl(*i*-Pr$_2$PPh)] to 0.31 in **113**, and 0.41 in **114**. The T-shaped complexes **113** and **114** provided the first, and so-far unique, evidence for M–B interactions supported by a single donor buttress. This also substantiated that M–B interactions are not restricted to 16e and 18e complexes, but may also be observed in 14e complexes.

At this stage, the formation of M–B interactions upon coordination of MPB **7b** and **7c** to Au and DPB **8a** to Rh, Pt, and Pd did not allow direct comparison to estimate the influence of the second phosphine buttress. We thus investigated the coordination of DPB ligands to AuCl. Complex **115a** was obtained in high yield from the reaction of **8a** with [AuCl(SMe$_2$)] in dichloromethane at room temperature (Scheme 66).[25]

8a R = *i*–Pr
8b R = Ph

115a R = *i*–Pr (90%)
115b R = Ph (84%)
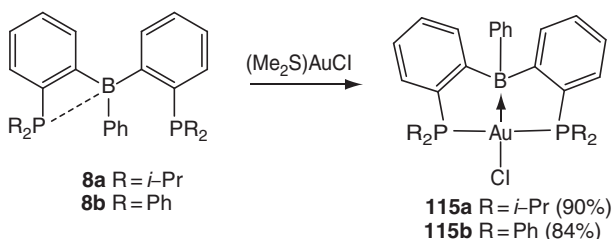
Scheme 66

X-ray diffraction analysis (Figure 42) revealed that (i) the gold center is tetracoordinate and adopts a square-planar geometry (ΣAu$_\alpha$ = 362.2°); (ii) the two phosphines span *trans* sites (PAuP = 160.2°); (iii) the Au–B distance (2.309(8) Å) is short; and (iv) the boron environment is strongly pyramidalized (ΣB$_\alpha$ = 341.2°). These data are indicative of a strong Au–B interaction in **115a**, in agreement with the low-frequency signal observed by ^{11}B NMR spectroscopy (δ = 24.6 ppm). Compared with the situation encountered in the related MPB complexes **113** and **114**, it is clear that the introduction of a second phosphine buttress significantly enforces the Au–B interaction. Then, the influence of the phosphorus substituents was probed by replacing the P*i*-Pr$_2$ groups for less electron-donating PPh$_2$ moieties. The corresponding complex **115b** was prepared following a similar procedure, and its molecular structure was authenticated crystallographically. The overall geometry of **115b** is very similar to that of **115a**, and the Au–B interaction is only marginally weakened [the Au–B distance (2.335(5) Å) is slightly elongated and the pyramidalization of the boron environment (ΣB$_\alpha$ = 343.8°) decreases slightly].

The square-planar geometry observed for both complexes **115a** and **115b** is intriguing and raises the question as to the very nature of dative
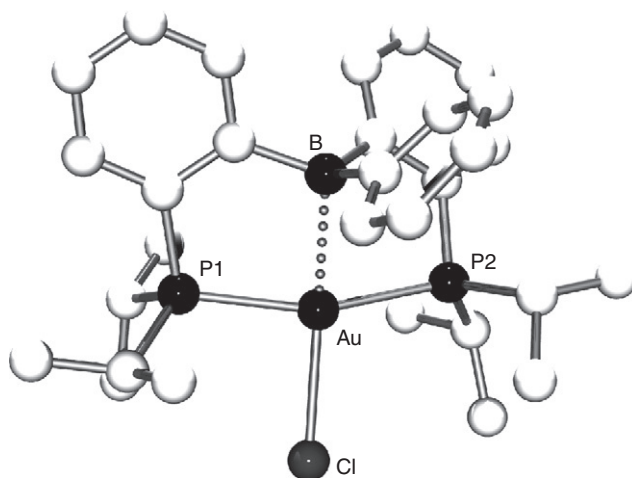
Figure 42   Molecular structure of **115a**.

M–Lewis acid interactions. In 2006, Hill[94] and Parkin[95] pointed out two different descriptions of the bonding situation in M–BR_3 complexes (Figure 43). These two formalisms are associated with two limiting fragment deconstructions that differ in the extent of electron-density transfer from M to B: (a) a coordinated neutral BR_3 ligand and retention of the original d^n configuration of the metal center, and (b) two-electron oxidation of the metal center resulting formally in a d^{n-2} configuration and a dianionic BR_3^{2-} ligand. As far as tetracoordinate gold complexes are concerned, the square-planar geometry is normally diagnostic for a d^8 gold(III) configuration, all known d^{10} gold(I) complexes adopting tetrahedral arrangements. At this stage, geometric considerations could thus be considered as supporting formalism b (see Figure 43) to depict the bonding situation in complexes **115**.

To further address this question, DFT calculations were carried out on the actual complexes **115a** and **115b**. Here also, second-order perturbative NBO analyses provided evidence for dative Au–B interactions. The corresponding NBO delocalization energies ($\sim$55 kcal/mol) are significantly higher than those found for the related MPB complexes **113** and **114**, which further corroborated the strengthening of the Au–B interactions

$$M : + \square BR_3 \quad a \qquad\qquad b \quad M^{2+}\square + : BR_3^{2-}$$
$$\Longleftarrow \boxed{\quad} M \longrightarrow BR_3 \boxed{\quad}\Longrightarrow$$
$$d^n \quad \text{Neutral} \qquad\qquad\qquad d^{n-2} \quad \text{Dianion}$$
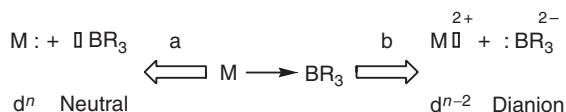
Figure 43   Schematic representation of the two limiting bonding situations suggested for dative M–BR_3 interactions.

upon introducing a second phosphine buttress. In addition, the gold to boron charge transfer could be estimated to roughly 0.4e by comparing the NBO charges for **115a** and **115b** with those of the free ligands **8a** and **8b** and borane-free complex [AuCl(PMe$_3$)$_2$]. Consistently, the computed electron configuration of the gold center in complexes **115a** and **115b** only marginally deviates from 5d^{10}, suggesting that **115a** and **115b** would be more appropriately described as gold(I) complexes. The unprecedented combination of square-planar geometry and d^{10} gold(I) configuration was definitely confirmed by ^{197}Au Mössbauer spectroscopy. The isomer shifts (IS ~ 3.35 mm s^{-1}) and quadrupole splittings (QS ~ 7.6 mm s^{-1}) for **115a** and **115b** are very similar to those reported for [AuCl(PCy$_3$)][96] (IS = 3.21 mm s^{-1} and QS = 7.59 mm s^{-1}) and clearly position complexes **115a** and **115b** among gold(I) and not gold(III) complexes (Figure 44). Overall, these results substantiate that the coordination of σ-acceptor ligands to transition metals (i) does not necessarily induce formal 2e oxidation, and (ii) may lead to geometries unknown for complexes featuring only σ-donor ligands.

The substantial strengthening of the Au–B interaction from MPB to DPB prompted us to investigate then the coordination of the related TPB ligand **9**.[97] The ensuing AuCl complex **116** was isolated in 92% yield as colorless crystals (Scheme 67). The X-ray diffraction analysis revealed a metal boratrane structure (Figure 45). The gold center is pentacoordinate and adopts trigonal-bipyramidal geometry. The three phosphorus atoms occupy the basal positions while the boron and chlorine atoms occupy the
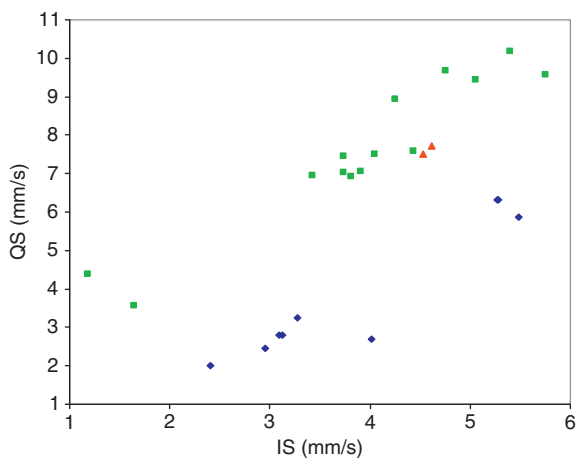
Figure 44   IS/QS relationship (IS = isomer shift and QS = quadrupole splitting) for complexes **115a** and **115b** (red triangles), representative phosphine Au(I) complexes (green squares) and Au(III) (blue rhombuses) complexes. (For interpretation of the references to color in this figure legend, the reader is referred to the Web version of this chapter.)

apical positions. The geometric features associated with the Au–B inter-action (AuB = 2.318(8) Å, ΣB_α = 339.3°) are similar to those of the related DPB complex **115a**, indicating only negligible influence of the third phosphine buttress. Complex **116** is the first pentacoordinate gold(I) complex without aurophilic interactions, which illustrates the ability of σ-acceptor ligands to form hypercoordinate complexes. Another salient feature of complex **116** is its C_3 symmetry, the three PCCBAu metallacycles adopting envelop conformations oriented in the same direction. This three-blade propeller geometry markedly contrasts with the C_{3v} symmetry typically observed in metal boratranes featuring tris(methimazolyl) borane ligands,[85c,g,h,m] and most likely results from steric congestion between the *i*-Pr groups of neighboring phosphine buttresses. Notably, the *exo/endo* environments for the CH(*i*-Pr) groups were distinguished by ^{1}H and ^{13}C NMR spectroscopy, and variable-temperature experiments allowed to estimate the inversion barrier of the three-blade propeller to 14.7 ± 0.5 kcal/mol.
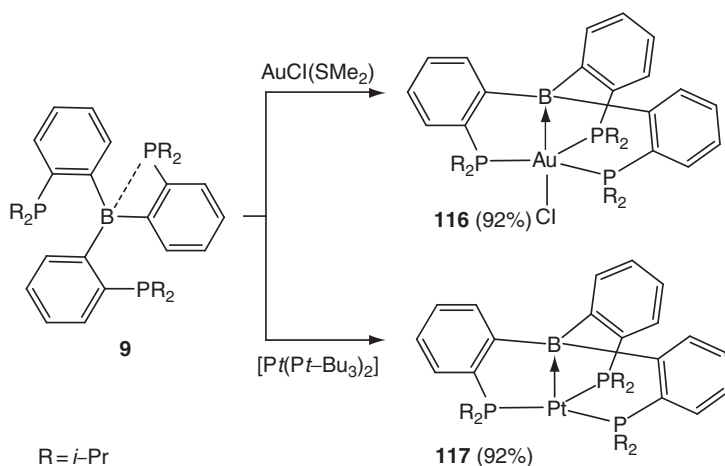
Scheme 67

To confirm the tendency of **9** to form C_3 symmetric metal boratranes, we prepared the platinum complex [Pt(TPB)] **117** by ligand displacement from [Pt(P*t*-Bu$_3$)$_2$]. Complex **117** adopts in the solid state a trigonal-pyramidal three-blade propeller geometry. The PtB distance (2.224(4) Å) is significantly shorter than the Au–B distance in **116** despite the slightly larger size of platinum compared to gold. Combined with the low-field shift of the ^{11}B NMR resonance signal (from δ = 27.7 ppm for **116** to 18.2 ppm for **117**), this indicates a slight strengthening of the M–B interaction from Pt to Au, in agreement with the higher basicity of Pt(0) vs. Au(I).
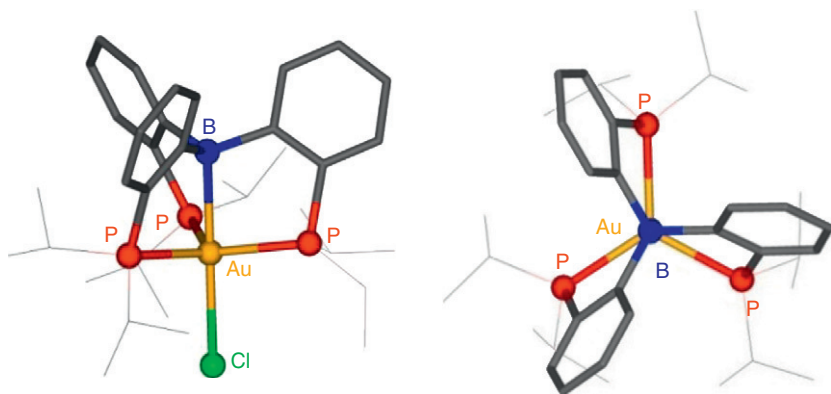
Figure 45 Side (left) and top (right) views of the molecular structure of **116**.

Remarkably, Pt(0) phosphine complexes are typically colorless or pale yellow, whereas complex **117** was isolated as deep red crystals ($\lambda_{max} = 541$ nm in toluene). These unusual optical properties were rationalized computationally. Indeed, TD-DFT calculations predicted two absorptions associated with allowed, quasi-degenerate transitions from the d(Pt)-centered HOMO and HOMO-1 orbitals to the 2p(B)-centered LUMO orbital (Figure 46). The LUMO orbital is readily accessible in energy, which explains why these transitions fall in the visible region ($\lambda \sim 520$ nm), whereas the highest wavelength of maximum absorption predicted for the related boron-free complex [Pt(i-Pr$_2$PPh)$_3$] was found at $\lambda \sim 350$ nm.

Here, we decided to prepare a complete series of homologous complexes in order to gain more insight into the very influence of the metal on the magnitude of M–B interactions.[98] The straightforward coordination of the TPB ligand gave us a unique opportunity to prepare isoelectronic complexes with both group 10 and 11 metals. The dark blue nickel complex **118** and deep red palladium complex **119** were obtained in ~80% yields by reacting TPB with [Ni(cod)$_2$] and [Pd(Pt-Bu$_3$)$_2$],
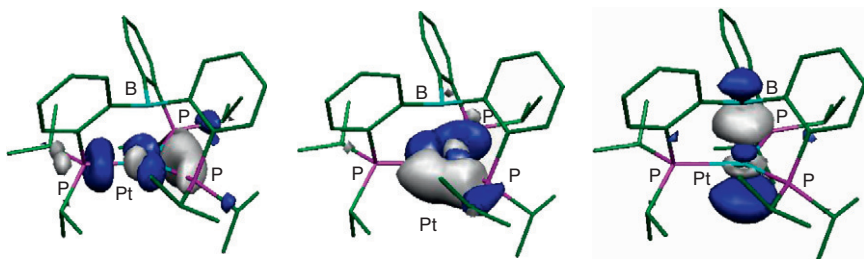
Figure 46 Molecular plots of the HOMO–1 (left), HOMO (middle), and LUMO (right) accounting for the lowest energy transitions of **117**.

respectively. The related copper and silver complexes **120** and **121** were readily prepared by adding TPB to dichloromethane suspensions of the corresponding metal(I) chlorides. The cationic gold boratrane **122** was also synthesized by chloride abstraction from the neutral complex **116** with GaCl$_3$. All complexes **118–122** were fully characterized by multinuclear NMR and UV spectroscopy, mass spectrometry, and X-ray diffraction analyses. They adopt trigonal pyramidal or bipyramidal (when a chlorine is bound to the metal) geometry organized around a central M–B interaction. Complexes **120** and **121** (Figure 47) provided the first examples of borane coordination to copper and silver.

In order to estimate and compare the magnitude of the M–B interactions in these isoelectronic complexes, a whole set of structural and spectroscopic parameters determined experimentally and/or computed theoretically were considered. This includes the M$\cdots$B distance d_{MB}, the ratio r between the M$\cdots$B distance and the sum of covalent radii (to take into account the different sizes of the metals involved), the pyramidalization of the boron environment ΣB_α, the ^{11}B NMR chemical shift δ ^{11}B, the difference Δq_B between the charge at boron in the metal boratrane and the free ligand TPB, the difference Δq_M between the charge at the metal in the metal boratrane and that in the related borane-free complex [M(i-Pr$_2$PPh)$_3$], and the NBO delocalization energy ΔE_{NBO} associated with the main donor–acceptor M–B interaction found at the second order in the NBO analysis (Table 2). Only the conclusions of this detailed analysis will be recalled here:

−All group 10 complexes feature a rather strong M–B interaction. Small, nonregular variations are observed in this triad, with Pd and Pt forming the weakest and strongest interactions, respectively.
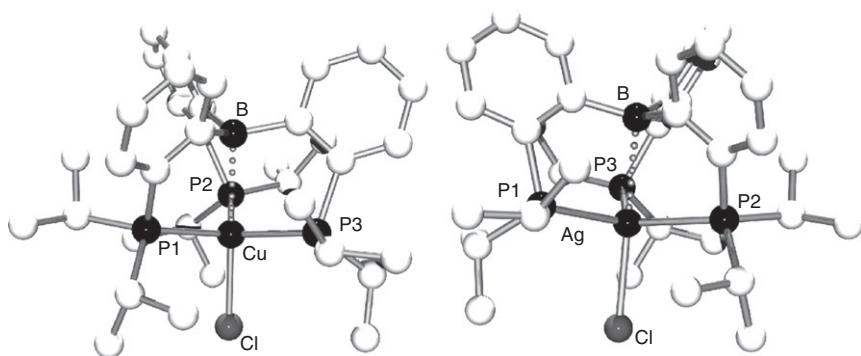
Figure 47   Molecular structures of **120** (left) and **121** (right).

Table 2 Selected data determined experimentally or predicted computationally for metal boratranes **116–122**

	(TPB)CuCl **120**	(TPB)AgCl **121**	(TPB)AuCl **116**	(TPB)Au$^+$ **122**	(TPB)Ni **118**	(TPB)Pd **119**	(TPB)Pt **117**
M–B[a]	2.508	2.540	2.318	2.448	2.168	2.254	2.220
av M–P[a]	2.358	2.499	2.424	2.390	2.199	2.349	2.296
ΣB_α[a]	347.0	347.4	339.3	351.3	339.1	341.8	336.7
$\delta\ ^{11}B$[b]	53.8	59.1	27.7	56.6	15.9	28.3	18.2
Δq_B[c]	−0.24	−0.30	−0.51	−0.20	−0.40	−0.34	−0.39
Δq_M[d]	+0.07	+0.11	+0.24	+0.14	+0.27	+0.23	+0.30
ΔE[e]	7.9	14.3	46.9	26.5	61.2	64.6	145.1

[a] Bond lengths in Å and bond angles in °.
[b] ^{11}B NMR chemical shifts (in ppm, relative to $BF_3 \cdot OEt_2$).
[c] NBO atomic charge $\Delta q_B = q_B$ (complex)$-q_B$ (free TPB ligand, open form).
[d] NBO atomic charge $\Delta q_M = q_M$ (TPB complex)$-q_M$ (borane-free complex).
[e] NBO stabilizing energy associated with the M–B interaction, in kcal/mol.

−Within neutral group 11 metal boratranes, the magnitude of the M–B interaction varies more significantly and increases progressively when going down the group to culminate with gold. This is consistent with the fact that the Lewis basicity of transition metals increases on going down a group.

−Among d^{10} complexes, group 10 metals form stronger M–B interactions than group 11 metals.

−The Au–B interaction persists upon cationization, but it is significantly weakened.

−The strongest M–B interactions are observed for the Pt and Au complexes for which the 5d orbitals are significantly destabilized by relativistic effects. As a result, the energy separation between the occupied $d_{z^2}(M)$ and vacant $2p(B)$ orbitals, and thus the magnitude of the M–B interaction, increases.

Note also that all of the metal boratranes **118–122** adopt C_3 symmetry both in the solid state and in solution. The degree of helicity (as quantified by the average P–M–B–C torsion angle $\theta \sim 27\pm3°$) and configurational stability (as estimated from the inversion barrier of the three-blade propeller $\Delta G^{\neq} \sim 16\pm2$ kcal/mol) are only moderately affected by the nature and magnitude of the central M–B interaction.

As mentioned in Section IV.C, the replacement of boron by its heavier congeners aluminium and gallium markedly affects the coordination behavior of the DPE ligands (E = group 13 element) toward AuCl. In particular, the zwitterionic and neutral forms of the diphosphine–gallane complex **103** were shown to coexist and interconvert in solution.[27]

Only **103$_{ZI}$** could be characterized crystallographically, but DFT calculations provided valuable insight into the Au–Ga interaction present in **103$_N$** (Figure 48). The relevant geometric features of the optimized structure (d_{AuGa} = 2.53 Å, $r = d_{AuGa}/\Sigma R_{cov}$ = 0.98 and ΣGa_α = 345°) are diagnostic of a rather strong interaction. The NBO analysis corroborated the presence of a dative Au–Ga interaction. The corresponding delocalization energy (33 kcal/mol) is intermediate between those predicted for the related borane and alane complexes. The presence of a third phosphine buttress at gallium prevents the interconversion between the zwitterionic and neutral forms, so that the coordination isomers **104$_{ZI}$** and **104$_N$** could be isolated and X-ray diffraction analyses were carried out on both compounds (Figure 49). As a result of the chloride transfer from Au to Ga, the gold center is pentacoordinate in **104$_N$** but tricoordinate in **104$_{ZI}$**. Accordingly, the overall geometry changes from trigonal bipyramidal in **104$_{ZI}$** to trigonal planar in **104$_N$**. The short Au–Ga distance (2.578(2) Å) and *inward* pyramidalization of the gallium environment (ΣGa_α = 347°) unambiguously indicate the presence of a significant Au–Ga interaction. Here also, no cumulative effect of the third phosphine buttress was found on the magnitude of the Au–Ga interaction. Very similar geometric features and NBO delocalization energies were predicted computationally for the complexes **103$_N$** and **104$_N$** deriving from di- and triphosphine-gallanes. Complex **104$_N$** provided the first evidence for a M–Ga interaction with a group 11 metal. Conversely, the Au···Ga distance is significantly longer in the zwitterionic form **104$_{ZI}$** (2.969(2) Å) and the pseudo-tetrahedral environment around the gallium center points toward chlorine rather than gold (slight *outward* pyramidalization, ΣGa_α = 356°).
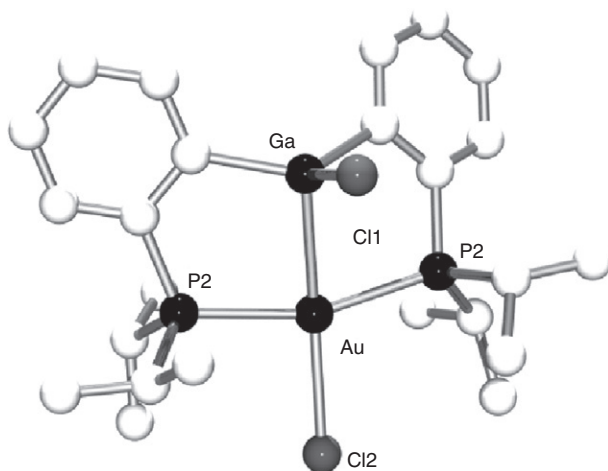
Figure 48   Optimized structure of **103$_N$**.
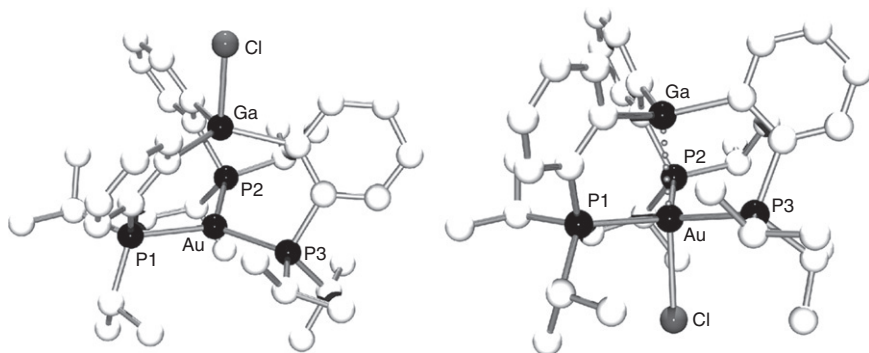
Figure 49 Molecular structures of **104$_{ZI}$** (left) and **104$_N$** (right).

Remarkably, the two complexes **104$_{ZI}$** and **104$_N$** display C_3 symmetry in the solid state, albeit with rather different degrees of helicity θ (19° for **104$_N$** vs. 27° for **104$_{ZI}$**). This further substantiates the propensity of the TPE ligands (E = group 13 element) to form three-blade propeller complexes even in the absence of a central M–E interaction.

The coordination of preformed ambiphilic ligands featuring group 13 Lewis acids has allowed significant extension of the scope of M–Z interactions, and a better understanding of their very nature as well as of the factors influencing their magnitude. The concept of σ-acceptor ligands appear much more general than initially believed, and current efforts seek to determine to which extent the Lewis acidity can be decreased while retaining the ability to form M–Z interactions. Taking into account that saturated heavier group 14 elements readily form hypervalent adducts through donor–acceptor interactions with organic Lewis bases, we recently became interested in the coordination of silane and stannanes as σ-acceptor ligands. Such a bonding situation has been previously invoked by Grobe upon coordination of the triphosphine-silane ligands **123–124** to nickel and palladium fragments, but the X-ray diffraction analyses revealed very long Ni···Si and Pd···Si distances (Ni–Si = 3.92–3.95 Å and Pd–Si = 3.87 Å) and tetrahedral geometries around silicon [Σ(CSiC) $\approx$ 348° and Σ(OSiO) $\approx$ 332°], suggesting little, if any, Ni–Si and Pd–Si interactions (Scheme 68).[99–101]

In addition, Wagler recently reported three cage complexes **129–131**, in which Pd–Si, Pt–Si, and Pd–Sn interactions are supported by four methimazolyl groups (Scheme 69).[102,103] Crystallographic analyses (Figure 50) revealed for all three complexes octahedral arrangements around both the metal and the group 14 element, resulting in lantern-like structures, and short PdSi (2.527(2)–2.569(1) Å), PtSi (2.447(3)–2.469(2) Å), and PdSn distances (2.605(1) Å).

To further assess the existence of M–Z interactions with heavier group 14 elements, we targeted the silane and stannane gold complexes
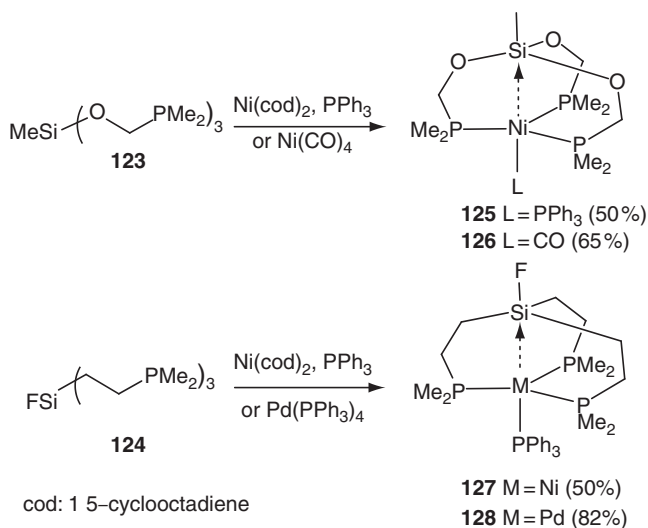
Scheme 68
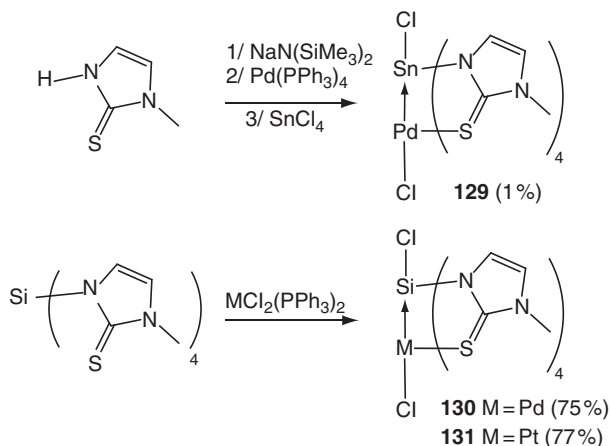
Scheme 69

analogous to **115a** and **115b**.[104] A chlorine or fluorine atom was intro-
duced at the heavier group 14 element in order to increase its Lewis
acidity (by lowering the energy of the corresponding σ* orbital). The
diphosphine-silane and -stannane ligands were readily prepared by
reacting the o-lithiated di(isopropyl)phenylphosphine with PhECl₃ (E =
Si or Sn) and chlorine to fluorine exchange was achieved with either
HF·collidine (collidine = 2,4,6-trimethylpyridine) (Si) or KF (Sn)
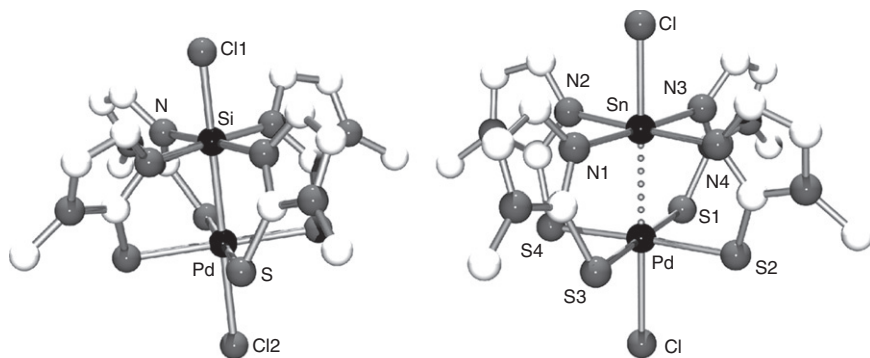
Figure 50   Molecular structures of **130** and **131**.

(Scheme 70). Upon reaction with [AuCl(SMe$_2$)], the desired complexes **134**, **135a**, and **135b** were obtained in high yields. Their most salient characteristics are listed in Table 3.

132 E = Si, X = F(DPSiF)
133a E = Sn, X = F (DPSnF)
133b E = Sn, X = Cl (DPSnCl)

134 E = Si, X = F (88%)
135a E = Sn, X = F (50%)
135b E = Sn, X = Cl (87%)
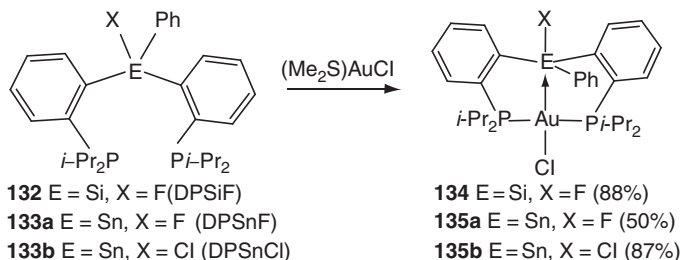
Scheme 70

The ^{29}Si and ^{119}Sn NMR resonance signals fall in the typical range for pentacoordinate species. The presence of Au–Si and Au–Sn interactions was further confirmed by X-ray diffraction analyses (Figure 51). The silicon and tin atoms come close to the gold center and their geometry changes from tetrahedral to slightly distorted trigonal-bipyramidal. The gold center occupies an axial position opposite to the halogen atom, inducing a slight elongation of the E–X bonds, and the geometry around gold is intermediate between tetrahedral and square-planar. All the geometric features indicate that tin binds more strongly than silicon to gold, something that parallels what is observed toward organic Lewis bases. No significant difference was observed between the fluoro- and chloro-stannane complexes **135a** and **135b**.

DFT calculations further confirmed the presence of Au–Si and Au–Sn interactions. NBO analyses identified donor–acceptor interactions from

Table 3 Geometric data (bond lengths in Å and bond angles in °) determined experimentally; NBO and AIM data predicted computationally for complexes **134** and **135a,b**

	(DPSiF).AuCl **134**	(DPSnF).AuCl **135a**	(DPSnCl).AuCl **135b**
Au–E[a]	3.090(2)	2.891(2)	2.873(3)
r[b]	1.25	1.05	1.04
E–X[a]	1.635(3)	2.018(3)	2.496(8)
Σ(C–E–C)[a]	353.51	359.90	359.57
P–Au–P	140.14(5)	159.91(6)	159.16(3)
XEAu[a]	166.11(2)	176.27(9)	173.73(2)
EAuCl[a]	141.54(4)	151.36(4)	161.43(2)
ΔE[c]	7.6	22.8	26.6
$\rho(r)$[d]	$2.13 \ 10^{-2}$	$3.50 \ 10^{-2}$	$3.56 \ 10^{-2}$

[a]E = Si or Sn and X = F or Cl;
[b]$r = d(M-B)/\Sigma(R_{cov})$.
[c]NBO stabilizing energy associated with the Au–E interaction, in kcal/mol.
[d]$\rho(r)_{AIM}$: electron density at the Bond Critical Point, in ebohr^{-3}.
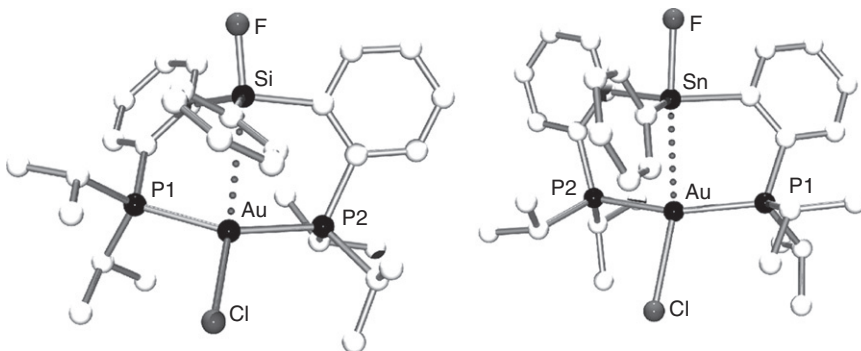
Figure 51 Molecular structures of **134** (left) and **135a** (right).

gold to the heavier group 14 element. The associated delocalization energies are about three times greater for tin than for silicon, but all remain significantly lower than those predicted for the related borane complex **115a** and **115b**. Atom in molecules (AIM) calculations were also carried out and bond critical points were localized between the gold center and the heavier group 14 element. The charge depletion at these BCP is consistent with the closed-shell, donor–acceptor nature of the Au–Si and Au–Sn interactions, and the values found for the electron density $\rho(r)$ at the BCP again indicate stronger interaction between tin and gold than between silicon and gold.

The silane and stannane complexes **134, 135a**, and **135b** provide unambiguous evidence that heavier group 14 centers may behave as σ-acceptor ligands. This extends the scope of Z-type ligands beyond group 13 Lewis acids, and provides evidence for a coordination mode of saturated moieties alternative to the side-one coordination of σ-bonds. In addition, complexes **134**, **135a**, and **135b** stand as (i) novel hypervalent derivatives of heavier group 14 elements featuring a transition metal as a substituent and (ii) stable analogs of the transition state postulated for the S_N2-type oxidative addition of $C_{sp}3$–X bonds to transition metals.[105]

E. η^3-BCC and η^2-BC coordinations

In addition to η^1-coordination of boranes as acceptor ligands, phosphine buttresses were shown to eventually support multicenter η^3-BCC and η^2-BC interactions involving a π-system at boron (phenyl ring or alkynyl moiety). η^3-BCC coordination was first evidenced by Emslie in the heterodinuclear complex **136** deriving from the tridentate ligand **32**: Phosphine-Sulfide-Borane (PSB) (Scheme 71).[76] The reaction of the chloro-bridged rhodium complex **91** with K[CpFe(CO)$_2$] was explored in order to probe if the removal of the chlorine at rhodium leads to some Rh–B interaction. The retention of a tetracoordinate environment around boron was apparent from ^{11}B NMR spectroscopy ($\delta = 11.5$ ppm for **91** and 2 ppm for **136**). In addition, some ^{1}H NMR signals associated with the phenyl rings at boron were found at unusually high fields, suggesting some π-coordination.
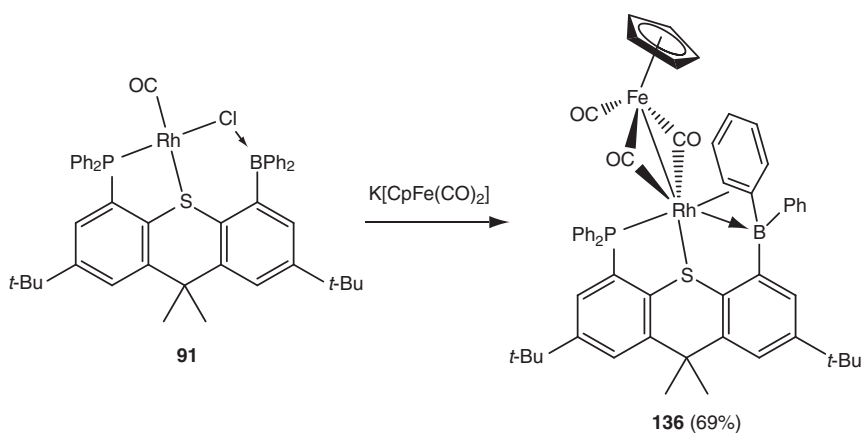
Scheme 71
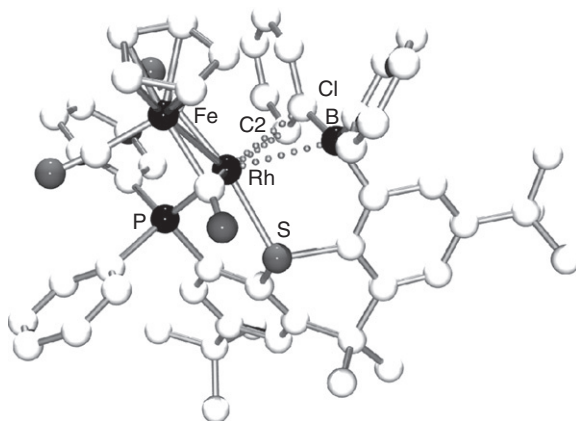
Figure 52   Molecular structure of **136**.

The solid-state structure of **136** (Figure 52) revealed the presence of a direct Rh–Fe bond with two bridging carbonyl ligands. In addition to phosphorus and sulfur, the PSB ligand is coordinated to rhodium by a $BC_{ipso}C_{ortho}$ fragment involving one of the phenyl rings. The boron, C_{ipso} and C_{ortho} atoms all remain in trigonal planar environments. The RhB distance (2.63(2) Å) is significantly longer than that observed in the DPB rhodium complexes **108–110** (2.29-2.37 Å),[23,94] but still appreciably shorter than the sum of van der Waals radii (3.80 Å). DFT calculations were carried out on a model complex featuring hydrogen atoms in place of the *t*-Bu groups. Three localized molecular orbitals were found to involve significant Rh/BCC bonding interactions, with noticeable mixing of the π(CC) and 2p(B) orbitals. The coordination behavior of the BCC fragment was thus considered intermediate between (i) the superposition of isolated borane and alkene moieties and (ii) a fully delocalized allyl-type BCC system.

To further illustrate the propensity of the PSB ligand to engage in such η^3-BCC interactions, Emslie then targeted related group 10 complexes.[71] The nickel complex **137** was directly obtained by mixing **32** and [Ni(cod)$_2$] (Scheme 72). The related palladium complex **138** was prepared either by reducing the chloro-bridged PdCl$_2$ precursor **92**, or by reacting the Pd (dba) precursor **94a** with lithium amides. Very similar spectroscopic and geometric features were observed for both complexes: (i) ^{11}B NMR signals ($\delta \sim 30$ ppm) at the upper limit of tetracoordinate boron environments, (ii) enforced η^3-BCC interactions, with M–B distances (2.297(4) Å for the nickel complex **137** and 2.320(5) Å for the palladium complex **138**) only slightly exceeding those reported in the related η^1-B complexes **118** and **119** deriving from the TPB ligand (2.168(2) Å for Ni and 2.254(2) Å for

Pd),[99] and quasi-symmetrical MC_{ipso} and MC_{ortho} contacts (2.019(3)/2.081
(3) Å for Ni, and 2.198(4)/2.325(4) Å for Pd). The preference for η^3-BCC
vs. η^1-B bonding of the PSB ligand in these complexes was attributed to
the coordinatively unsaturated nature of the metal fragments (formal 14e
counts when only the coordination of the phosphine and thioether moi-
eties are taken into account).

cod: 1,5-cyclooctadiene
dba: *trans, trans*-dibenzylideneacetone
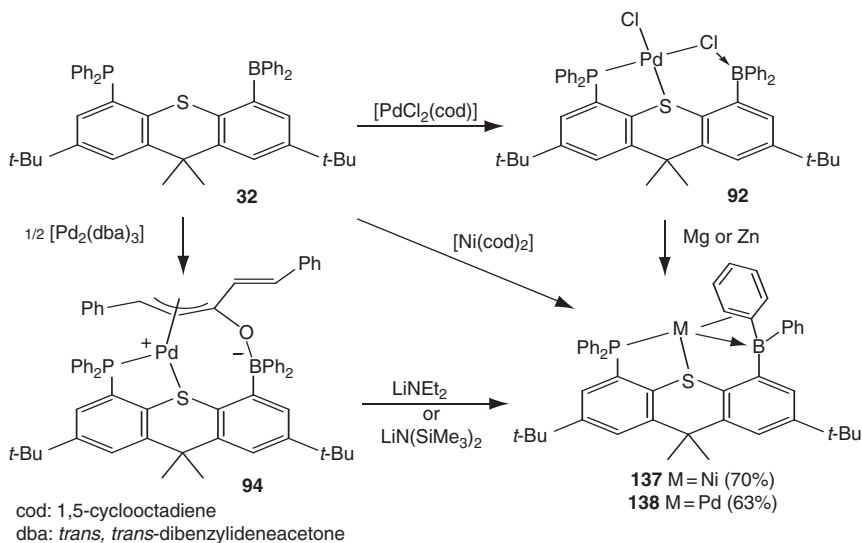
Scheme 72

Recently, we further extended the variety of such multicenter interac-
tions by examining the coordination properties of MPB and DPB ligands
toward CuCl.[21] In contrast with the η^1-B coordination observed in the
related TPB complex **120**, Cu–B interactions supported by arene coordi-
nation were evidenced within complexes **139–140a,b**. The MPB complex
139 adopts a chloro-bridged dimeric structure (Scheme 73) (Figure 53).
The copper center is surrounded by the phosphorus atom, two chlorine
atoms, and a BPh moiety organized in a tetrahedral environment. The
Cu···B distance (2.555(2) Å) is very similar to that of the (TPB)CuCl
complex **120** (2.508(2) Å),[98] and the CuC_{ipso}/CuC_{ortho} contacts (2.339(2)
and 2.596(2) Å) are in the typical range for η^2-CC arene complexes of
copper. The η^3-BCC coordination of the BPh_2 moiety in **139** markedly
contrasts with the pendant character of the BCy_2 group in the related
complex **73** (see Section IV.A), indicating some cooperative effect between
the coordination of the boron atom and phenyl ring in **139**.
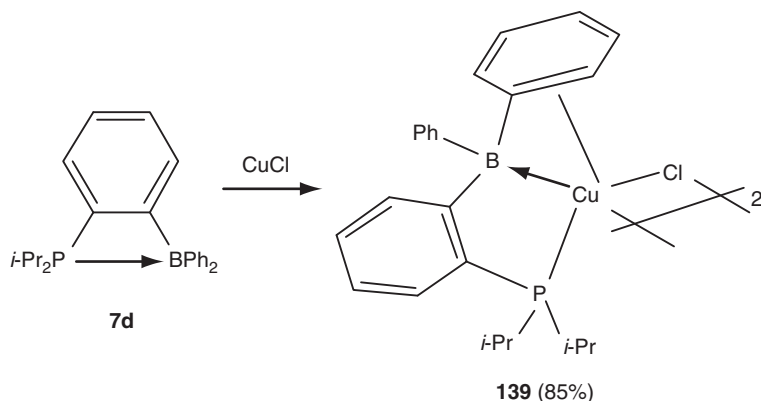
Scheme 73
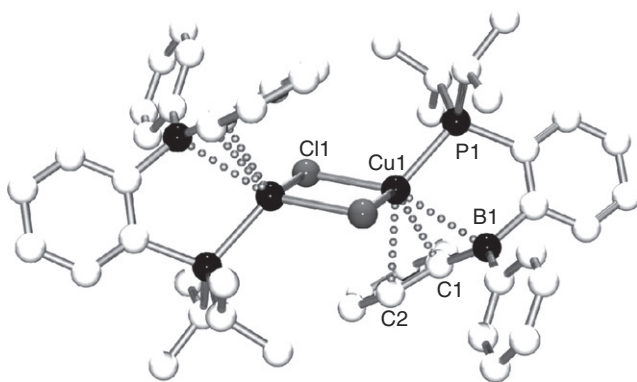
Figure 53   Molecular structure of **139**.

    In order to ascertain the influence of the presence of a second phos-
phine buttress, the DPB complexes **140a** and **140b** were also prepared and
fully characterized (Scheme 74). The participation of the B and C_{ipso} atoms
upon coordination was apparent by NMR: the corresponding signals
appear at δ ^{11}B $\sim$ 55 ppm (very similar to that of (TPB)CuCl) and
δ ^{13}C = 135 ppm (shifted to lower frequencies by about 13 ppm compared
to the free ligands). Both complexes were shown crystallographically to
adopt monomeric structures, with the copper centers in tetrahedral envir-
onments formed by the two phosphorus atoms, the chlorine atom, and the
BPh fragment (Figure 54). The metrical data indicate here η^2-BC rather
than η^3-BCC coordination, as observed in the MPB complex **139**. The Cu–B
distances (2.396(5) Å for **140a** and 2.379(5) Å for **140b**) are significantly
shorter than in the MPB and TPB complexes, and only C_{ipso} establishes a

short contact with copper (2.364(4) Å in **140a** and 2.414(4) in **140b**). In addition, the presence of four crystallographically independent molecules in the unit cell of **140b** suggested some flexibility in the coordination of the BPh fragment. Complexes **140a** and **140b** constitute the first examples of η^2-BC coordination involving a triarylborane, and thereby bridge the gap between the η^1-B and η^3-BCC coordination modes described previously. The bonding situations in **140a** and **140b** were thoroughly investigated by DFT calculations. The molecular orbital and NBO analyses clearly indicated the presence of three-center $CuBC_{ipso}$ interactions resulting from the superposition of several donor–acceptor interactions [Cu–B, $\pi(C_{ipso}C_{ortho}) \rightarrow 2p(B)$, $\eta(BC_{ipso}) \rightarrow Cu$ and $\pi(C_{ipso}C_{ortho}) \rightarrow Cu$]. In addition, the variation of the NPA atomic charges upon coordination substantiated some transfer of electron density from copper to boron (q_B decreases by about 0.23e while q_{Cu} increases by 0.14e). The existence of several minima of close energies but different positionings of the BPh fragment also supported the flexible character of the η^2-BC interaction.

R2P-----B-----PR2
         |
        Ph

8a R = *i*-Pr
8b R = Ph

CuCl →

140a R = Ph (94%)
140b R = *i*-Pr (43%)
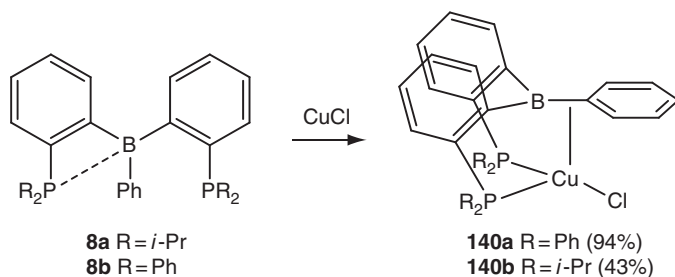
Scheme 74

Stephan examined the coordination of the ethynyl-bridge PB **5b** toward [Ni(cod)$_2$] and thereby gained evidence for unsupported η^3-BCC coordination (Scheme 75).[18] Diagnostic features for the coordination of the C≡C–B fragment in the ensuing complex **141** are the high-field ^{11}B NMR resonance signal ($\delta = 7.0$ ppm) and the low C≡C stretching frequency ($\nu = 1881$ cm^{-1} for **141**, vs. 2125 cm^{-1} in the free ligand).

X-ray diffraction analysis (Figure 55) revealed the pendant character of the phosphine moiety. The nickel center is surrounded by the bidentate cod ligand, the alkynyl fragment and the boron atom organized in a pseudo square-planar arrangement. The C≡C bond is elongated (1.254 (4) Å) and the PCCB skeleton significantly deviates from linearity (torsion angle of 159.4°), with the phosphorus atom and boron atoms in unusual
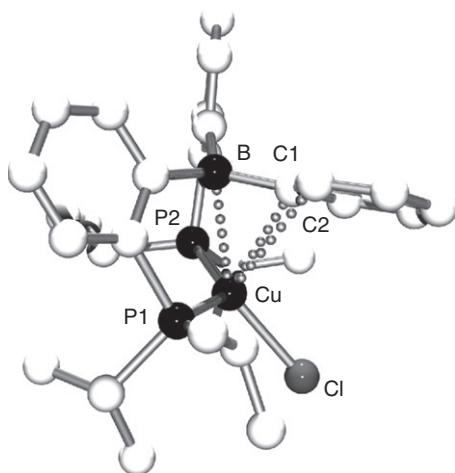
Figure 54   Molecular structure of **140b** (only one of the four independent molecules of the unit cell is shown for clarity).
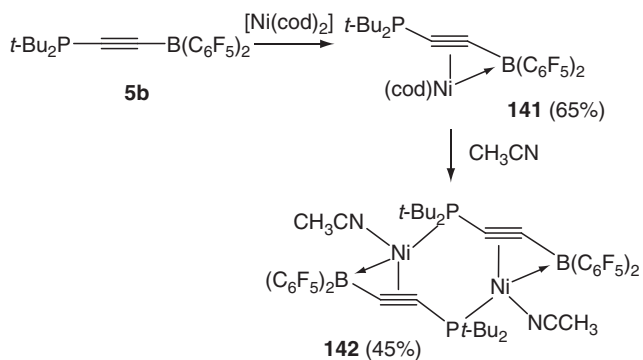
Scheme 75
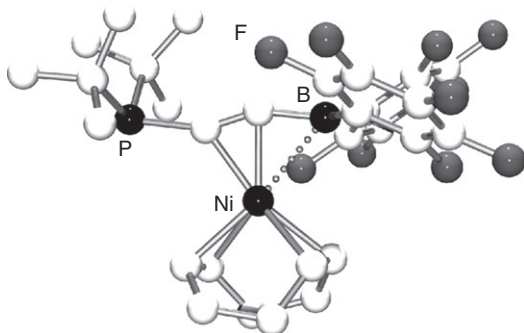
Figure 55   Molecular structure of **141**.

trans disposition. Despite the short Ni–B distance (2.358(3) Å) indicative of a substantial Ni–B interaction, the boron environment only marginally deviates from planarity ($\Sigma B_\alpha = 357.6°$). The bonding situation was analyzed by DFT calculations. Analysis of the molecular orbitals further confirmed the participation of both the C≡C triple bond and boron atom in the coordination, with significant mixing of the corresponding $\pi(CC)$ and $2p(B)$ orbitals. In addition, a NBO accounting for the Ni–B interaction was found, with major contribution from the 3d orbital at Ni (80.2%). The electron transfer from Ni to B was estimated to about 0.3e by comparing the NPA charge at boron in the complex **141** with that of the free ligand **5b**. The rather strong character of the Ni–B interaction was also substantiated experimentally by treating **141** with acetonitrile. The ensuing complex **142** adopts a centrosymmetric dimeric structure. The cod ligand but not the Ni–B interaction was displaced. One acetonitrile molecule coordinates to the nickel center, whose coordination sphere is further completed by the phosphorus atom. The key geometric features associated with the η^3-BCC coordination ($d_{CC} = 1.268$ (2) Å, $d_{NiB} = 2.324(2)$ Å) are very similar to those encountered in the mononuclear complex **141**.

F. B-H coordination

The strategy of supporting unusual M–B interactions by the coordination of phosphine buttresses has been recently extrapolated to the side-on coordination of a B–H bond. Alcaraz and Sabo-Etienne investigated the reaction of the PB **3c** with the dihydrido-bis(dihydrogen) ruthenium precursor **143** (Scheme 76).[14] Complex **144** resulting from the displacement of two dihydrogen ligand was fully characterized by multinuclear NMR spectroscopy and X-ray diffraction analysis (Figure 56). The ruthenium center is at the center of a distorted octahedron with the PB ligand coordinated in the equatorial plane by both the phosphorus lone pair and the $\sigma(B–H)$ bond. The B–H bond length (1.23(7) Å) is in the typical range for σ-borane complexes of ruthenium. The corresponding Ru···H distance (1.92(7) Å) is elongated by about 10% compared to the two ruthenium-hydride bond lengths (1.69(6)–1.77(7) Å), and the RuB distance (2.757(8) Å) significantly exceeds the sum of covalent radii (2.09 Å). The absence of significant Ru–B back-donation was further indicated by the strong N–B π-donation ($d_{NB} = 1.404(3)$ Å) and inappropriate orientation of the $2p(B)$ orbital. Interestingly, monitoring the reaction of **3c** with **143** allowed the spectroscopic authentication of the di(hydrido)-hydrogen complex **145** as an intermediate in the formation of **144**, and the hemilabile character of the PB ligand was substantiated by the back-formation of **145** upon pressurization of **144** with dihydrogen.
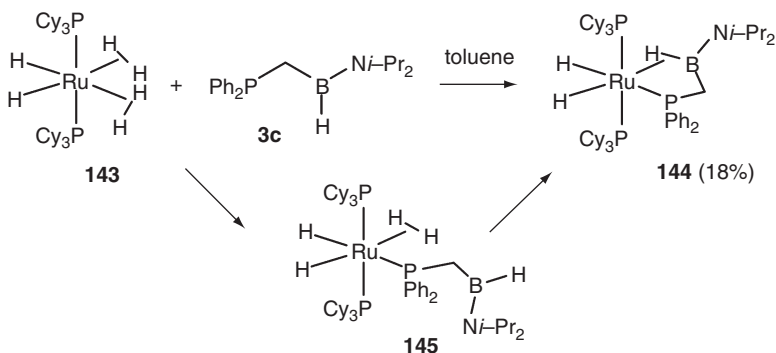
Scheme 76
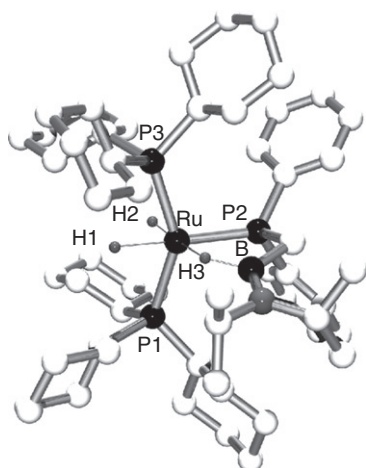
Figure 56   Molecular structure of **144**.

V. REACTIVITY AND CATALYTIC APPLICATION
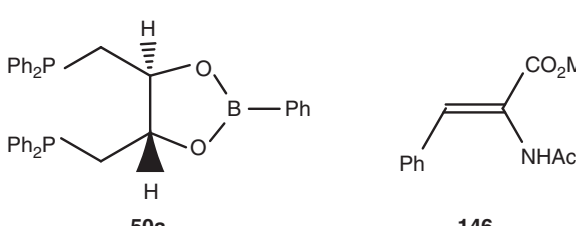
As discussed in the previous section, the coordination properties of PBs and related ambiphilic ligands have been quite extensively studied over the last decade. Comparatively, the reactivity and catalytic application of the ensuing complexes have only been scarcely explored. The few investigations reported in this area are summarized in this section. They nicely illustrate the various possibilities offered by the presence of the Lewis acid in the coordination sphere of a metal or at proximity.

A. Pendant Lewis acids as potential anchoring sites in catalysis

The presence of a pendant Lewis acid opens the way to secondary interactions with incoming substrates (see Section IV.A). This possibility was investigated early on by Kagan in Rh-catalyzed hydrogenation and hydrosilylation reactions.[61] The catalytic properties of the boraDIOP ligand **50a** featuring a remote boronate moiety were evaluated toward a variety of C=C and C=O containing substrates (Tables 4–6). When possible, solvents of low Lewis basicity were preferred to favor the formation of secondary interactions between the boron atom and the substrate. Rhodium complexes deriving from **50a** proved rather active catalysts, but no significant improvements in terms of activity or selectivity were observed compared to DIOP itself. This suggests only weak, if any, participation of the Lewis acid moiety.

A few years later, Landis drew similar conclusions for the 1,1′-ferrocenyldiphosphines **53a–c** featuring pendant benzoxaborolidine moieties.[63] Combined with rhodium precursors, these ambiphilic ligands lead to catalytically active species in hydrogenation and hydroformylation reactions (Tables 7 and 8), but the presence of the Lewis acid moiety has no significant effect on activity and selectivity (compared to ligands **51** and **52**).

Table 4 Rh-catalyzed hydrogenation of the *N*-acetyl dehydrophenylalanine derivative **146** with the DIOP and boraDIOP ligands

Ligand	Solvent	Yield (%) (time)	ee (%)
DIOP[a]	MeOH	100 (5 min)	66.9
boraDIOP **50a**[a]	MeOH	100 (0.5 h)	67.0
DIOP[b]	CH$_2$Cl$_2$	100 (3 h)	76.2
boraDIOP **50a**[b]	CH$_2$Cl$_2$	100 (3 h)	73.0

Reactions performed at 25 °C and 1 bar with 50 equiv. of substrate.
[a]Neutral catalyst prepared *in situ* from [Rh(μ-Cl)(cod)]$_2$ and the DIOP or boraDIOP ligand.
[b]Isolated cationic catalyst [Rh(cod)(DIOP)$^+$,PF$_6^-$] or [Rh(cod)(boraDIOP)$^+$,PF$_6^-$].

Table 5 Rh-catalyzed hydrogenation of ketone **147** and pyruvate **148** with the DIOP and boraDIOP ligands
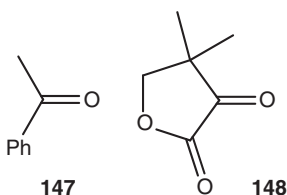
Ligand	Substrate	Solvent	Yield (%) (time)	ee (%)
DIOP	**147**	MeOH[a]	39 (4 d)	51.0
boraDIOP **50a**	**147**	MeOH[a]	41 (5 d)	3.6
DIOP	**148**	THF[b]	100 (3 d)	52.0
boraDIOP **50a**	**148**	THF[b]	100 (3 d)	54.3

Reactions performed at 50 bar with neutral catalysts prepared *in situ* from [Rh(μ-Cl)(cod)]$_2$ and the DIOP or boraDIOP ligand.
[a]25 °C, substrate:Rh = 170.
[b]50 °C, substrate:Rh = 100.

Table 6 Rh-catalyzed hydrosilylation of ketones **147** and **149** with the DIOP and boraDIOP ligands
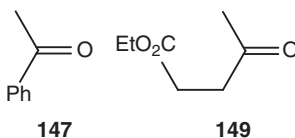
Ligand	Substrate	Yield (%) (time)	ee (%)
DIOP	**147**[a]	90 (3 h)	28.8
boraDIOP **50a**	**147**[a]	83 (1.5 h)	21.0
DIOP	**149**[b]	98	31.9
boraDIOP **50a**	**149**[b]	100	18.9

Reactions performed in toluene at 25 °C with 1.1 equiv. of Ph$_2$SiH$_2$ using neutral catalysts prepared *in situ* from [Rh(μ-Cl)(cod)]$_2$ and the DIOP or boraDIOP ligand.
[a]Substrate:Rh = 500.
[b]Substrate:Rh = 300.

Table 7 Rh-catalyzed hydrogenation of the *N*-acetyl dehydrophenylalanine derivative **146** with ferrocenyl diphosphines **51–53**

51   **52**   **53a** R = Me
                              53b R = Ph
                              53c R = *p*−ClC$_6$H$_4$
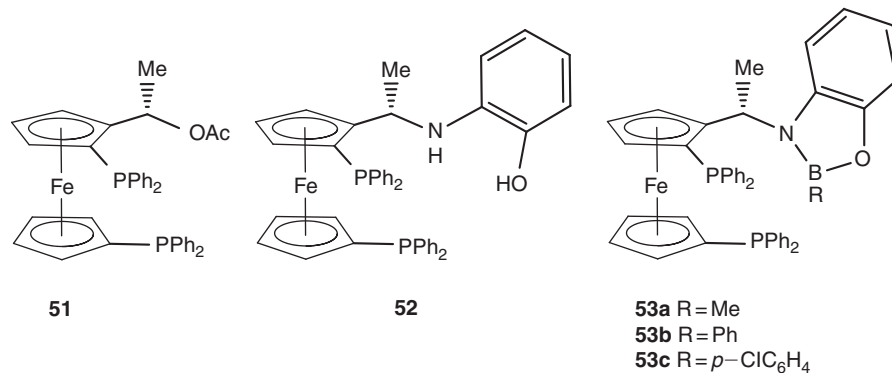
Ligand	Initial turnover freq. (min^{-1})	ee (%)
51	120	9
52	138	54
53a	149	39
53b	22	49
53c	127	53

Reactions performed in THF at 22 °C and 15 bar with 400 equiv. of substrate using [Rh(nbd)L][OTf] salts.

Table 8 Rh-catalyzed hydroformylation of styrene with ferrocenyl diphosphines **51–53**

Ligand	Initial turnover freq. (h^{-1})	b:l ratio
51	12	2
52	7	4
53a	6	4
53b	6	5
53c	13	4

Reactions performed with 120 equiv. of substrate.

The pioneering studies of Kagan and Landis pave the way to the use of remote Lewis acids, but strong evidence for substrate anchoring under catalytic conditions is still missing. Further developments in this area would probably be possible by finely tuning the position and electron-deficiency of the pendant Lewis acid.

B. Assistance of migratory insertion of CO by phosphine-alanes and -boranes

As early as in the 1980s, Miller and Labinger studied the migratory insertion of CO assisted by ambiphilic ligands. The iron precursor [CpFe(CO)$_2$Me] reacts only slowly or is even inert toward phosphines such as Ph$_2$PN(t-Bu)H. In marked contrast, migratory insertion proceeds within minutes at room temperature in the presence of the phosphine-alane Ph$_2$PN(t-Bu)AlEt$_2$ **1b**. The transient formation of the acyl complex **150** was supported by the structural characterization of its cyclized form **151**. The latter compound rearranged over a day to afford a mixture of the acetyl complex **152** (also characterized by X-ray diffraction analysis) and of its tautomeric complex **153** (Scheme 77).[9,10]

The ability of ambiphilic ligands to promote formyl formation from hydrido carbonyl complexes has also been studied. The phosphine-alanes **1b,c** rapidly react with [HMn(CO)$_5$] to give complexes **154b,c** analogous to **151** and formally resulting from the intramolecular attack of the phosphorus atom on the transient formyl complex (Scheme 78). However, monitoring the first stage of the reaction by NMR indicated the initial formation of a species containing a direct P–H bond
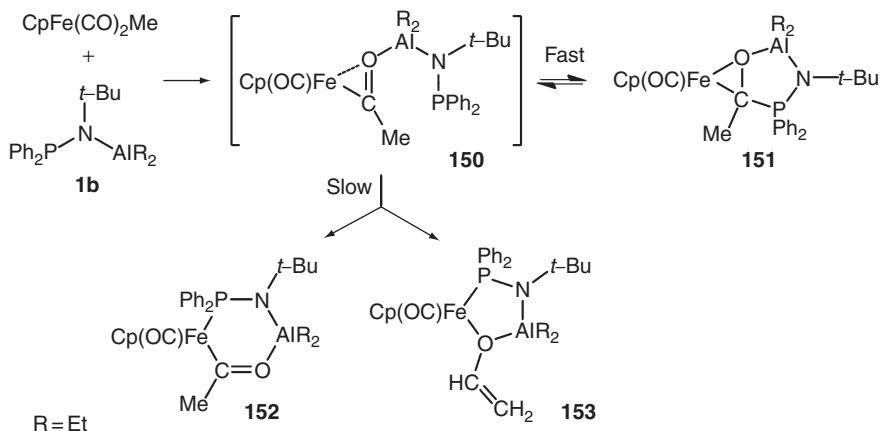
Scheme 77
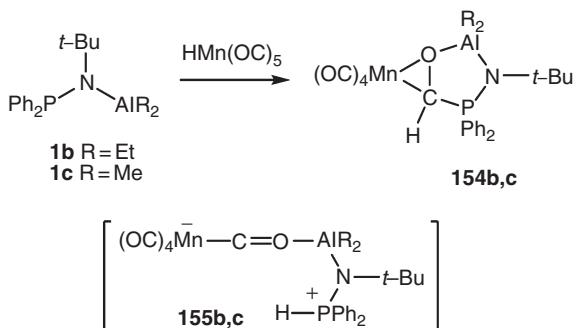
Scheme 78

(tentatively assigned to **155b,c**), ruling out the direct migration of hydride to CO in this case.[106]

Recently, Labinger and Bercaw investigated the ability of pendant boranes to act as hydride acceptors with the aim of transforming coordinated CO. The triphenylphosphine complex salt [Re(CO)$_4$(PPh$_3$)$_2$][BF$_4$] does not react with [HPt(dmpe)][PF$_6$] (dmpe = bis(dimethylphosphino) ethane) even in the presence of BEt$_3$, whereas complex **76** featuring two PB ligands readily affords complex **156** under the same conditions (Scheme 79).[72] This boroxycarbene complex **156** was characterized by multinuclear NMR and IR spectroscopy, and an X-ray diffraction study was performed on the corresponding dinuclear complex featuring bridging phosphine-boroxycarbene units. Attempts to crystallize **156** eventually led to the anionic carbene complex **157** that can be directly obtained by reacting **76** with two equivalents of hydride donor. A two-step
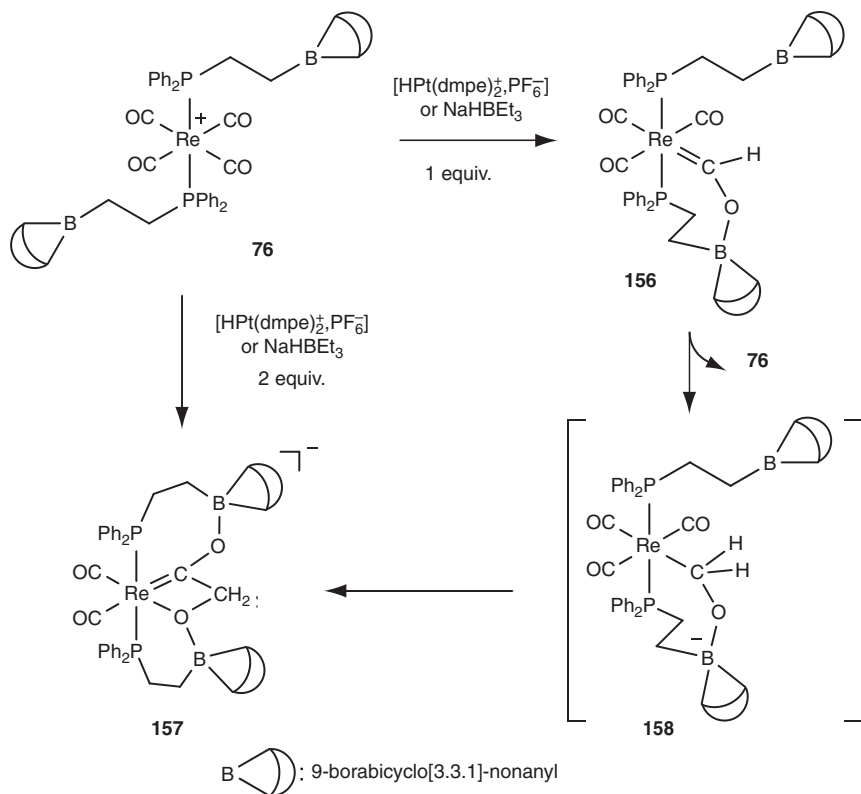
Scheme 79

mechanism was proposed to account for the formation of **157**: disproportionation of **156** by hydride transfer leading to **158**, followed by migratory insertion of CO into the Re–CH$_2$ bond. These results demonstrate that the incorporation of a pendant borane moiety can facilitate the formation of C–H and C–C bonds, and thereby promote the reductive coupling of CO in the coordination sphere of a transition metal.

C. Phosphine-alanes as bifunctional cocatalysts for the Ni-catalyzed dehydrogenative coupling of silanes

Fontaine and Zargarian reported in 2004 a seminal catalytic study involving an ambiphilic derivative. The dimeric phosphine-alane (Me$_2$PCH$_2$AlMe$_2$)$_2$ **2** was used as a bifunctional cocatalyst for the nickel-catalyzed

dehydrogenative coupling of phenylsilane PhSiH$_3$.[77] With the nickel complex [(1-MeInd)Ni(PPh$_3$)Me] (1-MeInd = 1-methylindenyl) **159**, the reaction proceeds very slowly, whereas vigorous evolution of H$_2$ occurs when the phosphine-alane **2** was added (Al/Ni ratio = 1). The turnover frequencies, as determined from manometric measurements of the rate of H$_2$ evolution, revealed a 50-fold rate enhancement (Table 9). According to ^{1}H NMR and GPC analyses, the reaction leads essentially to linear oligomers (trimers to hexamers) during the first hour, but cyclic oligomers predominate after prolonged reaction (∼24 h).

The stability of the active species was substantiated by a second feed experiment, similar rate of H$_2$ evolution being observed upon addition of a second batch of silane. With the aim of gaining more insight into the nature of the active species, a mixture of **2** and **159** was monitored by ^{31}P NMR spectroscopy. In the absence of substrate, no reaction took place. The displacement of PPh$_3$ at nickel by the more basic phosphine of the ambiphilic ligand is favorable, but requires the head-to-tail dimeric structure of **2** to be split. The addition of Lewis bases such as NEt$_3$ was investigated to promote the dissociation of **2**. The ensuing complex **160** featuring a pendant alane stabilized by NEt$_3$ was spectroscopically characterized (Scheme 80), and the ternary system **159**/**2**/NEt$_3$ led to a further rate enhancement by more than three orders of magnitude. Among the Lewis bases evaluated, the best results were obtained with NEt$_3$, tmeda (tetramethylethylene diamine), and tetrahydrofuran, while diethyl ether had almost no effect, and quinuclidine slowed down the reaction. Apparently, a compromise has to be found between the splitting of the dimeric structure of **2**, and the association of the Lewis base to the alane moiety.

Table 9 Catalytic rates for the dehydrogenative coupling of PhSiH$_3$ catalyzed by the nickel complex [(1-MeInd)Ni(PPh$_3$)Me] **159** in the presence of the phosphine-alane (Me$_2$PCH$_2$AlMe$_2$)$_2$ **2** and a Lewis base

Catalytic system	TOF (h^{-1})
159	11
159/**2**	554
159/**2**/NEt$_3$	1760
159/**2**/tmeda	1680
159/**2**/THF	1655
159/**2**/Et$_2$O	400
159/**2**/quinuclidine	280

Reactions performed in toluene at room temperature with 200 equiv. of substrate.
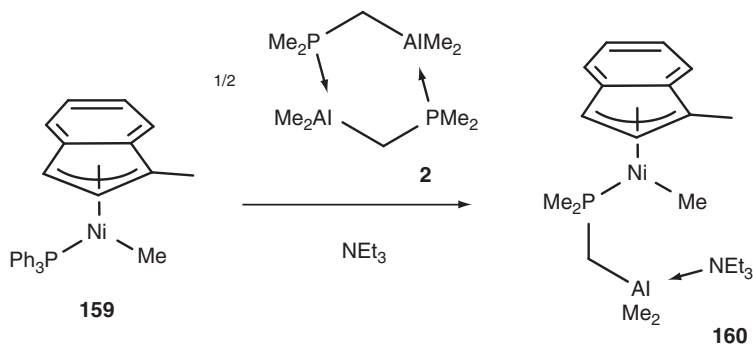
Scheme 80

D. (Phosphine-borane)-bridged zirconocenes as precatalysts for olefin polymerization

Taking advantage of the phosphorus/boron affinity, Ostoja Starzewski reported in 1999 a new class of *ansa*-metallocenes **161** featuring a donor–acceptor bridge (Figure 57).[107] In these complexes, one Cp-type ring features a phosphine group and the other bears a borane. The two π ligands are strongly bonded through intramolecular P–B interaction.

In contrast to conventional *ansa*-metallocenes, the synthesis of the phosphine-borane metallocenes **161** does not require the preparation of a bridging ligand, since the dative P–B interaction spontaneously forms when the two Cp-ligands are coordinated to the metal center. Accordingly, compound **161a** was readily obtained by reaction of the silylated phosphorus-containing precursor $Me_2P(Cp)SiMe_3$ with zirconium tetrachloride, and subsequent reaction of the resulting complex $Me_2P(Cp)ZrCl_3$ with the silylated boron-containing unit $Cl_2B(C_5H_4SiMe_3)$ (Scheme 81).[107]
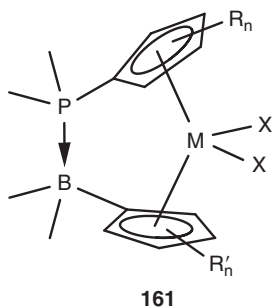
Figure 57 *Ansa*-metallocenes **161** featuring a phosphine-borane bridge.
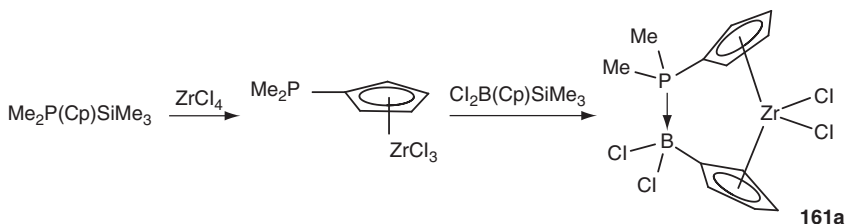
Scheme 81

The molecular structure of **161a** has been confirmed by an X-ray analysis (Figure 58). The PB bond length (1.983(2) Å) and the pyramidalization of the boron environment ($\Sigma B_\alpha = 333.9°$) are in the same range than those observed in the *closed* form of PBs featuring organic linkers (see Section III). The centroid–Zr–centroid angle (127.9°) is very comparable to that observed in the related *ansa*-zirconocene featuring the CH_2CH_2 bridge (128°). The presence of the P–B interaction in solution was unambiguously indicated by the ^{31}P and ^{11}B NMR data ($\delta\,^{31}P = -7.7$ ppm, $\delta\,^{11}B = -0.5$ ppm, and $^{1}J_{PB} = 120$ Hz). Remarkably, the donor–acceptor bridge proved to be highly thermally stable, no changes being observed by NMR up to 100 °C.

PB dichloro-zirconocenes **161** were found to be highly active precatalysts for the polymerization of ethylene under MAO activation.[107,108] At 100 °C under 10 bars of ethylene, complex **161a** led to high molecular weight polyethylene (PE) ($M_\eta = 106\times10^3$ g mol^{-1}) with an activity of about 118 t PE mol$_{Zr}^{-1}$ h^{-1}. When the polymerization was carried out at 60 °C, the activity of **161a** only slightly decreased, but the molecular weight of the resulting PE was significantly higher (Table 10). The
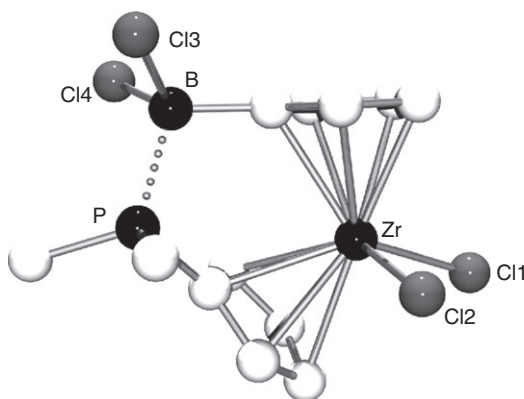
Figure 58 Molecular structure of the phosphine-borane metallocene **161a**.

Table 10 Ethylene polymerizations catalyzed by the phosphine-borane zirconocenes 161a–d

Phosphine-borane zirconocene	T (°C)	A (t $mol_{Zr}^{-1} h^{-1}$)	M_η (g mol^{-1})
$(Me_2PCp)(CpBCl_2)ZrCl_2$ **161a**	100	118	118.10^3
	60	90	264.10^3
$(Et_2PCp)[CpB(C_6F_5)_2]ZrCl_2$ **161b**	60	148	323.10^3
$(Et_2PFlu)[CpB(C_6F_5)_2]ZrCl_2$ **161c**	60	52	2110.10^3
$(Et_2PFlu)(CpBPh_2)ZrCl_2$ **161d**	60	28	3160.10^3
	40	40	3890.10^3

Reaction performed with MAO as cocatalyst (Al:Zr = 10,000) during 30 min at 10 bars of ethylene.

structure of the zirconocene precatalyst was modulated with the aim of favoring chain growth over chain transfer and termination reactions, in order to get high-performance ultrahigh molecular weight PEs (UHMW-PE, $M_\eta > 10^6$ g mol^{-1}). Complex **161b** featuring Et substituents at phosphorus and C_6F_5 groups at boron was found more active than **161a** (148 vs. 90 t $mol_{Zr}^{-1} h^{-1}$ at 60 °C) and afforded PE of higher molecular weight ($M_\eta = 323$ vs. 264×10^3 g mol^{-1}). The replacement of one Cp ring for a fluorenyl group (complexes **161c,d**) induced some decrease in activity, but further enhanced the selectivity in favor of propagation, leading to PE with M_η up to 3890×10^3 g mol^{-1} at 40 °C.

Due to the hindered rotation of the Cp rings, *ansa*-metallocenes are particularly suitable for stereocontrolled polymerization of propene. The racemic catalyst **161e**, in which both the donor and acceptor moieties have been introduced on 2-methylindenyl rings, has been investigated in this respect, and high molecular weight isotactic polypropenes were obtained (Table 11). ^{13}C NMR measurements indicated the absence of side 2,1- and 1,3-insertion reactions, and revealed very high isotacticity indexes, especially when the polymerizations were conducted at room temperature.[107]

Small centroid–metal–centroid angles make *ansa*-metallocenes particularly attractive for the polymerization and copolymerization of higher olefins. Thus, complexes **161** have also been evaluated for the preparation of ethylene/propylene copolymers and ethylene/propylene/5-ethylidene-2-norbornene terpolymers. These composites possess good elastic properties even at low temperature. So far, the use of conventional *ansa*-metallocenes and constrained-geometry half-sandwich complexes is limited by the accessible molecular weights ($<200 \times 10^3$ g mol^{-1}). Significant improvements were made with the phosphine-borane zirconocenes **161c,d,f** combining a Cp ring and a fluorenyl moiety (Table 12), and modulation of the substitution pattern at boron allowed to reach molecular weights as high as 1400×10^3 g mol^{-1}.[109]

Table 11 Propene polymerizations catalyzed by the phosphine-borane zirconocene **161e**

161 e
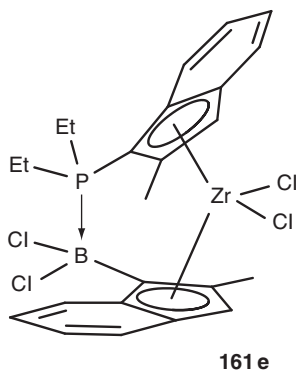
Solvent	Temperature	Isotacticity index (%)	M_η (g mol^{-1})
Toluene	RT	97	422.10^3
Bulk	RT	98	2000.10^3
Bulk	50 °C	92	434.10^3

Reactions performed under 2 bars of propene with tri-isobutylaluminium/dimethylanilinium-tetrakis(penta-fluorophenyl)borate as cocatalyst.

Table 12 Ethylene co- and terpolymerizations catalyzed by the phosphine-borane zirconocenes **161c,d,f**

Phosphine-borane zirconocene	A (t mol$_{zr}^{-1}$ h^{-1})	M_η (g mol^{-1})	P:ENB[a]
(Et$_2$PFlu)[CpB(C$_6$F$_5$)$_2$]ZrCl$_2$ **161c**	46	484.10^3	65:0
(Et$_2$PFlu)(CpBPh$_2$)ZrCl$_2$ **161d**	82	769.10^3	57:0
(Et$_2$PFlu)(CpBEt$_2$)ZrCl$_2$ **161f**	25	1400.10^3	45:0
(Et$_2$PFlu)[CpB(C$_6$F$_5$)$_2$]ZrCl$_2$ **161c**	59	536.10^3	60:5
(Et$_2$PFlu)(CpBPh$_2$)ZrCl$_2$ **161d**	49	949.10^3	51:4
(Et$_2$PFlu)(CpBEt$_2$)ZrCl$_2$ **161f**	22	1418.10^3	34:3

Reactions performed with MAO as cocatalyst (Al:Zr = 10,000) during 30 min at 40 °C and 4 bars of ethylene.
[a]Weight content in propene (P) and 5-ethylidene-2-norbornene (ENB).

VI. RECENT AND IN PRESS LITERATURE

Since the submission of this manuscript some papers related to the ambiphilic phosphine-boranes appeared in the literature. We have reported the preparation of the PB compound Ph$_2$P-(1,1′-ferrocenyl)-BMes$_2$ featuring a

1,1′-ferrocenyl spacer by ionic coupling starting from 1,1′-dibromoferro-
cene.[110]Its monomeric structure without P-B or Fe-B interactions was
revealed by multinuclear NMR and X-ray diffraction analysis. This PB
has been evaluated in Rh-catalyzed hydroformylation of 1-octene. The
linear product was obtained, the same activity and selectivity was
observed with the related boron free ligand FcPPh$_2$. These results indicate
that the BMes$_2$ moiety does not play any significant role during this
process, probably due to the flexibility of the spacer. The influence of
the rigidity of the linker between phosphorus and boron atoms was
then accessed by evaluating the activity of the related PB featuring an
o-phenylene spacer.[111] Under the same conditions, both the rate and
selectivity of the hydroformylation decrease. Steric rather than electronic
influence of the BMes$_2$ group was suggested by comparing these results
with those obtained using a related Buchwald-type biarylphosphine.

In the frame of dihydrogen activation by ''frustrated'' Lewis pairs, Wass
et al. reported the synthesis of two PB featuring three atom spacers, namely
t-Bu$_2$P-CH$_2$-CR$_2$-OB(C$_6$F$_5$)$_2$ (with R = H or CF$_3$) by ionic coupling between
the preformed lithium phosphino-alkoxide *t*-Bu$_2$P-CH$_2$-CR$_2$-OLi and ClB
(C$_6$F$_5$)$_2$.[112]According to ^{31}P, ^{11}B and ^{19}F NMR spectroscopy, the unsubsti-
tuted ethanoxy spacer (R = H) displays a monomeric open structure at room
temperature in solution. Variable temperature measurements revealed sub-
stantial modifications at lower temperature, suggesting the formation of a
P-B interaction. For the fluorinated PB (R = CF$_3$), a monomeric closed
structure resulting from intramolecular P-B interaction was apparent from
^{31}P, ^{11}B and ^{19}F NMR and confirmed by X-ray diffraction analysis.

VII. CONCLUSION

As prototypes of ambiphilic derivatives, PBs have attracted a surge of
interest over the last decade. Various synthetic strategies have been devel-
oped to assemble such polyfunctional compounds combining antagonist
sites. The factors governing their structure, with regards to the formation
of inter- or intramolecular P–B interactions have been elucidated.

Fundamental coordination studies have shown very versatile proper-
ties associated with different behaviors of the Lewis acid moiety. The
borane may remain pendant or interact with a coligand, leading ulti-
mately to zwitterionic complexes. In addition, the direct formation of
metal–borane interactions has allowed significant progress in the field
of σ-acceptor ligands. The scope of metal–Lewis acid interactions appears
now much more general than initially believed, and their bonding situa-
tion is better understood. Original multicenter interactions have also been
observed when the boron atom bears a π-system or a hydrogen atom.

The research on complexes deriving from ambiphilic ligands is still in its infancy, but the recent achievements summarized in this review will pave the way for further developments in the near future. Taking into account the great structural modularity of the ambiphilic framework, it is certain that other types of complexes featuring Lewis acids within the coordination sphere, or at proximity, will be prepared and new bonding situations are likely to be discovered. Besides structural considerations, much remains to be done regarding the influence of Lewis acid moieties on the electronic, geometric, and photophysical properties of metal complexes. The presence of a Lewis acid can also influence reactivity, something that clearly deserves further studies. This also holds true for the application of PBs and related ambiphilic ligands in catalysis. The use of Lewis acids as internal anchors, relays, or activators offers very promising perspectives. In this respect, not only complexes adopting a well-defined coordination mode but also ''dynamic'' systems susceptible to interconversion between different forms are highly desirable.

ACKNOWLEDGMENTS

REFERENCES

(1) Entwistle, C. D.; Marder, T. B. *Angew. Chem. Int. Ed.* **2002**, *41*, 2927.
(2) Welch, G. C.; San Juan, R. R.; Masuda, J. D.; Stephan, D. W. *Science* **2006**, *314*, 1124.
(3) (a) Stephan, D. W.; Erker, G. *Angew. Chem. Int. Ed.* **2010**, *49*, 46; (b) Stephan, D. W. *Dalton Trans.* **2009**, 3129.
(4) Moebs-Sanchez, S.; Bouhadir, G.; Saffon, N.; Maron, L.; Bourissou, D. *Chem. Commun.* **2008**, 3435.
(5) Bebbington, M. W. P.; Bontemps, S.; Bouhadir, G.; Bourissou, D. *Angew. Chem. Int. Ed.* **2007**, *46*, 3333.
(6) Fontaine, F. G.; Boudreau, J.; Thibault, M. H. *Eur. J. Inorg. Chem.* **2008**, 5439.
(7) Kuzu, I.; Krummenacher, I.; Meyer, J.; Armbruster, F.; Breher, F. *Dalton Trans.* **2008**, 5836.
(8) Clemens, D. F.; Sisler, H. H.; Brey, W. S., Jr. *Inorg. Chem.* **1966**, *5*, 527.
(9) Labinger, J. A.; Miller, J. S. *J. Am. Chem. Soc.* **1982**, *104*, 6856.
(10) Labinger, J. A.; Bonfiglio, J. N.; Grimmett, D. L.; Masuo, S. T.; Shearin, E.; Miller, J. S. *Organometallics* **1983**, *2*, 733.
(11) Karsch, H. H.; Appelt, A.; Koehler, F. H.; Mueller, G. *Organometallics* **1985**, *4*, 231.
(12) Rathke, J.; Schaeffer, R. *Inorg. Chem.* **1972**, *11*, 1150.
(13) Braunschweig, H.; Dirk, R.; Ganter, B. *J. Organomet. Chem.* **1997**, *545–546*, 257.

(14) Gloaguen, Y.; Alcaraz, G.; Pecharman, A. F.; Clot, E.; Vendier, L.; Sabo-Etienne, S. *Angew. Chem. Int. Ed.* **2009**, *48*, 2964.
(15) Thomas, J. C.; Peters, J. C. *Polyhedron* **2004**, *23*, 2901.
(16) Yuan, Z.; Taylor, N. J.; Sun, Y.; Marder, T. B.; Williams, I. D.; Cheng, L. T. *J. Organomet. Chem.* **1993**, *449*, 27.
(17) Dureen, M. A.; Stephan, D. W. *J. Am. Chem. Soc.* **2009**, *131*, 8396.
(18) Zhao, X.; Otten, E.; Song, D.; Stephan, D. W. *Chem. Eur. J.* **2010**, *16*, 2040.
(19) Balueva, A. S.; Nikonov, G. N.; Arbuzov, B. A.; Musin, R. Z.; Efremov, Y. *Izv. Akad. Nauk SSSR, Ser. Khim.* **1991**, 2397.
(20) Bontemps, S.; Bouhadir, G.; Miqueu, K.; Bourissou, D. *J. Am. Chem. Soc.* **2006**, *128*, 12056.
(21) Sircoglou, M.; Bontemps, S.; Mercy, M.; Miqueu, K.; Ladeira, S.; Saffon, N.; Maron, L.; Bouhadir, G.; Bourissou, D. *Inorg. Chem.* **2010**, *49*, 3983.
(22) Bontemps, S.; Bouhadir, G.; Apperley, D. C.; Dyer, P. W.; Miqueu, K.; Bourissou, D. *Chem. Asian J.* **2009**, *4*, 428.
(23) Bontemps, S.; Gornitzka, H.; Bouhadir, G.; Miqueu, K.; Bourissou, D. *Angew. Chem. Int. Ed.* **2006**, *45*, 1611.
(24) Bontemps, S.; Bouhadir, G.; Dyer, P. W.; Miqueu, K.; Bourissou, D. *Inorg. Chem.* **2007**, *46*, 5149.
(25) Sircoglou, M.; Bontemps, S.; Mercy, M.; Saffon, N.; Takahashi, M.; Bouhadir, G.; Maron, L.; Bourissou, D. *Angew. Chem. Int. Ed.* **2007**, *46*, 8583.
(26) Sircoglou, M.; Bouhadir, G.; Saffon, N.; Miqueu, K.; Bourissou, D. *Organometallics* **2008**, *27*, 1675.
(27) Sircoglou, M.; Mercy, M.; Saffon, N.; Coppel, Y.; Bouhadir, G.; Maron, L.; Bourissou, D. *Angew. Chem. Int. Ed.* **2009**, *48*, 3454.
(28) Agou, T.; Kobayashi, J.; Kawashima, T. *Org. Lett.* **2005**, *7*, 4373.
(29) Agou, T.; Kobayashi, J.; Kawashima, T. *Inorg. Chem.* **2006**, *45*, 9137.
(30) Kobayashi, J.; Agou, T.; Kawashima, T. *Phosphorus Sulfur Silicon Relat. Elem.* **2008**, *183*, 389.
(31) Morgan, I. R.; Di Paolo, A.; Vidovic, D.; Fallis, I. A.; Aldridge, S. *Chem. Commun.* **2009**, 7288.
(32) Welch, G. C.; Cabrera, L.; Chase, P. A.; Hollink, E.; Masuda, J. D.; Wei, P.; Stephan, D. W. *Dalton Trans.* **2007**, 3407.
(33) Schulz, F.; Sumerin, V.; Leskelae, M.; Repo, T.; Rieger, B. *Dalton Trans.* **2010**, *39*, 1920.
(34) Sasaki, S.; Murakami, F.; Murakami, M.; Watanabe, M.; Kato, K.; Sutoh, K.; Yoshifuji, M. *J. Organomet. Chem.* **2005**, *690*, 2664.
(35) Binger, P.; Koester, R. *J. Organomet. Chem.* **1974**, *73*, 205.
(36) Binger, P.; Benedikt, G.; Rotermund, G. W.; Köster, R. *Liebigs Ann. Chem.* **1968**, *717*, 21.
(37) Hagelee, L. A.; Köster, R. *Syn. React. Inorg. Metal-Org. Chem.* **1977**, 53.
(38) Balueva, A. S.; Erastov, O. A. *Izv. Akad. Nauk SSSR, Ser. Khim.* **1988**, 163.
(39) Balueva, A. S.; Nikonov, G. N. *Izv. Akad. Nauk, Ser. Khim.* **1993**, 378.
(40) Balueva, A. S.; Efremov, Y.; Nekhoroshkov, V. M.; Erastov, O. A. *Izv. Akad. Nauk SSSR, Ser. Khim.* **1989**, 2793.
(41) Grobe, J.; Goebelbecker, S.; Syndikus, D. *Z. Anorg. Allg. Chem.* **1992**, *608*, 43.
(42) Grobe, J.; Luetke-Brochtrup, K.; Krebs, B.; Laege, M.; Niemeyer, H. H.; Wuerthwein, E. U. *Z. Naturforsch. B: Chem. Sci.* **2006**, *61*, 882.
(43) Gaumont, A. C.; Carboni, B. *Sci. Synth.* **2004**, *6*, 485.
(44) Karsch, H. H.; Hanika, G.; Huber, B.; Meindl, K.; Koenig, S.; Krueger, C.; Mueller, G. *J. Chem. Soc. Chem. Commun.* **1989**, 373.
(45) Mueller, G.; Lachmann, J. *Z. Naturforsch. B: Chem. Sci.* **1993**, *48*, 1248.
(46) Braunschweig, H.; Dirk, R.; Englert, U. *Z. Anorg. Allg. Chem.* **1997**, *623*, 1093.

(47) Emslie, D. J. H.; Blackwell, J. M.; Britten, J. F.; Harrington, L. E. *Organometallics* **2006**, *25*, 2412.

(48) Bebbington, M. W. P.; Bouhadir, G.; Bourissou, D. *Eur. J. Org. Chem.* **2007**, 4483.

(49) Fukazawa, A.; Yamada, H.; Yamaguchi, S. *Angew. Chem. Int. Ed.* **2008**, *47*, 5582.

(50) Yuan, Z.; Taylor, N. J.; Marder, T. B.; Williams, I. D.; Kurtz, S. K.; Cheng, L. T. *J. Chem. Soc. Chem. Commun.* **1990**, 1489.

(51) Spies, P.; Schwendemann, S.; Lange, S.; Kehr, G.; Froehlich, R.; Erker, G. *Angew. Chem. Int. Ed.* **2008**, *47*, 7543.

(52) Spies, P.; Erker, G.; Kehr, G.; Bergander, K.; Froehlich, R.; Grimme, S.; Stephan, D. W. *Chem. Commun.* **2007**, 5072.

(53) Spies, P.; Kehr, G.; Bergander, K.; Wibbeling, B.; Froehlich, R.; Erker, G. *Dalton Trans.* **2009**, 1534.

(54) Fischbach, A.; Bazinet, P. R.; Waterman, R.; Tilley, T. D. *Organometallics* **2008**, *27*, 1135.

(55) Vergnaud, J.; Grellier, M.; Bouhadir, G.; Vendier, L.; Sabo-Etienne, S.; Bourissou, D. *Organometallics* **2008**, *27*, 1140.

(56) Thangavelu, S. G.; Hocker, K. E.; Cooke, S. R.; Muhoro, C. N. *J. Organomet. Chem.* **2008**, *693*, 562.

(57) Schmidbaur, H.; Sigl, M.; Schier, A. *J. Organomet. Chem.* **1997**, *529*, 323.

(58) Spies, P.; Froehlich, R.; Kehr, G.; Erker, G.; Grimme, S. *Chem. Eur. J.* **2008**, *14*, 333.

(59) Braun, J. *Compt. Rend. Acad. Sci.* **1965**, *260*, 218.

(60) Ashe, A. J.; Bajko, Z.; Carr, M. D.; Kampf, J. W. *Organometallics* **2003**, *22*, 910.

(61) Boerner, A.; Ward, J.; Kortus, K.; Kagan, H. *Tetrahedron: Asymmetry* **1993**, *4*, 2219.

(62) Fields, L. B.; Jacobsen, E. N. *Tetrahedron: Asymmetry* **1993**, *4*, 2229.

(63) Kimmich, B. F. M.; Landis, C. R.; Powell, D. R. *Organometallics* **1996**, *15*, 4141.

(64) Balueva, A. S.; Karaski, A. A.; Ayupova, E. I.; Musin, R. Z.; Nikohov, G. N. *Zh. Obshch. Khim.* **1994**, *64*, 1792.

(65) Brauer, D. J.; Hingst, M.; Kottsieper, K. W.; Liek, C.; Nickel, T.; Tepper, M.; Stelzer, O.; Sheldrick, W. S. *J. Organomet. Chem.* **2002**, *645*, 14.

(66) Chikkali, S.; Magens, S.; Gudat, D.; Nieger, M.; Hartenbach, I.; Schleid, T. *Eur. J. Inorg. Chem.* **2008**, 2207.

(67) Cordero, B.; Gomez, V.; Pletro-Prats, A. E.; Reves, M.; Echeverrýa, J.; Cremades, E.; Barragan, F.; Alvarez, S. *Dalton Trans.* **2008**, 2832.

(68) Batsanov, S. S. *Inorg. Mater.* **2001**, *37*, 871.

(69) Balueva, A. S.; Nikonov, G. N. *Zh. Obshch. Khim.* **1993**, *63*, 2704.

(70) Vul'fson, S. G.; Sarvarova, N. N.; Balueva, A. S.; Erastov, O. A.; Arbuzov, B. A. *Izv. Akad. Nauk SSSR, Ser. Khim.* **1988**, 1445.

(71) Emslie, D. J. H.; Harrington, L. E.; Jenkins, H. A.; Robertson, C. M.; Britten, J. F. *Organometallics* **2008**, *27*, 5317.

(72) (a) Miller, A. J. M.; Labinger, J. A.; Bercaw, J. E. *J. Am. Chem. Soc.* **2008**, *130*, 11874; (b) Miller, A. J. M.; Labinger, J. A.; Bercaw, J. E. *J. Am. Chem. Soc.* **2010**, *132*, 3301.

(73) Turculet, L.; Feldman, J. D.; Tilley, T. D. *Organometallics* **2004**, *23*, 2488.

(74) (a) A few reports describe the bridging coordination of M Cl bonds using other different donor buttresses:Lancaster, S. J.; Al-Benna, S.; Thornton-Pett, M.; Bochmann, M. *Organometallics* **2000**, *19*, 1599; (b) Crevier, T. J.; Bennett, B. K.; Soper, J. D.; Bowman, J. A.; Dehestani, A.; Hrovat, D. A.; Lovell, S.; Kaminsky, W.; Mayer, J. M. *J. Am. Chem. Soc.* **2001**, *123*, 1059.

(75) Baker, R. T.; Calabrese, J. C.; Westcott, S. A.; Marder, T. B. *J. Am. Chem. Soc.* **1995**, *117*, 8777.

(76) Oakley, S. R.; Parker, K. D.; Emslie, D. J. H.; Vargas-Baca, I.; Robertson, C. M.; Harrington, L. E.; Britten, J. F. *Organometallics* **2006**, *25*, 5835.

(77) Fontaine, F. G.; Zargarian, D. *J. Am. Chem. Soc.* **2004**, *126*, 8786.

(78) Thibault, M. H.; Boudreau, J.; Mathiotte, S.; Drouin, F.; Sigouin, O.; Michaud, A.; Fontaine, F. G. *Organometallics* **2007**, *26*, 3807.

(79) King, R. B. *Adv. Chem. Ser.* **1967**, 2, 203.

(80) Green, M. L. H. *J. Organomet. Chem.* **1995**, *500*, 127.

(81) (a) Early claims for transition metal-borane complexesShriver, D. F. *J. Am. Chem. Soc.* **1963**, *85*, 3509; (b) Parshall, G. W. *J. Am. Chem. Soc.* **1964**, *86*, 361; (c) Johnson, M. P.; Shriver, D. F. *J. Am. Chem. Soc.* **1966**, *88*, 301; (d) were not supported by structural authentication and their real identity has been strongly questioned: Braunschweig, H.; Wagner, T. *Chem. Ber.* **1994**, *127*, 1613; (e) Braunschweig, H.; Wagner, T. *Z. Naturforsch. B* **1996**, *51*, 1618; (f) Braunschweig, H.; Kollann, C. *Z. Naturforsch. B* **1999**, *54*, 839.

(82) Burlitch, J. M.; Burk, J. H.; Leonowicz, M. E.; Hugues, R. E. The borane complex $Et_4N^+[CpFe(CO)_2(BPh_3)]^-$ has been only spectroscopically characterized, *Inorg. Chem.* **1979**, *18*, 1702.

(83) Hill, A. F.; Owen, G. R.; White, A. J. P.; Williams, D. J. *Angew. Chem. Int. Ed.* **1999**, *38*, 2759.

(84) Foreman, M. R. St.J.; Hill, A. F.; White, A. J. P.; Williams, D. J. *Organometallics* **2004**, *23*, 913; (b) Crossley, I. R.; Hill, A. F. *Organometallics* **2004**, *23*, 5656; (c) Mihalcik, D. J.; White, J. L.; Tanski, J. M.; Zakharov, L. N.; Yap, G. P. A.; Incarvito, C. D.; Rheingold, A. L.; Rabinovitch, D. *Dalton Trans.* **2004**, 1626; (d) Crossley, I. R.; Hill, A. F.; Humphrey, E. R.; Willis, A. C. *Organometallics* **2005**, *24*, 4083; (e) Crossley, I. R.; Foreman, M. R. St.-J.; Hill, A. F.; White, A. J. P.; Williams, D. J. *Chem. Commun.* **2005**, *2005*, 221; (f) Landry, V. K.; Melnick, J. G.; Buccella, D.; Pang, K.; Ulichny, J. C.; Parkin, G. *Inorg. Chem.* **2006**, *45*, 2588; (g) Senda, S.; Ohki, Y.; Hirayama, T.; Toda, D.; Chen, J.-L.; Matsumoto, T.; Kawaguchi, H.; Tatsumi, K. *Inorg. Chem.* **2006**, *45*, 9914; (h) Pang, K.; Quan, S. M.; Parkin, G. *Chem. Commun.* **2006**, *2006*, 5015; (i) Figueroa, J. S.; Melnick, J. G.; Parkin, G. *Inorg. Chem.* **2006**, *45*, 7056; (j) Crossley, I. R.; Hill, A. F. *Dalton Trans.* **2008**, *2008*, 201; (k) Crossley, I. R.; Hill, A. F.; Willis, A. C. *Organometallics* **2008**, *27*, 312; (l) Crossley, I. R.; Foreman, M. R. St.-J.; Hill, A. F.; Owen, G. R.; White, A. J. P.; Williams, D. J.; Willis, A. C. *Organometallics* **2008**, *27*, 381; (m) Pang, K.; Tanski, J. M.; Parkin, G. *Chem. Commun.* **2008**, *2008*, 1008; (n) Crossley, I. R.; Hill, A. F.; Willis, A. C. *Organometallics* **2010**, *29*, 362; (o) Crossley, I. R.; Hill, A. F.; Willis, A. C. *Organometallics* **2007**, *26*, 3891; (p) Crossley, I. R.; Hill, A. F.; Willis, A. C. *Organometallics* **2005**, *24*, 4889.

(85) Crossley, I. R.; Hill, A. F.; Willis, A. C. *Organometallics* **2005**, *24*, 1062.

(86) Blagg, R. J.; Charmant Jonathan, P. H.; Connelly, N. G.; Haddow, M. F.; Orpen, A. G. *Chem. Commun.* **2006**, 2350.

(87) Blagg, R. J.; Adams, C. J.; Charmant, J. P. H.; Connelly, N. G.; Haddow, M. F.; Hamilton, A.; Knight, J.; Orpen, A. G.; Ridgway, B. M. *Dalton Trans.* **2009**, 8724.

(88) Owen, G. R.; Gould, P. H.; Hamilton, A.; Tsoureas, N. *Dalton Trans.* **2010**, 49.

(89) Owen, G. R.; Hugh Gould, P.; Charmant, J. P. H.; Hamilton, A.; Saithong, S. *Dalton Trans.* **2010**, *39*, 392.

(90) Tsoureas, N.; Haddow, M. F.; Hamilton, A.; Owen, G. R. *Chem. Commun.* **2009**, 2538.

(91) Tsoureas, N.; Bevis, T.; Butts, C. P.; Hamilton, A.; Owen, G. R. *Organometallics* **2009**, *28*, 5222.

(92) Grobe, J.; Martin, R. *Z. Anorg. Allg. Chem.* **1992**, *607*, 146.

(93) Bontemps, S.; Sircoglou, M.; Bouhadir, G.; Puschmann, H.; Howard, J. A. K.; Dyer, P. W.; Miqueu, K.; Bourissou, D. *Chem. Eur. J.* **2008**, *14*, 731.

(94) Hill, A. F. *Organometallics* **2006**, *25*, 4741.

(95) Parkin, G. *Organometallics* **2006**, *25*, 4744.

(96) Jones, P. G.; Maddock, A. G.; Mays, M. J.; Muir, M. M.; Williams, A. F. *J. Chem. Soc. Dalton Trans.* **1977**, 1434.

 (97) Bontemps, S.; Bouhadir, G.; Gu, W.; Mercy, M.; Chen, C. H.; Foxman, B. M.; Maron, L.; Ozerov, O. V.; Bourissou, D. *Angew. Chem. Int. Ed.* **2008**, *47*, 1481.

 (98) Sircoglou, M.; Bontemps, S.; Bouhadir, G.; Saffon, N.; Miqueu, K.; Gu, W.; Mercy, M.; Chen, C. H.; Foxman, B. M.; Maron, L.; Ozerov, O. V.; Bourissou, D. J. *Am. Chem. Soc.* **2008**, *130*, 16729.

 (99) Grobe, J.; Krummen, N.; Wehmschulte, R.; Krebs, B.; Laege, M. *Z. Anorg. Allg. Chem.* **1994**, *620*, 1645.

(100) Grobe, J.; Wehmschulte, R.; Krebs, B.; Laege, M. *Z. Anorg. Allg. Chem.* **1995**, *621*, 583.

(101) Grobe, J.; Luetke-Brochtrup, K.; Krebs, B.; Laege, M.; Niemeyer, H. H.; Wuerthwein, E. U. *Z. Naturforsch. B: Chem. Sci.* **2007**, *62*, 55.

(102) Wagler, J.; Hill, A. F.; Heine, T. *Eur. J. Inorg. Chem.* **2008**, 4225.

(103) Wagler, J.; Brendler, E. *Angew. Chem. Int. Ed.* **2010**, *49*, 624.

(104) (a) Gualco, P.; Lin, T. P.; Sircoglou, M.; Mercy, M.; Ladeira, S.; Bouhadir, G.; Perez, L. M.; Amgoune, A.; Maron, L.; Gabbai, F. P.; Bourissou, D. *Angew. Chem. Int. Ed.* **2009**, *48*, 9892; (b) Gualco, P.; Mercy, M.; Ladeira, S.; Coppel, Y.; Maron, L.; Amgoune, A.; Bourissou, D. *Chem. Eur. J.* **2010**, *16*, 10808.

(105) (a) Stille, J. K.; Lau, K. S. Y. *Acc. Chem. Res.* **1977**, *10*, 434; (b) Rodriguez, N.; Ramírez de Arellano, C.; Asensío, G.; Medio-Simón, M. *Chem. Eur. J.* **2007**, *13*, 4223; (c) Gourlaouen, C.; Ujaque, G.; Lledós, A.; Medio-Simón, M.; Asensio, G.; Maseras, F. *J. Org. Chem.* **2009**, *74*, 4049; (d) Luinstra, G. A.; Labinger, J. A.; Bercaw, J. E. *J. Am. Chem. Soc.* **1993**, *115*, 3004; (e) Vigalok, A. *Chem. Eur. J.* **2008**, *14*, 5102.

(106) (a) Grimmett, D. L.; Labinger, J. A.; Bonfiglio, J. N.; Masuo, S. T.; Shearin, E.; Miller, J. S. *J. Am. Chem. Soc.* **1982**, *104*, 6858; (b) Grimmett, D. L.; Labinger, J. A.; Bonfiglio, J. N.; Masuo, S. T.; Shearin, E.; Miller, J. S. *Organometallics* **1983**, *2*, 1325.

(107) (a) Ostoja Starzewski, K. A.; Kelly, W. M.; Stumpf, A.; Freitag, D. *Angew. Chem. Int. Ed.* **1999**, *38*, 2439; (b) Ostoja Starzewski, K. A. *Macromol. Symp.* **2004**, *213*, 47.

(108) Ostoja Starzewski, K. A.; Xin, B. S.; Steinhauser, N.; Schweer, J.; Benet-Buchholz, J. *Angew. Chem. Int. Ed.* **2006**, *45*, 1799.

(109) Ostoja Starzewski, K. A.; Steinhauser, N.; Xin, B. S. *Macromolecules* **2008**, *41*, 4095.

(110) Bebbington, M. W. P.; Bontemps, S.; Bouhadir, G.; Hanton, M. J.; Tooze, R. P.; van Rensburg, H.; Bourissou, D. *New. J. Chem.* **2010**, *34*, 1556.

(111) Hudnall, T. W.; Kim, Y.-M.; Bebbington, M. W. P.; Bourissou, D.; Gabbaï, F. P. *J. Am. Chem. Soc.* **2008**, *130*, 10890.

(112) Chapman, A. M.; Haddow, M. F.; Orton, J. P. H.; Wass, D. F. *DaltonTrans.* **2010**, *39*, 6184.

CHAPTER **2**

The Organometallic Chemistry of Group 10 Poly(pyrazolyl) borate Complexes

Ian R. Crossley*

Contents

Department of Chemistry, University of Sussex, Falmer, Brighton, UK

*Corresponding author.
E-mail address: i.crossley@sussex.ac.uk

I. INTRODUCTION

Poly(pyrazolyl)borate complexes of the group 10 triad are noticeably less numerous than for many transition metals. However, the study of these materials has typically proven more systematic than for many, dominated by investigation of reactivity traits, with limited incidence of purely derivative examples. Thus, though routinely included in generic studies of first-row complexes, those of Ni number far fewer than Cr, Fe, or Co, and while $Tp^xPd(\eta^3$-allyl) complexes are a standard target for successive generations of ''Tp^x'' ligand, there remain a modest number of examples. Indeed, the overwhelming emphasis would seem to lie with exploring *and* exploiting the phenomenon of C−H activation at Pd/Pt centers, and pursuing potential catalytic activity, albeit proving somewhat more elusive than one might anticipate.

This review is concerned only with those materials that conform to the generally accepted definition of ''organometallic,'' *and* those that, while not strictly ''organometallic,'' are or have the potential to be of interest and utility to the organometallic chemist. Thus, the inclusion of all complexes featuring an M−C linkage, along with related metal hydrides, phosphanes, and nitrosyls, is implicit. Beyond this, classical coordination compounds (e.g., homoleptic Tp^x complexes, halides, nitriles, sulfides, etc.) are included only where these possess substantiated or perceived utility to the field (e.g., synthetic precursors, catalysts) or serve to illustrate novel structural facets of far-reaching significance. Similar discretion is applied to the inclusion of more exotic materials that currently linger at the periphery of organometallic chemistry.

In organizing the review, one is immediately inclined to segregate the chemistry of nickel from that of its heavier congeners, in line with the limited extent to which the 3d metals mirror the 4d and 5d elements that are themselves conveniently considered in unison. Beyond this, material is subdivided according to the ligands of interest, prioritizing ''true'' organometallic pi and sigma complexes over metal hydrides and complexes of inorganic ligands (e.g., phosphanes). In general, where a complex embodies two or more *types* of ligand, it is classified on the basis of the greater chemical significance, and cross-referenced as appropriate. Purely derivative examples are treated as such and presented in tabular form. The final section considers the application of these materials to catalysis and other practical roles, drawing together information that is otherwise presented piecemeal throughout the review.

Standard conventions of poly(pyrazolyl)borate abbreviated nomenclature are applied; that is, Tp and Bp for the parent hydrotris- and dihydrobis(pyrazolyl)borate ligands, with pyrazole substituents denoted in the form $Tp^{R,4R',R''}$ where R, 4R', and R'' are substituents in the 3, 4, and 5

positions, respectively, omitted if none. Similarly, Tp^{R_2} denotes equivalent substituents in the 3/5 positions and Tp^{R_3} in all three positions. The nonsystematic, but commonly recognized abbreviations Tp* and Bp* will be used to denote the ligands derived from (3,5-dimethylpyrazole), that is, Tp^{Me_2} and Bp^{Me_2}. More complex systems will be defined as appropriate.

To the best of the author's knowledge, this review is comprehensive to the end of 2007 and includes selected material from the more recent literature. The reader should be aware that many palladium and platinum systems featured in a previous review in this journal, in the early 1990s.[1]

II. NICKEL

A. Homoleptic L$_2$Ni and heteroleptic LNiX and LL′Ni complexes

Relatively few simple homoleptic L_2Ni complexes have been prepared, among which only a handful are relevant here, by virtue of exhibiting agostic bridging between ligand and metal. The complexes Bp^{tBu}_2Ni (**1**) and $Bp^{tBu.Me}_2Ni$ (**2**),[2] prepared from $NiCl_2(py)_4$ and the respective $TlBp^x$, have both been crystallographically characterized with tetragonally distorted octahedral nickel(II) centers, comprising *trans* agostic $B-H\cdots M$ interactions [1.86(5) Å]. That these remain the sole such examples among Bp^x_2Ni complexes—even the simplest analogue Bp_2Ni (**3**) is devoid of $B-H\cdots M$ interactions[3,4]—implies some degree of steric promotion, though it is noted[2] that the agostic linkage exerts a bonding contribution to the stability of the complexes. It is also noteworthy that these compounds are pale-blue paramagnets (cf. orange and diamagnetic for most other cases).

More traditional agostic bonding has been suggested for the methylenic protons in complexes $\{Et_2Bp\}_2Ni$ (**4**) and $\{Bu_2Bp\}_2Ni$ (**5**),[5] on the basis of NMR studies. However, while a crystallographic study of **4** confirmed that these $C-H$ electron-pairs occupy apical positions close to nickel [2.459 Å],[6] there was no compelling evidence of an electronic interaction with the metal. Specifically, the lack of any perturbation in $Ni-N$ distances from those of other purely square-plane analogues mitigated against the $C-H$ functions behaving as apical ligands. A similar dearth of such interactions was reported for the related complex $\{Ph_2Bp\}_2Ni$ (**6**).[7]

Finally of note is the 1,5-cyclooctanediylbis(pyrazolyl)borate complex $\{BBN(pz)_2\}_2Ni$ (**7**, BBN = borabicyclononane),[8] which, as previously observed of its cobalt analogue,[8,9] exhibits significant agostic bonding between nickel and the bridgehead protons located above and below the N_4 plane. While this situation was confirmed crystallographically for the cobalt system, interactions in **7** were implied solely on the basis

of a strong, sharp infrared absorption (ν_{CH} 2800 cm^{-1}), the otherwise characteristic low-frequency ^{1}H NMR resonance for the bridging nuclei[5] being obscured by the remaining 1,5-cyclooctanediyl protons.

A somewhat wider range of heteroleptic LNiX (X = halide) complexes has been prepared, typically commencing from NiCl$_2$·6H$_2$O and alkali metal salts of the respective ligand. In an organometallic context, the complexes Tp^{x}NiX (X = Cl, Tp^x = Tp^{iPr_2} (**8**),[10] Tp^{Ph,Me} (**9**);[11] X = Br, Tp^x = Tp^{Me_2,4Br} (**10**)[12]) have served prominently as synthetic precursors, as have the labile acetonitrile complexes [Tp^{x}Ni(NCMe)$_3$]OTf (Tp^x = Tp^{iPr_2} **11.OTf**, Tp^{Ph,Me} **12.OTf**), generated by AgOTf metathesis of **8** and **9** in acetonitrile.[11] Beyond this, several Tp^{x}NiCl complexes have been demonstrated to be effective polymerization catalysts (Section IV.A). Thus, the mesitylpyrazole-derived complexes Tp^{x}NiCl (Tp^x = Tp^{Ms} (**13**), Tp^{Ms*} (**14**), Tp^{Ms**} (**15**); Tp^{Ms} = HB(3-mesityl)$_3$, Tp^{Ms*} = HB(3-mesityl)$_2$(5-mesityl), Tp^{Ms**} = HB (5-mesityl)$_2$(3-mesityl)) were each found to effect the oligomerization of ethylene in the presence of MAO with appreciable selectivity (>81%) for 1-butene.[13] Moreover, **13** was utilized in a tandem catalytic system with Cp$_2$ZrCl$_2$ for the generation of linear low-density polyethylene (LLDPE), the system activity, and polymer melting-point, increasing in line with the nickel mole-fraction.[14] Ethylene polymerization has also been demonstrated with Tp*NiCl (**16**), Tp^{tBu,Me}NiCl (**17**), and Tp^{Cum,Me}NiCl (**18**, Cum = cumyl),[15] and a comprehensive range of Tp^{x}NiX (X = F, Cl, Br) complexes are the subject of a patent[16] concerning their use as catalysts for the homo-, co-, and terpolymerization of α-olefins.

B. Hydrocarbyl π-complexes

There are, to date, no reports of discretely isolated neutral alkene complexes of the type [Tp^{x}Ni(η^2-alkene)], though one must presume their (transient) intermediacy in the polymerization of ethylene, which has been widely effected with a variety of nickel systems (Section IV.A). A single π-alkyne complex has been reported, the μ:η^2:η^2-alkyne-bridged, metal–metal bonded xenophilic complex **19** (Scheme 1), obtained by the interaction of diphenylacetylene with Tp^{Me_2,4Br}Ni−Co(CO)$_4$ (**20**).[17]
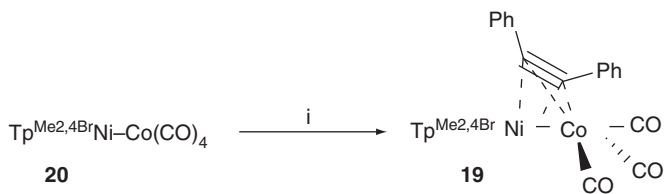
Scheme 1 Reagents: (i) PhC≡CPh.

A handful of complexes of monoanionic π-ligands are, however, known, including the η^3-allyls $Tp^xNi(\eta^3$-$C_3H_5)$ (Tp^x = Tp **21**,[18] Tp^{iPr_2} **22**[19]) and $Tp^{iPr_2}Ni(\eta^3$-$C_3H_3(Me_2$-3,3) (**23**)[20] (Scheme 2), all of which have been structurally characterized with essentially κ^3-Tp ligands, though the third N⋯Ni interaction is weak in each case. The chemistry of **22** has also been explored, to a limited extent, revealing that this material fails to liberate the alkene upon either protonolysis or hydrogenolysis, but will undergo oxygenation to afford the aldehyde CH_2=CHCHO.[20] It should also be noted that the use of complexes of the type $[Tp^xNi(\eta^3$-allyl)] as catalysts for olefin polymerization has been patented,[21] though their activity is significantly lower than the simple $[Tp^xNiCl]$ species.[16]
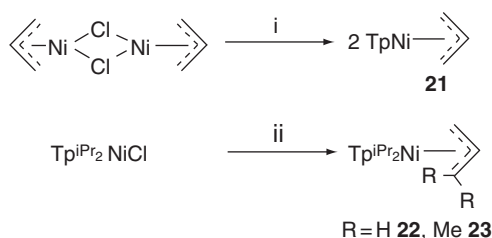
Scheme 2   Reagents and conditions: (i) KTp, thf, 24 h; (ii) $ClMgCH_2$=$CHCR_2$ (R = H, Me), thf, $-78\,°C\rightarrow$ r.t.

A somewhat larger range of mixed-sandwich complexes of the Tp^xNi fragment has been prepared, the earliest example being the 1,2,3-triphenylcyclopropenyl complex $Tp^*Ni(\eta^3$-$C_3Ph_3)$ (**24**), obtained from KTp* and $[Ni(\eta^3$-$C_3Ph_3)(PPh_3)_2]ClO_4$.[22] This complex was formulated on the basis of microanalytical data, and comparison of the ^{13}C NMR chemical shifts of the C_3Ph_3 unit with those of the structurally characterized [(triphos)Ni $(\eta^3$-$C_3Ph_3)$] (triphos = $CH_3C(CH_2PPh_2)_3$); κ^3-Tp* chelation was assumed.

The simplest Tp/Cp mixed sandwich, *viz.* TpNiCp (**25**) was originally prepared by the reaction of $[CpNi(PPh_3)Cl]$ with KTp,[18] which also affords 2 equiv. Tp_2Ni (**26**). Subsequent reaction of **25** with $LiCH_2C$ (Me)=CH_2 was also reported, resulting in displacement of the Tp fragment to afford $[CpNi(\eta^3$-C_3H_4Me-2)]$^+$. More recently, as part of a systematic investigation of $[TpMCp^x]$ (Cp^x = Cp, Cp*) complexes, **25** was resynthesized from $[CpNi(1,5$-cod)]$^+$,[23] a reaction that proceeds only in acetone and also affords variable quantities of **26** and Cp_2Ni, necessarily impacting upon the yield. Complex **25** is, however, isolable and moderately stable in the solid state, though somewhat air-sensitive in solution, properties mirrored by the structurally characterized analogue TpNiCp* (**27**), which was obtained more readily, commencing from $[Cp^*Ni(acac)]$ (acac = acetylacetonate). The chemical oxidation of **27** by $[Cp_2Fe]PF_6$ was

also effected, though it is noted that in coordinating solvents 27^+ decomposes with loss of Cp* to afford [TpNi(solvent)].

Electrochemical studies of both **25** and **27** were undertaken and revealed, *inter alia*, that the former is, surprisingly, slightly more difficult to oxidize than the latter, though both oxidation potentials are close to that of $NiCp_2$. In each case, a second redox event was also observed ($+585$ mV, irreversible. **27**; $+440$ mV, quasi-reversible **25**, relative to Fc^+/Fc couple), which was attributed to M(IV)/M(III) processes. The electronic and magnetic properties of $27/27^+$ were also explored in considerable detail,[24] revealing that the nominally 19-electron 27^+ obeys the Curie–Weiss law in the region 10–300 K, with μ_B greater than the spin-only value for 1 unpaired electron. No EPR signal was observed at room temperature, though a rhombic spectrum was recorded at 11 K, consistent with a $^2\Pi$ ground-state. In contrast, **27** displays Curie–Weiss behavior above 60 K, with μ_B consistent with $S = 1$, while below 30 K $1/\chi_M$ becomes independent of temperature. The large Zero-Field Splitting of a nondegenerate triplet ground state is deemed responsible for the lack of an EPR spectrum at 298 K, or below 20 K. The electronic structure of **27**, in comparison to the putative homoleptic systems Tp_2Ni and $NiCp^*_2$, was also investigated, using Density Functional Theory. This revealed, *inter alia*, three distinct sets of d-based orbitals of σ, δ, and π symmetry, of which the π-interaction is strongly antibonding. In respect of the Tp ligand this was attributed to σ-orbital overlap of the ''N lone pairs,'' while an antibonding component of the δ-orbital arises due to donation from the pyrazole π-MOs (two rings) augmented by a single ''N-lone pair'' donation, into the metal-based δ-orbitals. It was noted that the δ-orbitals of ''Tp''-based systems involve an appreciable ''Tp'' contribution (24% for **27**), while in Cp^*_2Ni the δ-orbital is overwhelmingly metal-based.

C. Complexes with σ-donor (alkyl, aryl) ligands

The literature includes few compounds of this type, with a particular dearth of metal-alkyls. Indeed, the synthesis of the ''simple'' alkyls $Tp^{iPr_2}Ni(R)$ from the respective chloride complex (**8**) and Grignard reagents has often proven difficult, attempts to prepare ethyl and *p*-methylbenzyl complexes in this way yielding only intractable decomposition mixtures upon warming to ambient temperature.[20,25] Formation of $Tp^{iPr_2}Ni(Et)$ (**28**) was, however, implied from the quantitative evolution of ethane during its decomposition. Moreover, by repeating the reaction under an atmosphere of CO,[20] **28** was ''trapped'' as the acyl complex $Tp^{iPr_2}Ni(CO)\{C(O)Et\}$ (**29**).[20,25] The *p*-methylbenzyl complex $[Tp^{iPr_2}Ni(CH_2C_6H_4Me\text{-}p)]$ (**30**) was similarly inferred, the analogous acyl (**31**)

being observed spectroscopically, though its propensity to lose CO precluded isolation.[20]

Despite these difficulties the related η^1-allyl complexes $Tp^{iPr_2}NiR$ (R = $CH_2CH=CHCH_3$ (crotyl) **32**; $CH_2CH=CMe_2$ (prenyl) **33**) have, apparently, been obtained via analogous methodology; that is, the reaction between **8** and RMgCl.[26] This is particularly remarkable, given that the latter reaction has been independently reported to afford exclusively the η^3-allyl complex **23**, with no evidence for formation of the η^1-prenyl species **33**.[20]

The remaining examples of relevant alkyl complexes, $BpNi(R)(PMe_3)$ (R = CH_2SiMe_3 **34**, CH_2CMe_3 **35**),[27] were readily obtained from the respective trans-$[Ni(R)Cl(PMe_3)_2]$ and KBp. Similarly, the aryl complexes $BpNi(Ph)(PMe_3)$ (**36**), $Tp*Ni(Ph)(PMe_3)$ (**37**), and $TpNi(C_6H_4X-o)(PMe_3)$ (R = H **38**, Me **39**) were obtained from trans-$[Ni(R)Br(PMe_3)_2]$ and the respective potassium salts, and each characterized as square-planar, κ^2-L (L = Bp, Tp^x) on the basis of spectroscopic data.[27] Analogous alkyl complexes proved inaccessible, the reactions of the respective $[Ni(R)X (PMe_3)_2]$ (R = CH_2SiMe_3, CH_2CMe_3, $CH_2C_6H_4Me-o$; X = Cl, Br) with KTp affording $[Tp_2Ni]$ (**26**) as the only isolable product; though for R = $CH_2C_6H_4Me-o$ in situ NMR studies revealed formation of $[Ni(PMe_3)_4]$ and $(C_8H_9)_2$ as by-products.[27] This lack of stability was attributed to the lower strength of the Ni-alkyl bond, relative to Ni-aryl.

In one final attempt to prepare nickel alkyls with Tp, the neophyl complexes trans-$[Ni(CH_2CMe_2C_6H_4R-p)Cl(PMe_3)_2]$ (R = H, Me) were treated with KTp, resulting in rearrangement of the neophyl ligand to afford the aryls $TpNi(1-C_6H_3-2-CMe_3-5-X)(PMe_3)$ (Scheme 3; X = H **40**, Me **41**). This rearrangement has literature precedent in the generation of $[CpNi(C_6H_4-o-CMe_3)(PPh_3)]$ as a by-product during the synthesis of $[CpNi(CH_2CMe_3Ph)(PPh_3)]$ from $[CpNiCl(PPh_3)]$ and the neophyl Grignard reagent.[28]
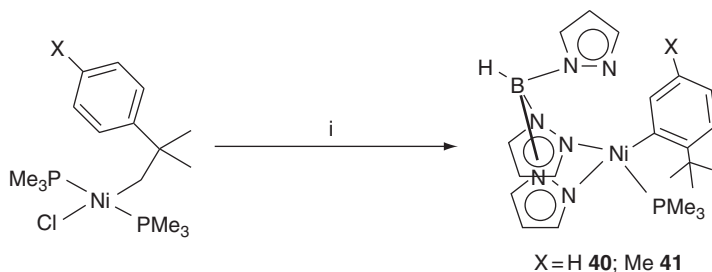
Scheme 3 Reagent: (i) KTp.

Difficulties were also encountered in the reactions between *trans*-[Ni(CH$_2$R)Cl(PMe$_3$)$_2$] (R = SiMe$_3$, CMe$_2$Ph, CN, CO$_2$Et) and TlBp^{tBu}, which failed to afford organometallic products, forming instead [Tp^{tBu}NiCl] (**42**).[2] The identity of **42** was determined on the basis of spectroscopic, microanalytical, and crystallographic data, the latter being obtained for 10 individual crystals to ensure reproducibility. The mechanism by which the Tp^{tBu} ligand was formed from [Bp^{tBu}]$^-$ under such mild conditions has not been established, though contamination of the TlBp^{tBu} salt with its Tp^{tBu} analogue has been ruled out; Lewis-acid-induced degradation of the Bp^{tBu} fragment was suggested.

The reactions of TlTp^{tBu} and TlBp^{tBu} with *trans*-[Ni(C$_6$H$_4$X-*p*)Br(PMe$_3$)$_2$] (X = H, Me, OMe, NMe$_2$) have also proven remarkable, resulting solely in displacement of bromide to afford *trans*-[Tp^{tBu}Ni(C$_6$H$_4$X-*p*)(PMe$_3$)$_2$] (X = H **43**,[29] Me **44**,[29] OMe **45**,[29] NMe$_2$ **46**)[27] and *trans*-[Bp^{tBu}Ni(C$_6$H$_4$X-*p*)(PMe$_3$)$_2$] (X = H **47**,[29] Me **48**,[29] OMe **49**,[29] NMe$_2$ **50**),[27] in which the poly(pyrazolyl)borate ligand adopts the rare κ^1 coordination mode. These compounds were initially formulated on the basis of microanalytical and spectroscopic data,[27,29] the latter also revealing a high barrier to rotation of the aryl group, and that fluxional equilibration of the pyrazolyl groups is apparently impeded by the high steric demand of the 3-*t*Bu substituent. Ultimately, the geometric arrangement of **44** was confirmed crystallographically (Figure 1).[27]

The reactivity of BpNi(R)(PMe$_3$), TpNi(R)(PMe$_3$), *trans*-[Tp^{tBu}Ni(C$_6$H$_4$X-*p*)(PMe$_3$)$_2$], and *trans*-[Bp^{tBu}Ni(C$_6$H$_4$X-*p*)(PMe$_3$)$_2$] toward CO
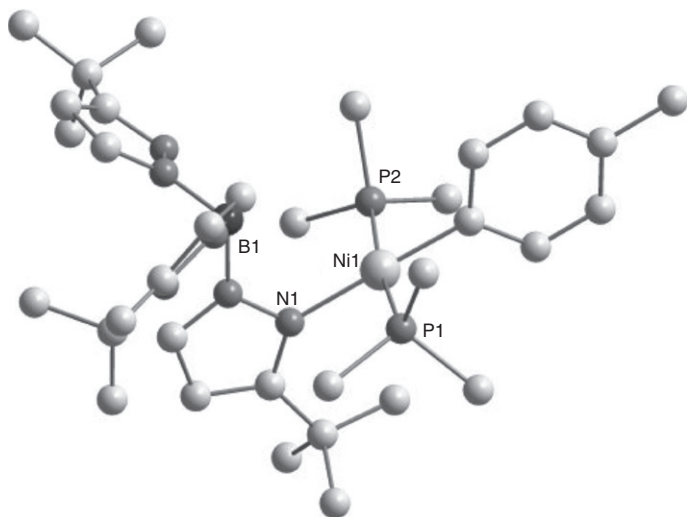
Figure 1 Molecular structure of Tp^{tBu}Ni(*p*-Tol)(PMe$_3$)$_2$ (**44**).

was briefly explored, revealing that the κ^2-Tp and κ^2-Bp complexes readily insert CO into the Ni$-$C linkage, affording the respective acyl and aroyl complexes (Section II.D.3).[27] In contrast, the κ^1-Tp^{tBu} and κ^1-Bp^{tBu} complexes fail to react with CO over periods of 5–10 min, but upon prolonged exposure undergo reduction to [Ni(CO)$_2$(PMe$_3$)$_2$].[27,29] Several aroyl complexes containing the κ^1-Tp^{tBu} or Bp^{tBu} ligands *have* been prepared, directly from the respective *trans*-[Ni{C(O)R}Br(PMe$_3$)$_2$] precursors, but are unstable toward the gradual loss of CO.[27,29] Complex **45** was also reacted with ZnCl$_2$, resulting in displacement of the Tp^{tBu} ligand by chloride.[27]

Finally, several aryl complexes have been derived from *trans*-[Ni(*o*-Tol)Br(PPh$_3$)$_2$] and used as catalysts in the copolymerization of carbon monoxide and ethylene. Thus, Tp^{Ph}Ni(*o*-Tol)(PPh$_3$) (**51**), prepared from TlTp^{Ph} and characterized crystallographically with a κ^2-Tp^{Ph} ligand, was found to be as effective a catalyst as more traditional palladium phosphane complexes, affording a strictly alternating polyketone above 20 °C and below 50 bar total pressure.[30] The potential of the flexible Tp^{Ph} ligand to alternate between κ^2 and κ^3 binding modes seems not to impede catalytic activity, and the presence of hard nitrogen donors is considered important in stabilizing the $+2$ oxidation state in the presence of CO, reduction to a Ni(0) carbonyl complex being the terminating step. The synthesis of analogous Tp, Tp*, and Tp$^{o\text{-}Tol,Me}$ complexes proved unsuccessful, however, Tp$^{o\text{-}Tol}$Ni(*o*-Tol)(PPh$_3$) (**52**) *was* obtained, but exhibited significantly less catalytic activity than **51**.[30]

In seeking to determine the importance of the B$-$H linkage in respect of catalytic activity, {BBN(pz)$_2$}Ni(*o*-Tol)(PPh$_3$) (**53**), which is devoid of a B$-$H functionality, was prepared from the K[BBN(pz)$_2$] salt.[31] Comparable activity to **51** was observed, though with somewhat lower efficiency; it was, however, established that neither the pendant pyrazolyl ring of **51**, nor the B$-$H functionality play any significant role in governing catalytic activity. An analogue of **53**, {κ^2-*N,O*-BBN(pz)(OH)}Ni(*o*-Tol)(PPh$_3$) (**54**), adventitiously obtained in the presence of trace moisture (presumed to partially hydrolyze [BBN(pz)$_2$]$^-$ since **53** cannot be directly hydrolyzed to **54**) was found to be completely inactive as a catalyst,[31] despite precedent for nickel centered N,O chelates to effectively catalyze polyketone formation.[32]

D. Complexes with σ-donor/π-acceptor ligands

1. Alkenyls and alkynyls

Surprisingly, there appear to be no examples of relevant nickel alkenyl compounds in the literature, nor is there any apparent reference to their unsuccessful pursuit. A single report describes the synthesis of an alkynyl complex, *viz.* the four-coordinate Tp^{iPr_2}Ni(C≡CCO$_2$Me) (**55**),[33] which was

identified on the basis of infrared spectroscopic data. Compound **55** was obtained in comparable fashion to its cobalt analogue, by condensation of HC≡CCO$_2$Me with the hydroxo-bridged precursor [{Tp^{iPr_2}Ni}$_2$(µ$_2$-OH)$_2$] (**56**). However, in contrast to cobalt, condensation of other terminal alkynes led only to intractable decomposition products, with the exception of HC≡CSiPh$_3$ which, as for cobalt, afforded exclusively [Tp^{iPr_2}NiO-SiPh$_3$] (**57**), due to preferential nucleophilic attack at the silicon atom by the oxygen donor.

2. Carbene complexes

Two such compounds have been obtained from the dimeric, alkylidene-bridged tetra-nickel complex **58** (Scheme 4), itself arising via α-H abstraction from metallacycle **59**, by an η^3-benzyl complex.[34] The reaction of **58** with KTp, resulted in cleavage of the halide bridges, with formation of **60**, which retains the µ-alkylidene unit, and was identified on the basis of analytical and spectroscopic data. Significantly, the spectroscopic data strongly implied the symmetric formulation of **60**, in which the Tp ligand adopts the κ^2-binding mode, rather than a nonsymmetric κ^3-Tp complex analogous to that obtained from **58** and NaCp. This disparity was further supported by observed similarities between the spectroscopic data for **60** and those for the Bp^{tBu} analogue **61**.
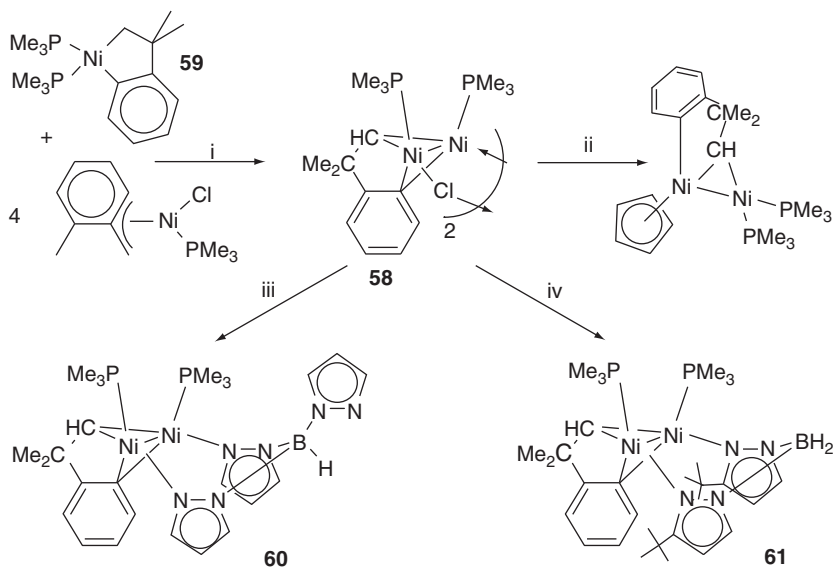
Scheme 4   Reagents and conditions: (i) Toluene; (ii) NaCp; (iii) KTp, (iv) TlBp^{tBu}.

One other carbene complex, a μ_2-vinylidene, has been prepared, from the xenophilic metal–metal bonded [$Tp^{Me_2,4Br}Ni$–$RuCp(CO)_2$] (**62**) upon its reaction with PhC≡CH. This affords **63**, which is bridged by both μ_2-C=C(H)Ph and μ_2-CO ligands (Scheme 5).[17]
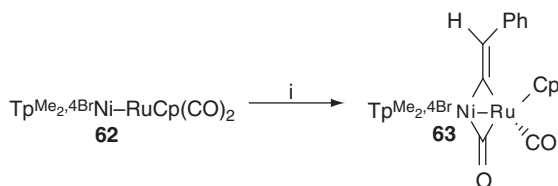
Scheme 5 Reagent: (i) PhC≡CH.

3. Carbonyls and acyls

Once again, few reports document the pursuit of such materials, and merely a handful are known. The only complexes of terminal carbonyls are the acyl species $Tp^{iPr_2}Ni(CO)\{C(O)R\}$ (R = Et **29**,[20,25] $CH_2C_6H_4Me$-p **31**),[20] obtained by alkylation of $Tp^{iPr_2}NiCl$ (**8**) under a CO atmosphere, or by *in situ* carbonylation of the respective alkyls $Tp^{iPr_2}Ni(R)$ (R = Et **28**,[20,25] $CH_2C_6H_4Me$-p **30**)[20] at −78 °C, the only conditions under which these are stable (Section II.D.3).

Carbonylation of BpNi(R)(PMe$_3$) (R = CH_2SiMe_3 **34**, CH_2CMe_3 **35**) and TpNi(Ph)(PMe$_3$) (**38**) has also been effected,[27] affording the respective acyls BpNi{C(O)R}(PMe$_3$) (R = CH_2SiMe_3 **64**, CH_2CMe_3 **65**) and TpNi{C(O)Ph}(PMe$_3$) (**66**), with no evidence for displacement of PMe$_3$. Similarly, carbonylation of TpNi(C_6H_4-o-tBu)(PMe$_3$) (**40**) affords TpNi{C(O)C_6H_4-o-tBu}(PMe$_3$) **67**, which was characterized *in situ*, due to a propensity to lose CO during workup; a similar issue was previously encountered with complex **31**. In contrast, carbonylation of the κ^1-Tp^{tBu} complexes *trans*-[$Tp^{tBu}Ni(C_6H_4X$-$p)(PMe_3)_2$] (**43–45**) resulted only in reduction to [Ni(CO)$_2$(PMe$_3$)$_2$]; the acyls *trans*-[$Tp^{tBu}Ni\{C(O)C_6H_4X$-$p\}(PMe_3)_2$] (X = H **68**, Me **69**, OMe **70**) were instead prepared directly from the respective *trans*-[Ni{C(O)C_6H_4X-p}(PMe$_3$)$_2$].[27,29] The same procedure was employed in the synthesis of Tp*Ni{C(O)Ph}(PMe$_3$) (**71**).[27]

Several carbonyl-bridged complexes have been encountered during the investigation of heteropolymetallic xenophilic complexes of the Tp^xNi fragment.[12,17,35] Thus, treating the nickel halides [Tp^xNiX] (Tp^x = Tp^{iPr_2}, $Tp^{Me_2,4Br}$; X = Cl, Br) with K[ML$_n$] (ML$_n$ = Co(CO)$_4$, Co(CO)$_3$(PPh$_3$), RuCp(CO)$_2$, Mn(CO)$_5$) affords the heterobimetallic, metal–metal bonded complexes Tp^xNi–Co(CO)$_4$ (Tp^x = $Tp^{Me_2,4Br}$ **20**, Tp^{iPr_2} **72**), $Tp^{Me_2,4Br}Ni$–Co(CO)$_3$(PPh$_3$) (**73**), $Tp^{Me_2,4Br}Ni$–RuCp(CO)$_2$ (**62**)[35], and the heterotrimetallic complex {$Tp^{Me_2,4Br}Ni(\mu_2$-CO)$_3$}$_2$Mn (**74**), which features bridging carbonyls.[17]

The interactions of **20** and **62** with a variety of donors have been investigated, revealing a tendency for hard donors to cleave the metal–metal bond, while soft donors tend to bind to the heterometallic (i.e., Co, Ru) fragment, typically inducing the carbonyl ligands to adopt a μ_2-bridging mode. Thus, treatment of **20** with the dppe and dppene (Scheme 6) or with tBuNC results in formation of the doubly bridged complexes **75–77**, while the interaction with diphenylacetylene preferentially affords the μ_2-η^2:η^2-alkyne-bridged species **19**, in which the carbonyls remain terminal to cobalt.[17]
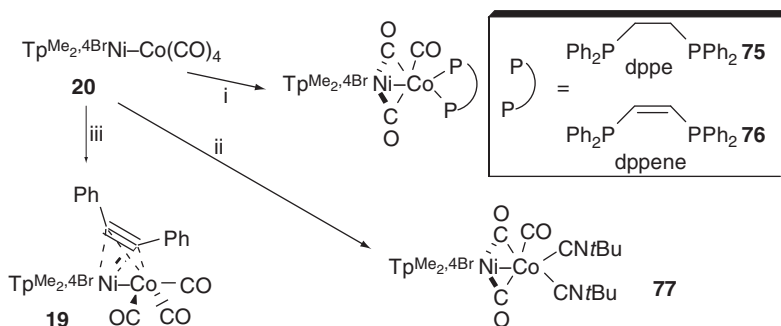
Scheme 6   Reagents: (i) dppe or dppene; (ii) tBuNC; (iii) PhC≡CPh.

Similarly, treatment of the nickel–ruthenium complex **62** with a variety of donors (CO, CNCy, NCtBu, PPh$_3$) affords the doubly bridged complexes **78–81** (Scheme 7), wherein the donor binds to ruthenium. However, upon treatment with PhC≡CH, only one carbonyl adopts a bridging mode, the second bridge being provided by a μ_2-vinylidene (**63**), derived from a 1,2-hydride shift within the PhC≡CH ligand.
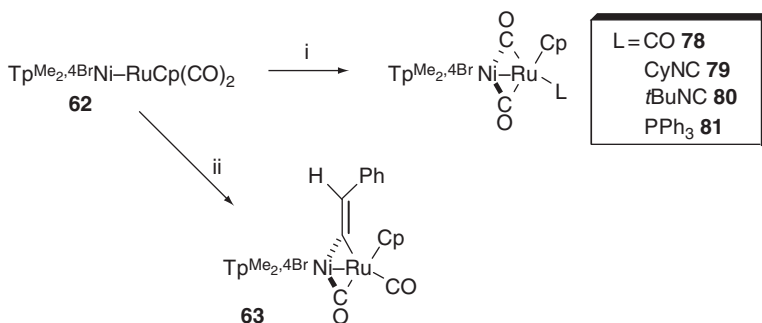
Scheme 7   Reagents: (i) L (CO, CyNC, tBuNC, PPh$_3$); (ii) PhC≡CH.

More complexity is observed in the case of the isothiocyanates CyN=C=S and PhN=C=S, which undergo fragmentation, speculated to be bimolecular in isothiocyanate (Scheme 8), to afford mixtures of the iminodithiocarbonato complexes **82** and **83** with the respective, carbonyl bridged, isonitrile complexes **79** and **84**.
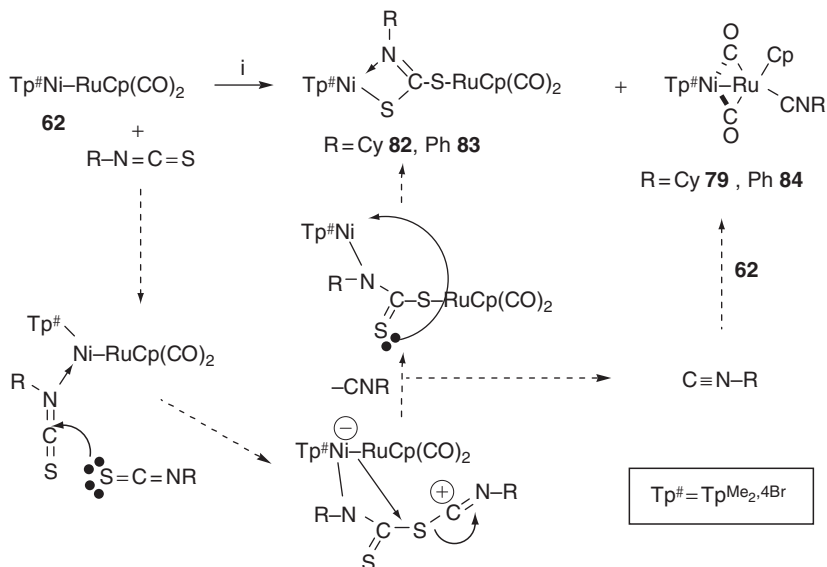
Scheme 8 Proposed mechanism for formation of **82/83** and **79/84** from the interaction of **62** with isothiocyanates.

4. Cyanide complexes

A single cyanide complex has been reported recently, the salt [Et$_4$N] [Tp*Ni(CN)$_2$] (**Et$_4$N[85]**),[36] obtained in the reaction of [Tp*Ni(OAc) (NCMe)] (**86**) with [Et$_4$N][CN]. Along with its cobalt and chromium analogues, **85**$^-$ was characterized on the basis of spectroscopic and crystallographic data, which revealed all three materials to be essentially isostructural. Moreover, in contrast to its congeners, **85**$^-$ was found to be diamagnetic.

5. Nitrosyl complexes

The first such complex, Tp*Ni(NO) (**87**), was very recently obtained from KTp* and [NiBr(NO)(PPh$_3$)$_2$], along with an analogue (**88**) based on the ''soft-scorpionate'' ligand hydrotris(2-seleno-1-mesitylimidazolyl)borate (Scheme 9).[37] In the same time frame Tp^{Ph_2}Ni(NO) (**89**) was independently

prepared in comparable fashion.[38] Both **87** and **88** were crystallographically characterized,[37] in each case demonstrating the presence of a linear NO ligand. The nature of the metal−NO bonding interaction in these complexes was studied by DFT calculations, leading the authors to conclude significant multiple-bond character, and to assign the metal a d^6 configuration, rather than the classically adopted d^{10}. It will be interesting to see how this work contributes to the apparently reigniting debate in respect of suitable treatise of the NO ligand, and how it applies to related systems.
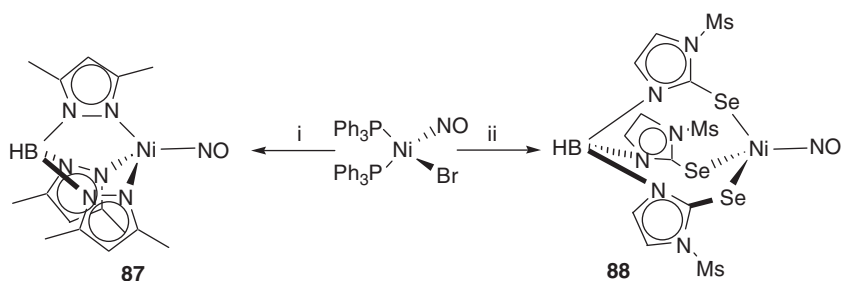
Scheme 9 Reagents: (i) KTp^{Me_2}, (ii) K[HB(C$_3$N$_2$(Mes)Se)$_3$].

E. Metallacarboranes

Like many late transition metals, nickel has featured, albeit briefly, in the pursuit of poly(pyrazolyl)borate–metal–carbollide complexes. Thus, [*closo*-3-(η^2-Ph$_2$Bp)-3,1,2-NiC$_2$B$_9$H$_{11}$]$^-$ (**90**$^-$) has been obtained as the tetramethylammonium salt,[39] via the reaction of [Me$_4$N][Ph$_2$Bp] with the neutral bisphosphine nickel dicarbollide [*closo*-3,3-(PhEt$_2$P)$_2$-3,1,2-
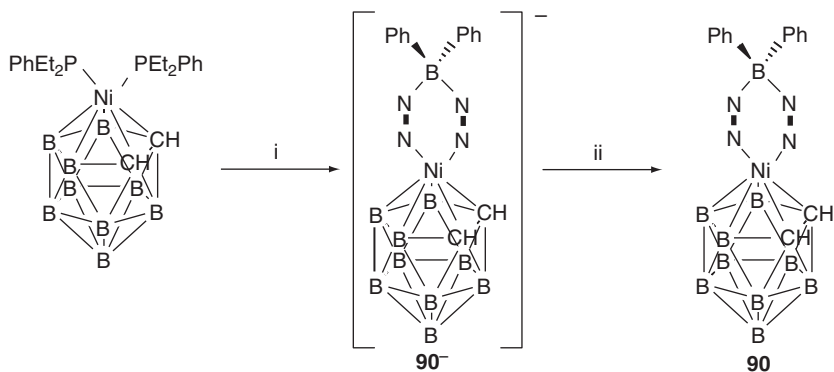
Scheme 10 Reagents: (i) [Me$_4$N][Ph$_2$Bp]; (ii) FeCl$_3$ (anhydr.), EtOH.
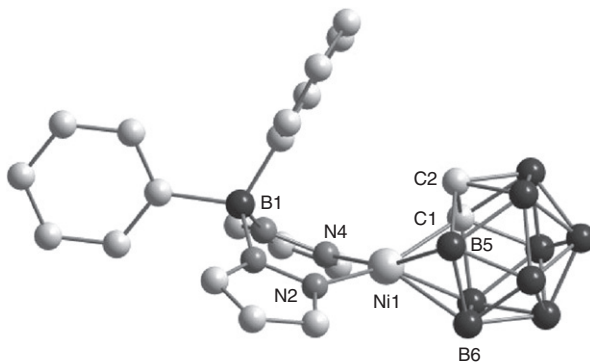
Figure 2   Molecular structure of [*closo*-3-(η^2-Ph$_2$Bp)-3,1,2-NiC$_2$B$_9$H$_{11}$]$^-$ (**90**$^-$).

NiC$_2$B$_9$H$_{11}$] (Scheme 10). Complex **90**$^-$ was fully characterized by ^{11}B{^{1}H} and ^{1}H NMR spectroscopy, confirming the anticipated local symmetry of the dicarbollide, and revealing dynamic behavior within the Ph$_2$Bp ligand, such that the *exo* and *endo* Ph groups are equivalent on the observational timescale. Crystallographic data for **90**$^-$ (Figure 2) revealed the anticipated geometry, which exhibits no distortion from an idealized *closo* cage; a feature mirrored in the bisphosphine precursor, but atypical among carbollides containing d^8 metals.

The oxidation of **90**$^-$ was effected with anhydrous ferric chloride in ethanol, affording the neutral d^7 nickelacarborane [*closo*-3-(κ^2-PhBp)-3,1,2-C$_2$B$_9$H$_{11}$] (**90**), which was found to be isostructural with its anionic congener.

One final nickel carbollide complex is noteworthy, albeit not strictly relevant insofar as it lacks a poly(pyrazolyl)borate ligand. This complex (**91**) is a so-called ''Venus Flytrap Cluster'' (VFC), in which Ni forms the capping vertex of two *closo*-carbollides, bridged by a pyrazole ring.[40] The VFC ligand is constructed in a single step from *closo*-1,8-C$_2$B$_9$H$_{11}$ by the pyrazole anion, then basified in solution to VFC^{3-}, which reacts with NiCl$_2 \cdot 6$H$_2$O to give **91** as a meso mixture of the D and L diastereoisomers (Scheme 11) that can be separated by recrystallization.

F. Metal hydrides

There are apparently no discrete Tp^{x}Ni hydrides in the literature, nor any dihydrogen complexes. A single borohydride complex, Tp*Ni(BH$_4$) (**92**), has been obtained recently via ligand metathesis from Tp*NiX (X = NO$_3$, Cl).[41] This complex was comprehensively characterized, and shown (crystallographically) to possess an octahedral nickel center, with facially tridentate Tp* and BH$_4$ ligands. In contrast to most nickel(II)
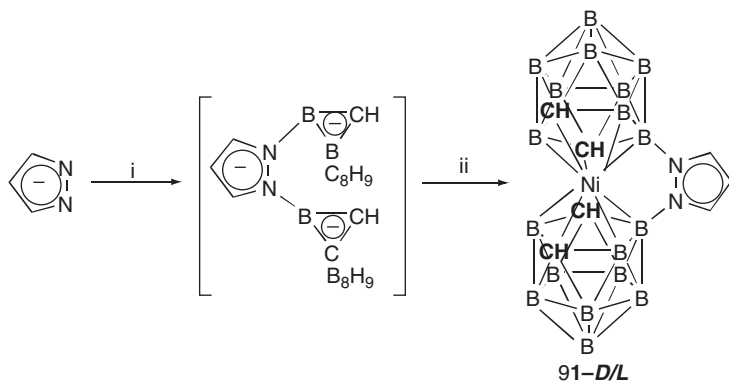
Scheme 11 Reagents: (i) $2C_2B_9H_{11}$; (ii) OH^-, $NiCl_2 \cdot 6H_2O$.

borohydrides, (e.g., $[Ni(BH_4)(PPh_3)_3]$),[42] wherein decomposition to Raney Nickel and nickel boride is prevalent,[43] **92** exhibits remarkable thermal, aerobic, and hydrolytic stability, and fails to catalyze hydrogenation reactions. However, **92** does readily effect the conversion of CX_4 (X = Cl, Br) and $CHBr_3$ to CX_2H_2 under ambient conditions, and reacts similarly with chloroform at elevated temperature. In contrast, dichloromethane is inert toward **92** even under reflux.[41] In the case of the CX_4 reactions, evolution of an infrared-silent gas was observed, the identity of which was inferred to be H_2 on the basis of a ^1H NMR signal at 4.65 ppm, which is also obtained from chloroform solutions of Tp*NiCl sparged with H_2.

G. Phosphane complexes

For nickel poly(pyrazolyl)borate complexes, phosphanes serve largely as ancillary ligands, and while undoubtedly exerting an influence upon the chemistry observed, are rarely directly involved therein. Indeed, in general, these ligands are spectators carried through from synthetic precursors. Thus, the square planar complexes $BpNi(R)(PMe_3)$ (R = CH_2SiMe_3 **34**, CH_2CMe_3 **35**, Ph **36**),[27] $Tp^xNi(R)(PMe_3)$ (Tp^x = Tp*, R = Ph **37**; Tp, R = Ph **38**, o-Tol **39**, C_6H_4-2-CMe_3 **40**, C_6H_3-2-CMe_3-5-Me **41**),[27] Tp^xNi (o-Tol)(PPh_3) (Tp^x = Tp^{Ph} **51**, $Tp^{o\text{-}Tol}$ **52**),[30] and $\{BBN(pz)_2\}Ni(o\text{-}Tol)(PPh_3)$ (**53**)[31] were all prepared directly from MTp^x (Tp^x = poly(pyrazolyl)borate, M = Na, K, Tl) and trans-$[Ni(R)X(PR_3)_2]$ (X = halide), with the exception of **40** and **41** that arose from trans-$[Ni(CH_2CMe_2C_6H_4R\text{-}p)Cl(PMe_3)_2]$ (R = H, Me)[27] via rearrangement of the neophyl ligand. The complex $\{\kappa^2\text{-}N,O\text{-}BBN(pz)(OH)\}Ni(o\text{-}Tol)(PPh_3)$ (**54**)[31] was also prepared from trans-$[Ni(o\text{-}Tol)Br(PPh_3)_2]$ and $K[BBN(pz)_2]$, but in the presence of moisture, it being noted that neither the free ligand, nor **53** hydrolyze independently.[31]

Complexes **34**, **35**, **38**, and **40** have been carbonylated to afford the respective acyls LNi{C(O)R}(PMe$_3$) (L = Bp, Tp; **64–67**), in which the phosphane ligand is retained.[27] In contrast, Tp*Ni{C(O)Ph}(PMe$_3$) (**71**) was prepared directly from *trans*-[Ni{C(O)Ph}Br(PMe$_3$)$_2$] and KTp*.[27] However, when the same complex is treated with TlTp^{tBu}, the bis(phosphane) complex *trans*-[κ^1-N-Tp^{tBu}Ni{C(O)Ph}(PMe$_3$)$_2$] (**68**)[27,29] is instead obtained, in which the Tp^{tBu} ligand adopts the rare κ^1 coordination mode. The analogues *trans*-[κ^1-N-Tp^{tBu}Ni{C(O)C$_6$H$_4$X-p}(PMe$_3$)$_2$] (X = Me **69**, OMe **70**)[27,29] have been similarly prepared, as have the parent aryl complexes *trans*-[κ^1-Tp^{tBu}Ni(C$_6$H$_4$X-p)(PMe$_3$)$_2$] (X = H **43**,[29] Me **44**,[29] OMe **45**,[29] NMe$_2$ **46**),[27] and *trans*-[κ^1-Bp^{tBu}Ni(C$_6$H$_4$X-p)(PMe$_3$)$_2$] (X = H **47**,[29] Me **48**,[29] OMe **49**,[29] NMe$_2$ **50**).[27] It is noted that carbonylation of these aryl complexes does not afford the respective acyls. Rather, short exposure leads to no reaction, while over prolonged periods reduction to [Ni(CO)$_2$(PMe$_3$)$_2$] prevails exclusively. See also Sections II.C and II.D.3.

Finally, the bimetallic alkylidene-bridged complex Ni$_2$(μ$_2$-CHCMe$_2$-o-C$_6$H$_4$)(μ$_2$-κ^1:κ^1-Tp)(PMe$_3$)$_2$ (**60**) and its Bp analogue **61**, in which each metal center bears one phosphane ligand, were prepared by cleavage of the chloride-bridged dimer [Ni$_2$(μ$_2$-CHCMe$_2$-o-C$_6$H$_4$)(μ$_2$-Cl)(PMe$_3$)$_2$]$_2$ with KTp and KBp, respectively (Scheme 4, Section II.D.2).[34]

H. Nonorganometallic coordination compounds

Few other such materials have significance in an organometallic context. However, it is noteworthy that a recent report has described the synthesis of what are seemingly the first nickel dithiocarbamates and organoxanthates supported by poly(pyrazolyl)borate ligands, *viz.* Tp^{Ph,Me}Ni(S$_2$CNR$_2$) (R = Et **93**, Ph **94**) and Tp^{Ph,Me}Ni(S$_2$COEt) (**95**).[44] These paramagnetic materials were prepared by metathesis of the respective sodium salts with Tp^{Ph,Me}NiCl (**9**) and were fully characterized spectroscopically (infrared, UV–Vis and tractable ^{1}H NMR) and crystallographically, revealing the dithiocarbamates to adopt square-planar solid-state geometries, while the xanthate adopts a 5-coordinate square-pyramidal motif.

III. PALLADIUM AND PLATINUM

A. Homoleptic L$_2$M and heteroleptic LMX$_{2−n}$(solv)$_n$ (n = 0, 1) complexes

In contrast to nickel, simple homoleptic Tp^x or Bp^x, and heteroleptic pyrazolylborate–halide complexes of palladium and platinum are largely unexplored. Indeed, while for 3d metals these are ''standard'' targets for each successive generation of poly(pyrazolyl)borate ligand, for the

heavier metals of group 10 this role has been exclusively filled by palladium allyls (Section III.B.2). Nonetheless, a handful relevant materials has been reported, the first, [(Bpz$_4$)$_2$Pd] (**96**), obtained as the sole, unexpected, product of reaction between NaBpz$_4$ (pzTpNa) and [Pd(C,N-C$_6$H$_4$CH=NPh)Cl]$_2$.[45] More recently, {BBN(pz)$_2$}$_2$Pd (**97**, BBN = borabicyclononane) was deliberately prepared from PdCl$_2$ and K[BBN(pz)$_2$], and also encountered fortuitously upon reacting the potassium salt with [Pd(η^3-C$_3$H$_5$)Cl]$_2$ under benzene reflux.[46] Though **97** has not received extensive study, magnetic inequivalence of the two (BC)H protons in the 9-BBN fragment suggest that, in common with nickel analogue **7**,[8] cobalt[8,9] and rhodium[47] congeners one of these protons from each ligand engages in an agostic interaction with the metal, though the extent of this remains unquantified. It should be noted that the related complex (Et$_2$Bp)$_2$Pd (**98**) has also been reported,[48] though its structural features have not been discussed.
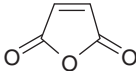
There is a single relevant heteroleptic metal halide complex, *viz.* Cl$_2$Pd (pz)$_2$B(pz)$_2$B(pz)$_2$PdCl$_2$ (**99**),[49] obtained from PdCl$_2$ and 0.5 equiv. of the B,B-tetrakis(pyrazolyl)pyrazabole (pz)$_2$B(pz)$_2$B(pz)$_2$, which was prepared from pyrazole and H$_2$B(pz)$_2$BH$_2$,[50] the latter generated from equimolar amounts of pyrazole and BH$_3$·NMe$_3$.[51] Complex **99** belongs to a class of pyrazolyl-bridged spirocomplexes, derived from B(pz)$_4$[52] and its pyrazabole homologues {B(pz)$_2$}$_n$, that were briefly the subject of intense study in the late 1960s and early 1970s. Much of this work employed organometallic capping groups of the type M(η^3-C$_3$H$_4$R) (M = Pd, Pt; R = H, alkyl), which are considered later (Section III.B.2).

B. Hydrocarbyl π-complexes

1. η^2-Alkene, alkyne, and allene complexes

Relatively few group 10 poly(pyrazolyl)borates complexes of this type are known, and most are based on platinum. Indeed, the first such materials reported were a series of 5-coordinate complexes of the type TpPt(Me)(η^2-L), where L = alkene, alkyne, allene. Complexes **100–125** (Table 1) were each prepared by treatment of the insoluble, and presumed polymeric, complex TpPtMe (**126**)[53–56] with the respective unsaturated hydrocarbon, and fully characterized by NMR spectroscopy. It was thus confirmed that the Tp ligand adopts a static κ^3-binding mode, since a 2:1 ratio is observed for the pyrazolyl 4-proton resonances, each of which exhibit coupling to the platinum center. In the case of the nonsymmetric acetylene complexes (**117–122**), the observation of three unique pyrazolyl environments in the ^{1}H NMR spectra suggested that the RC≡CR′ unit is constrained to the trigonal plane,[54,56] a situation subsequently confirmed crystallographically for the hexafluorobut-2-yne complex **115**.[57] An analogous situation was observed for the tetrakis(pyrazolyl)borate complexes **127–129**, which

Table 1 Summary of complexes of the type Tp^{x}PtMe(L) where L = alkene, alkyne

L	Cmpd	Ref#	L	Cmpd	Ref#
			TpPt(Me)(η^2-L)		
C_2H_4	**100**	60	*Trans*-C(CN)H=C(CN)H	**107**	60
C_2F_4	**101**	53,55	CH_2=C(CF_3)(CN)	**108**	53,55
CF_2=CH_2	**102**	53,55	CH_2=CH(CN)	**109**	54,55
CF_2=CFH	**103**	53,55	CH_2=C(Me)(CN)	**110**	54,55
cis-MeO$_2$CH=CHCO$_2$Me	**104**	54,55	*trans*-MeCH=CH(CHO)	**111**	54,55
trans-EtO$_2$CH=CHCO$_2$Et	**105**	54,55	CH_2=CHCO$_2$Me	**112**	54,55
	106	54,55		**113**	54,55
PhC≡CPh	**114**	56	PhC≡CMe	**119**	54,56
CF$_3$C≡CCF$_3$	**115**	54,56	HC≡CCO$_2$Me	**120**	56
MeO$_2$C≡CCO$_2$Me	**116**	54,56	HC≡COMe	**121**	56
MeC≡CCO$_2$Me	**117**	56	HC≡CCF$_3$	**122**	56
PhC≡CCO$_2$Me	**118**	56			
Me$_2$C=C=CMe$_2$	**123**	54,55	MeCH=C=CH$_2$	**125**	55
Me$_2$C=C=CH$_2$	**124**	54,55			
			[B(pz)$_4$Pt(Me)(η^2-L)]		
MeO$_2$C≡CCO$_2$Me	**127**	56	CF$_3$C≡CCF$_3$	**129**	56
PhC≡CPh	**128**	56			

For compound **106**: O=⟨cyclohexadiene⟩=O

For compound **113**: maleic anhydride structure (O=⟨ring⟩=O with O)

were prepared from pzTpPtMe (**130**), and found not to exhibit fluxion-
ality of either alkyne or B(pz)$_4$ ligands up to 90 °C.[56] Finally, infrared
spectroscopic data[54,56,58] for the alkyne complexes **114–122** revealed an
appreciable level of Pt(d_π)→C≡C(π^*) retrodonation, a corollary of the
donor properties of Tp, which serve to render these 5-coordinate Pt(II)
species unusually stable.

The allene complexes **123–125** were also determined to adopt trigonal
Static coordination in the trigonal plane was also established for the
alkene complexes **100–113**, on the basis of NMR spectroscopic,[54,55] and for
101 crystallographic,[59] data, though with the intrinsic potential for adopt-
ing multiple geometrical isomers, due to inequivalence of the upper and
lower faces of the alkene. While the *cis*-1,2 disubstituted alkenes dimethyl
maleate, maleic anhydride, and benzoquinone afforded single isomers
(R$_1$=R$_2$=substituents, R$_3$=R$_4$=H), isomeric mixtures were encountered
for the majority of unsymmetrical alkenes. Though these were not all
unequivocally identified, simple 1:1 mixtures were obtained with acrylo-
nitrile (**109**), methacrylonitrile (**110**), and *trans*-crotonaldehyde (**111**),
while methylacrylate (**112**) gave a 2:1 mixture. Similar mixtures (1:1)
were also encountered with CF$_2$=CFH and CH$_2$=C(CF$_3$)CN, though in
these cases the presence of the ^{19}F NMR reporter enabled unequivocal
assignment to **103a/b** and **108a/b**, respectively.[53,55] As with the alkyne
complexes, a significant amount of Pt(d_π)→C=C(π^*) retrodonation was
established on the basis of in-depth ^{13}C NMR spectroscopic studies.[60] One
further notable feature of all of the fluoro-olefin complexes **101–103** and
108 is the observation of a significantly enhanced coupling interaction
between the Pt−Me protons and spatially proximal ^{19}F-nuclei. Indeed,
only these proximal centers engage in coupling to the methyl protons,
hence a ''through-space'' mechanism was invoked.[53,55]

The allene complexes **123–125** were also determined to adopt trigonal
bipyramidal structures with the allene unit assuming a stereochemically
rigid position in the trigonal plane, even at 110 °C.[54] In the case of 1,1′-
dimethylallene (**124**), coordination is exclusively through the CH$_2$=C-
double bond,[54,55] while for methylallene (**125**) at least two of the four
possible geometric isomers were obtained, though their stereochemistry
remains undetermined, due to the complexity of the spectra (Chart 1).
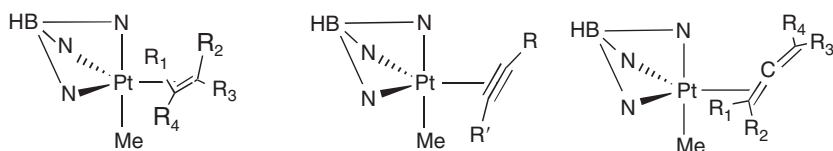
Chart 1   TpPt(Me)(η^2-L) geometries.

Attempts to prepare dihydrobis(pyrazolyl)borate analogues of the alkyne complexes **114–122** were unsuccessful, yielding immediately platinum metal.[56] However, it was subsequently found that the cyclooctadiene bridged dimers {(R$_2$Bp)PtMe}$_2$(cod) (R = Et **131**, Ph **132**), obtained from [PtMe(cod)(Me$_2$CO)]$^+$PF$_6$ and Na[R$_2$Bp],[61] react with a variety of donors to afford the respective square-planar complexes (R$_2$Bp)PtMe(L) (see also Sections III.C.3, III.D.2, III.F). Thus, Et$_2$BpPt(Me)(η^2-PhC≡CPh) (**133**), Et$_2$BpPt(Me)(η^2-PhC≡CMe) (**134**), and Ph$_2$BpPt(Me)(η^2-PhC≡CMe) (**135**) were obtained as crystalline materials and fully characterized spectroscopically,[61] and in the case of **134** crystallographically,[62] thus verifying the approximate square-planar geometry. The related complexes (Me$_2$Epz$_2$) PtMe(L) (L = PhC≡CPh, E = B **136**; Ga **137**) were similarly prepared directly from [PtMe(cod)Cl] and the respective Na[Me$_2$Epz$_2$], with subsequent addition of PhC≡CPh[63] (cf. formation of **131** and **132** which require pre-abstraction of the halide). In contrast, attempts to induce the reaction of **131** or **132** with but-2-yne, styrene, maleic anhydride, and dimethyl fumarate afforded only the starting materials,[61] while PhC≡CH, HC≡CCOMe, and C$_2$(CN)$_4$ yielded intractable mixtures.[61]

A key feature of the Tp acetylene complexes **114–122** is their apparent inertness toward alkyne insertion into the Pt–Me linkage,[54,56] and a similar situation is observed for **133–137**, which are recovered unaltered after prolonged benzene reflux.[61,63] In contrast, the electron deficient alkyne CF$_3$C≡CCF$_3$ rapidly inserted into the Pt–Me linkage of **131/132** to afford the respective alkenyls, which were isolated as the PPh$_3$ adducts R$_2$BpPt{C(CF$_3$)=C(CF$_3$)(Me)}(PPh$_3$) (R = Et **138**, Ph **139**). Similarly, DMAD immediately inserts to afford a mixture of two products, identified as *cis*-[R$_2$BpPt{C(CO$_2$Me)=C(CO$_2$Me)(Me)}] (R = Et **140**, Ph **141**; not isolated) and the chelate (**142/143**).[61] Comparable insertions are observed when using the Me$_2$Bp and Me$_2$Ga(pz)$_2$ ligands, though the products were not isolated.[63]
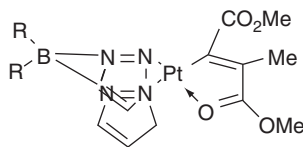
R = Et **142**; Ph **143**

The general stability of TpPtMe(η^2-RC≡CR) complexes, and their capacity to release the alkyne upon carbonylation,[56,63] has rendered the "TpPtMe" unit a potentially useful alkyne protecting group[64] affording stability under reactive conditions that might degrade the free alkyne. This was demonstrated by coordinating a series of bis(amide)acetylenes (complexes **144–149**, Scheme 12), then placing **144** under conditions of
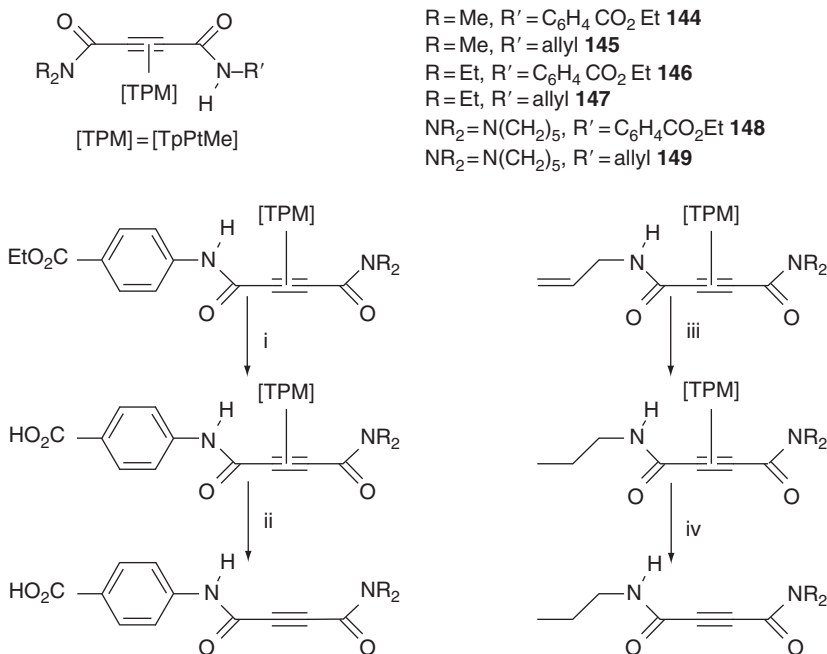
Scheme 12 Conditions and reagents: (i) LiOH, H_2O-THF; (ii) 60 atm., CO; (iii) H_2 Pd/C ethanol.

basic hydrolysis, while **145** was catalytically hydrogenated. Both complexes were then cleaved under 60 atm. CO, thus affording the free acetylenes and TpPt(Me)(CO) (**150**, Sections III.C.2, IV.A).

Despite this significant early work, the chemistry of η^2-hydrocarbyl complexes has not been appreciably further developed, and relatively few examples of ''simple'' η^2-hydrocarbyl ligands are recorded. Indeed, TpPtMe(η^2-C_2H_4) (**100**)[60] was the sole complex of C_2H_4 known before 2000, and only six more have been reported since. These were obtained by low-temperature protonation of the hydride complexes Tp*Pt(R)$_n$H$_{3-n}$ (R = Me, $n = 2$ **151**,[65] $n = 1$ **152**;[66] R = Ph, $n = 2$ **153**,[67] see also Section III.E) with [H(OEt$_2$)]BArf$_4$ (Ar^f = $C_6H_3(CF_3)_2$-3,5) under an atmosphere of C_2H_4, thus affording respectively the N-protonated complex cations [κ^2-N,N-(HTp*)Pt(R)(η^2-C_2H_4)]$^+$ (R = Me **154**$^+$,[65] H **155**$^+$,[66] Ph **156**$^{+}$[67]). In each case, the κ^2-HTp* ligand was identified on the basis of ^{1}H NMR and infrared spectroscopic data, and for **154**$^+$ by a single crystal X-ray diffraction study.[65]

Both **154**$^+$ and **156**$^+$ are deprotonated by treatment with NaH in THF to afford the respective neutral complexes Tp*Pt(R)(η^2-C_2H_4) (R = Me **157**,[65] Ph **158**[67]), while **158** is also obtained spontaneously from the ambient-temperature protonation of **153** under C_2H_4.[67]

The protonation of Tp*PtH$_3$ (**159**) in the presence of C$_2$H$_3$R (R = H, Me, Et, n-Pr) has also been described, affording [κ^2-N,N-{HTp*}Pt(H)(η^2-CH$_2$=CHR)]$^+$ (R = H **154**$^+$, Me **160**$^+$, Et **161**$^+$, n-Pr **162**$^+$) (Section III.E).[68]

The neutral 1-pentene complex Tp*Pt(H)(η^2-CH$_2$=CHn-Pr) (**163**) has also been obtained, upon the thermal reaction of Tp*PtMe$_2$H (**151**) with B(C$_6$F$_5$)$_3$ in n-pentane, an approach by which Tp*PtH(η^2-cycloalkene) (cycloalkene = cyclopentene **164**, cyclohexane **165**, cyclooctene **166**) were also generated from the respective cycloalkanes, and Tp*PtH(η^2-neohexene) (**167**) from *tert*-butylethane.[69] These reactions proceed via borane-induced methane elimination, followed by C−H activation of the solvent to afford the intermediate alkyls Tp*PtMe(R)H (R = C$_5$H$_{11}$ **168**, c-C$_5$H$_8$ **169**, c-C$_6$H$_{10}$ **170**, c-C$_8$H$_{14}$ **171**, CH$_2$CH$_2$^{t}Bu **172**), which are detectable by *in situ* ^{1}H NMR spectroscopy at low, constant concentrations. Continued heating results in loss of a second equivalent of methane, followed by β-elimination to afford the respective η^2-alkene complexes. The regioselectivity of this process was illustrated in the exclusive formation of the 1-pentyl and *tert*-butylethyl complexes **168** and **172**, and their conversion to alkene complexes **163** and **167**. Partial formation of the η^2-pent-2-ene complex **173** was, however, observed upon prolonged heating of **163**, and attributed to isomerization via 2,1-insertion into the Pt−H linkage and subsequent β-elimination. Similarly, while low-temperature protonation–deprotonation of Tp*PtPh$_2$H (**153**) in the presence of n-pentane afforded exclusively **163**, when the temperature was allowed to rise prior to the deprotonation step mixtures of **163** and **173** were obtained, presumably resulting from a similar isomerization process. It is noted that low-temperature protonation of the cycloalkene complexes **164** and **165** with [H(OEt$_2$)$_2$]BAr$^f_4$ was effected, affording the respective complexes [κ^2-HTp*PtH(η^2-cycloalkene)]$^+$ (c-C$_5$H$_8$ **174**$^+$, c-C$_6$H$_{10}$ **175**$^+$), which were also crystallographically characterized.

Beyond this work, the chemistry of neutral η^2-ethylene complexes remains largely unexplored. However, it has been reported that in the presence of B(C$_6$F$_5$)$_3$ at 60 °C, **158** converts to the platinacyclic complex **176** (Scheme 13).[67] This conversion, which also occurs in the absence of the borane at 80 °C, results from ethylene insertion into the Pt−Ph linkage, followed by rapid intramolecular orthometallation. A comparable reaction has also been noted with propene, though in this instance the intermediate η^2-complexes are never observed (see also Section III.C.1).

The low-temperature protonation chemistry of the dihydride Tp*Pt(Ph)(H)$_2$ (**177**) has also been explored, resulting in isolation of the η^2-benzene complex [κ^2-(HTp*)PtH(η^2-C$_6$H$_6$)]BAr$^f_4$ (**178.BAr$^f_4$**),[70] the identity of which was established on the basis of ^{1}H NMR spectroscopic studies, and ultimately by single crystal X-ray diffraction. The slow loss of benzene from **178**$^+$ is observed at 0 °C, affording a dihydride bridged dimer (Section III.E). However, below this temperature no exchange
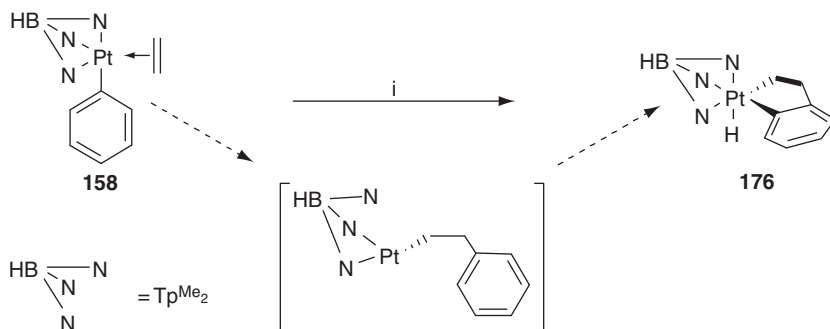
Scheme 13   Conditions and reagents: (i) B(C$_6$F$_5$)$_3$, 60 °C; *or* 80 °C.

occurs with free benzene, though at -20 °C evidence of exchange between the η^2-C$_6$H$_6$ and hydride ligands *is* observed, indicative of an equilibrium between aromatic C−H activation and elimination (Chart 2). Though the 5-coordinate species postulated to arise from the C−H activation step has not been discretely isolated, at temperatures below -30 °C it can be trapped as a 6-coordinate complex by the addition of nitriles. At higher temperatures, this results in displacement of the π-arene (Sections III.C.1.c, III.C.3).[71]
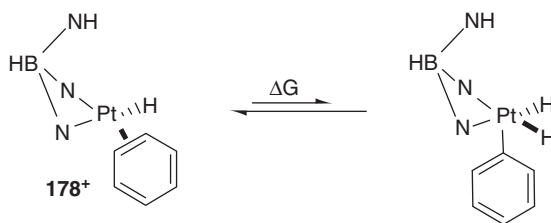
Chart 2   Equilibrium between η^2-benzene and σ-hydridophenyl complexes.

This work was extended to consider the analogous toluene (**179**$^+$) and *p*-xylene (**180**$^+$) systems, and [κ^2-(HTp*)Pt(Ph)(η^2-C$_6$H$_6$)]$^+$ (**181**$^+$, Scheme 14). Each of these were obtained by protonation of the respective aryl hydride complex Tp*Pt(R)H(Ar) (R = H, Ar = Tol **182**, 2,5-Xyl **183**; R = Ar = Ph **153**).[72] As with **178**$^+$, no evidence for arene dissociation is observed for either **179**$^+$ or **180**$^+$ below 0 °C, though both lose the arene above this temperature to afford the same dihydride-bridged dimer. In contrast, **181**$^+$ slowly exchanges coordinated benzene with the solvent at -100 °C.

Kinetic studies revealed that increased methyl substitution on the η^2-arene ligand resulted in a higher barrier to C−H activation ($\Delta G^{\ddagger} = 13.6$ kcal mol^{-1} **179**$^+$, 14.2 kcal mol^{-1} **180**$^+$), while the steric bulk of the ancillary ligand exerts a negligible effect ($\Delta G^{\ddagger} = 12.7$ kcal mol^{-1} **179**$^+$, 12.9 kcal mol^{-1} **181**$^+$).
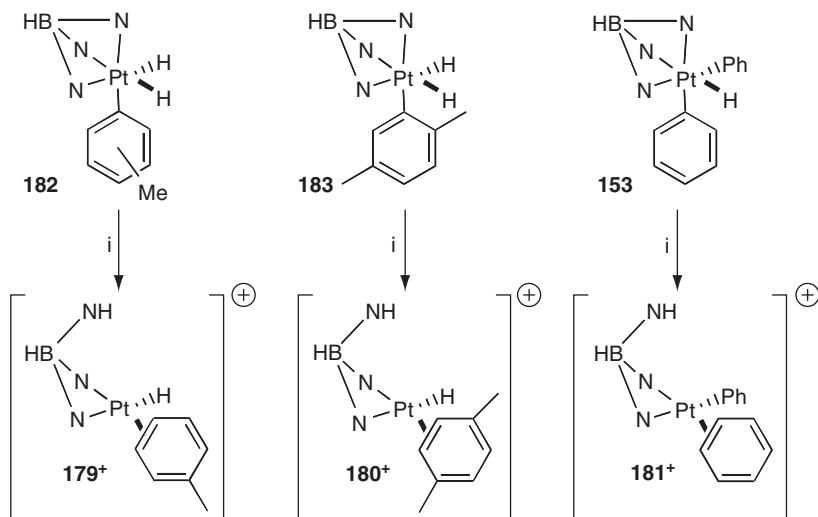
Scheme 14   Conditions and reagents: (i) [H(OEt$_2$)$_2$][BAr$^f_4$], −78 °C.

One final series of η^2-alkene complexes has been reported, which include the only examples of palladium-based poly(pyrazolyl)borate complexes with neutral alkene ligands. The complexes TpM(η^1:η^2-C$_8$H$_{12}$OMe) (M = Pd **184**, Pt **185**) and BpPt(η^1:η^2-C$_8$H$_{12}$OMe) (**186**), together with their cationic poly(pyrazolyl)methane analogues [(HCpz$_3$)M(η^1:η^2-C$_8$H$_{12}$OMe)]PF$_6$ (M = Pd **187.PF$_6$**, Pt **188.PF$_6$**) and [(H$_2$Cpz$_2$)M(η^1:η^2-C$_8$H$_{12}$OMe)]PF$_6$ (M = Pd **189.PF$_6$**, Pt **190.PF$_6$**) were obtained directly from the respective proligands and [M(η^1:η^2-C$_8$H$_{12}$OMe)Cl]$_2$, which was prepared from [M(η^4-C$_8$H$_{12}$)Cl$_2$] and methoxide (Scheme 15).[73] Attempts to prepare the palladium analogue of Bp complex **186** were unsuccessful, yielding only Pd metal. Comprehensive NMR spectroscopic studies confirmed the formulations of each of the isolated complexes, supported in the cases of **184** and **187.PF$_6$** by crystallographic data, and also revealed dynamic exchange of the pyrazolyl rings. For the bis(pyrazolyl) systems, this exchange was accompanied by inversion of the boat-like chelate, thus affording two isomers (A and B, Chart 3), both of which were present in solution, but could not be individually assigned.
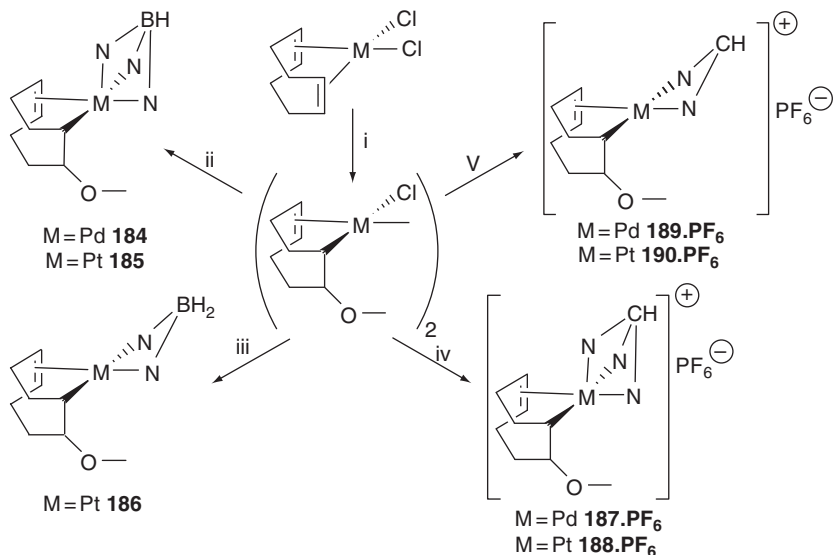
Scheme 15   Reagents: (i) NaOMe, (ii) NaTp, MeOH; (iii) NaBp, MeOH; (iv) HC(pz)$_3$, NaPF$_6$, MeOH; (v) H$_2$C(pz)$_2$, NaPF$_6$, MeOH.
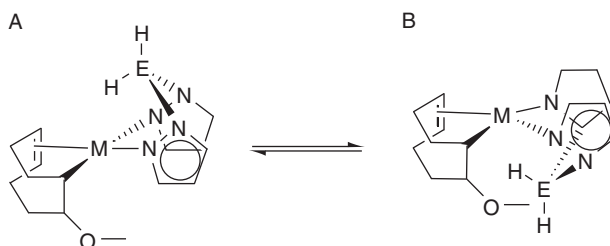
Chart 3   Inversion isomers of the BN$_2$M boat.

2. η^3-Allyl complexes

Whereas η^2-hydrocarbyl complexes are dominated by platinum, for η^3-allyl ligands palladium is the metal of choice. Indeed, TpPd(η^3-C$_3$H$_5$) (**191**) and pzTpPd(η^3-C$_3$H$_5$) (**192**), prepared from [PdCl(η^3-C$_3$H$_5$)]$_2$ and KTp or K[pzTp], respectively, were the first reported palladium(II) poly (pyrazolyl)borate complexes.[74] In the years since, LPd(η^3-allyl) have become "standard targets" for successive generations of "new" scorpionate ligands, typically attracting little or no discussion. Thus, the complexes LPd(η^3-CH$_2$CR′CH$_2$) (**193–210** L = Tp^x, (pz^x)Tp^x, R$_2$Bp^x; R′ = H, Me; Table 2, Chart 4), Tp^{Ph}Pd(η^3-CH$_2$C(Ph)CH$_2$) (**211**),[75] the related poly (1,2,4-triazolyl)borates {Et$_2$B(tz)$_2$}Pd(η^3-CH$_2$CRCH$_2$) (R = H **212**, Me **213** tz = 1,2,4-triazolyl) and {BBN(tz)$_2$Pd(η^3-CH$_2$CRCH$_2$) (R = H **214**, Me

Table 2 Summary of generic Tp^x and Bp^x palladium allyls

L	Cmpd	Ref#	L	Cmpd	Ref#
		$[LPd(\eta^3\text{-}C_3H_5)]$			
Et_2Bp	**193**	48	Ph_2Bp	**195**	48
$n\text{-}Pr_2Bp$	**194**	48	Tp^*	**196**	15
		$[LPd(\eta^3\text{-}CH_2C(Me)CH_2)]$			
Tp^{tBu}	**197**	75	Tp^{Me_2}	**204**	78
$(pz^{tBu})Tp^{tBu}$	**198**	75	Tp^{Br_3}	**205**	78
Tp^{Ph}	**199**	75	$Tp^{Ph,Me}$	**206**	79
$(pz^{Ph})Tp^{Ph}$	**200**	75	Tp^{4tBu}	**207**	80
Tp^{CHPh_2}	**201**	81	Tp^a	**208**	79
Tp^{Ms}	**202**	82	$Tp^{a,Me}$	**209**	79
Tp^{Ms*}	**203**	82	Tp^b	**210**	79
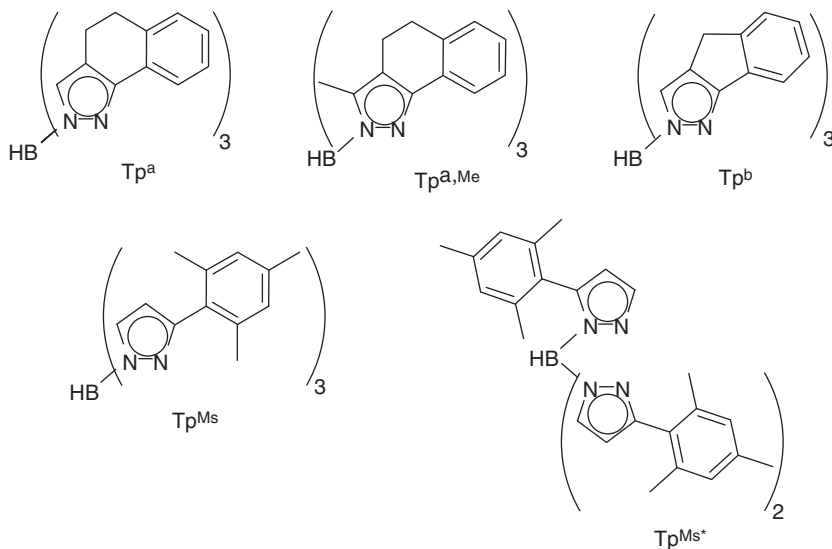
Chart 4 Polycyclic scorpionate ligands.

215,[76] and the poly(benzo-1,2,3-triazolyl)borates $\{H_nB(btz)_{4-n}\}Pd(\eta^3\text{-}C_3H_5)$ ($n = 1$ **216**, 0 **217**, btz = benzotriazolyl),[77] each obtained from the respective palladium allyl dimer and potassium salts, are all recorded in the literature without particular comment.

These compounds were all deemed to adopt square-planar geometries in the solid state, supported by crystallographic data for **191**,[83] **198**,[84] **204**,[78] and **205**,[78] though solution-phase NMR spectroscopic data illustrate

the dynamic behavior that has become a ubiquitous facet of such materials. Thus, coordinated and free pyrazole rings equilibrate on the NMR timescale, typically rapidly,[85] though in the case of **201** the steric bulk of the ''3-CHPh$_2$'' substituent imposes a slower exchange limit, such that resonances are significantly broadened.[82] Meanwhile, inversion of the boat-like chelate ring[84] and rotation of the η^3-allyl ligand about the Pd−B axis[82] serve to equilibrate both faces of the BN$_2$Pd plane.

Somewhat greater complexity is encountered with the 9-BBN-derived ligand BBN(pz)$_2$, in the complexes BBN(pz)$_2$Pd(η^3-CH$_2$CRCH$_2$) (R = H **218**,[8,46] Me **219**,[8] Ph **220**[8]), obtained from the respective [Pd(η^3-allyl)Cl]$_2$ and sodium[46] or thallium[8] salt of [BBN(pz)$_2$]$^-$. In each case, two isomers, corresponding to two possible rotameric conformations of the η^3-allyl ligand, were observed, in the ratios 1:1 (**218**) and 2:1 (**219** and **220**), the least sterically demanding isomer being presumed to dominate.[8] The possibility of agostic interaction between the bridgehead protons of the BBNpz$_2$ ligand and Pd, as seen for the homoleptic {BBN(pz)$_2$}$_2$Pd (**97**) and Ni (**7**),[8] Co and Rh[8,9] analogues, was suggested for both **218** and **219**, though no definitive evidence was presented. A similar situation was encountered with the somewhat more elaborate complexes Et$_2$Bp^{Fc}Pd (η^3-C$_3$H$_5$) (**221**) and {BBN(pz^{Fc})$_2$Pd(η^3-C$_3$H$_5$) (**222**), in which the pyrazole rings bear a 3-ferrocenyl substituent.[86] These complexes also exhibit four unique ^{1}H and ^{13}C NMR resonances for the four CH units of the pyrazole-bound C$_5$H$_4$ ring, which has been attributed to interaction between some of these units and the η^3-allyl ligand.

The most detailed body of work on allyls has focussed on the basic κ^2-B(pz)$_4$ ligand motif within the complexes pzTpPd(η^3-CH$_2$CRCH$_2$) (R = H **192**,[74] Me **223**,[49] Ph **224**[49]) and a rare example of a platinum methallyl, pzTpPt(η^3-CH$_2$CMeCH$_2$) (**225**, Scheme 16).[87] In each case, the two pendant pyrazole donors have been demonstrated to accommodate a second metal, or other Lewis acidic fragment, to afford a series of cationic spirocomplexes. Thus, in the presence of NaPF$_6$, equimolar amounts of Na[pzTp] and the respective [Pd(η^3-CH$_2$CRCH$_2$)Cl]$_2$ afford the symmetric salts [(η^3-CH$_2$CRCH$_2$)Pd(pz)$_2$B(pz)$_2$Pd(η^3-CH$_2$CRCH$_2$)]PF$_6$ (R = H **226.PF$_6$**,[52] Me **227.PF$_6$**, Ph **228.PF$_6$**).[49] These are also accessible by treating **192**, **223**, or **224** with one equivalent of the respective [Pd(η^3-CH$_2$CRCH$_2$) (solv)$_2$]BF$_4$, a route by which diplatinum complex **229**$^+$ was prepared from **225**.[87] This latter approach also affords access to asymmetric spiro cations, as demonstrated in the synthesis of [H(pz$_2$)B(pz)$_2$M(η^3-CH$_2$CMeCH$_2$)]$^+$ (M = Pd **230**$^+$, Pt **231**$^+$) from **223/225** and HBF$_4$, and [Et$_2$B(pz)$_2$B(pz)$_2$Pd(η^3-CH$_2$CRCH$_2$)]$^+$ (R = H **232**$^+$,[52] Me **233**$^+$, Ph **234**$^+$)[49] from pzTpPd(η^3-allyl) (**192**) and Et$_2$BOTs; these can also be accessed from Et$_2$B(pz)$_2$B(pz)$_2$ and [Pd(η^3-allyl)Cl]$_2$.[49,52] The neutral bimetallic complex (C$_6$F$_5$)$_2$Pd(pz)$_2$B(pz)$_2$Pd(η^3-CH$_2$CMeCH$_2$) (**235**) has been similarly obtained from **223** and cis-[(C$_6$F$_5$)$_2$Pd(NCPh)$_2$],[88] while the asymmetric
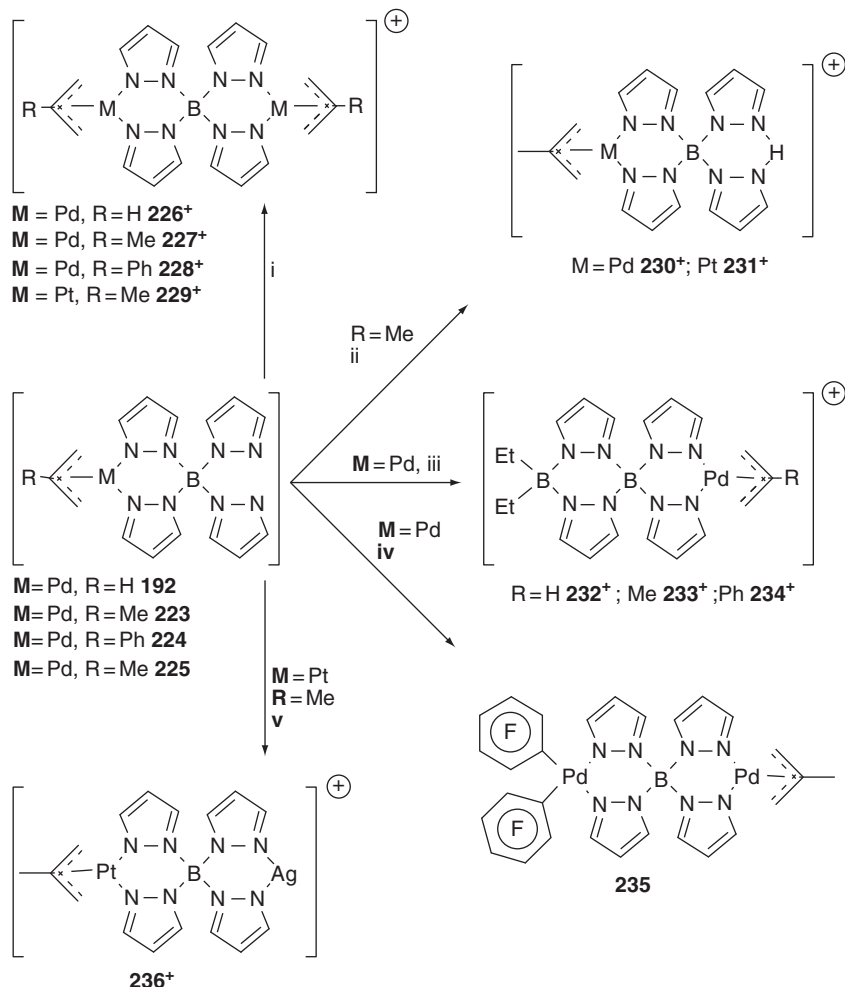
Scheme 16 Conditions and reagents: (i) $[M(\eta^3\text{-}CH_2CRCH_2)]BF_4$; (ii) HBF_4; (iii) Et_2BOTs; (iv) $[(C_6F_5)_2Pd(NCPh)_2]$; (v) $AgBF_4$.

complex cation $[Ag(pz)_2B(pz)_2Pt(\eta^3\text{-}CH_2CMeCH_2)]^+$ (236^+), of which no palladium analogue is known, is afforded upon treatment of **225** with $AgBF_4$.[87] In a further elaboration of the ''pyrazabole'' concept the dications 237^{2+}–239^{2+} were prepared from the respective $[Pd(\eta^3\text{-allyl})Cl]_2$ and $(pz)_2B(pz)_2B(pz)_2$ in the presence of 2 equiv. $NaPF_6$ (Scheme 17).[49,52]

Unsurprisingly, dynamic exchange of pyrazolyl groups on the NMR timescale was universally observed, equivalence of all pyrazolyl groups being noted for **192**, **223**, and **224** at ambient temperature, with the process slowed at $-40\,^\circ C$.[49,52] In contrast, the platinum analogue **225** exhibits

R=H **237²⁺**; Me **238²⁺**; Ph **239²⁺**
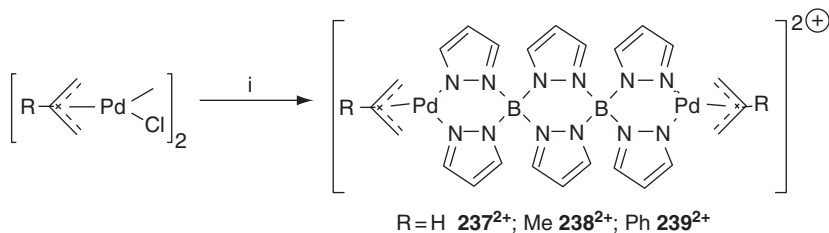
Scheme 17 Conditions and reagents: (i) (pz)$_2$B(pz)$_2$B(pz)$_2$, 2NaPF$_6$.

three pyrazolyl environments (2:1:1) between -90 °C and room temperature. Similar situations are encountered for the spirocomplexes, for which the favored conformation of the M(pz)$_2$B ring has become of key interest. Thus, the observation, below -38 °C, of two pyrazolyl environments in each of **226⁺**–**228⁺** led the authors to conclude that both Bpz$_2$Pd rings are puckered into ''boat-like'' conformations.[49,52] In contrast, the related ''pyrazabole'' complexes **232⁺**–**234⁺** each exhibit three pyrazole environments at low temperature (1:1:2), simplifying to two (2:2) at higher temperatures. These data were interpreted in terms of a planar Et$_2$B(pz)$_2$B fragment with magnetically inequivalent pyrazoles, due to the influence of the B(pz)$_2$Pd(η^3-allyl) boat,[49,52] which inverts at elevated temperatures to afford time-averaged C_{2v} symmetry. Similar geometries were concluded for the dicationic **237²⁺**–**239²⁺**, which appear highly symmetrical, with a B(pz)$_2$B unit and two rapidly inverting B(pz)$_2$Pd boats.[49,52] It should also be noted that a slow intermolecular exchange process was identified in the case of the simple spiro cations **228⁺** (Pd) and **229⁺** (Pt), demonstrated by equimolar mixtures of the two in CDCl$_3$ gradually giving rise to the mixed bimetallic complex (η^3-C$_3$H$_4$Me-2)Pt(pz)$_2$B (pz)$_2$Pd(η^3-C$_3$H$_4$Me-2) (**240**).[87]

Uniquely among group 10 poly(pyrazolyl)borate allyl complexes, some, albeit limited, reaction chemistry of the methallyls pzTpM(η^3-C$_3$H$_4$Me-2) (M = Pd **223**, Pt **225**) has been described.[87] Aside from the formation of spiro cations (*vide supra*) by both complexes, **225** was found to react rapidly with one equivalent of PPh$_3$ to afford the η^1-methallyl complex pzTpPt(η^1-CH$_2$CMe=CH$_2$)(PPh$_3$) (**241**, Scheme 18). The failure of palladium analogue **223** to react even with excess PPh$_3$ was attributed to the relative ease of $\eta^3 \rightarrow \eta^1$ allyl rearrangement for the two metals, that is, Pt $\gg$ Pd. The attempted synthesis of a phosphane-bridged analogue of **241** through reaction of **225** with ½ equiv. dppe resulted only in displacement of the B(pz)$_4$ ligand to afford the ion pair [(η^3-C$_3$H$_4$Me-2)Pd(κ^2-dppe)]$^+$[B(pz)$_4$]$^-$ **[242][B(pz)$_4$]**; however, the goal was achieved with 0.5 equiv. of dppb, affording **243** in good yields.
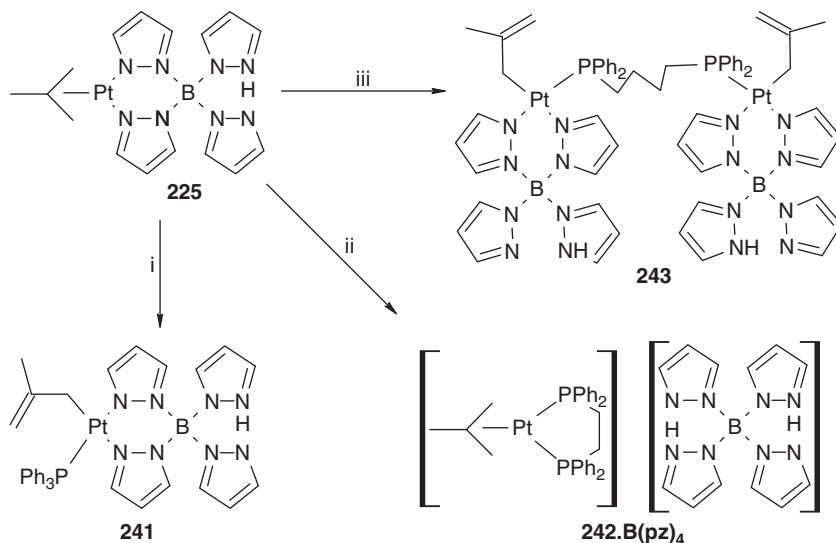
Scheme 18 Conditions and reagents: (i) PPh$_3$; (ii) dppe; (iii) Ph$_2$P(CH$_2$)$_4$PPh$_2$.

The chloromethallyl complex pzTpPd{η^3-C$_3$H$_4$(CH$_2$Cl)-2} (**244**) has also been prepared and reacted with NaSO$_2$Ph to afford the S-alkylated pzTpPd{η^3-C$_3$H$_4$(CH$_2$SO$_2$Ph)-2} (**245**).[89] This contrasts with the related Cp* systems that undergo O-alkylation of the sulfinate anion, a fact attributed to the donor capacity of the Cp* ligand.

Finally, there are two allyl complexes of the somewhat more exotic poly(pyrazolyl)borate ligand, (pz)$_3$B−B(pz)$_3$, obtained as the dipotassium salt from Kpz, pyrazole, and (Me$_2$N)$_2$B−B(NMe$_2$)$_2$.[90] In solution, these complexes, (η^3-CH$_2$CRCH$_2$)Pd(pz)$_2$B(pz)−B(pz)(pz)$_2$Pd(η^3-CH$_2$CRCH$_2$) (R = H **246**, Me **247**), undergo rapid exchange of the pyrazole groups, all of which appear equivalent on the ^{1}H NMR timescale. The formulation of κ^2,κ^2-(pz)$_3$B−B(pz)$_3$ binding in the solid state was, however, established on the basis of a single crystal X-ray study of **246**.

C. Complexes with σ-donor (alkyl, aryl) ligands

These are the most extensively studied class of poly(pyrazolyl)borate compounds for platinum and palladium, and rank among the most numerous and varied. The literature includes examples of M(II) and M(IV) centers in cationic, neutral, and anionic complexes, with all possible coordination numbers four to six represented; moreover, many of these complexes are readily interconverted. This section will therefore be organized according to oxidation state, as the most logical approach.

1. M(IV) complexes

The first example of a group 10 poly(pyrazolyl)borate complex in the $+4$ oxidation state was the dialkyl cation $[(\kappa^2\text{-pzTp})PtMe_2(PMe_2Ph)_2]PF_6$ (**248.PF$_6$**), prepared by reaction of $Na[B(pz)_4]$ with the dicationic $[PtMe_2(PMe_2Ph)_2](PF_6)_2$.[91] Though briefly commented upon for the magnitude of $J_{Pt-H(Me)}$ as an indicator of the level of 6s character at the platinum center,[56] **248$^+$** has received no further study, nor have any analogues been prepared.

a. Trimethyl M(IV) complexes   The first true ''study'' of M(IV) complexes described the isolation of the archetypal trimethylplatinum(IV) compounds pzTpPtMe$_3$ (**249**) and TpPtMe$_3$ (**250**)[1] from the ubiquitous $[Me_3PtI]_4$;[92] a route subsequently applied to the synthesis of Tp^{x}PtMe$_3$ (Tp^x = Tp* **251**,[93] Tp$^{(CF3)2}$ **252**)[94] via the intermediacy of the triflate $[Me_3Pt(OTf)]_4$. In each of the Tp^x systems spectroscopic data revealed a single pyrazolyl environment, consistent with facial coordination in complexes of C_{3v} symmetry. A single pyrazolyl environment was also observed in the B(pz)$_4$ complex **249** even down to -60 °C, indicating rapid dynamic exchange of coordinated and uncoordinated pyrazolyl groups on the NMR timescale.[92] The data for **251** and **252** also demonstrate significantly weaker Pt−N bonding for the fluorinated analogue, implicit from the reduced magnitude of $^4J_{Pt-H}$ to the pyrazole methine protons, in support of the crystallographic data.[94] Moreover, a long-range $^{19}F-^1H$ coupling was reported ($J = 3$ Hz), which, as in the fluoro-olefin π-complexes (Sections III.B.1, III.C.2) was attributed to a through-space interaction.

The original study also described the reaction between $[Me_3Pt]PF_6$ and KBp to afford BpPtMe$_3$ (**253**), also obtained from the iodide tetramer alongside unreacted $[Me_3PtI]_4$, in which the Bp ligand adopts the rare $\kappa^3\text{-}N,N,H$ binding mode.[92] This was the first example of Bp adopting an agostic binding motif at a group 10 metal. The assignment of this agostic mode from a strong ν_{BH} stretch (2039 cm^{-1}) was confirmed by synthesis of the deuterated (D$_2$Bpz$_2$) analogue **253-d_2**, and also by displacement of the B−H−Pt linkage with P(OMe)$_3$ to afford BpPtMe$_3\{P(OMe)_3\}$ (**254**), the agostic B−H infrared stretch being lost in both cases. Complex **254** was alternatively generated without isolation of **253**, by including P(OMe)$_3$ in the reaction of $[Me_3PtI]_4$ with KBp; by similar means the inherently unstable monocarbonyl BpPtMe$_3$(CO) (**255**) was also obtained and characterized *in situ* (ν_{CO} 2125 cm^{-1}) before loss of CO predominated. The isolable complexes BpPtMe$_3$(L) (L = pzH **256**, pz*H **257**) were similarly prepared. The pyridine adduct BpPtMe$_3$(py) (**258**) has also been reported,

---

[1] Complex **250** was also obtained upon reaction of Cp*PtMe$_3$ with KTp, demonstrating a high tendency for formation of this motif.

but obtained directly from [Me$_3$PtI(py)] and KBp,[95] and treated with PMe$_2$Ph to afford BpPtMe$_3$(PMe$_2$Ph) (**259**).

An alternative route to trimethyl-M(IV) complexes that has seen some utility is *in situ* methylation, by MeI, of the putative M(II) complex anions [Tp^{x}MMe$_2$]$^-$, which form on treatment of [PtMe$_2$(SEt$_2$)]$_2$ or [PdMe$_2$(tmeda)] with the respective KTp^x. Thus, the novel hydrotris (indolyl)borate complexes {HB(ind)$_3$}MMe$_3$ (M = Pt **260**, Pd **261**) were prepared from [{HB(ind)$_3$}MMe$_2$]$^-$K$^+$ (M = Pt **K.262**, Pd **K.263**),[96] and the dimethylbis(pyridyl)borate complex Me$_2$B(py)$_2$PtMe$_3$ (**264**) from [Me$_2$B (py)$_2$PtMe$_2$]$^-$ (**265**$^-$).[97] Complex **264** is remarkable in exhibiting facile methyl transfer from boron to platinum when oxidized by O$_2$ or MeI in alcohol solvents, thus affording κ^3-*N,N,O*-MeB(py)$_2$(OR)PtMe$_3$ (R = Me **266**, Et **267**) and methane; detailed mechanistic studies revealed the methane to originate from the parent PtMe$_3$ fragment.

This synthetic route has proven to be the method of choice for preparing trimethylpalladium (and other triorgano-group 10, *vide infra*) species, having also been applied to the synthesis of pzTpPdMe$_3$ (**268**),[98] TpPdMe$_3$ (**269**)[98] from the respective unisolated Pd(II) anions (pzTp **270**$^-$, Tp **271**$^-$), and the generation at -70 °C of BpPdMe$_3$(L) (L = py **272**, PMe$_2$Ph **273**), both of which undergo reductive elimination above 0 °C to afford BpPdMe(L) (L = py **274**, PMe$_2$Ph **275**), which were not isolated.[95]

Complex **269** has also been generated by water-oxidation of [TpPdMe$_2$]$^-$ (**271**$^-$),[99] which affords ''TpPdMe'' as a by-product that is isolable as the phosphane adduct TpPdMe(PPh$_3$) (**276**),[99] and results in liberation of H$_2$, as determined by *in situ* ^{1}H NMR spectroscopic studies.[100] This reaction was presumed to result from the slow oxidation of **271**$^-$ to an unobserved Pd(IV) species of the type ''TpPdMe$_2$(OH)'' (in equilibrium with [TpPdMe$_2$(OH$_2$)]$^+$) that is then attacked by **271**$^-$, resulting in methyl transfer from the Pd(IV) to Pd(II) center, a reaction for which precedent exists.[101,102] Evidence in support of this reaction sequence was sought by treating the anionic palladacyclic complex [TpPd(C$_4$H$_8$)]$^-$ (**277**$^-$, Scheme 19) with water, or more effectively H$_2$O$_2$, resulting in isolation of the moderately stable (-20 °C) TpPd(OH)(C$_4$H$_8$) (**278**), which is intrinsically inert toward alkyl transfer.[103] Structural data for **278** were obtained by virtue its forming crystalline adducts with phenol,[100] *m*-cresol[100,104], and pentafluorophenol,[100,104] each of which exhibit extensive levels of hydrogen bonding between the phenolic and Pd(OH) functions. In the case of **278.(C$_6$F$_5$OH)**, a somewhat foreshortened C–O distance within the C$_6$F$_5$OH unit [d(CO) 1.300(7) Å], relative to those in both C$_6$F$_5$O$^-$ and other hydrogen-bonded C$_6$F$_5$OH complexes,[100] led the authors to conclude that protonation had occurred, to afford the aquapalladium(IV) complex [TpPd(OH$_2$)(C$_4$H$_8$)]$^+$C$_6$F$_5$O$^-$ (**279.C$_6$F$_5$O**), further supporting the original postulate.

Scheme 19   Conditions and reagents: (i) H$_2$O, (ii) C$_6$F$_5$OH.

As was the case with **271**$^-$, the treatment of palladacycle **277**$^-$ with water also results in the liberation of H$_2$, the mechanistic features of which were studied theoretically, using the somewhat simplified model complex PdMe$_2${(H$_2$C=N-NH)$_3$BH},[105] and proceeding from the assumption that an unstable palladium-hydride species is involved. It was thus concluded that reduction of H$_2$O to H$_2$ involves two proton-transfers to palladium, each proceeding with protonation of the pendant pyrazolyl donor, which then behaves as an intramolecular nucleophile (Scheme 20).

b. Triorgano M(IV) complexes   The oxidation of diorganoplatinum(II) and palladium(II) complex anions by organohalides (*vide supra*) has become an important general synthetic route to M(IV) complexes bearing alkyl or aryl ligands. The complexes TpPdMe$_2$R (R = Me **269**,[98,99] Ph **280**,[98,99] Et **281**,[98] Bz **282**,[98] η^1-C$_3$H$_5$ **283**,[98]), TpPdMePhR (R = Ph **284**,[99] Bz **285**,[98,99] η^1-allyl **286**[98]), pzTpPdMe$_3$ (**268**),[98] pzTpPdMePhEt (**287**),[98] TpPd(C$_4$H$_8$)R (R = Me **288**,[98,106] Et **289**,[98] Bz **290**,[98,106] η^1-allyl **291**[98]), TpPtMe(p-Tol)$_2$ (**292**),[107] and Tp*PtR$_3$ (R$_3$ = Me$_3$ **251**, MePh$_2$ **293**)[108] were thus all obtained from the respective anions [TpPdMeR]$^-$ (R = Me **271**$^-$, Ph **294**$^-$),[99] [pzTpPdMeR]$^-$ (R = Me **270**$^-$, Ph **295**$^-$),[98] [TpPd(C$_4$H$_8$)]$^-$ (**277**$^-$),[98,106] [TpPt(p-Tol)$_2$]$^-$ (**296**$^-$),[107] or [Tp*PtR$_2$]$^-$ (R = Me **297**$^-$, Ph **298**$^-$)[108] and organohalides RX (R = MeI, EtI, BzBr, C$_3$H$_5$I). In similar fashion, treatment of the palladacyclic anion [TpPd{κ^2-CH$_2$CMe$_2$-o-C$_6$H$_4$}]$^-$ (**299**$^-$) with CH$_2$Cl$_2$ affords the chloromethyl complex TpPd{κ^2-CH$_2$CMe$_2$-o-C$_6$H$_4$}(CH$_2$Cl) (**300**, Scheme 21),[109] which in contrast to many Pd(IV) complexes demonstrates appreciable thermal stability, remaining unchanged upon heating to 90 °C.

The bis(pyrazolyl)borate complexes BpPdMeR(mq) (R = Me **301**, Ph **302**)[110] and BpPtMe$_2$(mq) (**303**,[95,110] Scheme 22, mq = 8-methylquinolinyl)
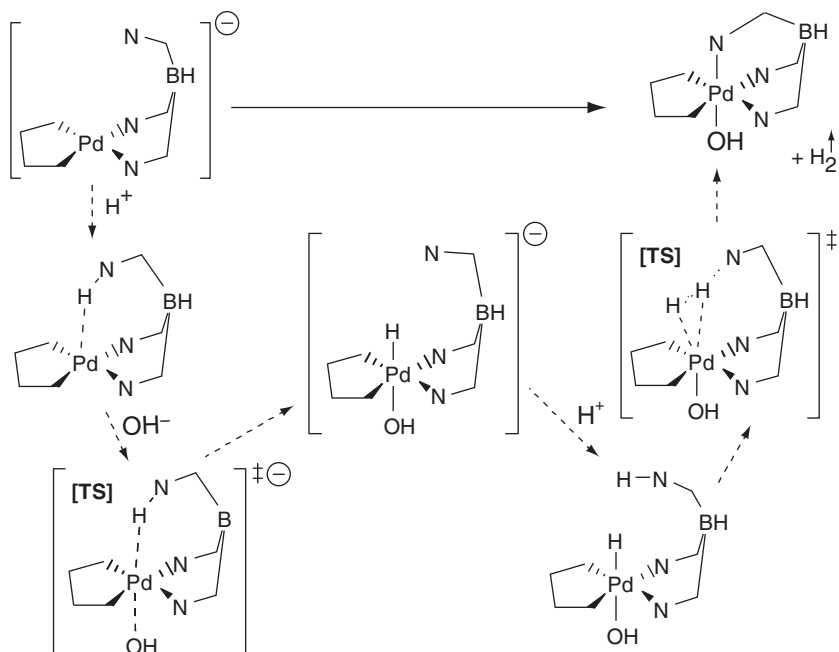
Scheme 20 Proposed mechanism of H_2O reduction to H_2 by **271**, based on DFT calculations of the theoretical $PdMe_2\{(H_2C=N-NH)_3BH\}$.
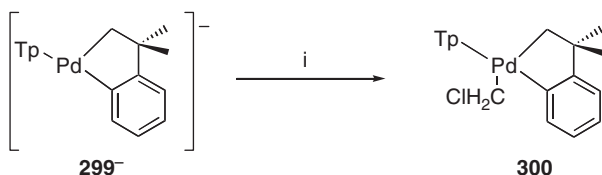
Scheme 21 Condition: (i) CH_2Cl_2.

have also been prepared from $[BpMMeR]^-$ (M = Pd, R = Me **304**⁻, Ph **305**⁻; Pt, R = Me **306**⁻),[110] generated *in situ*, and 8-methylquinolinylbromide.

Palladium complexes TpPdMe₃ (**269**) and TpPdMe₂Ph (**280**) were alternatively obtained by water oxidation of the complex anions $[TpPdMe_2]^-$ (**271**⁻) and $[TpPdMePh]^-$ (**294**⁻), respectively, believed to result from methyl transfer to the anions from the respective Pd(IV) hydroxo complexes that form slowly under aqueous conditions (*vide supra*).[100,106] The by-products "TpPdR" are isolable as the PPh₃ adducts TpPdR(PPh₃) (R = Me **276**, Ph **307**). Comparable results are observed upon treatment of **271**⁻ and **294**⁻ with dihalogens, though at an accelerated rate, the reactions being complete within 30 min.[100] In contrast, when the palladacyclopentane anion [TpPd
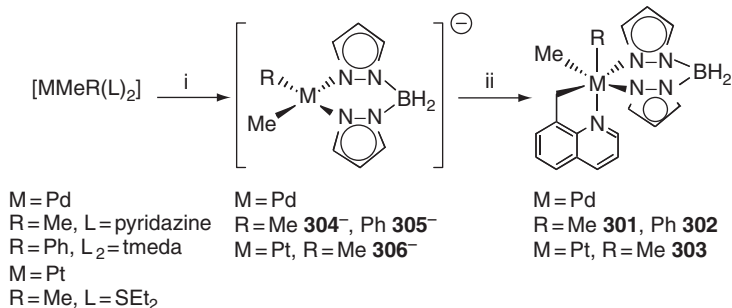
Scheme 22 Conditions and reagents: (i) KBp; (ii) 8-Br(mq).

$(C_4H_8)]^-$ (**277**$^-$), in which the alkyl fragment is inert toward transfer, or less labile platinum anions [TpPtMe$_2$]$^-$ (**308**$^-$), [pzTpPtMe$_2$]$^-$ (**309**$^-$), and [TpPt(p-Tol)$_2$]$^-$ (**296**$^-$) are treated with water, the respective hydroxo complexes TpPd(OH)(C$_4$H$_8$) (**278**),[100,103] TpPtMe$_2$(OH) (**310**),[103,107] pzTpPtMe$_2$(OH) (**311**),[107] and TpPt(p-Tol)$_2$(OH) (**312**)[107] are isolated exclusively. Similarly, both **277**$^-$ and [Tp*PtPh$_2$]$^-$ (**298**$^-$) react with PhICl$_2$, Br$_2$, and/or I$_2$, to afford, respectively, the halide complexes TpPd(C$_4$H$_8$)X (X = Cl **313**, Br **314**, I **315**),[100,103] and Tp*PtPh$_2$I (**316**).[108]

Interestingly, similar halide complexes are obtained when the related palladacyclic anion [TpPd{κ^2-CH$_2$CMe$_2$-o-C$_6$H$_4$}]$^-$ (**299**$^-$) is treated with CH$_2$X$_2$ (X = Br, I, Scheme 23), affording TpPd{κ^2-CH$_2$CMe$_2$-o-C$_6$H$_4$}X (X = Br **317**, I **318**) as the dominant species in admixture with TpPd{κ^2-CH$_2$CMe$_2$-o-C$_6$H$_4$CH$_2$}X (X = Br **319**, I **320**); both **319** and **320** eliminate 1,1-dimethylindane upon prolonged standing in solution.[109] The formation of **317** and **318** in these reactions has been reconciled with a radical process that competes with S$_N$2 substitution, and is the more facile with CH$_2$X$_2$ (X = Br, I), whereas for CH$_2$Cl$_2$ substitution alone is observed, affording only the chloromethyl complex **300** (*vide supra*). The formation of **319** and **320**, which result from formal insertion of CH$_2$ into the Pd−C$_{aryl}$ linkage, remains to be unequivocally explained, though two mechanisms have been proposed, *viz.* (i) reductive coupling of the CH$_2$X and aryl groups, with subsequent intramolecular C−X oxidative addition; (ii) halide loss from an intermediate halomethyl Pd(IV) species to afford a transient Pd(IV) carbene that undergoes subsequent migratory insertion into the Pd−C$_{aryl}$ linkage.

Several Pd(IV) complex salts were also prepared by oxidation of **299**$^-$, in this instance with the chemical oxidant [Cp$_2$Fe][BF$_4$], in the presence of *para*-substituted pyridines, affording the complexes [TpPd(CH$_2$CMe$_2$-o-C$_6$H$_4$)(NC$_5$H$_4$R)]$^+$ (R = NMe$_2$ **321**$^+$, H **322**$^+$, CN **323**$^+$).[111] The Tp* analogues (R = NMe$_2$ **324**$^+$, H **325**$^+$, CN **326**$^+$) were similarly obtained from [Tp*Pd(CH$_2$CMe$_2$-o-C$_6$H$_4$)]$^-$ (**327**$^-$). These salts, identified on the basis of
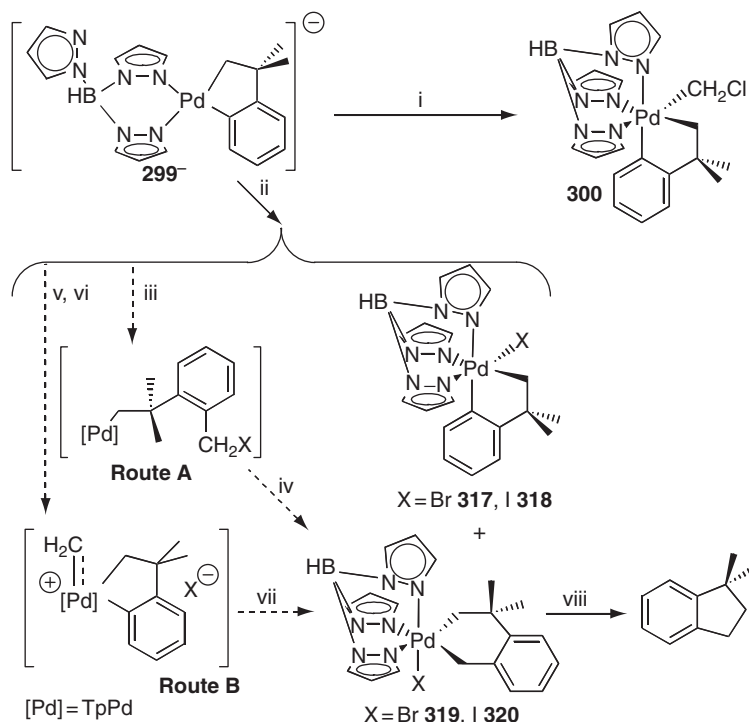
Scheme 23   Reagents and conditions: (i) CH_2Cl_2; (ii) CH_2X_2 (X = Br, I), $-80\ °C$; (iii)reductive coupling; (iv) oxidative addition; (v) S_N2; (vi) halide abstraction; (vii) migratory insertion; (viii) CD_2Cl_2, r.t.

comprehensive spectroscopic data, were also studied electrochemically, which revealed the stability of the Pd(IV) state to be dependent on the donor capacity of both the pyridine ligand (stronger donor = more stable) and the Tp^x ligand (Tp* complexes more easily reduced than Tp).

Oxidation of M(II) anions by dichalcogenides has also been explored, with $[TpMMe_2]^-$ (M = Pd **271**$^-$, Pt **308**$^-$) and $[TpPd(C_4H_8)]^-$ (**277**$^-$). For platinum, this results in formation of the chalcogenide complexes $TpPtMe_2(ER)$ (ER = O_2CPh **328**, SMe **329**, SPh **330**, SeMe **331**, SePh **332**),[112] each of which was comprehensively characterized spectroscopically. The palladium reactions, however, proved more complex (Scheme 24), the simplest example being the low-temperature reaction between **271**$^-$ and $(O_2CPh)_2$, which once again resulted in methyl transfer to afford $TpPdMe_3$ (**269**) and "TpPdMe," the latter isolated as its PPh_3 adduct **276**. In contrast, treatment with $(SPh)_2$ and $(SePh)_2$ afforded unstable species that decompose with formation of Me−Me, Me−EPh, and EPh_2, as determined by GC–MS and NMR spectroscopy. On the basis of
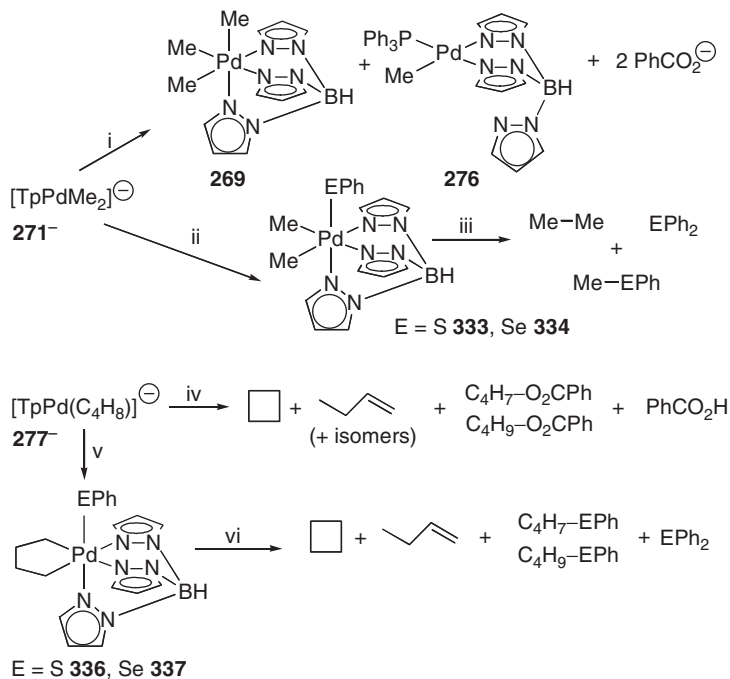
Scheme 24 Conditions and reagents: (i) $(O_2CPh)_2$, PPh_3, $-50\ °C$; (ii) $(EPh)_2$ ($S -10\ °C$, Se $0\ °C$); (iii) $S -10\ °C$, Se $0\ °C$; (iv) $(O_2CPh)_2$, $-20\ °C$; (v) $(EPh)_2$, $-20\ °C$; (vi) $-20\ °C$.

these results and *in situ* ^1H NMR studies, it was concluded that these unstable palladium species are direct analogues of the platinum compounds, *viz.* $TpPdMe_2(EPh)$ ($E = S$ **333**, Se **334**). Similarly, the palladacyclic **277**⁻ is believed to give rise to the intermediate species $TpPd(C_4H_8)$ (ER) (ER = O_2CPh **335**, SPh **336**, SePh **337**), both the sulfide and selenide being observed *in situ*, prior to eliminating cyclobutane, C_4H_9-ER, ER_2 and, via fragmentation of the palladacycle, isomeric butenes.

All three anions were also treated with the weaker oxidant $BrSnMe_3$, which reacted only with the platinum salt, affording $TpPtMe_2(SnMe_3)$ (**338**),[112] subsequently characterized crystallographically.[113] The chlorodimethyltin analogue $TpPtMe_2(SnMe_2Cl)$ (**339**) was similarly prepared from $SnMe_2Cl_2$.[113]

c. Organohydrido M(IV) complexes   The oxidation of anionic M(II) complexes has also been exploited in the synthesis of a small number of diorganohydrido complexes, their protonation being effected with a variety of acids, and even phenol. Thus, $[TpPtMe_2]^-$ (**308**⁻) and $[pzTpPtMe_2]^-$ (**309**⁻) are protonated by phenol to afford $TpPt(Me)_2H$ (**340**)[114] and $pzTpPtHMe_2$ (**341**).[107] In contrast, the protonation of $[TpPt(p-Tol)_2]^-$

(296^-) to TpPt(p-Tol)$_2$H (**342**) is only effected by the stronger acids CH$_3$CO$_2$H, CF$_3$CO$_2$H, or HBF$_4$.[107] Similarly, Tp*PtR$_2$H (R = Me **151**, Ph **153**), both of which have proven remarkably stable toward reductive elimination, were obtained from [Tp*PtR$_2$]$^-$ (R = Me 297^-, Ph 298^-) and anhydrous HCl.[108] The mechanism of protonation was investigated theoretically, using the ''model'' ligand HB(NH−N=CH$_2$)$_3$ that is deemed a suitable substitute for Tp.[114] It was thus concluded that protonation proceeds directly at the metal, on the face opposite to the uncoordinated pyrazole donor (κ^2-Tp), rather than via initial N-protonation and subsequent proton transfer.

These complexes are indefinitely stable in acidic solution, but unstable under neutral or basic conditions. Thus, treatment of **340** with 10% aqueous NaOH regenerates the parent anion [TpPtMe$_2$]$^-$ (308^-) in admixture with the hydroxo complex TpPtMe$_2$(OH) (**310**), which ultimately becomes the sole product.[107] The analogous Tp* complex Tp*PtMe$_2$(OH) (**343**) has also been generated from its respective hydride [Tp*PtMe$_2$H] (**151**), both by treatment with N$_2$O, and indirectly from the structurally characterized hydroperoxide complex Tp*PtMe$_2$(OOH) (**344**), either by prolonged thermolysis in C$_6$D$_6$, or treatment with PR$_3$ (R = Ph, Me).[115] The formation of **344** from **151** was established to result from O$_2$ insertion into the Pt−H linkage, believed to proceed via a radical chain process on the basis of observed catalysis by light and the radical initiator AIBN, and retardation by the radical inhibitor 1,4-cyclohexadiene. Comparable reactivity has very recently been demonstrated for both Tp*PtPh$_2$H (**153**) and TpPtMe$_2$H (**340**), affording, respectively, Tp*PtPh$_2$(OOH) (**345**) and TpPtMe$_2$(OOH) (**346**), and a detailed investigation of the radical mechanism has been described.[116]

In two notable examples, the dihydrides Tp^{x}PtMe(H)$_2$ (Tp^x = Tp **347**,[117,118] Tp* **152**[66]) have been generated by hydrolysis of the respective Pt(II) carbonyls Tp^{x}PtMe(CO) (Tp^x = Tp **150**, Tp* **348**), upon heating in 1:1 acetone:H$_2$O. These conversions were proposed to occur in a two-step process, involving in initial nucleophilic attack of the carbonyl by H$_2$O, in a manner reminiscent of the water-gas shift (WGS) reaction, subsequent CO$_2$ liberation affording ''[Tp^{x}PtMeH]$^-$'' which then undergoes protonation to afford the dihydrides (Scheme 25).[117] This suggestion was supported by a number of mechanistic investigations that enabled observation of liberated CO$_2$ (by labeling studies) and demonstrated that direct protonation of **150** or **348** proceeds preferentially at an uncoordinated pyrazole group, rather than the metal center, thus confirming WGS as the initial step.[117] It should be noted, however, that a very recent study has demonstrated that the interaction of **150** with water is a reversible process, occurring rapidly with respect to formation of **348**; thus, in the presence of D$_2$O the methyl protons of **150** exchange to form all possible isotopomers (**150-d_1, d_2, d_3**).[119] On the basis of experimental

and theoretical (DFT) studies, the mechanism for this was proposed to involve formation and deprotonation of a ''sticky σ-methane'' ligand, by way of a multistep ''proton-walk'' that transfers $H(D)^+$ from an activated water molecule, via the uncoordinated pyrazole donor, to the platinum-methyl linkage, and back again.
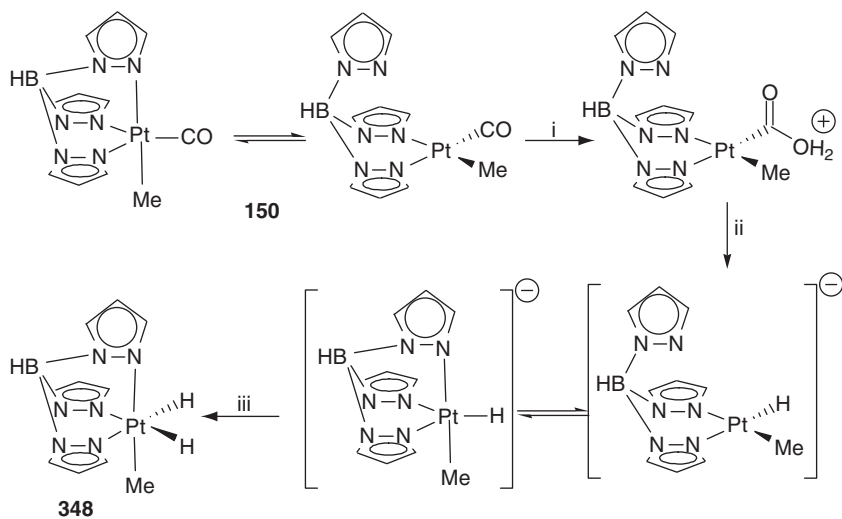
Scheme 25 Reagents and conditions: (i) H_2O; (ii) $-CO_2$; (iii) H_3O^+.

The interaction of Tp*PtMe(CO) (**348**) with nucleophilic reagents of the type RLi has also been reported, affording initially the anionic Pt(II) acyl complexes $[Tp*PtMe\{C(=O)R\}]^-$ (R = Me **349**⁻, Ph **350**⁻), which were identified by *in situ* NMR spectroscopic observations.[120] As for other anionic Pt(II) salts (*vide supra*), these are oxidized by R′X(R′X = MeI, HCl) to afford the Pt(IV) acyl complexes Tp*PtMe{C(=O)R}R′ (R = Me, R′ = Me **351**, H **352**; R = Ph, R′ = Me **353**, H **354**, Scheme 26).[120] Similarly, treating **348** with NaHBEt₃ affords initially the anionic formyl complex $[Tp*PtMe\{C(=O)H\}]^-$ (**355**⁻), which is protonated to afford the chiral Tp*PtMe{C(=O)H}H (**356**, Section III.D.2). Though unequivocally identified spectroscopically, the isolation of **356** has thus far proven elusive, due to its propensity for decarbonylation, yielding dihydride **152**.

An unsurprisingly prevalent route to organohydrido species has been via C−H activation of hydrocarbon solvents by Pt(II) precursors. This was first exploited in the synthesis of Tp*PtMeRH (R = Ph **357**, C₅H₁₁ **168**, Cy **170**), commencing from the Pt(II) anion $[Tp*PtMe_2]^-$ (**297**⁻), which was crystallographically characterized as its PPN salt.[121] Treatment of **K[297]** with the strongly electrophilic $B(C_6F_5)_3$ in benzene, *n*-pentane, and cyclohexane led to formation of the respective Pt(IV) complexes **357**, **168**,
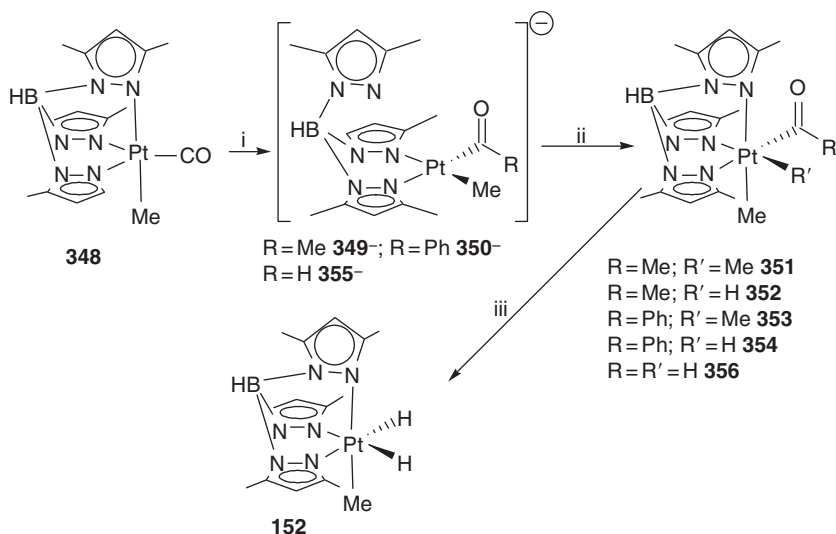
Scheme 26 Conditions and reagents: (i) RLi or NaHBEt$_3$; (ii) MeI or HCl·OEt$_2$; (iii) R=R′= H, −CO.

and **170** in admixture with K[MeB(C$_6$F$_5$)$_3$] and "significant proportions" of Tp*PtMe$_2$H (**151**); this mixture has defied separation. The formation of **151** was attributed to adventitious water, which is seemingly supported by the reaction in C$_6$D$_6$, which affords **357-d$_6$** with no incorporation of deuterium into by-product **151**. The mechanism by which the hydridodialkyls form is believed to involve methyl abstraction from **297⁻** by the borane to afford an active "Tp*PtMe" fragment that undergoes oxidative addition of the solvent. It was noted that the reaction in *n*-pentane results exclusively in activation of a primary C−H linkage, to afford only the *n*-pentyl product (**168**).

Complex **168** also forms, with complete selectivity, in the thermal reaction of Tp*PtMe$_2$H (**151**) with substoichiometric B(C$_6$F$_5$)$_3$ in *n*-pentane, though was not isolated. Continued heating effects complete conversion to the 1-pentene complex Tp*PtH(η^2-C$_5$H$_{10}$) (**163**).[69] The complexes Tp*PtMe (R)H (R = *c*-C$_5$H$_9$ **169**, *c*-C$_6$H$_{11}$ **170**, *c*-C$_8$H$_{14}$ **171**, CH$_2$CH$_2$^{t}Bu **172**) are similarly generated from the respective alkanes and have been observed *in situ* as intermediates *en route* to the respective hydridoalkene complexes (**164–167**), which form via loss of a second equivalent of methane and subsequent β-hydride abstraction.

Several diarylhydridoplatinum complexes have been obtained under ambient conditions upon the treatment of Tp*PtMe(H)$_2$ (**152**) with substoichiometric amounts of B(C$_6$F$_5$)$_3$ in aromatic solvents; thus, Tp*PtR(H)$_2$ (R = Ph **177**,[122] Tol **182**,[122] C$_6$H$_4$Et **358**,[67] C$_6$H$_4$C(H)Me$_2$ **359**,[67] 2,5-Xyl **183**,[122] 3,4-Xyl **360**,[122] 3,5-Xyl **361**[122]) were each isolated in >50% yield (Scheme 27). For **182**, **358**, and **359** three regio-isomers are encountered,

corresponding to CH activation *para* (**a**), *meta* (**b**), and *ortho* (**c**) to the ring substituent. A statistical ratio (2:1) of *meta:para* isomers is obtained in each case, while only a trace of the *ortho* isomer was observed for **182** (none for **358** and **359**), a fact attributed to *ortho*-activation being sterically disfavored.[122] For each of the remaining arenes a single product was obtained, though these typically exhibited dynamic behavior (i.e. ring rotation) that could be frozen-out at low temperature, in which limit **360** shows preference (1:1.8) for the rotamers in which the meta-methyl group points away from the Tp* ligand. The 2,5-Xylyl complex **183** is unique in exhibiting no dynamic behavior.
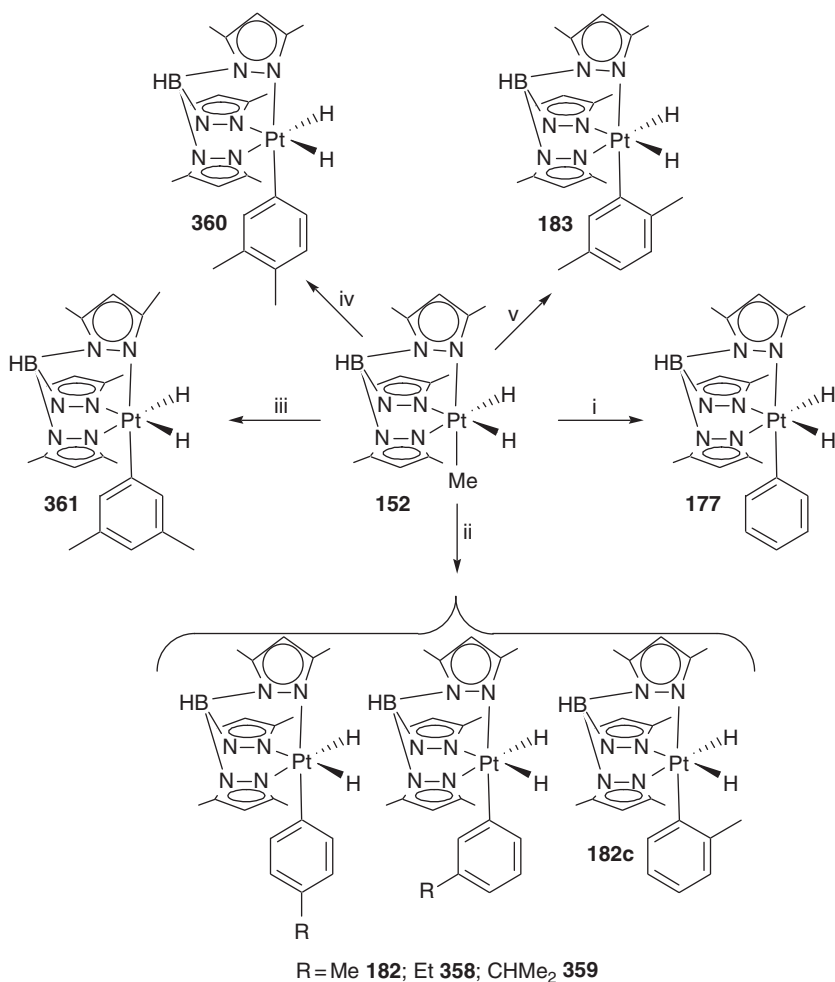
Scheme 27   Conditions and reagents: B(C$_6$F$_5$)$_3$, r.t. in (i) C$_6$H$_6$; (ii) C$_6$H$_4$R (R = Me, Et, CHMe$_2$); (iii) *m*-Xylene; (iv) *o*-Xylene; (v) *p*-Xylene.

The role of the borane in these conversions is to catalyze methane elimination from **152**, presumably giving rise to an active species of the type ''Tp*PtH(solv).'' This was established on the basis that only substoichiometric quantities of the borane are necessary,[122] while in its absence the loss of methane is observed only at elevated temperature.[123] The mechanism of catalysis remains to be firmly established; however, it is believed to involve borane-assisted dechelation of one pyrazole donor from (κ^3-Tp*)PtMe(H)$_2$ (**152**) to afford the free coordination site necessary for methane elimination.[122,123] Indeed, a mechanism of this type has been demonstrated to prevail upon protonation of complexes Tp*PtR$_2$H (R = Me **151**, Ph **153**) and Tp*PtR(H)$_2$ (R = Me **152**, Ph **177**). Thus, treatment of **151** (in CD$_2$Cl$_2$) with [H(OEt$_2$)$_2$][BAr$^f_4$] at -78 °C results in immediate liberation of methane to afford the spectroscopically observable complex salt [{κ^2-N,N'-HTp*}Pt(Me)(CD$_2$Cl$_2$)]BAr$^f_4$ (**362.BAr$^f_4$**),[65] which decomposes above 0 °C but can be trapped by addition of excess Lewis base as the isolable adducts [{κ^2-N,N'-HTp*}Pt(Me)(L)]BAr$^f_4$ (L = NCMe **363$^+$**, CN^{t}Bu **364$^+$**, CO **365$^+$**, py **366$^+$**, η^2-C$_2$H$_4$ **154$^+$**). The analogous PMe$_2$Ph complex (**367$^+$**) is obtained using a single equivalent of the phosphane, with excess resulting in further reaction (Section III.F). The phenyl complex salts [{κ^2-N,N'-HTp*}Pt(Ph)(L)]BAr$^f_4$ (L = C$_2$H$_4$ **156$^+$**, NCMe **368$^+$**) were similarly obtained,[65] as were the hydrido salts [{κ^2-N,N'-HTp*}PtH (L)]$^+$ (L = CO **369$^+$**,[68] NCMe **370$^+$**,[66] η^2-C$_2$H$_4$ **155$^+$** [66]), commencing from **153** and **152**, respectively. Deprotonation of **363$^+$**–**367$^+$** and **154$^+$** can be effected by a variety of bases (most efficiently NaH in thf), though with the BAr$^f_4$ anion the products are not readily purified, a difficulty circumvented by use of the BF$_4$ salts, which can be cleanly deprotonated *in situ* to afford the respective neutral complexes [Tp*Pt(R)(L)] (R = Me, L = NCMe **371**,[65] CN^{t}Bu **372**,[65] CO **348**,[65] py **373**,[65] η^2-C$_2$H$_4$ **157**,[65] SMe$_2$ **374**;[65] R = Ph, L = NCMe **375**,[65] η^2-C$_2$H$_4$ **158**,[67] CO **376**[67]).

Deuteration of **151** and **152** with [D(OEt$_2$)$_2$]BAr$^f_4$ results in no deuterium incorporation in either the eliminated methane or at the metal-hydride position, demonstrating conclusively that protonation occurs only at the pyrazolyl donor.[65,66] However, under comparable conditions **152-d_2** (Tp*PtMe(D)$_2$) undergoes scrambling between the methyl and hydrido centers, liberating both CH$_3$D and CH$_2$D$_2$, with appreciable incorporation of hydrogen in the solvento-cation [κ^2-N,N'-HTp*PtH (Solv)]$^+$.[66] These data were deemed to implicate the reversible formation of a methane σ-complex as a prelude to methane elimination. A similar scenario has been thermally induced for TpPtMe(H)$_2$ (**347**) in deuteromethanol, resulting in complete conversion to TpPt(CD$_3$)D$_2$ (**347-d_5**); regeneration of **347** is effected on heating in MeOH.[124] This is believed to result from a fast pre-exchange between the hydridic protons and the solvent, with subsequent reversible formation of an σ-methane complex. Significantly, in this instance, no methane elimination is observed, nor is

C−H activation of the solvent; however, upon addition of a strong donor (PMe_3) dihydrogen elimination *is* induced, affording $TpPt(Me)(PMe_3)$ (**377**). Definitive explanations for this observation, the facility of H/D scrambling and reluctance toward methane elimination have yet to be established, but are the subject of on-going experimental[124] and theoretical studies.[125]

The validity of the acid-assisted dechelation step has been demonstrated by protonation (-78 °C) of the putative dihydrido-silyl complex $Tp*PtH_2(SiEt_3)$ (**378**), obtained by prolonged thermolysis of $Tp*PtMe_2H$ (**151**) with Et_3SiH,[126] which affords the isolable, and crystallographically characterized, five-coordinate complex [{κ^2-*N,N'*-HTp*}$PtH_2(SiEt_3)$]BAr$^f_4$ (**379.BAr$^f_4$**).[127] Though **379$^+$** is observed to undergo solution-phase decomposition to $Tp*PtH_3$ (**159**), no evidence was observed for formation of a silane σ-complex. However, direct evidence for this step of the reaction *has* been observed upon protonation of $Tp*PtPh(H)_2$ (**177**), which affords a chiral compound, identified spectroscopically, and ultimately crystallographically (Figure 3) as the η^2-benzene adduct [(κ^2-*N,N'*-HTp*)$PtH(\eta^2$-C_6H_6)]BAr$^f_4$ (**178.BAr$^f_4$**).[70] Though no exchange between coordinated and free benzene was observed for **178$^+$** on the NMR timescale, exchange between the hydridic and aromatic protons was apparent at 252 K, indicating reversible formation of the η^2-beznene adduct (ΔG_{exch} = 12.7 kcal mol^{-1}); this scenario is similar to the resistance of **347** toward methane loss (*vide supra*).[124] However, upon prolonged standing **178$^+$** does slowly lose benzene to afford the cationic Pt(II) dihydride [{(κ^2-*N, N'*-HTp*)Pt(µ-H)}$_2$][BAr$^f_4$]$_2$ (**380.2BAr$^f_4$**).[66,70]

The interaction of both **178$^+$** and its analogue [(κ^2-*N,N'*-HTp*)PtPh(η^2-C_6H_6)]$^+$ (**181$^+$**), generated from $Tp*PtPh_2H$ (**153**), with excess of nitriles
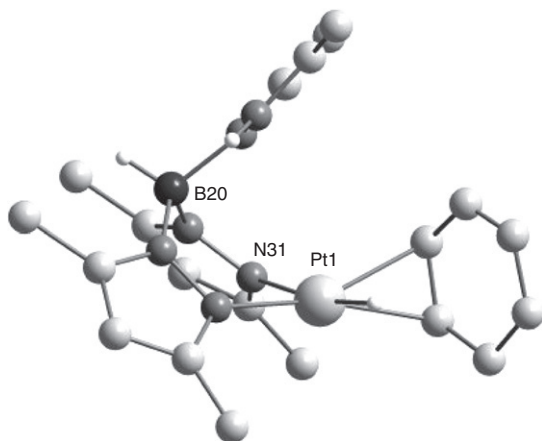
Figure 3   Molecular structure of [(κ^2-*N,N'*-HTp*)Tp*PtH(η^2-C_6H_6)]$^+$ (**178$^+$**).

R′CN (for 178^+ R′ = Me, tBu; 181^+ R′ = tBu) allows for trapping of the five-coordinate intermediate resulting from benzene C$-$H activation; *viz.* [(κ^2-*N,N′*-HTp*)PtPh(H)R(NCR′)]$^+$ (R = H, R′ = Me 381^+, CMe$_3$ 382^+; R = Ph, R′ = CMe$_3$ 383^+, Scheme 28).[71] These complexes are obtained, at 193 K, as an equilibrium mixture with the respective η^2-benzene complexes, the latter being favored upon warming to 223 K, though the equilibrium mixture is reestablished upon re-cooling; however, attempts to isolate exclusively 381^+–383^+ at lower temperatures were unsuccessful. The electronic influence of the nitrile in these reactions was probed by treating 178^+ with a series of *para*-substituted benzonitriles to obtain the respective complexes [(κ^2-*N,N′*-HTp*)PtPh(H)$_2$(NCC$_6$H$_4$Y-4)]$^+$ (Y = H 384^+, Me 385^+, OMe 386^+, Cl 387^+, CF$_3$ 388^+); this revealed the Pt(IV) aryldihydrides to be stabilized by more electron-rich nitriles.

Above -30 °C complexes 381^+–383^+ each give way to complete replacement of benzene by the nitrile, to afford the Pt(II) complexes [(κ^2-*N,N′*-HTp*)PtR(NCR′)]$^+$ (R = H, R′ = Me 370^+, CMe$_3$ 389^+; R = Ph, R′ = CMe$_3$ 390^+), directly analogous to those obtained via protonation of Tp*PtMe$_2$H (**151**), Tp*PtMeH$_2$ (**152**), and Tp*PtPh$_2$H (**153**) and their subsequent treatment with excess acetonitrile (Section III.E).[65]

R=H **178⁺**, Ph **181⁺**   + R′CN

R=H, R′=Me **381⁺** CMe₃ **382⁺**
R=Ph, R′=CMe₃ **383⁺**
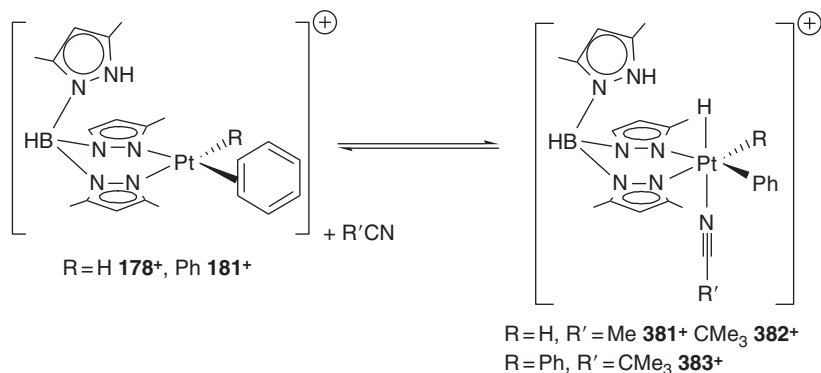
Scheme 28   Conditions: <-30 °C.

The acid-assisted dechelation of a κ^3-Tp* ligand has also been employed to induce, at elevated temperatures, insertion of ethylene into the Pt$-$Ar linkage of the five-coordinate Pt(II) complex Tp*PtPh(η^2-C$_2$H$_4$) (**158**), resulting in an unanticipated C$-$H activation of the resulting ethylbenzene to afford a Pt(IV) hydrido complex. Thus, upon treatment with substoichiometric B(C$_6$F$_5$)$_3$ at 60 °C, benzene solutions of **158** afford exclusively the chiral platinacycle **176**, identified on the basis of NMR spectroscopic data, and ultimately crystallographically. This complex is

presumed to form via the intermediacy of a coordinately unsaturated σ-ethylbenzene complex, which undergoes aromatic C−H activation (Scheme 29).[67] As in previous examples (*vide supra*) protonation of **176** (with [H(OEt₂)₂][BArᶠ₄]) results in dechelation of one pyrazole donor, enabling reductive elimination of the alkyl and hydride functionalities to afford the solvento-cation [κ²-HTp*Pt(C₆H₄Et-2)(OEt₂)]⁺ (**391**⁺), which in the presence of NCMe is trapped as the more stable acetonitrile complex **392**⁺. The exclusive reductive elimination of the alkyl, rather than aryl function, was attributed to the greater strength of M-aryl versus M-alkyl linkages; however, aryl elimination followed by immediate rearrangement of the σ-ethylbenzene to 2-ethylphenyl could not be excluded.
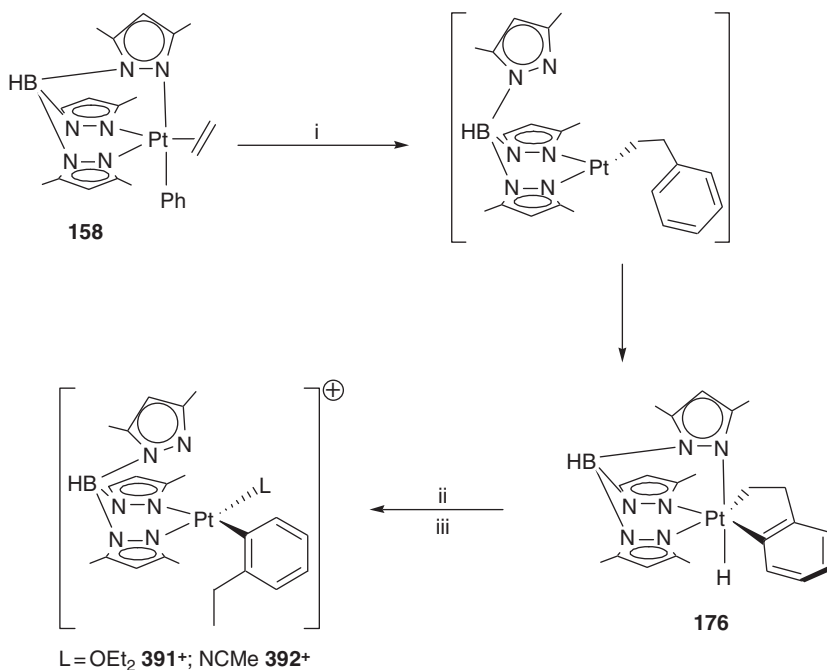
Scheme 29 Conditions and reagents: (i) B(C₆F₅)₃, C₆H₆, 60 °C *or* C₆H₆, 80 °C; (ii) [H(OEt₂)₂][BArᶠ₄]; (iii) NCMe.

This alkene-insertion/oxidative addition chemistry has proven more facile with the propylene analogue of **158**, which is itself not isolable. Indeed, protonation (with HBF₄ at −78 °C) of diphenylhydride **153** and subsequent sparging with propylene while warming to ambient temperature (2 h) affords, after deprotonation of the putative but unisolable η²-C₂H₃Me intermediate, three platinum hydride species, identified as the platinacycle **393** (major) and two diastereoisomers of **394** (Scheme 30).

The 2,1-insertion product **393** was confirmed as the kinetic product by treating the low-temperature reaction mixture with NEt$_3$, enabling its isolation as the major product. Subsequent heating to 80 °C in the NMR probe allowed for observation of its clean conversion to **394a/b**.
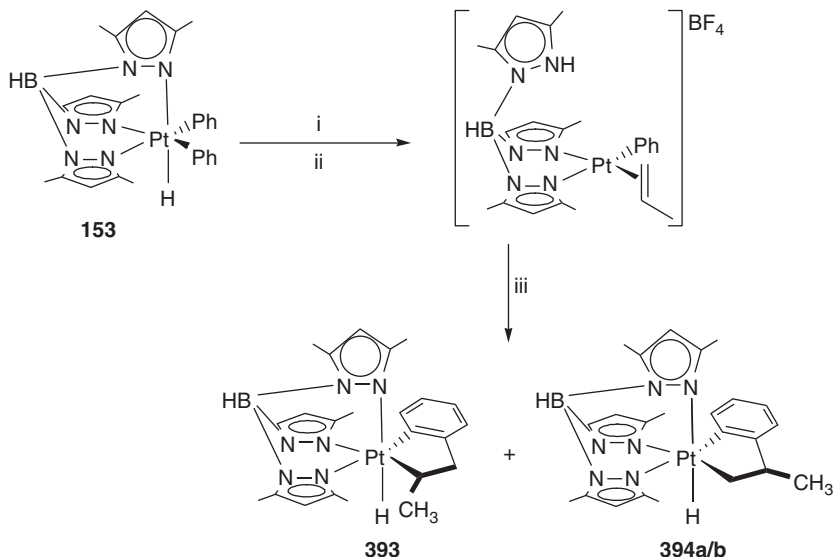
Scheme 30   Conditions and reagents: (i) HBF$_4$, −78 °C; (ii) CH$_2$=CH(CH$_3$), −78 °C→ r.t.; (iii) NaH or NEt$_3$, −78 °C → r.t.

Complexes **176** and **394** have also been obtained via the borane-assisted activation of alkylarenes by Tp*PtMe$_2$H (**151**), as has the related complex **395** (Scheme 31). These reactions presumably proceed by borane-

R = R′ = H **176**
R = Me, R′ = H **394a/b**
R = H, R′ = Et **395**
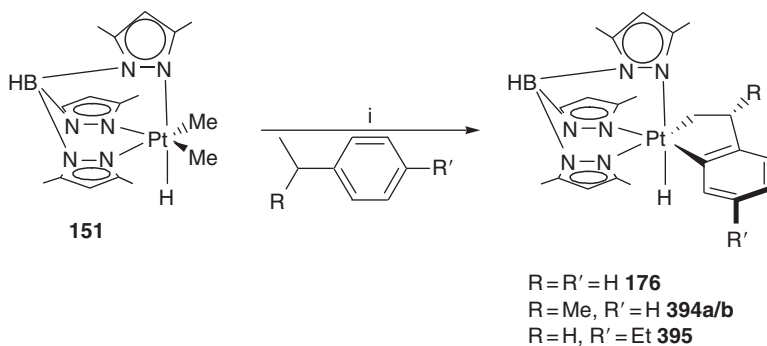
Scheme 31   Reagents and conditions: (i) B(C$_6$F$_5$), mild heating.

assisted methane loss and subsequent C−H activation of the substrate. In this respect, activation of an aryl C−H is believed to precede that of the alkyl, consistent with the established facility of aromatic C−H activation, and supported by the observation that both ethyl- and propylbenzene activate solely at the aromatic ring (*vide supra*).

2. 5-coordinate M(II) complexes

Among the earliest group 10 poly(pyrazolyl)borate compounds bearing σ-donor ligands were the 5-coordinate platinum complexes TpPtMe (η^2-L) (**100–125**) and (pzTp)PtMe(η^2-L) (**127–129**) where L = alkene, alkyne, or allene (Table 1, Section III.B.1).[53–56,60] These were obtained by hydrocarbyl cleavage of the appropriate, polymeric, LPtMe (L = Tp **126**, pzTp **130**), in turn prepared from [PtMe(η^4-C$_8$H$_{12}$)]PF$_6$ and KTp or K [(pzTp)], respectively. The role of the methyl group in these π-complexes is essentially as a spectator, though an electronic interaction between this and ligated fluoro-olefins was observed within TpPt(Me)(η^2−L) (L = C$_2$F$_4$ **101**, CF$_2$=CH$_2$ **102**, CF$_2$=CFH **103**, CH$_2$=C(CF$_3$)(CN) **108**),[53,55] manifest in an increased-magnitude of the ^{1}H–^{19}F coupling constant for the proximal centers, and thus attributed to a ''through-space'' mechanism. No reactivity has been observed of the methyl ligand, nor indeed of the complexes themselves, other than the ready displacement of the π-alkynes from **114–122** under pressure of CO to afford TpPt(Me)(CO) (**150**). Consequently, the ''TpPtMe'' fragment is a viable protecting group for alkynes of the type R$_2$NC(O)C≡C(O)NR'H (R' = allyl, C$_6$H$_4$CO$_2$Et), which when coordinated (complexes **144−149**) can undergo selective hydrogenation and base-hydrolysis of the R' group; conditions of which the free alkynes are intolerant.[64]

The carbonyl complex **150** has also been obtained by cleaving [TpPt (Me)]$_n$ (**126**) with CO,[55] as has pzTpPt(Me)(CO) (**396**).[55,128] The related complexes TpPt(Me)(L) (L = CN^{i}Bu **397**, CNCy **398**, P(OMe)$_3$ **399**) have been similarly prepared from the respective donors.[128] Each complex was assigned a stereochemically nonrigid 5-coordinate geometry in solution, on the basis of NMR spectroscopic data, *viz.* (i) the resolution of coupling between ^{195}Pt and all three coordinated pyrazole rings, and (ii) observed dynamic equilibration of all pyrazoles at ambient temperatures, which is frozen out around −100 °C.[54,55,128] However, in the solid state, both **150**[129,130] and **396**[131] adopt slightly distorted square-planar (κ^2-Tp) geometries. The authors had difficulty reconciling this with spectroscopic data, concluding only that a Pt−N bond-breaking process was involved in the solution-phase dynamic exchange, giving rise to a 4-coordinate intermediate in the high-temperature exchange process.[128]

Finally, a series of 5-coordinate M(II) complexes, which include the only examples based on palladium, are derived from [M(η^1:η^2-C$_8$H$_{12}$OMe)Cl]$_2$, which comprises a σ,π-chelating cyclooctenyl ligand.

Thus, upon treatment with NaTp or $HCpz_3/NH_4PF_6$, the complexes TpM $(\eta^1:\eta^2\text{-}C_8H_{12}OMe)$ (M = Pd **184**, Pt **185**) and their anionic tris(pyrazolyl) methane counterparts $[(HCpz_3)M(\eta^1:\eta^2\text{-}C_8H_{12}OMe)]PF_6$ (M = Pd **187. PF_6**, Pt **188.PF_6**) were obtained in high yield as moderately moisture-sensitive materials (Scheme 15, Section III.B.1). These compounds were confirmed to be 5-coordinate in the solid state (by X-ray) and fluxional in solution, resulting in equilibration of all three pyrazole donors.

3. 4-coordinate M(II) complexes

a. Diorgano M(II) complexes   The most prominent such compounds are the complex anions $[Tp^xMRR']^-$, which have been widely exploited as precursors to organo and hydrido M(IV) species (*vide supra*). Numerous M(IV) complexes have been obtained via oxidation of the anionic M(II) salts $K[\{HB(ind)_3\}MMe_2]$ (M = Pt **K.262**, Pd **K.263**),[96] $K[TpPdMeR]$ (R = Me **K.271**; Ph **K.294**),[99] $K[pzTpPdMeR]$ (R = Me **K.270**; Ph **K.295**),[98] $K[TpPd(C_4H_8)]$ (**K.277**),[98,106] $K[TpPt(p\text{-}Tol)_2]$ (**K.296**),[107] $K[Tp*PtR_2]$ (R = Me **K.297**, Ph **K.298**),[108] $K[TpPtMe_2]$ (**K.308**),[100,103] $K[pzTpPtMe_2]$ (**K.309**),[100,103] $K[BpPdMeR]$ (R = Me **K.304**, Ph **K.305**),[110] $K[BpPtMe_2]$ (**K.306**),[110] which are typically obtained from the respective KTp^x and M (II) precursors $[MR_2(LL)]$ (LL = tmeda, pyridazine, etc.), or in the case of the palladacyclopentanes from $[Pd(C_4H_8)(tmeda)]$. Subsequent reaction with alkyl halides, either *in situ* or of the isolated salts, affords the complexes $Tp^xMRR'R''$ (**251**, **268**, **269**, and **280**−**293**, *vide supra*)[98,99,106–108] while **308**$^-$ has also been found to react with dichalcogenides to give $[TpPtMe_2(ER)]$ (ER = O_2CPh **328**, SMe **329**, SPh **330**, SeMe **331**, SePh **332**).[112] Protic acids have been utilized to generate metal hydrides, the more basic anions **306**$^-$ and **309**$^-$ being readily protonated by phenol to afford $TpPtMe_2H$ (**338**)[114] and $pzTpPtMe_2H$ (**341**),[107] while conversion of the less reactive **296**$^-$ to $TpPtH(p\text{-}Tol)_2$ (**342**) requires either CH_3CO_2H, CF_3CO_2H or HBF_4.[107] Similarly, $Tp*PtR_2H$ (R = Me **151**, Ph **153**) are obtained from **297**$^-$ and **298**$^-$, respectively, but require the stronger acid HCl.[108]

In contrast, protonation of the complex anion $[(Ph_2Bp)PtMe_2]^-$ (**400**$^-$) fails to afford an isolable metal hydride; rather, treatment with $[HN^iPr_2Et]$ BPh_4 leads to methane elimination, the presence of extraneous donors enabling isolation of the adducts $(Ph_2Bp)PtMe(L)$ (L = NCMe **401**, CO **402**, $P(C_6F_5)_3$ **403**).[132] Moreover, in benzene solution, in the absence of other donors, methane loss is followed by C−H activation of the solvent, affording $[(Ph_2Bp)PtPh_2]^-$ (**404**$^-$). In the presence of NCMe, protonation of **404**$^-$ affords $(Ph_2Bp)PtPh(NCMe)$ (**405**). This somewhat distinct reactivity of **400**$^-$ is attributed to the formation of an unobserved, unisolable metal hydride in which the final octahedral site is occupied by a weak solvent interaction (cf. *N*-donor in Tp^x derivatives). This avails the required vacant site for methane elimination via a σ-complex, for which

evidence was obtained from deuterium scrambling studies. The resulting ''(Ph$_2$Bp)PtR'' fragment is then trapped as an η^2-benzene adduct that undergoes rapid C−H addition to the metal. This reaction has been effected with greater facility using [H(OEt$_2$)]BAr$^f_4$, and is also promoted by B(C$_6$F$_5$)$_3$, acting to abstract methide. Finally, **400**$^-$ has been shown to preferentially activate sp^3 C−H bonds, its protonation in mesitylene affording (Ph$_2$Bp)PtCH$_2$(C$_6$H$_3$Me$_2$-2,4) (**406**) as the major product.

Water-oxidation of diorgano anions has also been described,[99,100,103–105,107] resulting, for [TpPdMeR]$^-$ (R = Me **271**$^-$, Ph **294**$^-$), in quantitative formation of 1:1 mixtures of [TpPdMe$_2$R] (R = Me **269**, Ph **280**) and ''[TpPdR],'' the latter being identified by trapping as the PPh$_3$ adducts TpPdR(PPh$_3$) (R = Me **276**, Ph **307**),[100,107] which have also been synthesized independently, along with the analogous pzTpPdR(PPh$_3$) (R = Me **407**, Ph **408**), directly from [PdMe(SMe$_2$)(μ-I)]$_2$ and [PdIPh(tmeda)], respectively.[83] The formation of TpPdMe$_2$R is believed to proceed by methyl transfer from a transient Pd(IV) hydroxo complex to the Pd(II) center; indeed, while the hydroxo intermediates remain unobserved, the analogues TpPdC$_4$H$_8$(OH) (**278**),[100,103] TpPtMe$_2$(OH) (**310**),[103,107] pzTpPtMe$_2$(OH) (**311**),[107] and TpPt(p-Tol)$_2$(OH) (**312**)[107] have been obtained upon water oxidation of the respective, less labile, [TpMR$_2$]$^-$ anions, with no evidence for subsequent methyl transfer. However, treatment of **271**$^-$ with water in the presence of [TpPtMe$_2$]$^-$ (**308**$^-$) results in formation (observed by NMR) of TpPtMe$_3$ (**251**),[100] consistent with the known facility of methyl transfer from Pd(IV) to Pt(II) (see also Section III.C.1). This process has also been studied theoretically using DFT methods.[105]

The differing lability of comparable Pd(II) and Pt(II) systems is also illustrated upon oxidation of [TpMMe$_2$]$^-$ with dichalcogenides,[112] which with Pt afford stable, isolable Pt(IV) complexes (*vide supra*). In contrast, oxidation of **271**$^-$ with (O$_2$CPh)$_2$ again results in methyl transfer to afford **267** and ''TpPdMe,'' while the initial products obtained with (SPh)$_2$ and (SePh)$_2$ spontaneously decompose to mixtures of ethane, EPhMe, and EPh$_2$ (Scheme 24, Section III.C.1.b). The oxidation of [TpPd(C$_4$H$_8$)]$^-$ (**277**$^-$) has also been effected with PhICl$_2$, Br$_2$, and I$_2$ to afford the stable Pd(IV) halides TpPd(C$_4$H$_8$)X (X = Cl **313**, Br **314**, I **315**);[100,103] the related platinum complex Tp*PtPh$_2$I (**316**) has been similarly obtained. However, there are no reports of halide oxidation of **271**$^-$, though this would presumably again result in immediate decomposition.

The related palladium halide complexes TpPd(κ^2-CH$_2$CMe$_2$-o-C$_6$H$_4$)X (X = Br **317**, I **318**) have also been obtained, upon treatment with CH$_2$X$_2$ of [TpPd(κ^2-CH$_2$CMe$_2$-o-C$_6$H$_4$)]$^-$ (**299**$^-$), formed from [Pd(κ^2-CH$_2$CMe$_2$-o-C$_6$H$_4$)(cod)] and KTp.[109] These reactions are believed to be radical in nature, and compete with the predominant S$_N$2 attack of dihalomethane, which culminates with CH$_2$ insertion into the organic ligand to afford a

series of Pd(IV) metallacycles (Scheme 23, Section III.C.1.b). In contrast, the interaction of **299**$^-$ with CH_2Cl_2 yields exclusively the chloromethyl complex TpPd(κ^2-CH_2CMe_2-o-C_6H_4)(CH_2Cl) (**300**).

Complex anion **299**$^-$, and its Tp* analogue **327**$^-$, have also served as precursors to the metal nitrosyls Tp^{x}Pd(κ^2-CH_2CMe_2-o-C_6H_4)NO (Tp **409**, Tp* **410**), upon treatment with Diazald (*N*-methyl-*N*-nitroso-*p*-toluenesulfonamide) or, less reproducibly, [NO]BF$_4$ (Section III.D.3).[133] The nitro complex TpPd(κ^2-CH_2CMe_2-o-C_6H_4)NO$_2$ (**411**) was also prepared by NO$_2$ oxidation of **299**$^-$. Chemical oxidation of **299**$^-$ and **327**$^-$ has also been effected with [Cp$_2$Fe]BF$_4$ in the presence of *para*-substituted pyridine donors, affording the salts [Tp^{x}Pd(κ^2-CH_2CMe_2-o-C_6H_4)(NC$_5$H$_4$R)]$^+$ (Tp, R = NMe$_2$ **321**$^+$, H **322**$^+$, CN **323**$^+$; Tp*, NMe$_2$ **324**$^+$, H **325**$^+$, CN **326**$^+$).[111]

Finally for this section, a small number of pentafluorophenyl complexes bearing the pzTp ligand have been prepared, including the bimetallic complex anions [(C$_6$F$_5$)$_2$M(pz)$_2$B(pz)$_2$M(C$_6$F$_5$)$_2$]$^-$ (Pd **412**$^-$, Pt **413**$^-$). These were obtained from the CH_2Cl_2-mediated reaction of the respective [(C$_6$F$_5$)$_2$M(NCPh)$_2$] and K[pzTp] (2:1), and fully characterized spectroscopically, revealing equivalence of the pyrazole groups on the NMR timescale. This was interpreted to imply rapid intramolecular conversion of conformational isomers, resulting from ring inversion of the M(N–N)$_2$B boat (Scheme 32).[88] The palladium species **412**$^-$ was also characterized crystallographically (Figure 4).
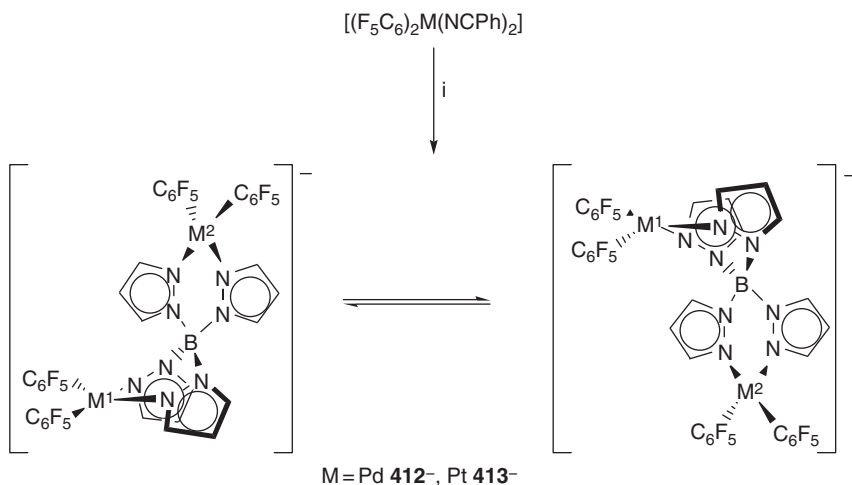
Scheme 32   Reagents: (i) CH_2Cl_2, K[pzTp].

The monometallic fragments [pzTpM(C$_6$F$_5$)$_2$]$^-$ (Pd **414**$^-$, Pt **415**$^-$) were similarly obtained from a 1:1 ratio of the reagents, though these form in
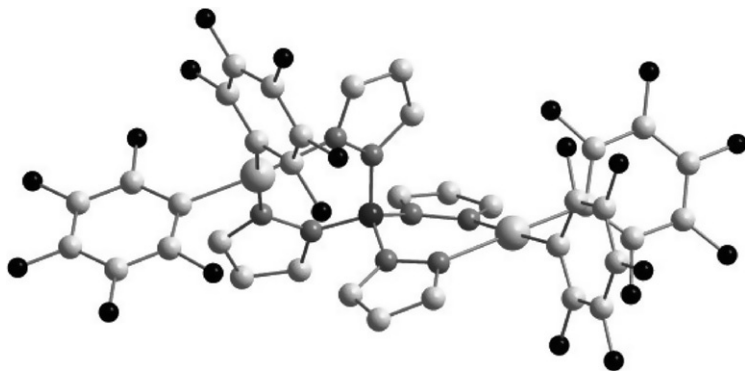
Figure 4   Molecular structure of [(C$_6$F$_5$)$_2$Pd(pz)$_2$B(pz)$_2$Pd(C$_6$F$_5$)$_2$]$^-$ (**412**$^-$).

admixture with **412**$^-$ or **413**$^-$ respectively, and have defied separation. Finally, the neutral, asymmetric-bimetallic complex (C$_6$F$_5$)$_2$Pd(pz)$_2$B (pz)$_2$Pd(η^3-C$_3$H$_4$Me-2) (**235**) was prepared from the palladium allyl pzTpPd(η^3-CH$_2$CMeCH$_2$) (**223**) and [(C$_6$F$_5$)$_2$M(NCPh)$_2$]. The NMR spectroscopic data for **235** indicated two unique pentafluorophenyl environments and a 2:1:1 ratio of pyrazole environments, with no change in dynamic behavior in the temperature range -70 to $+50°$C. These data were reconciled with a structure in which the (C$_6$F$_5$)$_2$Pd(pz)$_2$B ring is rapidly inverting, even at low temperature, while the B(pz)$_2$Pd(η^3-CH$_2$CMeCH$_2$) ring is puckered in a boat conformation.

b. Monoorgano M(II) complexes   The earliest examples of this type were the diorganobis(pyrazolyl)borate complexes (R$_2$Bp)PtMe(L) (R = Et, L = PhC≡CPh **133**, PhC≡CMe **134**, CN(C$_6$H$_4$Me-p) **416**, PMe$_2$Ph **417**, PPh$_3$ **418**, CO **419**; R = Ph, L = PhC≡CMe **135**) and the bimetallic species [Et$_2$BpPt(Me)]$_2${dppe} (**420**). Each of these was readily obtained from the respective donor and [{(R$_2$Bp)Pt(Me)}$_2$(cod)] (R = Et **131**, Ph **132**), which were in turn prepared from [Pt(Me)(cod)(solv)]PF$_6$ and Na[R$_2$Bp],[61] the direct reaction between Na[R$_2$Bp] and [PtMeCl(cod)] in the presence of the donor having proven ineffective.[56] In contrast, (Me$_2$Bp)Pt(Me)(η^2-PhC≡CPh) (**136**) was subsequently prepared via this direct route, as were the dimethylbis(pyrazolyl)gallate complexes (Me$_2$Ga(pz)$_2$)Pt(Me) (L) (L = PhC≡CPh **137**, PPh$_3$ **421**, CO **422**).[63] More recently, Ph$_2$BpPtMe (L) (L = NCMe **401**, CO **402**, P(C$_6$F$_5$)$_3$ **403**) and Ph$_2$BpPtPh(NCMe) (**405**) were obtained via the protonation of [Ph$_2$BpPtMe$_2$]$^-$ (**400**$^-$) and [Ph$_2$BpPtPh$_2$]$^-$ (**404**$^-$), respectively, in the presence of the donors.[132]

   The impetus for the earliest studies was to circumvent the persistent innocence of the Pt−Me linkage in 5-coordinate TpPtMe(L) complexes, which unlike related non-Tp^x systems[134] had proven inert toward alkyne

insertion. However, in isolation, acetylene complexes **133–136** are similarly inert, while the presence of CO effects alkyne displacement exclusively.[61,63] Insertion was, however, spontaneous upon treatment of **131** with $CF_3C{\equiv}CCF_3$, subsequent addition of PPh_3 enabling isolation of the *cis*-alkenyl $(Et_2Bp)Pt\{C(CF_3){=}C(CF_3)Me\}(PPh_3)$ (**138**). Similarly, **131** reacts with DMAD to afford the isolable chelating *cis*-alkenyl $(Et_2Bp)Pt\{\kappa^2\text{-}C,O\text{-}C(CO_2Me){=}C(CO_2Me)\}$ (**142**), and a comparable reaction was inferred for $(Me_2Ga(pz)_2)Pt(Me)(cod)$ (not isolated), on the basis of NMR spectroscopic data.[63]

Simple Bp^x (cf. R_2Bp) complexes of this type were initially deemed inaccessible;[56] indeed, there remain no examples with platinum. However, $NaBp^x$ ($Bp^x = Bp$, Bp^*) react with $[Pd(Me)Cl(cod)]$ in the presence of PR_3 (R = Ph, Cy) to give $Bp^xPd(Me)(L)$ (Bp, L = PPh_3 **423**, PCy_3 **424**; Bp^*, L = PPh_3 **425**, PCy_3 **426**),[135] while $Bp^xPd(CH_2R)(PMe_3)$ (Bp, R = CMe_2Ph **427**, $SiMe_3$ **428**; Bp^*, R = CMe_2Ph **429**, $SiMe_3$ **430**) were prepared from the respective $[PdCl(CH_2R)(PMe_3)_2]$ precursors.[136] These complexes are fluxional with respect to inversion of the BN_2M boat, exemplified in **427** and **428** by equivalence of the methylenic protons in the CH_2R moiety, at ambient temperature on the NMR timescale. In contrast, the bulkier Bp^* ligand slows this exchange process, such that inequivalent methylenic centers are resolved at ambient temperature.[136] A somewhat more intriguing situation has been reported for complex **426**, for which a single pyrazolyl ^{1}H NMR environment is observed at 20 °C, decoalescence occurring below this temperature such that unique environments are clearly resolved at −30 °C. The participation of a phosphane-exchange process was discounted on the basis of experimental observations, leading the authors to suggest a mechanism involving dissociation–reassociation of one pyrazole donor (i.e., $\kappa^1\text{-}Bp^*{\leftrightarrow}\kappa^2\text{-}Bp^*$), induced by steric repulsion between the pyrazolyl methyl substituent and bulky PCy_3 ligand.[135]

Each of **423–430** inserts CO into the Pd−C linkage, affording the respective acyl complexes $Bp^xPd\{C(O)Me\}(L)$ (Bp, L = PPh_3 **431**, PCy_3 **432**; Bp^*, L = PPh_3 **433**, PCy_3 **434**)[135] and $Bp^xPd\{C(O)CH_2R\}(PMe_3)$ (Bp, R = CMe_2Ph **435**, $SiMe_3$ **436**; Bp^*, R = CMe_2Ph **437**, $SiMe_3$ **438**).[136] Once again, boat-inversion was observed to be rapid at ambient temperatures for the Bp complexes **435** and **436** but slower for Bp^* analogues,[136] while the acetyl complex **434** exhibited the same apparent $\kappa^1{\leftrightarrow}\kappa^2$ equilibrium as the parent methyl complex **426**; the related complexes **431–433** showed no such exchange at ambient temperatures.[135] It is noteworthy that none of these complexes (**423–438**) will catalyze olefin polymerization, or CO/olefin copolymerization, the pursuit of which motivated their study.

The pursuit of related Tp^x complexes (i.e., $[\kappa^2\text{-}Tp^xPd(R)(L)]$) has been less focussed, though $Tp^*Pt(R)(L)$ (R = Me, L = CO **348**,[65] NCMe **371**,[65] CN^tBu **372**,[65] py **373**,[65] $\eta^2\text{-}C_2H_4$ **157**,[65] SMe_2 **374**;[65] R = Ph, L = $\eta^2\text{-}C_2H_4$

158,[67] NCMe **375**,[65] CO **376**[67]), and TpPt(Me)(PMe$_3$) (**377**) have been obtained by deprotonation of the respective [{κ^2-N,N'-HTp^x}Pt(R)(L)]$^+$ salts, derived from Pt(IV) diorganylhydrides (Section III.C.1.b). A further handful have been prepared directly from MTp^x and suitable Pd(II) organyls; thus, TpPd(R)(PPh$_3$) (R = Me **276**, Ph **307**) and pzTpPd(R) (PPh$_3$) (R = Me **407**, Ph **408**) were prepared from [PdMe(SMe$_2$)(μ-I)]$_2$ and [PdIPh(tmeda)] in the presence of PPh$_3$,[83] and Tp*Pd(R)(PPh$_3$) (R = Me **439**, p-Tol **440**) from [Pd(R)Cl(cod)],[137] while the 2-furfuryl complexes Tp^{x}Pd(CH$_2$Fu)(PPh$_3$) (Tp **441**, pzTp **442**; Fu = 2-C$_4$H$_3$O) were prepared from [PdCl(CH$_2$Fu)(PPh$_3$)$_2$] and the respective NaTp^x.[138] More unusually, Tp*Pd{CH(CN)R}(py) (R = CN **443**, C(O)OMe **444**, C(O)Ph **445**) have been obtained by condensation of the respective alkanes H$_2$C(CN)R with Tp*Pd(OH)(py) (**446**).[139] Fluxionality is universally observed on the NMR timescale, though only for **439** and **440** has this been studied. In the case of **439**, C_3 symmetry is attained in both low- and high-temperature regimes (coalescence ca. 20 °C) while **440** exhibits no symmetry at low temperature, with coalescence at ca. 20 °C.[137] Nonetheless, comparable exchange processes were postulated for both systems, *viz.* intramolecular substitution of coordinated and uncoordinated pyrazolyl donors. Both materials undergo slow (~1 day) insertion of CO at atmospheric pressure to afford Tp*Pd{C(O)R}(PPh$_3$) (R = Me **447**, p-Tol **448**), which exhibit comparable fluxional processes, mirroring the temperature dependence of **440**. Significantly, **448** slowly (>1 day) inserts norbornadiene to afford Tp*PdC$_7$H$_8$C (O)p-Tol) (**449**); however, when **440** is simultaneously exposed to both CO and norbornadiene, catalytic copolymerization is effected, resulting in polyketone formation within hours.[140,141] A mechanism involving rapid interception of the intermediate Tp*Pd{η^2-O,C-O=C(p-Tol)} by nbd, which is impeded by the presence of excess PPh$_3$, has been proposed (Section IV.A).[140]

The synthesis of Tp^{tBu}Pd(Ph)(PMe$_3$) was unsuccessfully attempted via the reaction of TlTp^{tBu} and [PdCl(Ph)(PMe$_3$)$_2$], which affords instead the unprecedented κ^1-Tp^{tBu}Pd(Ph)(PMe$_3$)$_2$ (**450**).[29] This rare example of the Tp^{tBu} ligand adopting the κ^1-coordination mode mirrors the case of the directly analogous nickel system (Section II.C), which has been studied at greater length.[27,29]

Several pentafluorophenyl complexes have also been reported, involving Bpz$_4$ as both a bridging and terminal ligand. Thus, the bimetallic complex salts [(C$_6$F$_5$)(L)Pd(pz)$_2$B(pz)$_2$Pd(L)(C$_6$F$_5$)]ClO$_4$ (L = CN^{t}Bu **451**$^+$, NCPh **452**$^+$, PPh$_3$ **453**$^+$, PEt$_3$ **454**$^+$, PMe$_2$Ph **455**$^+$, AsPh$_3$ **456**$^+$, Scheme 33) were each obtained by sequential treatment of the respective [(C$_6$F$_5$)(L)Pd(μ-X)]$_2$ (X = Cl, Br) with AgClO$_4$ (1:2) and K[Bpz$_4$] (1:1), while the analogous reaction with L = tetrahydrothiophene (tht) in the presence of NBu$_4$Cl afforded NBu$_4$[(C$_6$F$_5$)(Cl)Pd(pz)$_2$B(pz)$_2$Pd(Cl)(C$_6$F$_5$] (**NBu$_4$.457**).[88] The neutral monomeric species (κ^2-pzTp)Pd(C$_6$F$_5$)(CN^{t}Bu)

(**458**) was similarly obtained using a 1:2 ratio of the dipalladium precursor and [pzTp]$^-$. NMR spectroscopic data for the bimetallics **451$^+$**–**457$^-$** revealed them to adopt a unique arrangement in solution, each exhibiting a single environment for both the pentafluorophenyl and L ligands. The ^{1}H NMR spectra revealed two unique pyrazole environments, resulting from *trans* dispositions relative to C$_6$F$_5$ and L respectively, but no apparent fluxionality, leading the authors to conclude that the ubiquitous "boat-inversion" process was proceeding rapidly on the NMR timescale. For the isocyanide complex **451$^+$** the proposed geometry was confirmed in the solid state by an X-ray diffraction study. In contrast, the monomeric **458** exhibits broad ^{1}H NMR spectra at ambient temperature, due to fluxional exchange of the four pyrazolyl groups, attributed to a combination of "tumbling" (mediated by a κ^3-5-coordiante geometry) and inversion of the Pd$-$(N$-$N)$_2$$-$B boat. Low-temperature limiting spectra for this material were obtained at $-60\ ^\circ$C, under which conditions inequivalence of all four pyrazolyl groups is apparent.
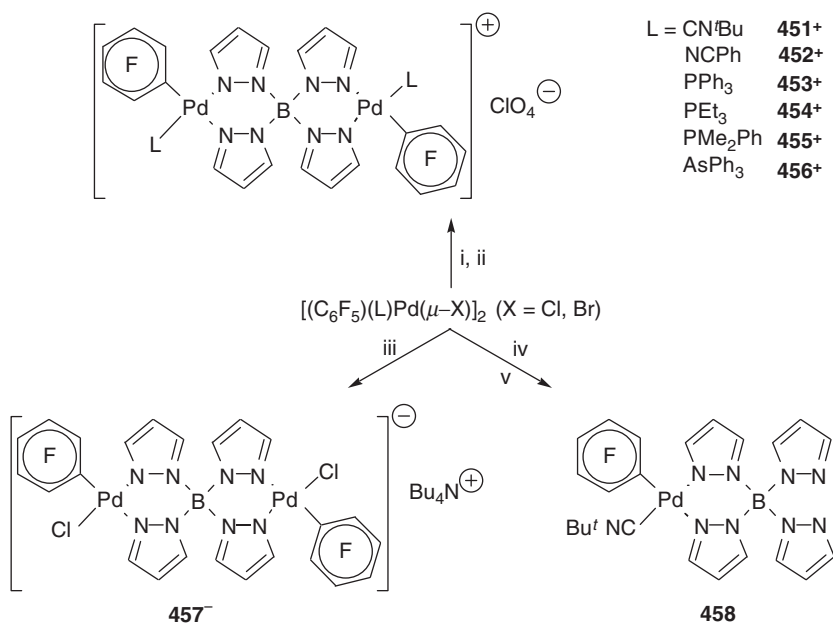
Scheme 33 Reagents: (i) 2 AgClO$_4$; (ii) K[Bpz$_4$]; (iii) K[Bpz$_4$]/Bu$_4$NCl (L = THT); (iv) 2 AgClO$_4$; (v) 2K[Bpz$_4$].

A handful of bimetallic complexes with bridging ancillary ligands have also been reported, of which four are based on platinum. These include [(κ^2-pzTp)Pt(η^1-C$_3$H$_4$Me)]$_2$(μ-dppb) (**243**, Section III.B.2), obtained by treatment of pzTpPt(η^3-C$_3$H$_4$Me) (**225**) with ½ equiv.

dppb,[87] a procedure that fails with dppe, and the 1,5-cod bridged complex [{(Et$_2$Bp)PtMe}]$_2$(µ-cod) (**131**),[61] which *does* react with dppe to afford [{(Et$_2$Bp)PtMe}]$_2$(µ-dppe) (**420**). These materials have not been further elaborated.

Two palladium bimetallics are known (Scheme 34), obtained in low yields (<30%) by treatment of the 2-picolyl bridged precursor [Pd(2-picolyl)Cl(PPh$_3$)]$_2$ with Na[pzTp] and KBp, respectively.[142] The dimeric nature of these materials was established on the basis of molecular weight determinations, and the observation that the ^{1}H NMR spectroscopic data for the 2-picolyl bridge were consistent with those of the parent compound. This latter fact also led the authors to conclude that this ligand retains the rigid boat-like form of the parent. The hindrance this bridge imposes upon the notionally vacant axial coordination site of the metal was invoked to account for the lack of any discernible fluxionality within the pzTp ligand of **459** up to 52 °C, following from the assumption that equilibration is initiated by coordination of a vacant pyrazolyl donor.
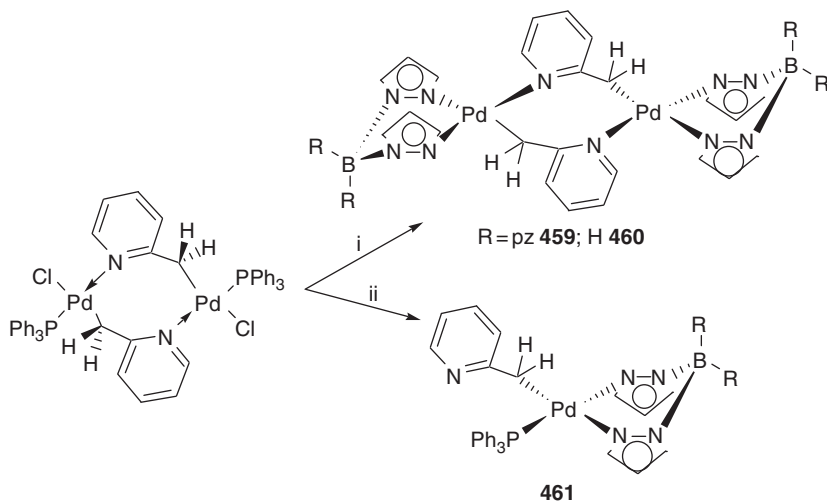
Scheme 34 Conditions and reagents: (i) Na[pzTp] or KBp; (ii) NaTp.

In contrast, the analogous reaction with NaTp affords exclusively the monomeric complex **461**, in which fluxionality of the κ^2-Tp ligand was noted in the temperature range 28 to −31 °C.[142] Moreover, free rotation of the 2-picolyl ligand was inferred from the equivalence of the methylenic protons (cf. inequivalent in **459**, **460**, and the parent), and a discernible [31]P−[1]H coupling of 5 Hz confirmed a *cis* disposition relative to the PPh$_3$ ligand.

A series of complexes (Chart 5) have been reported that comprise both a poly(pyrazolyl)borate ligand and an intramolecularly chelating, mono-anionic coligand. These are typically obtained via halide displacement and dimer cleavage by the respective sodium or potassium poly(pyrazolyl)borate salt, a means by which **462−466**,[45] **467−469**,[143] and **470−479**[144,145] were each prepared in good yield, while the related poly(pyrazolyl)methane complexes **480**[+]**−483**[+] were isolated as their perchlorate salts in the presence of NaClO$_4$.[145]
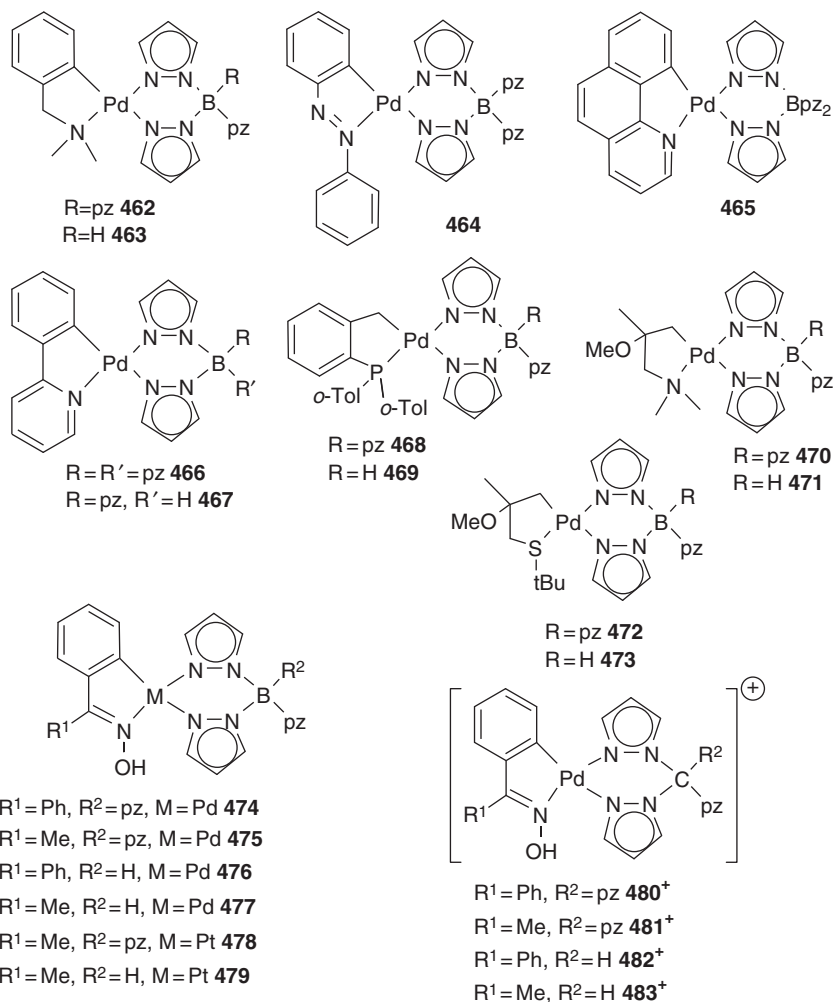
Chart 5 Summary of generic Tp^x and Bp^x complexes with chelating coligands.

As one would anticipate, the palladium Tp complexes all undergo ambient temperature equilibration of the three pyrazole groups on the NMR timescale, via the commonly accepted "tumbling" process[45] by which the free pyrazole coordinates to metal center with subsequent dissociation of another. This process is diminished at low temperature, though limiting spectra for the slow-exchange regime have been obtained only for **469** ($-80\ °C$)[144] and **473** ($-36\ °C$).[143] The pzTp complexes exhibit greater stereochemical rigidity, with slow-exchange limits lying at, or marginally below, ambient temperature, while the fast-exchange limit is typically unattainable. Indeed, only above 50 °C does the dimethylaminobenzyl complex **462** exhibit any fluxionality,[45] while for both **470** and the related alkenyl complex pzTpPd{C,N-C(Cl)=CHCMe$_2$NMe$_2$} (**484**, Section III.D.1) fast exchange is approached at 80 °C, but no limiting spectra have been obtained.[143] Interestingly, the related 2-[(dimethylamino)methyl]naphthalene complex **485** (Chart 6)[146] exhibits significant
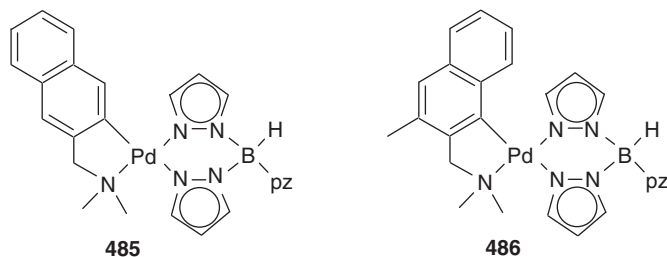
Chart 6   2-[(dimethylamino)methyl]naphthalene complexes of pzTpPd

fluxionality on the NMR timescale at 25 °C, despite its steric and electronic similarity to **462**; no explanation for this discrepancy was found. The 2-[(dimethylamino)methyl]-3methyl-naphthalene complex **486**, an analogue of **485**, has also been prepared,[147] but has received no comment.

The two platinum complexes **478** and **479** are less fluxional, the pzTp complex **478** being stereochemically rigid below 110 °C, above which it becomes unstable in solution, while for the Tp analogue **479** equivalence of the pyrazole groups is achieved at 85 °C. This equilibration slows at ambient temperature, but poor solubility below 10 °C precluded acquisition of limiting spectra.

For only four of these cyclometallated complexes has any chemistry been pursued, *viz.* the C^2,N^1-2-phenylpyridine chelates **466** and **467**, and the P,C-2-phospinobenzyl chelates **468** and **469**, which were each treated with a series of electrophiles and monitored by ^{1}H and ^{31}P NMR spectroscopy. All were unreactive toward MeI, BzBr, PhI, and p-BrC$_6$H$_4$OMe up to ambient temperature, while I$_2$ and the chlorinating agent PhICl$_2$ both induced decomposition.[143]

Recently, a nascent utility has emerged for generic group 8−10 metal complexes bearing cyclometallated 2-phenylpyridines, in the guise of tuneable luminescent materials for application to Organic ElectroLuminescent Devices (OLEDs). This has inspired a search for suitable coligands, which has included poly(pyrazolyl)borates. Though less prevalent than for other metals a handful of cycloplatinated complexes have thus been prepared, comprising the ligands Et_2Bp (**487**),[148] Bp, and Bp* (**488**–**493**, Scheme 35).[149] While **487** was prepared by a classical dimer-cleavage reaction with $Na[Et_2Bp]$, the remaining materials were obtained from monomeric species, the authors describing difficulty in isolation of the respective dimers.

$R^1 = R^2 = H, R^3 = H$ **488**
$R^1 = R^2 = H, R^3 = Me$ **489**
$R^1 = CH_2OH, R^2 = H, R^3 = H$ **490**
$R^1 = CH_2OH, R^2 = H, R^3 = Me$ **491**
$R^1 = H, R^2 = OHex, R^3 = H,$ **492**
$R^1 = H, R^2 = OHex, R^3 = Me$ **493**
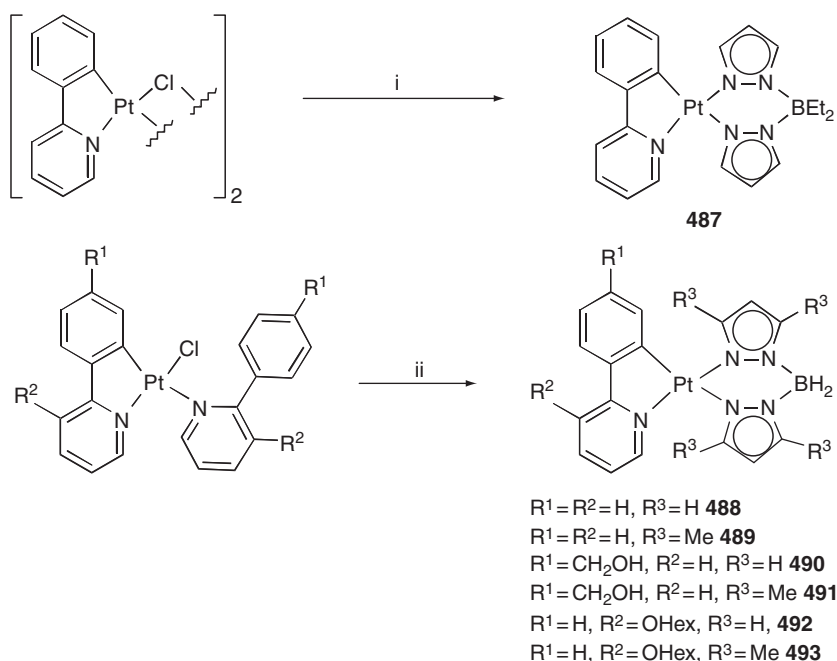
Scheme 35 Conditions and reagents: (i) $Na[Et_2Bp]$, CH_2Cl_2, r.t. 12 h; (ii) KBp^x, CH_2Cl_2, r.t. 5 h.

The (pyrazolyl)borate coligand was established to effect a blue-shift of ca. 20–30 nm in the absorption spectra of **488** and **489**, relative to that in $[\kappa^2\text{-}C^2,N\text{-phenylpyridine})Pt(dpm)]$ (dpm = 2,2,66-tetramethyheptanedionate), though apparently has little effect upon the luminescent emission. These complexes do, however, possess significantly longer apparent lifetimes (5.7 and 8.6 μs) than related dpm compounds (2.6 μs), though the

photoluminescent quantum yields (<1%) are appreciably diminished relative to benchmarks (1−25%), a consequence of an enhanced quenching mechanism.[149] Though no further studies have been specifically described, platinum complexes of this type feature generically in a growing body of patent literature.[150–159]

Finally in this section, the platinum complex BpPt(η^1:η^2-$C_8H_{12}OMe$) (**186**) and related bis(pyrazolyl)methane complex salts [(H_2Cpz_2)M(η^1:η^2-$C_8H_{12}OMe$)]PF_6 (M = Pd **189.PF$_6$**, Pt **190.PF$_6$**) have been obtained from [M (η^1:η^2-$C_8H_{12}OMe$)Cl]$_2$ and NaBp, or H_2Cpz_2/NH_4PF_6, respectively (Scheme 15, Section III.B.1).[73] The palladium analogue of **186** has proven inaccessible. These complexes all exhibit fluxionality, ascribed to inversion of the EN_2M boat (E = B, C).

D. Complexes with σ-donor/π-acceptor ligands

1. Alkenyl and alkynyl compounds

Merely a handful of alkenyl complexes of this type are known. The first examples were obtained spontaneously upon treatment of [$R_2BpPtMe$]$_2$(-cod) (R = Et **131**, Ph **132**) with the electron deficient alkynes $F_3CC{\equiv}CCF_3$ and DMAD, which insert into the Pt−Me linkage to afford vinyl complexes. The 1,2-bis(trifluoromethyl)vinyls were isolated by trapping as the PPh_3 adducts cis-[R_2BpPt{C(CF_3)=C(CF_3)Me}(PPh_3)$] (R = Et **138**, Ph **139**), while the analogous cis-insertion products from DMAD (R = Et **140**, Ph **141**) were merely observed in situ.[61] These species were, however, accompanied by the isolable chelates R_2BpPt{\kappa^2$-C,O-C(CO_2Me)=C(CO_2Me)Me}$ (R = Et **142**, Ph **143**), resulting from trans insertion; the rate of formation of these chelates was found to be solvent dependent, viz. $CH_2Cl_2 > CHCl_3 \gg$ $(CH_3)_2CO$. These outcomes all provide stark contrast to the analogous reactions between **131/132** and less activated alkynes (e.g., PhC≡CPh, PhC≡CH, etc.), which afford exclusively 5-coordinate π-complexes that are inert toward alkyne insertion into the Pt−Me linkage (Sections III.B.1, III.C.2). Neither the chemistry nor properties of **138–143** have been further elaborated.

The first palladium alkenyls, pzTpPd{C,N-C(Cl)=CHCMe$_2$NMe$_2$} (**484**)[144] and the 3-oxo-hexenyl complex **493**,[160] were obtained systematically by halide displacement and dimer cleavage (Scheme 36). In common with alkyl and aryl systems (**462–479**, Section III.C.3), the pzTp ligand was in each case concluded to adopt a κ^2-coordination mode in solution, on the basis of (i) spectroscopic data, (ii) literature precedent, and (iii) the assumption that the Pd(II) centers in these complexes were too electron rich to permit coordination of the third pyrazole; no solid-state data were reported. Both materials are fluxional in solution, and for **484** the slow-exchange limit was attained at −30 °C, with equilibration of the pyrazolyl environments becoming rapid at 79 °C, though the fast exchange limit

was not reached. Fluxionality was established to involve three separate exchange processes, *viz.* (i) inversion of the boat, (ii) rotation of the pz rings, (iii) the ubiquitous ''tumbling'' process. Line-shape analysis of the ^{1}H NMR spectra revealed the boat inversion to be six times more rapid than exchange of the coordinated and uncoordinated pyrazolyl rings, and also enabled calculation of the activation parameters for the process ($E_a = 17.8\pm1.7$ kcal mol^{-1}, $\Delta G^{\#}_{298} = 14.5$ kcal mol^{-1}, $\Delta H^{\#}_{298} = 17.2$ kcal mol^{-1}, $\Delta S^{\#} = 9.1$ cal deg^{-1}mol^{-1}).[144] A similar situation was reported for **494**, which is fluxional between 50 and $-30\,°C$, though neither the fast nor slow-exchange limiting spectra were obtained.[160]
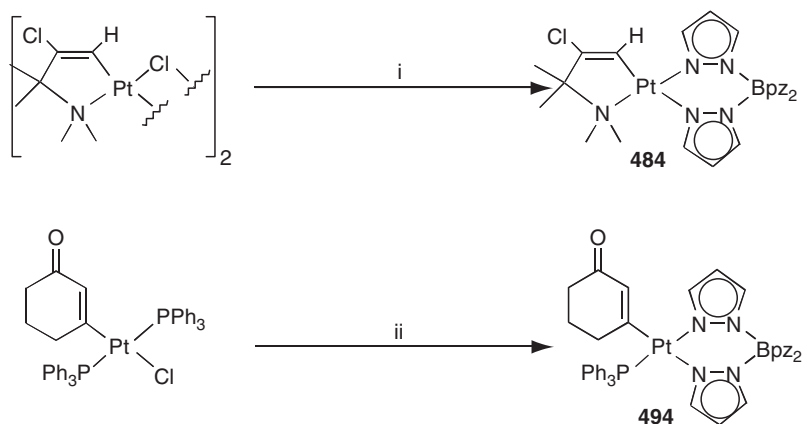
Scheme 36   Conditions and reagents: (i) Na[pzTp], C$_6$H$_6$, 16 h r.t.; (ii) Na[pzTp], C$_6$H$_6$, Δ, 3 h.

The remaining examples are a series of M(IV) allenyl complexes, obtained, along with several propargyl species, from [TpMR$_2$]$^-$ precursors upon treatment with HC≡CCH$_2$Br and MeC≡CCH$_2$Br as part of a study of the propargyl-allenyl tautomeric equilibrium.[161] Thus, while treatment of [TpMMe$_2$]$^-$ (M = Pd **271**$^-$, Pt **308**$^-$) and [TpPd(C$_4$H$_8$)]$^-$ (**277**$^-$) with MeC≡CCH$_2$Br affords only the propargyl complexes **495**–**497** (Scheme 37), comparable reactions with HC≡CCH$_2$Br result in exclusive formation of the palladium allenyls **498** and **499**, while with platinum an equilibrium is established between the allenyl (**500**) and propargyl (**501**) tautomers. No firm conclusions in respect of these equilibria for M(IV) complexes were established from this study.

2. Carbonyls and acyls

The pursuit of metal carbonyls has been relatively limited and only a handful of discrete examples have been reported. Among the earliest of these was BpPtMe$_3$(CO) (**255**), obtained from NaBp and [Me$_3$PtI]$_4$ under an atmosphere of CO, which remains the sole example with the metal
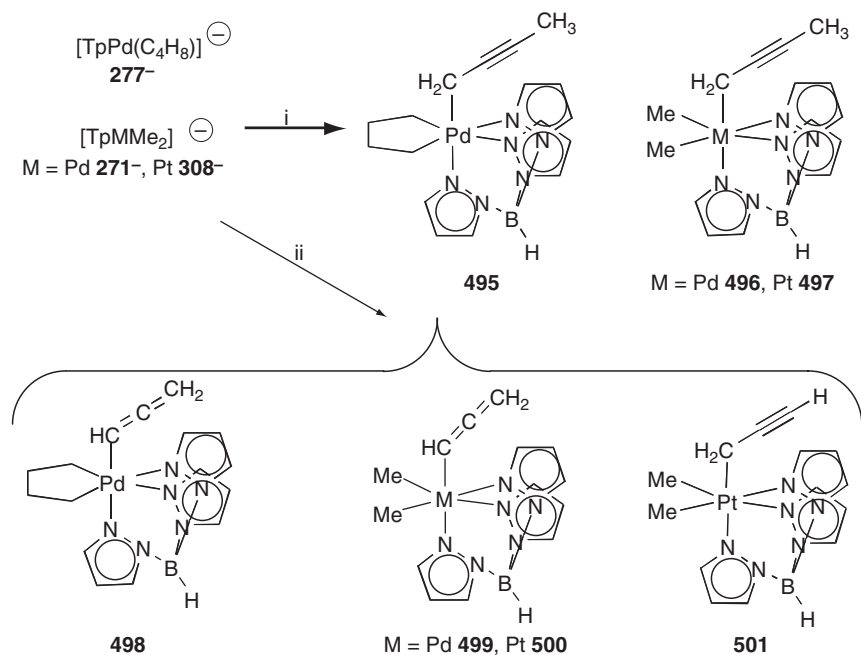
Scheme 37   Reagents: (i) MeC≡CCH₂Br, (ii) HC≡CCH₂Br.

formally in the +4 oxidation state.[92] Given the consequentially low electron density at Pt it is unsurprising that **255** readily loses CO to afford BpPtMe₃ (**249**), which involves an agostic B−H−Pt linkage.

More stable are TpˣPtMe(CO) (Tp **150**,[54] pzTp **396**[128]) both of which form readily upon cleavage of the polymeric [TpˣPtMe]ₙ (Tp **126**, pzTp **130**) by CO; the related Et₂BpPtMe(CO) (**419**)[61] and Me₂Ga(pz)₂PtMe(CO) (**422**)[63] have been similarly prepared by ligand displacement from [Et₂BpPtMe]₂(cod)[61] and Me₂Ga(pz)₂PtMe(cod) (*in situ*) or Me₂Ga (pz)₂PtMe(η²-PhC≡CPh) (**137**),[63] respectively. In contrast, Ph₂BpPtMe (CO) (**402**) was obtained by protonation of [Ph₂BpPtMe₂]⁻ (**400⁻**, Section III.C.3.a) under a CO atmosphere.[132] Complexes **150** and **396** were concluded to adopt 5-coordinate (κ³-Tpˣ) structures on the basis of the limiting low-temperature ¹H and ¹³C NMR spectra, which revealed stereochemically rigid geometries in which Pt satellites were resolved for each of the three pyrazolyl groups, while at higher temperatures fluxionality resulted in equilibration of the pyrazolyl groups. However, a single crystal X-ray diffraction study of **150** revealed a slightly distorted square-planar (κ²-Tp) geometry,[129,130] which has been argued to represent an intermediate in the pyrazolyl equilibration process—that is, the exchange involves a Pt−N bond-breaking process. Though initially considered unlikely,[128] this argument has been supported by the demonstration

that the analogue Tp*PtMe(CO) (**348**) adopts both κ^2- and κ^3 coordination modes in solution, determined by the presence of two B−H stretching modes, while a single mode, consistent with κ^3-coordination, is apparent in the solid state.[65] Though structural data for **348** remain elusive, a recent X-ray study of Tp*PtH(CO) (**502**) clearly demonstrated a 5-coordinate geometry, albeit that the third pyrazole donor interacts only weakly with the metal (d(Pt−N) 2.489 Å, cf. 2.088, 2.139 Å).[68]

Synthesis of the Tp* derivatives utilized octahedral Pt(IV) precursors of the type Tp*PtRR′(R = Me, H; R′ = Me, Ph) which upon low-temperature protonation under a CO atmosphere afford the cationic complexes [(κ^2-HTp*PtR(CO)]$^+$ (R = Me **365$^+$**,[65] H **369$^+$**;[68] Scheme 38, also Section III.C.1), which are isolable as the BAr$^f_4$ salts. When protonation is instead effected with HBF$_4$, the resulting cations are cleanly deprotonated *in situ* with NaH, affording the neutral Pt(II) carbonyls, though in the case of **369$^+$** deprotonation was effected with NEt$_3$.[68] The same approach has been applied to the synthesis of Tp*PtPh(CO) (**376**), though the cation [(κ^2-HTp*PtPh (CO)]$^+$ (**503$^+$**) was not isolated.[67]
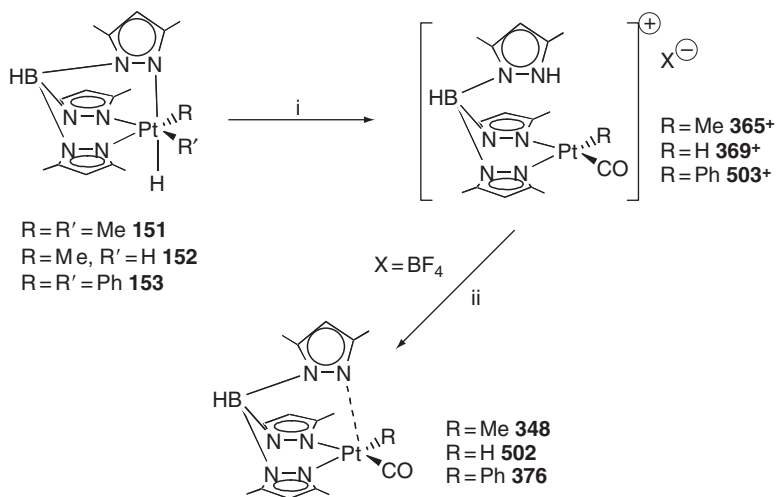
Scheme 38 Conditions and reagents: (i) CH$_2$Cl$_2$, −78 °C, [H(OEt$_2$)$_2$]BAr$^f_4$ *or* HBF$_4$; (ii) NaH, thf, −78 °C.

The notional reverse of these syntheses, that is, conversion of the Pt(II) carbonyls into Pt(IV) hydridoorganyls, has also been described. This was first demonstrated with the water oxidation of **150** in acetone solutions, which within 24 h at ambient temperature affords good yields of TpPtMeH$_2$ (**347**).[117] The mechanism of this conversion was proposed to

involve attack of H_2O at the carbonyl with subsequent loss of CO_2, analogous to the WGS reaction, followed by protonation of the resulting intermediate $[TpPtMeH]^-$ anion, facilitated by the presence of trace carbonic acid from dissolved CO_2. This was supported by ^{13}CO labeling studies, which confirmed loss of $^{13}CO_2$, while the prevalence of the WGS reaction over protonation was established, given that **150** preferentially protonates at pyrazole to afford $[\kappa^2\text{-}HTpPtMe(CO)]^+$ (**504**$^+$), which was isolated and structurally characterized as the BF_4 salt.

More recently, a modified water oxidation procedure was employed in the synthesis of the trihydride Tp*PtH$_3$ (**159**) from Tp*PtH(CO) (**502**) under ''slightly basic'' conditions in refluxing acetone. This process is reversed when **159** is treated with $[H(OEt_2)_2]BAr^f_4$ under an atmosphere of CO,[68] the formation of **502** being consistent with loss of H_2, though in the absence of CO no evidence for this was observed under ambient conditions. Low-temperature protonation studies, under CO, enabled observation of an intermediate species comprising three hydrides (2:1 ratio), which was attributed to the 6-coordinate Pt(IV) complex $[(\kappa^2\text{-}HTp^*)PtH_3(CO)]BAr^f_4$ (**505.BAr$^f_4$**) in which the unique hydride occupies a position *trans* to the carbonyl. On allowing this species to attain ambient temperature, loss of H_2 was readily observed by ^1H NMR spectroscopy, supporting the supposition.

The susceptibility of the Pt(II) carbonyls toward nucleophilic attack (i.e., by H_2O, in initiating the WGS reaction) is perhaps unsurprising, given the relatively high carbonyl stretching frequencies (ν_{CO}/cm^{-1} 2057 **348**, 2070 **502**, 2090 **376**) that illustrate limited π-retrodonation from the metal, and thus imply appreciable electrophilicity in the carbonyl ligand. This has been exploited, in the case of **348**, as a means of generating acyl and, unprecedented, formyl complexes. Thus, treatment of **348** with RLi (R = Me, Ph) cleanly affords the anionic complexes $[Tp^*PtMe\{C(=O)R\}]^-$ (R = Me **349**$^-$, Ph **350**$^-$), characterized on the basis of NMR spectroscopic data, which was consistent with square-planar geometries based on chiral Pt(II) centers.[120] Quenching of these anions with HCl·Et$_2$O or MeI affords high yields of the chiral, Pt(IV) acyls Tp*PdMe{C(O)R}R′(R = Me, R′= Me **351**, H **352**; R = Ph, R′= Me **353**, H **354**), conclusively characterized on the basis of ^1H and ^{13}C NMR spectroscopic data.

Treatment of **348** with Na[HBEt$_3$] has also been reported, affording initially the Pt(II) formyl complex anion $[Tp^*PtMe\{C(O)H\}]^-$ (**355**$^-$), as determined by ^1H and ^{13}C NMR spectroscopic data that again reveal a chiral metal center. At 193 K two formyl environments (2:1 ratio) are apparent, which coalesce at 201 K. These are attributed to restricted rotation about the Pt−C linkage, and $\Delta G^{\#}$ for conversion of the minor to major isomer was calculated at 8.8 kcal mol^{-1}.[120] Protonation of **355**$^-$ affords exclusively the Pt(IV) formyl complex Tp*PtMe{C(O)H}H (**356**), with no evidence for protonation of either pyrazole or the formyl, or

indeed formation of H_2. Though the identity of **356** was firmly established from NMR spectroscopic data, its isolation was precluded by a propensity toward decarbonylation, affording the dihydride Tp*PtMe(H)$_2$ (**152**). A comparable situation is reported for the generation of Tp*PtH$_2$(CHO) (**506**) from Tp*PtH(CO) (**502**), the former being observed by *in situ* ^{1}H NMR studies, prior to spontaneous decarbonylation to the trihydride Tp*PtH$_3$ (**159**).

A more general range of Pd(II) acyl complexes has been prepared by carbonylation of organometallic precursors. Thus, Bp^{x}Pd{C(O)Me}(PR$_3$) (Bp, R = Ph **431**, Cy **432**; Bp*, R = Ph **433**, Cy **434**),[135] Bp^{x}Pd{C(O)CH$_2$R} (PMe$_3$) (Bp, R = CMe$_2$Ph **435**, SiMe$_3$ **436**; Bp*, CMe$_2$Ph **437**, SiMe$_3$ **438**),[136] and Tp*Pd{C(O)R}(PPh$_3$) (R = Me **447**, *p*-Tol **448**)[137] have each been obtained upon carbonylation (2 atm.) of the alkyls **423–426**, **427–430**, and **439–440**, respectively. All of the Bp^x systems exhibit the ubiquitous boat-inversion fluxionality, which for Bp derivatives is typically rapid at ambient temperatures, while with Bp* the process is retarded on the NMR timescale under comparable conditions.[136] Uniquely among these complexes, **434**, which comprises two ''bulky'' ligands (*viz.* Bp* and PCy$_3$) exhibits fluxionality attributed to dechelation of one pyrazole group, a consequence of steric crowding between the 3-methyl substituent and cyclohexyl groups.[135] A directly analogous scenario was observed for the parent alkyl **426**. The Tp* systems also exhibit fluxionality, attributed to an intramolecular exchange of coordinated and uncoordinated pyrazole groups,[137] a process for which limiting spectra were not obtained.

A key impetus in the study of these materials was the pursuit of catalytic CO/olefin copolymerization, reactivity to which **431–438** and **447** and their parent alkyls are entirely inert. Though **448** *has* been found to react with norbornadiene, affording the insertion product Tp*PdC$_7$H$_8$C (O)*p*-Tol) (**449**), it does so slowly (>1 day). However, when the parent *p*-Tolyl complex **440** is simultaneously exposed to both CO and norbornadiene, catalytic copolymerization ensues, affording the polyketone within hours (Section IV.A).[140,141]

The synthesis of complexes **435–438** has also been effected directly from KBp^x and the respective acyl precursors [PdCl{C(O)CH$_2$R}(PMe$_3$)$_2$], a route that has also been utilized to prepare the more exotic ferrocenylacyls LPd(PPh$_3$){C(O)Fc} (L = pzTp **507** Tp **508**, Bp **509**).[162] Both **507** and **508** are stable in the solid state and solution; however, the Bp derivative **509** was reported to decompose in halogenated solvents, and proved less soluble than its congeners in nonhalogenated solvent. All three materials were fully characterized spectroscopically, revealing the ubiquitous fluxionality of **507** and **508** on the NMR timescale. Thus, equivalence within the pzTp ligand was observed at 51 °C but frozen out to a static κ^2-structure -31 °C, while for Tp equivalence was apparent at 23 °C,

slowing at $-45\,^{\circ}$C, though no limiting spectrum was obtained. No special fluxional processes were identified for **509**.

Cyclic Voltammetry (platinum electrode) was undertaken for each of these materials as MeCN solutions in the presence of 0.1 mol dm^{-3} of NH$_4$PF$_6$. This revealed readily reversible redox couples for both **507** and **508**, with ΔE_p (62 mV) close to the theoretical value of 59 mV, and oxidation products that were stable during the sweep. In contrast, the corresponding redox-couple for **509** had $\Delta E_p = 147$ mV, leading the authors to describe this process as quasi-reversible. These redox processes were all attributed to the Fe(II)/Fe(III) couple of the ferrocenyl moiety, and for each the observed E^0 was more anodic than for ferrocene itself. This was attributed to the electron withdrawing effect of the palladiocarbonyl moiety, which appeared most pronounced for the pzTp ligand, resulting from the greater scope for delocalization across four pyrazolyl groups. An irreversible oxidation of the Pd(II) center was also observed for each complex above 1300 mV.

3. Isonitriles

The first such materials, TpPtMe(CNR) (R = ^{t}Bu **397**, Cy **398**),[128] were prepared by isocyanide cleavage of the polymeric [TpPtMe]$_n$ (**126**), directly analogous to the synthesis of the carbonyl complex TpPtMe (CO) (**150**, *vide supra*),[128] while Et$_2$BpPtMe(CNTol) (**416**) was similarly obtained by displacement of cyclooctadiene from [Et$_2$BpPtMe]$_2$(cod) (**131**).[61] Like the carbonyl analogue **150**, both **397** and **398** are fluxional in solution, while an X-ray diffraction study of **397** revealed a 4-coordinate geometry in the solid state,[131] directly analogous to that of **150**.[129,130] More recently, the Tp* analogue of **397**, *viz.* Tp*PtMe(CN^{t}Bu) (**372**) was obtained from the Pt(IV) precursor Tp*PtMe$_2$H (**151**), which when protonated in the presence of ^{t}BuNC gives rise to the cationic [(κ^2-HTp*)PtMe (CN^{t}Bu)]$^+$ (**364$^+$**), subsequent deprotonation *in situ* affording **372**.[65]

Only two further terminal isocyanide complexes have been reported, the bimetallic **451$^+$** and monometallic **458**, obtained in accordance with Scheme 33 (Section III.C.3.b).[88] The bimetallic complex **451$^+$** was demonstrated to adopt a static structure, comprising a single type of pentafluorophenyl group and two different pyrazolyl environments, distinguished by the *trans* disposed ligands (C$_6$F$_5$ vs. CNtBu). A very rapid intramolecular interconversion between conformational isomers, corresponding to inversion of the M(N–N)$_2$B boat, was thus concluded. In contrast, at ambient temperatures **458** exhibits a single pyrazolyl environment, consistent with equilibration of the four pyrazoles on the NMR timescale, fluxionality that is frozen out at $-60\,^{\circ}$C.

Finally, there is a single example of an isocyanide-bridged bimetallic complex, *viz.* the metal−metal bonded [TpPd(μ-CNXyl)]$_2$ (**510**, Figure 5), prepared from [Pd$_2$Cl$_2$(CNXyl)$_4$] and NaTp, alongside a variety of
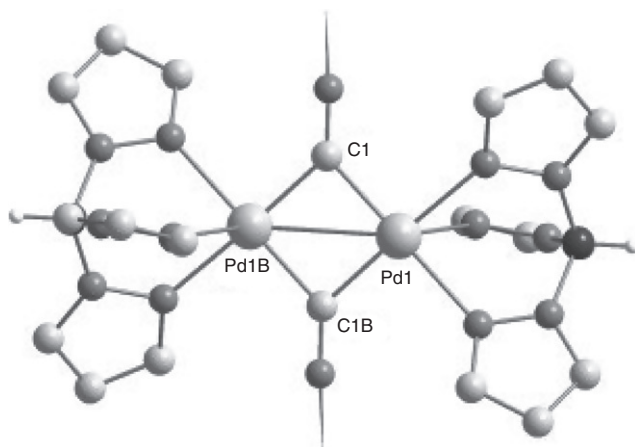
Figure 5   Molecular structure of [TpPd(μ-CNXyl)]$_2$ (**510**) with Xylyl groups and hydrogen atoms omitted for clarity.

Cp′derivatives.[163] In the sold state, the two Tp ligands of **510** bind in an asymmetric κ^3 fashion, such that two pyrazolyl donors are strongly bound (d(Pd−N) 2.16 Å), while the third interacts weakly (d(Pd−N) 2.64 Å). This was interpreted as a formal 5-coordinate geometry correlating with the presumed intermediate responsible for equilibration of all pyrazolyl groups in the solution phase. The metal−metal bond of **510** was considered to be weak, on the basis of full occupancy of the σ* and π* orbitals of the Pd$_2$(CNXyl)$_2$ core.

4. Nitrosyls

Only two nitrosyl complexes have thus far been reported, obtained from the reaction of the anions [Tp^{x}Pd(κ^2-CH$_2$CMe$_2$-o-C$_6$H$_4$)]$^-$ (Tp **299**$^-$, Tp* **327**$^-$) and Diazald, affording Tp^{x}Pd(κ^2-CH$_2$CMe$_2$-o-C$_6$H$_4$)NO (Tp **409**, Tp* **410**, Scheme 39).[133] Both materials were assigned stereochemically

R=H **299**$^-$; Me **327**$^-$

R=H **409**; Me **410**
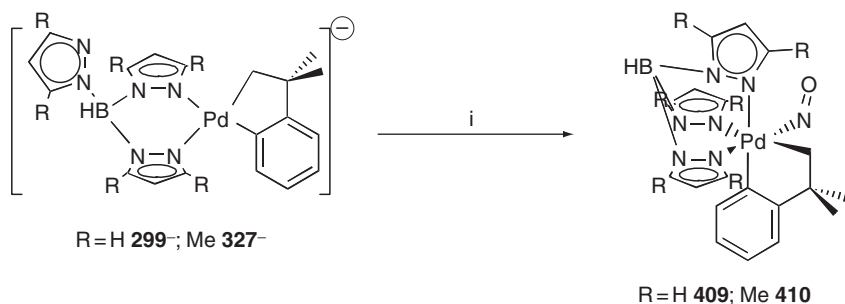
Scheme 39   Reagents: (i) Diazald (N-methyl-N-nitroso-p-toluenesulfonamide).
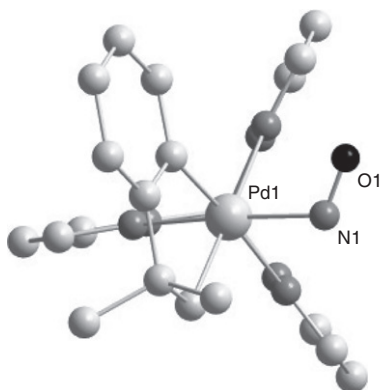
Figure 6   Molecular structure of **409** projected along the Pd−B vector.

rigid, 6-coordinate geometries (κ^3-Tp^x) in solution on the basis of spectro-scopic data, and were described as {Pd(NO)}^{8} systems, with Pd(IV) centers and "bent" NO$^-$ ligands. Indeed, the "bent" NO geometry was supported, albeit equivocally, by the infrared v_{NO} data (1650 cm^{-1} **409**, 1660 cm^{-1} **410**) and for **409** was confirmed by a single crystal X-ray diffraction study ($\angle$ Pd−N−O 118.4(5)°, d(N−O) 1.151(7) Å; Figure 6). Theoretical calcula-tions on the model complexes (κ^3-Tp^x)PdMe$_2$(NO) (Tp^x = Tp, Tp*) using DFT (B3LYP/LANL2DZ*) also supported these assignments, showing good agreement with the experimentally derived structure of **409**.

The reaction of both complexes with dioxygen was explored, affording in the case of **410** an intractable mixture. However, **409** reacts to afford the Pd(IV) nitrate complex TpPd(κ^2-CH$_2$CMe$_2$-o-C$_6$H$_4$)ONO$_2$ (**511**, Scheme 40) in 50% yield, *inter alia* intractable materials. The identity of **511** was assigned on the basis of: (i) infrared spectroscopic data that support the presence of a coordinated NO$_3$ group (v 1500, 1275, 985 cm^{-1}); (ii) its behaviour as a nonelectrolyte, and (iii) its conversion to the complex salt [TpPd(κ^2-CH$_2$CMe$_2$-o-C$_6$H$_4$)(PMe$_3$)]$^+$NO$_3^-$ (**512.NO$_3$**) upon treatment with PMe$_3$, the presence of free NO$_3^-$ being confirmed by a strong infrared absorption v_{as}(NO) = 1375 cm^{-1}. The mechanism by which **511** is obtained remains to be fully established, however, the intermediacy of the nitrocomplex TpPd(κ^2-CH$_2$CMe$_2$-o-C$_6$H$_4$)NO$_2$ (**411**) was discounted, since an isolated sample of this material, obtained by NO$_2$ oxidation of **299**$^-$, failed to convert to **511** upon exposure to O$_2$.

E. Hydrides

Complexes of this type are relative few in number; indeed, there remain no examples of discrete palladium hydrides, though an agostic hydrogen inter-action was reported for Pd{(pz)$_2$BBN} (**96**)[46] between Pd and the bridgehead
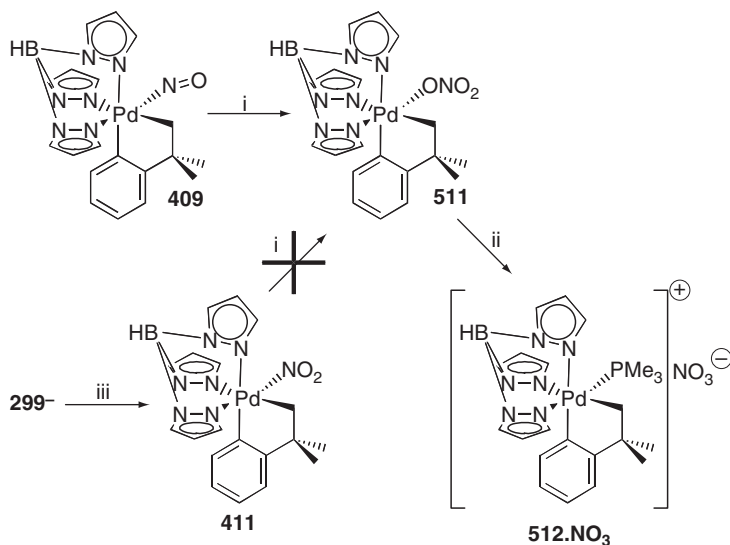
Scheme 40   Reagents: (i) O_2; (ii) PMe_3; (iii) NO_2.

C—H unit, as seen for Co,[8,9] Rh[47] and Ni (**7**)[8] analogues. The extent of this interaction has, however, not been established. Similarly, an agostic interaction was convincingly invoked for the Pt(IV) complex $BpPtMe_3$ (**253**), on the basis of the assumed octahedral geometry, and a strong infrared band at 2039 cm^{-1} (v_{BHPt}), which was absent from the D_2Bpz_2 analogue, and lost upon reaction with $P(OMe)_3$ to give $BpPtMe_3\{P(OMe)_3\}$ (**254**).[92] Though no structural or NMR spectroscopic evidence in support of this agostic linkage have ever been reported, such data were recently obtained for an analogous complex based upon the $H_2B(mt)_2$ (mt = methimazolyl) ligand, *viz.* $\{\kappa^2\text{-}S,S',$ $H\text{-}H_2B(mt)_2\}PtMe_3$ and its Me_3PtI adduct.[164]

1. Diorganohydrides

All examples of discrete metal hydrides are based on platinum and are either organohydrides of the type $Tp^xPtR_nH_{3-n}$, or derived from these. The first such materials, Tp^xPtMe_2H ($Tp^x = Tp^*$ **151**,[108] Tp **340**,[114] pzTp **341**[107]), Tp^*PtPh_2H (**153**),[108] and $TpPt(Tol)_2H$ (**342**),[107] were obtained from the respective Pt(II) diorganyl anions $[Tp^xPtR_2]^-$ upon protonation by acids, varying in strength from phenol[107,114] to CF_3CO_2H[107] and HCl[108] (Section III.C.1). These materials all exhibit remarkable stability, both as solids and in solution, being resistant to reductive elimination of RH under ambient conditions. Indeed, the Tp* complex **151** eliminates methane only above 190 °C,[108] while Tp analogue **340** is stable to above 140 °C.[107] Similarly the diphenyl complex **153** survives above 230 °C,[108] while **342**

decomposes with loss of toluene and ditolyls above 90 °C.[107] Nonetheless, thermolysis of **151** in benzene has been demonstrated to afford Tp*PtPh$_2$H (**153**), by way of the intermediate Tp*PtMePhH (**357**), which arises via thermal elimination of methane and subsequent C−H activation of the solvent, a process that then repeats.[123] The mechanism of this conversion was explored at some length (see also Sections III.C.1, IV.A), deuterium labeling studies revealing H/D scrambling between the organo and hydrido ligands, consistent with the intermediacy of an alkyl σ-complex during the elimination step. The coordinately unsaturated product of methane elimination, *viz.* ''Tp*PtMe'' was trapped by effecting thermolysis in C$_6$F$_6$/NCMe, thus affording Tp*PtMe(NCMe) (**371**).

Methane elimination from **151** has also been effected using acids, protonation with [H(OEt$_2$)$_2$]BAr$^f_4$ at −78 °C affording the solvent adduct [κ^2-HTp*PtMe(solv)]$^+$, which was observed *in situ* and also trapped with a variety of donor ligands (Section III.C.3).[65] The protonation step proceeds exclusively at a pyrazolyl nitrogen center, as demonstrated through use of [D(OEt$_2$)$_2$]BAr$^f_4$, which results in no deuterium incorporation into either the hydridic or methyl positions; subsequent crystallographic studies of adducts [HTp*PtMe(L)]$^+$ also clearly demonstrated the κ^2-*N,N'*-(Hpz*)BH(pz)$_2$ mode of the HTp* ligand. It is considered that this facilitates κ^3→κ^2 dechelation of the Tp* ligand, to avail the requisite coordinate unsaturation for reductive elimination to proceed.

This role is also served by the borane B(C$_6$F$_5$)$_3$, which has been employed in thermal reactions between **151** and a variety of alkanes, leading to formation of Tp*PtMe(R)H (R = *n*-C$_5$H$_{11}$ **168**, *c*-C$_5$H$_9$ **169**, *c*-C$_6$H$_{11}$ **170**, *c*-C$_8$H$_{14}$ **171**, CH$_2$CH$_2$^{t}Bu **172**).[69] These, in turn, eliminate a second equivalent of methane and undergo β-hydride abstraction to afford the respective alkene complexes Tp*PtH(η^2-alkene) (alkene = CH$_2$=CH*n*Pr **163**, *c*-C$_5$H$_8$ **164**, *c*-C$_6$H$_{10}$ **165**, *c*-C$_8$H$_{14}$ **166**, CH$_2$=CH*t*Bu **167**). Interestingly, the synthesis of **168** and **170** was previously effected, alongside that of Tp*PtPhMeH (**357**), by utilizing B(C$_6$F$_5$)$_3$ to abstract ''Me$^-$'' from the salt K[Tp*PtMe$_2$] (**K.297**) in the presence of pentane, cyclohexane, and benzene, respectively.[121] On that occasion, no evidence for further reaction to afford **163** or **164** was reported.

The diphenyl complex **153** has also been utilized in similar chemistry, its protonation at −78 °C inducing reductive elimination of the hydride and one phenyl ligand to afford the intermediate η^2-benzene complex [κ^2-HTp*PtPh(η^2-C$_6$H$_6$)]$^+$ (**181$^+$**),[72] from which benzene is displaced by the donors CO and C$_2$H$_4$, *in situ* deprotonation with NEt$_3$ affording Tp*PtPh(L) (L = CO **376**, C$_2$H$_4$ **158**).[67] Subsequent treatment of **158** with B(C$_6$F$_5$)$_3$ at 60 °C induces insertion of the C$_2$H$_4$ ligand into the Pt−Ph linkage, followed by spontaneous C−H activation to afford the chiral platinacycle Tp*PtH(κ^2-C$_6$H$_4$-2-CH$_2$CH$_2$) (**176**, also Scheme 29, Section III.C.1.c), protonation of which induces reductive elimination of

the alkyl and hydrido functions. The insertion/oxidative addition process is appreciably more facile in the propene analogue of **158**, which is non-isolable. Protonation/deprotonation of **153** in the presence of propene affords only the platinacycles **391** (major) and two diastereoisomers of **394** (Scheme 30, Section III.C.1.c). The 2,1-insertion product **393** was established as the kinetic product by preparing it cleanly, from mixing $[\kappa^2\text{-HTp*PtPh}(\eta^2\text{-}C_6H_6)]BF_4$ (**181.BF$_4$**) and propylene with NEt$_3$, then observing (^{1}H NMR spectroscopy) its clean conversion to **394a/b** at 80 °C. Complexes **176** and **394**, and the related species **395**, have also been obtained via the borane-assisted activation of alkylarenes by Tp*PtMe$_2$H (**151**).

R = R′ = H **176**
R = Me, R′ = H **394a/b**
R = H, R′ = Et **395**
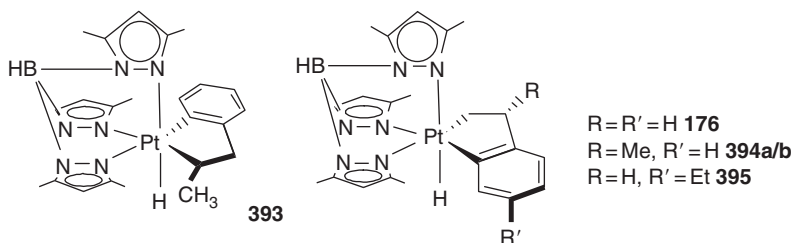
One final piece of reactivity chemistry has been described, *viz.* the reactions of Tp*PtR$_2$H (R = Me **151**, Ph **153**) and TpPtMe$_2$H (**340**) with dioxygen. These afford cleanly the Pt(IV) hydroperoxide complexes Tp*PtR$_2$(OOH) (R = Me **344**,[115] Ph **345**)[116] and TpPtMe$_2$(OOH) (**346**),[116] which were comprehensively characterized, including a single crystal X-ray diffraction analysis of **344**.[115] These reactions were established to proceed via a radical chain mechanism, largely comparable to the autoxidation of alkanes,[116] being facilitated by UV irradiation, while in the dark the thermal process is enhanced by addition of a radical initiator, and impeded by radical inhibitors. Though the importance of this result to the pursuit of commercially viable homogeneous catalytic alkane oxidation was emphasized, no further work on these complexes has been reported.

2. Dihydridoorganyls

The seminal synthesis of this type of complex, specifically TpPt(H)$_2$Me (**347**), barely a decade ago, resulted from stirring TpPtMe(CO) (**150**) in 1:1 acetone/H$_2$O for 24 h,[117] a process that was subsequently patented.[118] A modified, base-catalyzed, variation of this process was independently applied to the synthesis of Tp*Pt(H)$_2$Me (**151**) from Tp*PtMe(CO) (**348**).[66] The initial step of this conversion is believed to be analogous to the WGS reaction, *viz.* nucleophilic attack (H$_2$O *or* $^-$OH) at the carbonyl inducing loss of CO$_2$, a process supported by ^{13}CO labeling studies that confirmed loss of ^{13}CO$_2$.[117] Resultant traces of carbonic acid then facilitate protonation of the intermediate [Tp^{x}PtMeH]$^-$ anion.

As with the monohydrides, these materials exhibit appreciable reluctance toward the elimination of methane; indeed, prolonged heating at 70 °C in methanol leaves **347** apparently unchanged, with no evidence for CH_4 liberation.[124] However, in CH_3OD comparable conditions effect complete H/D exchange in both the methyl and hydridic positions, implicating a methane σ-complex that is unusually resistant toward dissociation; the process is reversed in CH_3OH. This σ-complex was established to involve an η^2-C−H coordination mode, on the basis of DFT studies,[125] which, in combination with kinetic data,[124,125] also indicated a significantly greater barrier to elimination ($\Delta G^{\ddagger}$ 11.9 kcal mol^{-1}) compared with C−H activation ($\Delta G^{\ddagger}$ 6.6 kcal mol^{-1}) and the essentially barrier-less process of methane rotation; hence the observed stability. Interestingly, attempts to induce methane elimination through addition of PMe_3 failed to displace the alkyl ligand, inducing instead loss of H_2 to give $TpPtMe(PMe_3)$ (**377**),[124] via the intermediacy of κ^2-$TpPtMe(PMe_3)_2$ (**513**). Despite further DFT studies, no acceptable explanation for the prevalence of this process has yet been determined.[125] Methane elimination from **347** can, however, be effected thermally, heating to 130 °C in benzene for 8 days resulting in formation of $TpPtPh(H)_2$ (**514**) via the ubiquitous methane-elimination/C−H activation protocol.[125]

Acid-catalyzed elimination of RH has again proven a valuable tool, applied most extensively to $Tp^*Pt(H)_2Me$ (**152**). Thus, protonation of **152** with $[H(OEt_2)_2]BAr^f_4$ affords the anticipated solvento complex
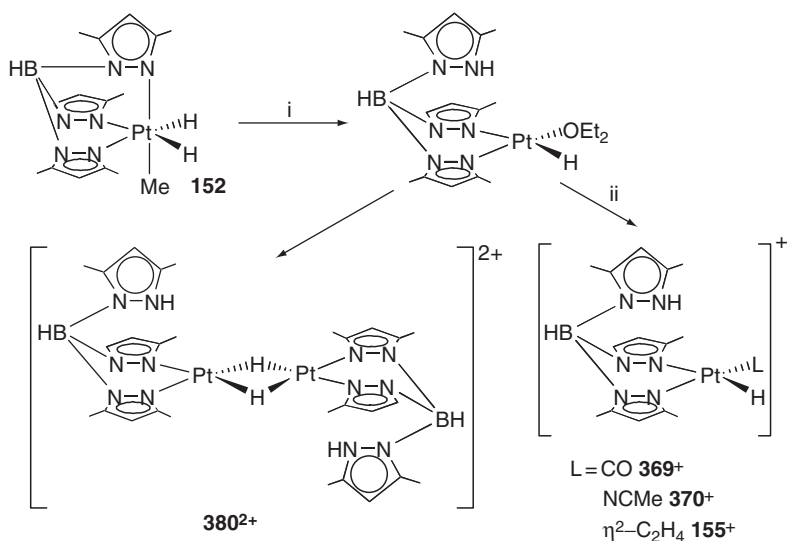
Scheme 41 Reagents and conditions: (i) [H(OEt$_2$)$_2$]BAr$^f_4$, −78 °C, CH$_2$Cl$_2$; (ii) L (L = CO, NCMe, C$_2$H$_4$).

$[\kappa^2\text{-HTp*Pt(H)(solv)}]^+$, which was trapped with excess donors as $[\kappa^2\text{-HTp*Pt(H)(L)}]^+$ (L = CO **369**$^+$,[68] NCMe **370**$^+$,[66] $\eta^2\text{-C}_2\text{H}_4$ **155**$^{+66}$). In the absence of extraneous donors, the solvento complex dimerizes to the hydride-bridged dication $[\{(\kappa^2\text{-HTp*})\text{Pt}(\eta\text{-H})\}_2]^{2+}$ (**380**$^{2+}$, Scheme 41), as confirmed both crystallographically and by ^{1}H NMR spectroscopy, though only with long-acquisition times could the ^{195}Pt satellites be resolved for the bridging hydride ligands.[66] In contrast to the monomeric species, **380**$^{2+}$ is deep red in color, a property that was probed by electronic spectroscopy and DFT studies, revealing two low-energy transitions (v 562 and 355 nm) to a low-lying metal−metal nonbonding MO of the 3c-2e Pt(μ-H)$_2$Pt moiety.

Treatment of **152** with substoichiometric amounts of B(C$_6$F$_5$)$_3$ in the presence of a variety of aromatic solvents has also been described, resulting in loss of methane and subsequent C−H activation to yield the complexes Tp*Pt(H)$_2$Ar (Ar = Ph **177**,[122] Tol **182**,[122] C$_6$H$_4$Et **358**,[67] C$_6$H$_4$CHMe$_2$ **359**,[67] 2,5-Xyl **183**,[122] 3,4-Xyl **360**,[122] 3,5-Xyl **361**,[122] Scheme 27, Section III.C.1.c). Among these, the *p*-Xylene derivative **183** is unique in exhibiting no dynamic behavior at room temperature, while the others all participate in ring rotation, which can be frozen out at low temperature to avail several rotameric forms.[122] For **182**, **358**, and **359** regioisomers are also observed.[67,122]

Several of these aryl compounds have been demonstrated to undergo protonation at a pyrazole group to afford moderately stable cationic η^2-arene complexes, *viz.* $[\kappa^2\text{-HTp*Pt(H)}(\eta^2\text{-Ar})]^+$ (Ar = C$_6$H$_6$ **178**$^+$,[70] Tol **179**$^+$,[72] *p*-Xyl **180**$^+$,[72] Scheme 14, Section III.B.1), directly analogous to the protonation of Tp*Pt(H)$_2$Me (**152**) and Tp*PtPh$_2$H (**153**) (*vide supra*). Each complex was convincingly identified on the basis of spectroscopic data, and for **178**$^{+70}$ and **180**$^{+72}$ supported by a single crystal X-ray diffraction study. In all cases, migration of the platinum around the ring is observed, and this can be frozen out for the xylene adduct, enabling calculation of the barrier to fluxionality (9.2 kcal mol^{-1}).[72] While the adduct **178**$^+$ shows no evidence for exchange with free benzene, nor indeed dissociation of the η^2 benzene ligand, both the toluene and xylene adducts slowly lose the arene above 273 K, resulting in formation of the previously noted dihydride-bridged dimer **380**$^{2+}$.[72] All three adducts exhibit intramolecular scrambling between the aryl and hydride ligands, once again postulated to proceed via a 5-coordinate intermediate of the type κ^2-HTp*Pt (H)$_2$Ar, existing as the minor component of an equilibrium with the arene π-complexes. Activation barriers for this intrinsic C−H activation process were calculated as $\Delta G^{\ddagger}$ = 12.7, 13.6, and 14.2 kcal mol^{-1} for **178**$^+$, **179**$^+$, and **180**$^+$, respectively.[72]

Evidence in support of the postulated 5-coordinate intermediate κ^2-HTp*Pt(H)$_2$Ph was obtained when **178**$^+$, generated *in situ* from **177**, was treated at 193 K with excess of nitriles RCN, which afforded

spectroscopically observable mixtures of 178^+ and the cationic nitrile adducts [{κ^2-HTp}Pt(H)$_2$Ph(NCR)]$^+$ (R = Me 381^+, tBu 382^+, Ph 384^+, C$_6$H$_4$Me-4, 385^+, C$_6$H$_4$OMe-4 386^+, C$_6$H$_4$Cl-4 387^+, C$_6$H$_4$CF$_3$-4 388^+, Scheme 28, Section III.C.1.c).[71] Similarly, addition of NCtBu to [{κ^2-HTp*}PtPh(η^2-C$_6$H$_6$)]$^+$ (372^+) afforded [{κ^2-HTp}Pt(H)Ph$_2$(NCtBu)]$^+$ (383^+). Complete consumption of the η^2-benzene adducts was not observed, rather a dynamic equilibrium is established with the trapped C−H addition product; this equilibrium shifts in favor of the η^2-benzene adduct on warming to 232 K, but is reestablished on cooling back to 193 K. Kinetic studies of the 178^+/381^+ system revealed activation barriers for the C−H addition and NCMe trapping processes of 13.4 and 12.8 kcal mol^{-1}, respectively, while the rate of insertion into the Ph−H bond was established to be comparable to the rate of trapping at 230 K. It was also established that the dihydride species are more stabilized by electron-rich nitriles.

Isolation of the nitrile adducts at low temperature proved ineffective, and upon warming above −30 °C elimination of benzene was observed; thus, 381^+, 382^+, and 383^+ gave rise to [{κ^2-HTp*}PtR(NCR')]$^+$ (R = H, R' = Me 370^+, R'= tBu 389^+; R = Ph, R' = tBu 390^+), analogous to the reactions observed upon protonation of Tp*PtMe$_2$H (151) and Tp*Pt(H)$_2$Me (152) in the presence of NCMe, for which comparable 6-coordinate nitrile adducts were not observed (Section III.C.1.c).[65,66]

The first stable 5-coordinate dihydride of this type to be discretely isolated was [{κ^2-HTp*}Pt(H)$_2$(SiEt$_3$)]$^+$ (379^+), which was accessed by protonation, with [H(OEt$_2$)$_2$]BAr$^f_4$, of the parent Tp*Pt(H)$_2$(SiEt$_3$) (378),[127] itself obtained via thermal activation of Et$_3$SiH by Tp*PtMe$_2$H (151).[126] The latter reaction was proposed to involve initial loss of methane and activation of one Et$_3$SiH molecule to afford the unobserved intermediate Tp*PtMe(SiEt$_3$)H (A, Scheme 42) that then irreversibly eliminates Et$_3$SiMe, activation of a second molecule of Et$_3$SiH affording 378. No evidence was observed for the more intuitive elimination of a second equivalent of methane to ultimately afford Tp*Pt(SiEt$_3$)$_2$H (B), and precedent for preferential reductive elimination of an Si−C linkage over C−H was cited.[165]

The 5-coordinate salt 379^+ has also been accessed, with greater facility, via low-temperature protonation of Tp*PtH$_2$Me (152) and ''trapping'' of the resulting solvento-complex with Et$_3$SiH.[127] Similarly, employing either Ph$_3$SiH or Ph$_2$SiH$_2$ in place of Et$_3$SiH results in formation of [(κ^2-HTp*)Pt(SiPh$_2$R)(H)$_2$]$^+$ (R = Ph 515^+, H 516^+).

The formulation of 379^+, 515^+, and 516^+ as 5-coorinate silyldihydrides was established on the basis of a single crystal X-ray diffraction study of 379^+ (Figure 7)[127] and characteristic spectroscopic data, $viz.$ ^{1}H NMR resonances associated with (i) the NH of the protonated pyrazole group (9–10 ppm) and (ii) a discrete terminal hydride (−15 to −17 ppm) that
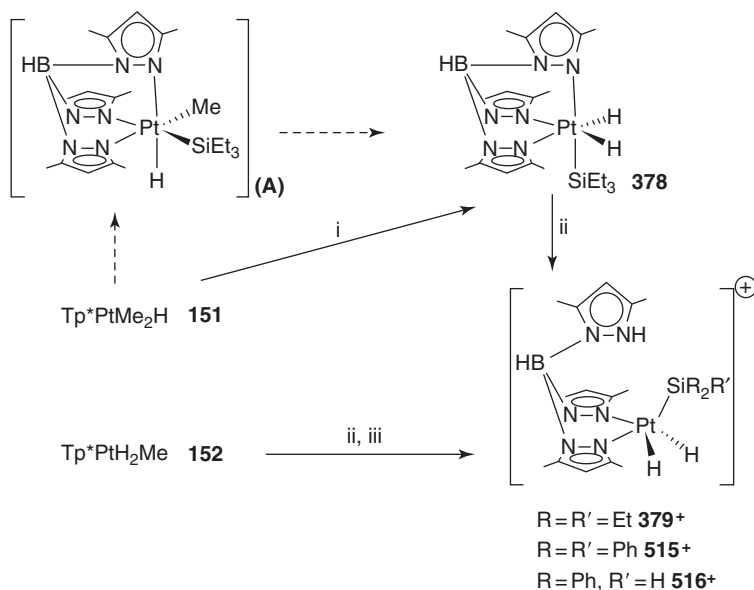
Scheme 42   Reagents and conditions: (i) Et$_3$SiH, Δ, 7 h.; (ii) [H(OEt$_2$)$_2$]BAr$^f_4$, −78 °C, CH$_2$Cl$_2$; (iii) HSiR$_2$R′.
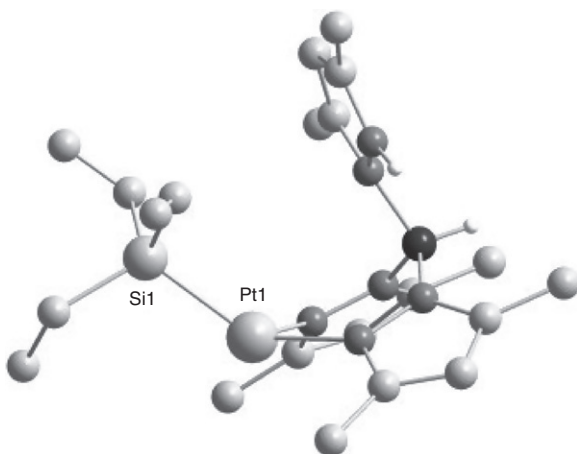
Figure 7   Molecular structure of [κ^2-HTp*Pt(H)$_2$(SiEt$_3$)]$^+$ (**379**$^+$) with hydrogen atoms omitted for clarity.

integrates for two nuclei. The possibility of these structures being based upon Pt(II) silane σ-complexes undergoing rapid hydride exchange was excluded on the basis of NMR studies illustrating: (i) the inability of

donors to displace silane; (ii) the absence of $^1J_{SiH}$ coupling of the hydride resonances; (iii) a negligible isotope shift (0.06 ppm) for the hydride resonance of $[\{\kappa^2\text{-}HTp^*\}Pt(SiEt_3)(D)(H)]^+$ (379-d_1^+) relative to 379$^+$. Moreover, the diphenylsilyl complex 516$^+$ shows no evidence of exchange between the Pt−H and Si−H functionalities, which would be anticipated if a silane σ-complex were involved.

3. Trihydrides

The initial impetus to prepare the silyldihydride 378 was as an intermediate step, *en route* to the synthesis of the first, and still only, trihydride of a group 10 poly(pyrazolyl)borate complex, *viz.* Tp*PtH$_3$ (159).[127] This synthesis was originally achieved by refluxing 378 in MeOH/CH$_2$Cl$_2$, affording 159 in 13% overall yield, based upon consumption of Tp*PtMe$_2$H (151), the precursor to 378; the monodeuterated analogue Tp*PtH$_2$D (159-d_1) was similarly obtained from MeOD. A longer (four steps), but ultimately higher yielding synthesis for 159 was subsequently established,[68] utilizing an analogue of the WGS reaction, as previously employed in the synthesis of TpPtH$_2$Me (347)[117,118] and Tp*PtH$_2$Me (152, *vide supra*).[66] Thus, protonation of 152 and purging with CO affords the cation $[\kappa^2\text{-}HTp^*PtH(CO)]^+$ (369$^+$), which is then deprotonated *in situ* with NEt$_3$ to the neutral Tp*PtH(CO) (502). Reflux of 502 in 1:1 acetone/H$_2$O under slightly basic conditions effects quantitative conversion to 159, isolated in 64% overall yield (Scheme 43).[68]
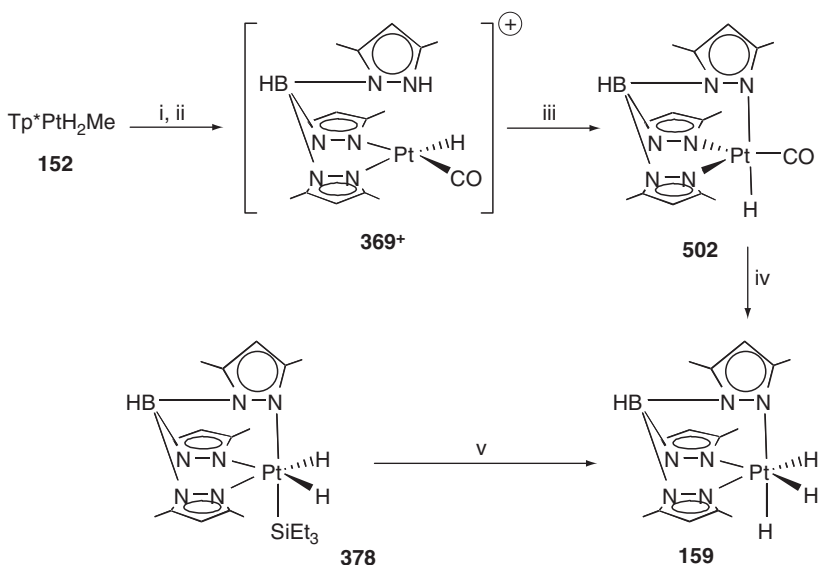
Scheme 43 Reagents and conditions: (i) [H(OEt$_2$)$_2$]BAr$^f_4$, −78 °C, CH$_2$Cl$_2$; (ii) purge CO, −78 °C→r.t ; (iii) NEt$_3$, −78 °C; (iv) H$_2$O/Me$_2$CO, $^-$OH, Δ; (v) MeOH/CH$_2$Cl$_2$, Δ.

Though no structural data have been reported for **159**, its formulation followed convincingly from spectroscopic observations.[127] The infrared spectrum exhibits absorptions for both B—H (ν_{BH} 2524 cm^{-1}) and Pt—H (ν_{PtH} 2247 cm^{-1}) stretching vibrations, the latter showing no significant vibrational coupling, while the ^{1}H NMR spectrum exhibited resonances for single pyrazolyl (3 resonances) and hydride (δ_H −20.03 ppm) environments, reflecting the anticipated C_{3v} symmetry on the NMR timescale. That **159** is a classical trihydride was established from T_1 measurement of the hydridic resonance (T_1 = 1.25s at 20 °C; cf. milliseconds for H$_2$ complexes), and from the spectroscopic data of **159-d_1**, which indicate the presence of a discrete Pt—D linkage with no measurable J_{HD} coupling, nor is there significant change in the chemical shift of the hydridic resonance (δ_H −20 ppm) relative to **159**, both of which would be expected of a dihydrogen complex.

In common with the mono- and dihydrides, the protonation chemistry of **159** has been explored in some detail,[68] though this is apparently difficult, low-temperature (−78 °C) treatment with [H(OEt$_2$)$_2$]BAr$^f_4$ being unsuccessful, **159** alone being observed spectroscopically; moreover, upon warming to ambient temperature, 50% of the initial **159** remains intact, the rest decomposing to Tp*H and Pt black. However, in the presence of CO, the same reaction affords [{κ^2-HTp*}PtH(CO)]$^+$ (**369$^+$**), the result of H$_2$ elimination from the intermediate [{κ^2-HTp*} PtH$_3$(CO)]$^+$ (**505$^+$**), which was observed at low temperature. With other donor ligands H$_2$ elimination is more facile, such that trihydride intermediates cannot be observed *en route* to [{κ^2-HTp*}Pt(H)(L)]$^+$ (L = C$_2$H$_4$ **155$^+$**, H$_2$C=CHMe **160$^+$**, H$_2$C=CHEt **161$^+$**, H$_2$C=CHnPr **162$^+$**, Scheme 44). In contrast, the acetonitrile complex [{κ^2-HTp*}PtH$_3$(NCMe)]$^+$ (**517$^+$**) *was* observed at low temperature, but dissociates the nitrile on warming, regenerating **159** with 50% decomposition products. Both PMe$_3$ and PMe$_2$Ph induce a small amount of H$_2$ elimination, though side reactions have precluded detailed study.

The loss of H$_2$ from trihydride intermediate **505$^+$** was probed, leading the authors to conclude a direct elimination mechanism from this 6-coordinate species (cf. typical requirement of a free coordination site). It was also established, *inter alia*, that H$_2$ loss is irreversible, and dissociation of the carbonyl is facile, though the direct relationship between CO pressure and rate of H$_2$ loss precluded this as a prelude to H$_2$ elimination. The possibility of a CO migratory insertion/deinsertion to a Pt—H linkage was also excluded on the grounds that the formyl Tp*Pt(H)$_2$(CHO) (**506**), prepared by successive addition of H$^-$ and H$^+$ to Tp*PtH(CO) (**502**), rapidly loses CO, but not H$_2$, affording only Tp*PtH$_3$ (**159**). A comparable situation was previously reported for the formyls Tp*PtMe{C(=O)R}H (R = Me **352**; Ph **354**; H **356**, Section III.D.2).[120]

50 % **159**

HB————N—N

N—N
N—N—Pt····H
N—N   H
          H
159

i →

HB————N—NH

N—N   +

N=N   Pt$_{black}$

ii

iv

+

N—NH

HB

              L
N—N—Pt····H
N=N   H
          H

L = CO **505**$^+$; NCMe **517**$^+$
(observed at low T)

iii ←

+

HB————N—NH

N—N
N—N—Pt····H
N=N   L

L = CO **369**$^+$;
C$_2$H$_4$ **155**$^+$
CH$_2$=CHMe **160**$^+$
CH$_2$=CHEt **161**$^+$
CH$_2$=CH nPr **162**$^+$

Scheme 44 Conditions and reagents: (i) [H(OEt$_2$)$_2$]BAr$^f_4$, −78 °C → r.t.; (ii) [H(OEt$_2$)$_2$] BAr$^f_4$, −78 °C, L (L = CO, NCMe (observed) C$_2$H$_3$R (R = H, Me, Et, nPr, not observed); (iii) r.t. (not NCMe); (iv) r.t. NCMe.

4. Application of hydrides in catalysis
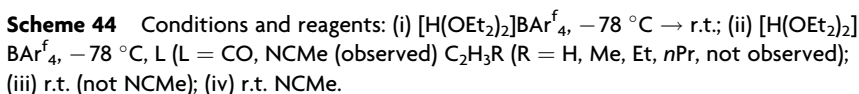
In concluding this section, it is noteworthy that several monohydrides have been explored as catalysts for dehydrogenative coupling of hydrosilanes to aryl and aliphatic hydrocarbons, with considerable success.[166] Thus, over 24 h at 200 °C, TpPtMe$_2$H (**340**), Tp*PtMe$_2$H (**152**), and Tp*PtPh$_2$H (**153**), at 5 mol%, achieved >70% yield for the coupling of benzene and Et$_3$SiH. Similar success was reported for the silanes HSiR$_2$R′ (R=R′=Et, n-Pr; R=Me, R′=Ph; R=Ph, R′=Me) and in intramolecular dehydrogenative coupling of both 2-phenylethylsilanes and tributylsilane. These are discussed more fully in Section IV.A.

F. Phosphane complexes

It is perhaps unsurprising that the role of phosphane ligands in group 10 poly(pyrazolyl)borate complexes can often be summarized as "spectatorial," and in many instances is incidental in respect of chemistry. Indeed, the dominant utility of these ligands is as donors with which to trap or stabilize coordinately unsaturated materials.

As trapping agents, phosphanes have enabled isolation of the vinyl complexes $(R_2Bp)PtC(CF_3)=C(CF_3)Me)(PPh_3)$ (R = Et **138**, Ph **139**),[61] which result from spontaneous insertion of hexafluorobut-2-yne into the Pt−Me linkage of the unobserved ''$R_2BpPtMe\{\eta^2-C_2(CF_3)_2\}$'' (Sections III. B.1, III.D.1), and TpPdR(PPh$_3$) (R = Me **276**, Ph **307**),[99] thus confirming the formation of ''TpPdR'' as a by-product in the water oxidation of [TpPdRMe]$^-$ (R = Me **271**$^-$, Ph **294**$^-$), which also affords the Pd(IV) complexes TpPdMe$_2$R (R = Me **269**, Ph **280**), respectively. Both **276** and **307** were also deliberately prepared, alongside their pzTp analogues pzTpPdR(PPh$_3$) (R = Me **407**, Ph **408**) from [PdMe(SMe$_2$)(μ-I)$_2$] or [PdIPh(tmeda)], PPh$_3$, and the respective KTp^x.[83] The related TpPtMe{P (OMe$_3$)} (**399**) has been prepared directly from the polymeric ''TpPtMe'' (**126**) and P(OMe)$_3$ in what may formally be termed ''ligand displacement'' by the phosphite.[60]

Ligand displacements are ubiquitous in this area, first exploited to afford BpPtMe$_3$\{P(OMe)$_3$\} (**254**) from the B−H−Pd agostic complex BpPtMe$_3$ (**253**),[92] while the displacement of pyridine from BpMMe$_3$(py) (M = Pt **258**, Pd **272**) with PMe$_2$Ph gave BpMMe$_3$(PMe$_2$Ph) (M = Pt **259**, Pd **273**), of which **273** is stable only below −70 °C, above which it eliminates ethane to afford BpPdMe(PMe$_2$Ph) (**275**).[95] Displacement of cyclooctadiene from the dimeric \{Et$_2$BpPtMe\}$_2$(cod) (**131**) was utilized to prepare Et$_2$BpPtMe(L) (L = PMe$_3$Ph **417**, PPh$_3$ **418**) and the dppe bridged complex \{Et$_2$BpPtMe\}$_2$(dppe) (**420**),[61] while Me$_2$Ga(pz)$_2$PtMe(PPh$_3$) (**421**) was similarly prepared from ''Me$_2$Ga(pz)$_2$PtMe(cod),'' generated *in situ* from PtCl(Me)(cod) and Na[Me$_2$Ga(pz)$_2$].[63] In contrast, Ph$_2$BpPtMe\{P (C$_6$F$_5$)$_3$\} (**403**) was obtained upon protonation of the anionic [Ph$_2$BpPtMe$_2$]$^-$ (**400**$^-$), which liberates methane to transiently generate the otherwise unisolable ''Ph$_2$BpPtMe.''[132]

In situ displacements have seen wider utility, being employed in the synthesis of Tp*Pd(R)(PPh$_3$) (R = Me **439**, *p*-Tol **440**)[137] and Bp^{x}PdMe (PR$_3$) (Bp, R = Ph **423**, Cy **424**; Bp*, R = Ph **425**, Cy **426**)[135] from PdCl(Me) (cod) or PdI(*p*-Tol)(tmeda) and KTp^x(Bp^x). All of these materials have been carbonylated to afford Tp*Pd\{C(O)R\}(PPh$_3$) (R = Me **447**, *p*-Tol **448**)[137] and Bp^{x}Pd\{C(O)Me\}(PR$_3$) (Bp, R = Ph **431**, Cy **432**; Bp*, R = Ph **433**, Cy **434**).[135] Significantly, the *p*-toluoyl complex **448** has been shown to slowly insert norbornadiene, affording the chelate complex Tp*Pd\{C$_7$H$_8$C (O)*p*-Tol\} (**449**); moreover, when the parent tolyl **440** is simultaneously exposed to CO and norbornadiene, copolymerization is achieved (Sections III.D.2, IV.A).[140,141] However, in neither instance does the phosphane exceed the role of ''labile donor,'' stabilizing the latent coordination site necessary for these reactions. In contrast, the phosphane is of great significance in complexes **426** and **434**, insofar as the bulky cyclohexyl substituents seemingly induce fluxionality in the Bp* ligand by virtue of steric crowding with the pyrazolyl 3-methyl substituents.[135] Thus, whereas

423−**425** and **431**−**433** adopt static, square-planar geometries, for both **426** and **434** the Bp* ligand is apparently in equilibrium between κ^2 and, the very rare, κ^1 coordination modes (Section III.C.3, III.D.2).

A prominent example of a discrete complex comprising a κ^1-poly(pyrazolyl)borate ligand was encountered upon *in situ* treatment with PMe_2Ph of the solvento cation $[\{\kappa^2$-$HTp^*\}PtMe(CH_2Cl_2)]^+$ (**362$^+$**), generated at −78 °C by acid-induced methane elimination from Tp^*PtMe_2H (**151**).[65] Thus, while a single equivalent of PMe_2Ph displaces dichloromethane to afford $[\{\kappa^2$-$HTp^*\}PtMe(PMe_2Ph)]^+$ (**367$^+$**), excess leads also to displacement of one pyrazolyl donor, affording $[\{\kappa^1$-$HTp^*\}PtMe(PMe_2Ph)_2]^+$ (**518$^+$**), which was identified both from ^1H NMR spectroscopic data and by single crystal X-ray diffraction (Figure 8).

The remaining examples of compounds obtained by phosphane displacement of ancillary ligands embody somewhat greater novelty, and thus warrant individual consideration. Firstly, $pzTpPt(\eta^3$-methallyl) (**225**) was found to react with both PPh_3, and ½ equiv. bis(diphenylphosphino)butane to afford, respectively, $pzTpPt(\eta^1$-$CH_2CMe{=}CH_2)(PPh_3)$ (**241**) and $\{pzTpPt(\eta^1$-$CH_2CMe{=}CH_2)\}_2(dppb)$ (**243**, Scheme 18, Section III.B.2).[87] In contrast, treatment of **225** with ½ equiv. dppe results only in displacement of the pzTp ligand to give the ion pair $[(dppe)Pt(\eta^3$-methallyl)]$^+[B(pz)_4]^-$ (**242.B(pz)$_4$**). The monomeric complex **241** reacts with mineral acids HX (X = Cl, Br) to effect cleavage of the η^1-methallyl ligand, affording $pzTpPtX(PPh_3)$ (X = Cl **519**, Br **520**), both of which undergo halide exchange with NaI to give the respective iodide complex **521**.

Displacement of nitrate from $TpPd(\kappa^2$-C_6H_4-o-CMe_2CH_2-$)(ONO_2)$ (**511**), obtained by O_2 oxidation of the nitrosyl $TpPd(\kappa^2$-C_6H_4-o-CMe_2CH_2-$)(NO)$ (**409**), has been effected by PMe_3 to afford the complex
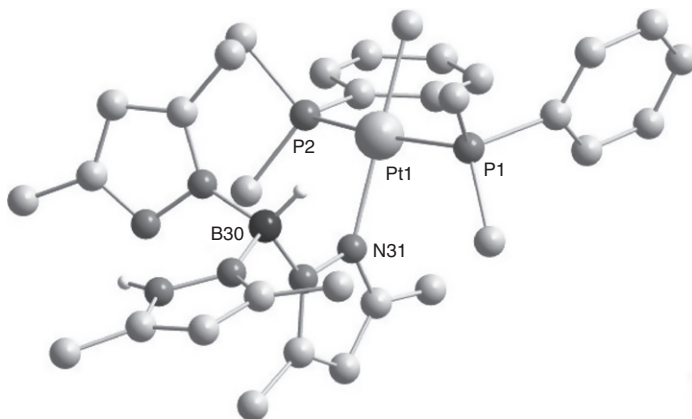
Figure 8   Molecular structure of $[\kappa^1$-$HTp^*PtMe(PMe_2Ph)_2]^+$ (**518$^+$**) with hydrogen atoms omitted for clarity.

salt [TpPd(κ^2-C_6H_4-o-C(Me)$_2$CH$_2$-)(PMe$_3$)]$^+$NO$_3^-$ (**512.NO$_3$**, Scheme 40, Section III.D.4).[133] These remain the sole examples of nitrosyl, nitrite, and nitrate complexes of Pd or Pt poly(pyrazolyl)borates.

The putative hydroperoxide complex Tp^{iPr}Pd(OOH)(py) (**522**), obtained by dehydrative condensation of Tp^{iPr}Pd(OH)(py) (**523**), reacts with PPh$_3$ to afford orange crystals of Tp^{iPr}Pd(OOH)(PPh$_3$) (**524**).[167] A single crystal X-ray diffraction study of **524**, which is stable as a solid and in solution, revealed a significant hydrogen bonding interaction between the free pyrazole donor and the hydroperoxide ligand. Moreover, the particularly high-frequency resonance for the hydroperoxide proton (δ_H 8.93) revealed this interaction to be retained in solution, and a similarly high-frequency resonance for **522** (δ_H 6.86) would seem to imply a comparable scenario. Indeed, the incidence of these interactions was cited as a possible reason for the remarkable stability exhibited by both **522** and **524**.

Finally, a more elaborate example of ligand displacement by extraneous phosphane is observed upon treatment of TpPtH$_2$Me (**347**) with PMe$_3$, which induces elimination of dihydrogen via a mechanism that has not been conclusively established. However, the 5-coordinate intermediate κ^2-TpPtMe(PMe$_3$)$_2$ (**513**) has been observed, and is believed to initially adopt a *cis* disposition of phosphanes, before slowly isomerizing to a *trans* complex, which then loses PMe$_3$ to finally afford TpPtMe(PMe$_3$) (**377**).[124]

The most prevalent source of phosphane ligands for Pt and Pd poly-(pyrazolyl)borate complexes is their retention from precursors, hence their role is, in many cases, entirely ancillary. Thus, pzTpPt(3-oxo-1-cyclohexenyl)(PPh$_3$) (**494**),[160] Tp^{x}Pd(CH$_2$Fu)(PPh$_3$) (Tp^x = Tp **441**, pzTp **442**),[138] and LPd{C(O)Fc}(PPh$_3$) (L = pzTp **507**, Tp **508**, Bp **509**),[162] were all obtained from the respective MRCl(PPh$_3$)$_2$, while Bp^{x}Pd(CH$_2$R)(PMe$_3$) (Bp, R = CMe$_2$Ph **427**, SiMe$_3$ **428**; Bp*, R = CMe$_2$Ph **429**, SiMe$_3$ **430**) and Bp^{x}Pd(C(O)CH$_2$R)(PMe$_3$) (Bp, R = CMe$_2$Ph **435**, SiMe$_3$ **436**; Bp*, R = CMe$_2$Ph **437**, SiMe$_3$ **438**) are derived from [PdCl(CH$_2$R)(PMe$_3$)$_2$] and [PdCl(C(O)CH$_2$R)(PMe$_3$)$_2$], respectively;[136] the acyls **435–438** are alternatively accessible via carbonylation of **427–430**.[136] Beyond it being noted that **427**−**430** and **435**−**438** fail to undergo exchange with free PMe$_3$, study of these materials has seemingly focussed exclusively on the organic fragments, as discussed elsewhere.

It should be noted that the accessibility of such materials from bis(phosphane) precursors is not universal. Indeed, when PdIPh(PMe$_3$)$_2$ is treated with one equivalent of TlTp^{tBu} the sole product is the bis(phosphane) complex κ^1-Tp^{tBu}PdPh(PMe$_3$)$_2$ (**450**), again illustrating the rare κ^1-coordination mode for the Tp^x ligand.[29] Analogous results were also obtained with nickel systems, *viz. trans*-[Tp^{tBu}Ni(C$_6$H$_4$R)(PMe$_3$)$_2$] (R = H **43**, Me **44**, OMe **45**, NMe$_2$ **46**), *trans*-[Bp^{tBu}Ni(C$_6$H$_4$R)(PMe$_3$)$_2$] (R = h **47**, Me **48**, OMe **49**, NMe$_2$ **50**), *trans*-[Tp^{tBu}Ni{C(O)C$_6$H$_4$R}(PMe$_3$)$_2$] (R = H **68**, Me **69**, OMe **70**, Section II.G),[27,29] and while their formation was attributed

to the presence of the bulky 3-*t*Bu substituents, exactly why this should fail to displace a PMe$_3$ ligand has not, thus far, been established.

The systematic pursuit of phosphane complexes has prominently employed dimer-cleavage by suitable MTp^x (M = Na, K) reagents. The first example of this was in fact fortuitous, and followed from treatment of the 2-picolyl bridged dimer [PdCl(CH$_2$C$_5$H$_3$N)(PPh$_3$)]$_2$ with KTp, affording the monomeric κ^2-TpPd(CH$_2$C$_5$H$_3$N)(PPh$_3$) (**461**, Scheme 34, Section III.C.3.b). This contrasts the analogous reactions with KBp and K{pzTp}, which preferentially displace PPh$_3$ (cf. the picolyl nitrogen) to afford phosphane-free dimers.

More systematic was the synthesis of a range of complexes of general formula [{(C$_6$F$_5$)Pd(L)}$_2$(B(pz)$_4$)]$^+$ (L = PPh$_3$ **453**$^+$, PEt$_3$ **454**$^+$ PMe$_2$Ph **455**$^+$ AsPh$_3$ **456**$^+$) from the halide-bridged dimers [{(C$_6$F$_5$)Pd(L)(μ-X)}$_2$] (X = Cl, Br).[88] Precleavage of the dimer with 2 equiv. of AgClO$_4$, followed by addition of one equivalent K[B(pz)$_4$] afforded **453**$^+$–**456**$^+$ as the perchlorate salts, all of which behave as 1:1 electrolytes in acetone solution. NMR spectroscopic studies revealed single environments for both the C$_6$F$_5$ and L ligands, and evidence for rapid fluxionality attributed to inversion of the M(N–N)$_2$B boats. The synthetic approach to these materials in many respects mirrors the first ever synthesis of a Tp^{x}Pt phosphane complex, the Pt(IV) salt [(κ^2-pzTp)PtMe$_2$(PMe$_2$Ph)$_2$]$^+$ (**248**$^+$), which was prepared by addition of Na[B(pz)$_4$] to a solution of [PtMe$_2$(PMe$_2$Ph)$_2$]$^{2+}$, generated *in situ* from PtMe$_2$I$_2$(PMe$_2$Ph)$_2$ with 2 AgPF$_6$.[91] In this instance, however, it proved impossible to obtain the dimeric B(pz)$_4$ bridged complexes, all efforts affording only the monomeric **248**$^+$. This study did, however, demonstrate that κ^2-B(pz)$_4$ occupies a position between pyridine and bipyridyl in the NMR *trans*-influence series.

A somewhat more comprehensive study was undertaken in pursuit of complexes of the type LMX(PR$_3$) (L = Bp^x, Tp^x) that might serve as organometallic precursors. The starting points for this work were the halide-bridged dimers [MX$_2$(PEt$_3$)]$_2$ (M = Pt, Pd; X = Cl, Br), which, in the case of Pt, react with KBp to afford BpPtX(PEt$_3$) (X = Cl **525**, Br **526**), as determined by multinuclear (^{1}H, ^{31}P, ^{11}B, ^{13}C) NMR spectroscopic studies. In combination with infrared data for the B−H stretching modes, these led the authors to conclude classical square-planar geometries, with no evidence for agostic B−H−Pt association.[168] Complexes **525** and **526** were not, however, obtained in pure form, both forming in admixture with a second, minor, product that defied separation; these secondary contaminants were not identified. Moreover, attempts to prepare PPh$_3$ analogues also resulted in formation of two products, though their identity has not been disclosed. In contrast, treatment of [MCl$_2$(PEt$_3$)]$_2$ (M = Pt, Pd) with Na[Bu$_2$Bp] was independently shown to form Bu$_2$BpMCl(PEt$_3$) (M = Pt **527**, Pd **528**), which are readily purified by chromatography on silica,[169] though it was noted that the same reaction with KBp afforded only Pd metal.

The comparable reaction with NaTp also affords two products, in 3:1 ratio,[168] and though separable by chromatography on silica, these could only be isolated in small amounts. In contrast, when a single equivalence of NaTp was reacted with $[PtBr_2(PEt_3)]_2$ the major of these two materials formed exclusively, and was identified as the Tp-bridged dimer **529** (Scheme 45), on the basis of a single crystal X-ray diffraction study (Figure 9) that correlated with NMR spectroscopic data; the chloride analogue **530** was similarly prepared. Both materials exhibit considerable stability, failing to react with either excess of NaTp, or indeed PEt_3. This was considered surprising, given that polymeric ''TpPtMe'' (**126**), which presumably also involves a bridging Tp ligand, is readily cleaved by alkenes, alkynes, and other donors.[55]

X = Br **529**, Cl **530**
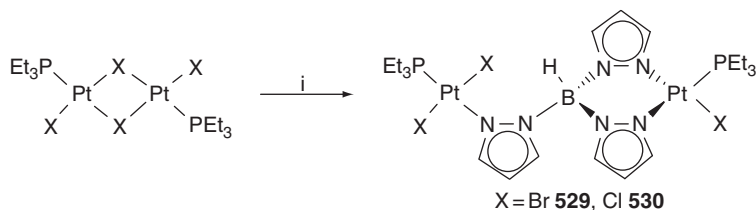
Scheme 45 Reagents and conditions: (i) NaTp.

The target complexes $TpMX(PEt_3)$ have never been obtained, however, the analogue $Tp*PdCl(PPh_3)$ (**531**) was, more recently, prepared via an alternative route: the interaction of $KTp*$ with $PdCl_2(NCMe)_2$ and subsequent addition of PPh_3.[170] The phosphane was added as a supporting ligand, since in its absence the reaction afforded only intractable mixtures. Moreover, the rate of phosphane addition was found to be critical, slow
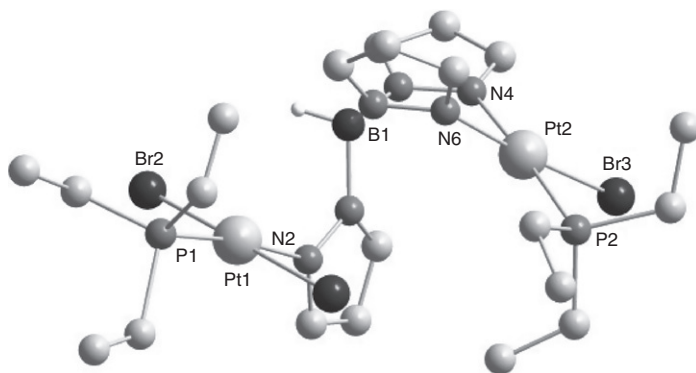
Figure 9 Molecular structure of dimeric **529**.

addition resulting in optimal formation of **531** in admixture with a small amount of $PdCl_2(PPh_3)_2$, while more rapid addition led to a predominance of the latter. Indeed, it was found that **531** reacts with PPh_3 to afford $PdCl_2(PPh_3)_2$, a fact that must presumably preclude the latter from acting as precursor to **524**, through reaction with KTp*. A stepwise dechelation of the Tp* ligand from **531** was suggested to prevail upon PPh_3 addition, though no evidence for this was obtained. It should also be noted that **531** is relatively unusual in exhibiting no fluxionality of the Tp* ligand on the NMR timescale.

A similarly nonfluxional geometry is reported for $pzTpPtBr(PEt_3)$ (**532**), which forms cleanly from $[PtBr_2(PEt_3)]_2$ and $KB(pz)_4$ (cf. the reactions with KBp and KTp, *vide supra*),[168] and exhibits four unique pyrazolyl environments in the ^1H NMR spectrum. On this basis, and the generally low barrier to equilibration of uncoordinated pyrazolyl donors in κ^2-pzTp complexes, it was concluded that **532** is 5-coordinate (κ^3-pzTp). In contrast, the chloride analogue **533**, prepared independently,[169] was found to exhibit only three pyrazolyl environments under ambient conditions, and thus concluded to adopt a κ^2-pzTp coordination mode, equilibration of the free pyrazole donors being ''frozen out'' at $-35\ °C$. It is noteworthy that a more recent attempt to prepare the $B(pz^{tBu})_4$ analogue of **533** via analogous synthetic methodology has proven unsuccessful, resulting instead in cleavage of the ligand $B-N$ bonds to afford $PdCl_2\{3(5)-Hpz^{tBu}\}(PEt_3)$.[84]

Finally, there are two examples of intramolecular *C,P* chelates, *viz.* LPd $\{\kappa^2$-*C,P*-2-$CH_2C_6H_4P(o$-Tol)$_2\}$ (L = Tp **468**, Bp **469**), both prepared by cleavage of the halide bridged dimer with KL (Scheme 46).[143] These complexes were targeted to explore their potential in the guise of catalysts for organic synthesis, a role to which the cyclopalladated tris(*o*-tolyl) phosphane precursor had been previously applied. However, this preliminary study revealed these materials to be unreactive toward electrophiles (see also Section III.C.3.b), and no further investigations have been reported.
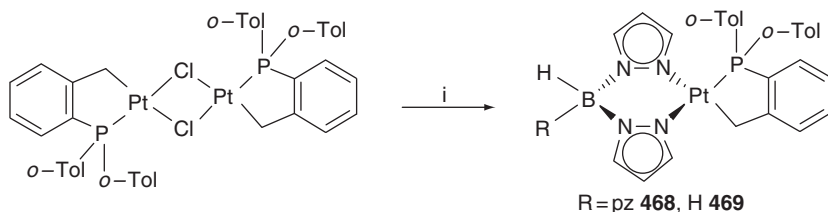
Scheme 46 Reagents and conditions: (i) Na[HB(pz)$_2$R], R = pz, H.

IV. PERSPECTIVES: CATALYSIS AND C−H ACTIVATION

It is an axiom of modern organometallic chemistry that the pursuit of late transition metal complexes is ultimately driven by the need to formulate ever more efficient catalysts and reagents for chemical synthesis. In this respect, the field of poly(pyrazolyl)borate chemistry is no different from any other, albeit that in the case of the group 10 triad the breadth of study is perhaps more limited than for other metals and/or ligands. This section provides an overview of prominent results in respect of both catalysis and the C−H activation processes that underpin them.

A. Catalysis

Though widely pursued, there are few examples of catalytic activity among group 10 poly(pyrazolyl)borate complexes, and these are relatively recent developments. The first such report appeared in 1998, describing κ^2-Tp^{Ph}Ni(o-Tol)(PPh$_3$) (**51**) as an effective,[30] albeit "mediocre,"[15] catalyst for the copolymerization of ethylene and carbon monoxide, operating above 20 °C and below 50 bar total pressure. Though the mechanism of this process remains unclear, it was established that neither the pendant pyrazole donor, nor B−H functionality exert any influence upon it, since BBNpz$_2$Ni(o-Tol)(PPh$_3$) (**53**), which is devoid of both, shows comparable activity under the same conditions.[31] It was, however, believed that the hard nitrogen donors are key to maintaining nickel in the +2 oxidation state in the presence of CO, its reduction being the primary termination pathway.[30] Moreover, the nature of the pyrazolyl 3-substituent seems fundamentally important, given that κ^2-Tp^{Tol}Ni(o-Tol)(PPh$_3$) (**52**) a direct analogue of **51**, exhibits appreciably reduced reactivity relative to the latter, despite minimal perturbation of electronic and steric character.

It was also noted that {κ^2-N,O-BBN(pz)(OH)}Ni(o-Tol)(PPh$_3$) (**54**), formed by *in situ* hydrolysis during the synthesis of **53**, is catalytically inactive under comparable conditions. This was perhaps a surprising observation given the growing prevalence of N,O chelating ligands in this role and this anomaly remains to be explained. Moreover, there is a surprising dearth of palladium systems capable of effecting olefin/CO copolymerization, despite the wealth of documented Pd(II) alkyl, aryl, and acyl complexes. Indeed, Bp^{x}Pd(Me)(L) (Bp, L = PPh$_3$ **423**, PCy$_3$ **424**; Bp*, L = PPh$_3$ **425**, PCy$_3$ **426**),[135] Bp^{x}Pd(CH$_2$R)(PMe$_3$) (Bp, R = CMe$_2$Ph **427**, SiMe$_3$ **428**; Bp*, R = CMe$_2$Ph **429**, SiMe$_3$ **430**), Bp^{x}Pd{C(O)Me}(PR$_3$) (Bp, R = Ph **431**, Cy **432**; Bp*, R = Ph **433**, Cy **434**),[135] Bp^{x}Pd{C(O)CH$_2$R}(PMe$_3$) (Bp, R = CMe$_2$Ph **435**, SiMe$_3$ **436**; Bp*, CMe$_2$Ph **437**, SiMe$_3$ **438**),[136] and Tp*Pd{C(O)Me}(PPh$_3$) (**447**)[137] have all proven entirely ineffective in

this role. In contrast, Tp*Pd{C(O)p-Tol}(PPh$_3$) (**448**)[137] has been demonstrated to slowly (>1d) insert norbornadiene to afford Tp*PdC$_7$H$_8$C(O)p-Tol (**449**).[140,141] More importantly, when the parent p-Tolyl complex Tp*Pd(p-Tol)(PPh$_3$) (**440**) is carbonylated (1 bar) in the presence of norbornadiene, catalytic formation of the polyketone ensues in a matter of hours (Scheme 47).[140,141]
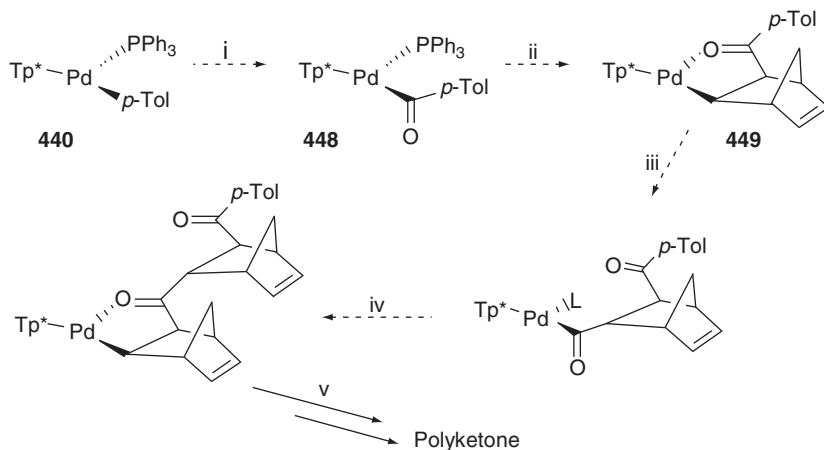
Scheme 47 Proposed mechanism for copolymerization of CO and nbd by **440**. Conditions: (i) CO; (ii) nbd, $-$ PPh$_3$; (iii) CO, L (L = PPh$_3$, nbd); (iv) nbd, $-$L; (v) n(nbd), n(CO).

Somewhat greater success has been reported in respect of homo-oligo-merization of olefins, though once again reports are few, and focused predominantly on nickel. The complexes Tp^{X}NiCl (Tp^X = Tp^{Ms} **13**, Tp^{Ms*} **14**, Tp^{Ms**} **15**; Ms = mesityl, Tp^{Ms*} = HB(pz^{Ms})$_2$(pz^{5Ms}), Tp^{Ms**} = HB(pz^{Ms}) (pz^{5Ms})$_2$) were screened in the presence of methylaluminoxane (MAO) cocatalyst at 0 °C under 30 bar ethylene. Under these conditions, both **13** and **14** showed appreciable activity, with very high selectivity for 1-butene (95–96%) within the C$_4$ fraction, equivalent to 81% selectivity overall.[13] In contrast, **15** was found to be completely inactive under these conditions.

The influence of reaction conditions upon activity was explored, revealing that **13** is 16 times more active than is **14**, a fact that can perhaps be attributed to the enhanced steric bulk of the former. This property has previously been identified as fundamentally important in avoiding termination by the β-hydride elimination pathway.[171,172] The activity of the **13**/MAO system was further probed, revealing a significant increase in turn-over number (TON) upon varying the pressure in the range 1.1 → 30 bar (5.4→29.2 × 10^3 h^{-1} at 0 °C; 2.2→34.6 × 10^3 h^{-1} at 30 °C) as might be anticipated from an increase in ethylene concentration.[13] It was also noted that selectivity for α-olefins decreased (20%) as the pressure was lowered

owing to parallel isomerization reactions, though there was little variation in selectivity for dimers (C_4) over trimers (C_6) which remained ca. 86:13. Finally, it was reported that switching to the **13**/TMA system increased the turn-over frequency under comparable conditions to **13**/MAO, though at the expense of selectivity for C_4 oligomers, and indeed life-time of the catalytically active species (30 min at 1.1 bar, cf. >60 min for **13**/MAO).

Significantly, **13** was subsequently employed alongside Cp_2ZrCl_2 as a tandem catalyst system for ''copolymerization'' of ethylene and α-olefins, facilitating the synthesis of linear low-density polyethylene (LLDPE) using ethylene as the only olefin feed-stock.[14] A ''plausible'' catalytic cycle for this process was proposed (Scheme 48), based upon the *in situ* generation of ''$Tp^{Ms}NiH$,'' which has never been observed, as the ''active species'' for homo-oligomerization of ethylene to 1-butene, which is then incorporated into the growing polyethylene chain of the $Cp_2Zr(P)^+$ species.
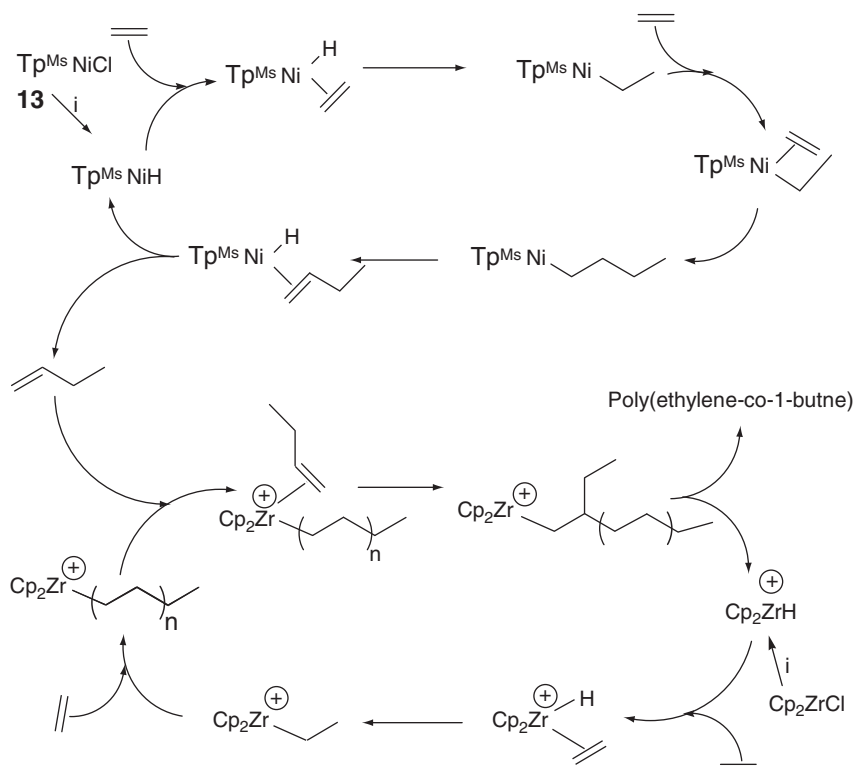
Scheme 48 Proposed tandem catalysis cycle for **13**/Cp_2ZrCl_2. Reagents: (i) MAO activation.

Utilizing MAO/TMA as the cocatalyst and operating in toluene at 0 °C, **13** effects oligomerization of ethylene with a TON of 5.4×10^3 h^{-1}, while Cp$_2$ZrCl$_2$ forms linear high-density polyethylene (LHDPE) with a turn-over of 7.9×10^3 mol[C$_2$H$_4$]/mol[Zr] h^{-1}. Under the same conditions the TON of the **13**/Cp$_2$ZrCl$_2$ tandem system is highly dependent upon the nickel mole-fraction (χ_{Ni}), ranging between 6.6×10^3 and 37.1×10^3 h^{-1}. The polymer molecular weight (M_w) was observed to increase with decreasing χ_{Ni}, in the range 4.226×10^3 g mol^{-1} ($\chi_{Ni} = 0.80$) to 570×10^3 g mol^{-1} ($\chi_{Ni} = 0$); as was the melting temperature ($T_m = 98$ °C ($\chi_{Ni} = 0.98$) cf. 138 °C ($\chi_{Ni} = 0$)). Below $\chi_{Ni} = 0.2$ a broad range of T_m was observed, consistent with formation of polymers with different fractions of comonomer/short-chain branches.

The nickel complexes Tp*NiCl (**16**), Tp^{tBu,Me}NiCl (**17**), and Tp^{Cum,Me}NiCl (**18**, Cum = cumyl) are also active ethylene polymerization catalysts (toluene solution, 1 bar ethylene, 55 °C). Once again the activity was found to be highly dependent upon the nature of the pyrazolyl 3-substituent.[15] Thus, the enhanced steric bulk of **17** results in a ca. sixfold activity increase over **16**, while **18** is 12 times more active. This latter observation was deemed inconsistent with the relatively small increase in steric shielding of the metal center upon introducing the cumyl substituent, but was reconciled with the concomitant reduction in pyrazolyl donor strength for this system, which thus favors olefin coordination. The influence of the cocatalyst was also probed, revealing significant increases in PE production as the MAO/catalyst ratio is increased from 50 to 1000 (35% for **17**, 20% for **18**). Switching the activator to Bu$_2$Mg resulted in lower activity, while AlEt$_2$Cl was completely inactive. It was also noted that the palladium(II) complex Tp*Pd(η^3-C$_3$H$_5$) (**196**) is a dramatically poorer catalyst than any of the above.

The relative success of these nickel-based catalysts has led to generic complexes of the type Tp^{x}NiX (X = Cl, Br, F) being patented in this role,[16] as were Tp^{x}Ni(η^3-allyl),[21] though these are significantly less active than the halide complexes.

In respect of ''Tp^x'' complexes of the heavier group 10 metals, the focus lies with their application to catalyzed molecular synthesis, rather than polymerization, given their demonstrated ineptitude for the latter. Nonetheless, there remains a paucity of examples.

The first instance involves the Pt(II) fragment ''TpPdMe,'' used not as a catalyst, but rather as a protecting function for alkynes during catalytic, and indeed stoichiometric, processes, a role that followed from the noted stability of TpPtMe(η^2-RC≡CR) complexes, and their capacity to release the alkyne by carbonylation.[56,63] Thus, π-complexes with a series of bis(amide)acetylenes (**144–149**, Scheme 12, Section III.B.1), formed from the polymeric TpPtMe (**126**), could be subjected to conditions of catalytic hydrogenation, or basic hydrolysis of the pendant functions, without

compromising the triple-bond. The free alkynes were then displaced from the ''TpPtMe'' fragment under 60 atm. CO.[64] Despite the clear importance of this work, it has yet to be exploited in practical syntheses.

As regards catalytic behavior, little early progress is apparent, seemingly impeded by an intrinsic reluctance of Pd and Pt substrates toward requisite reactivity. For instance, while the P,C-chelate ligand ''2-$CH_2C_6H_4P(o\text{-}Tol)_2$'' typically affords effective Pd(II) catalysts that are believed to operate via Pd(IV) intermediates, the pyrazolyl(borate) complexes $Tp^xPd\{\kappa^2\text{-}P,C\text{-}2\text{-}CH_2C_6H_4P(o\text{-}Tol)_2\}(Tp^x = Tp$ **468**, pzTp **469**) failed to oxidatively add even the archetypal electrophiles MeI, BzI, PhI, and IC_6H_4OMe.[143] Moreover, in the presence of I_2 or $PhICl_2$ decomposition ensued. This confounded attempts to explore the chemistry of the postulated ''Pd(IV)'' intermediates using Tp^x systems.

Nonetheless, very recent work has established the utility of a series of organohydride complexes in the catalytic dehydrogenative coupling of hydrosilanes with aromatic or aliphatic C−H functions.[166] The complexes $TpPtMe_2H$ (**340**), Tp^*PtMe_2H (**151**), Tp^*PtH_2Me (**152**), and Tp^*PtPh_2H (**153**) were each employed at 5 mol% in the thermal reaction of Et_3SiH and benzene (200 °C, 48 h, Scheme 49), resulting in ca. 80% yield of Et_3SiPh using **340**, **151**, and **153**, though dihydride **152** afforded only 6%.
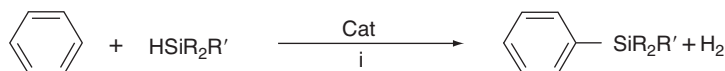
	Cat	Yield
	TpPtMe$_2$H **340**	72 %
R = R′ = Et	Tp*PtMe$_2$H **151**	86 %
	Tp*PtMeH$_2$ **152**	6 %
	Tp*PtPh$_2$H **153**	78 %
R = R′ = *n*Pr		86 %
R = Me, R′ = Ph	Tp*PtMe$_2$H **151**	71 %
R = Ph, R′ = Me		64 %

Scheme 49 Conditions: (i) 200 °C, 48 h.

Further investigations of this silylation process were undertaken, using **151** as the more efficient catalyst. It was thus established that there is fair tolerance of mixed aryl-alkylsilanes, benzene being readily silylated with $^nPr_3SiH$, Ph_2MeSiH, and Me_2PhSiH under comparable conditions, with yields in excess of 60%. In contrast, $^tBuMe_2SiH$ and $PhCl_2SiH$ failed to react when **151** was investigated as a possible catalyst. In respect of the arene, poor tolerance for functional groups was established with haloarenes resulting in low turn-overs; moreover, negligible

ortho-silylation was observed, while a modest selectivity for *meta* over *para* silylation was noted for toluene (1.9:1) and trifluorotoluene (2.1:1). For *o*-Xylene, a 96:4 preference for the 4-silyl, over 3-silyl, product was noted. Intermolecular selectivity for electron-poor arenes was observed upon conducting the reaction in the solvent mixtures toluene/trifluorotoluene and *m*-xylene/1,3-$(CF_3)_2C_6H_4$, which afforded, respectively, 1.5:1 and 3.3:1 product ratios in favor of the electron-poor arene.

The methodology was also extended to the intramolecular silylation of dimethyl-2-phenylethylsilane and diethyl-2-phenylpropylsilane (Scheme 50), and more significantly of tri-*n*-butylsilane, which constituted the first high-yield example of coupling between an Si−H and purely aliphatic C−H linkage (Scheme 51).

n = 1, R = Me 70 %
n = 2, R = Et 64 %
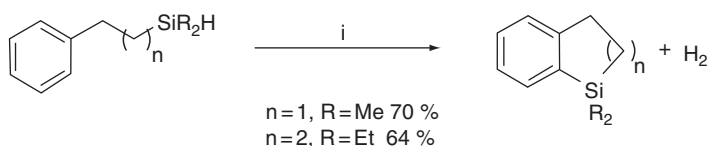
Scheme 50   Reagents and conditions: (i) Tp*PtMe$_2$H (**151**), 200 °C, 48 h.

88 %
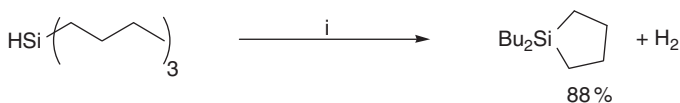
Scheme 51   Reagents and conditions: (i) Tp*PtMe$_2$H (**151**), 200 °C, 72 h.

Finally, preliminary investigation of the thermodynamics of these catalyzed silylation reactions established that the silylation step is irreversible, as determined by the exclusive generation of $^nPr_3SiPh$ in the presence of 1.5 equiv. of p-$CF_3C_6H_4SiEt_3$, which remains 98% intact, and the failure to regenerate *m*-xylene when m-$Et_3SiC_6H_4Me$ was heated at 200 °C under 10 atm. H_2.

B. C−H activation and functionalization

1. Probing C−H addition/elimination in Pt(II)/Pt(IV) systems

The importance of oxidative addition of aromatic and aliphatic C−H bonds to Pt(II) centers and its microscopic reverse, reductive elimination of C−H from Pt(IV) species, is ubiquitous in the context of both catalysis and synthesis. It is thus inevitable that the chemical, mechanistic, and kinetic facets of such reactions have become a prominent focus of group 10 poly(pyrazolyl)borate research, although this remains a relatively nascent area.

In this context, the first incidence of C–H activation was reported to ensue upon treatment of K[Tp*PtMe$_2$] (**K.297**) with stoichiometric B (C$_6$F$_5$)$_3$ in hydrocarbons (benzene, pentane, cyclohexane).[121] Methide abstraction by the borane was deemed to afford the intermediary ''Tp*PtMe,'' which then inserts into the solvent C–H bond to afford Tp*PtMeRH (R = Ph **357**, C$_5$H$_{11}$ **168**, Cy **170**), albeit in admixture with often inseparable by-products (Section III.C.1). This seminal work offered the first example of aryl and alkyl C–H bonds oxidatively adding to Pt(II) centers to give *stable* Pt(IV) species; a consequence of the variable hapticity in the Tp* ligand affording coordinate saturation (octahedral, κ^3-Tp*) and thus precluding reductive elimination of RH, which necessitates a 5-coordinate intermediate. Indeed, κ^3-Tp*PtMe$_2$H (**151**) was noted to show considerable reluctance toward elimination of methane under ambient conditions,[108] though a number of subsequent studies have induced methane loss thermolytically, exploiting subsequent C–H activation as a route to further Pt(IV) compounds. Thus, when heated in the presence of Et$_3$SiH, **151** was cleanly converted to Tp*Pt(SiEt$_3$)H$_2$ (**378**), the result of sequential methane-loss /silane-addition to afford the presumed intermediate Tp*Pt(SiEt$_3$)MeH, which preferentially eliminates MeSiEt$_3$ (over MeH) and activates a further equivalent of silane to give **378**.[126] More intuitively, thermolysis of **151** in benzene affords cleanly Tp*PtPh$_2$H (**153**), the result of two sequential methane-elimination/C–H activation steps.[123]

This thermolytic process has been studied at some length,[123] experiments in C$_6$D$_6$ illustrating first-order kinetics with respect to consumption of **151**, with an observed rate constant of $k_{obs} = 6.73 \times 10^{-5}$ s^{-1} reported for the generation of **153-d_{11}**. A small systematic deviation in the kinetic modeling for the concentration of both **151** and the intermediate monophenyl complex Tp*PtMe(C$_6$D$_5$)D (**357-d_6**) was noted, apparently consistent with the rate constant for conversion of **357-d_6** to **153-d_{11}** (i.e., k_{obs}(**357-d_6**)) increasing with time. This was attributed to relatively fast exchange between the hydridic and methyl protons, coupled with a slower exchange between the hydridic and phenyl positions, which result in observed H/D scrambling, with generation of CH$_3$D, CH$_2$D$_2$, and isotopomers of **357** and **153**. Consequently, k_{obs} is perturbed through a weighted sum of k_H and k_D, though this kinetic effect is small (<5%) such that an averaged value for k_{obs}(**357-d_6**) of 8.3×10^{-5} s^{-1} was determinable. The incidence of an inverse kinetic isotope effect for each methane elimination step was confirmed by studying the rate of CD$_4$ elimination from Tp*Pt(CD$_3$)$_2$D (**151-d_7**), enabling calculation of k_H/k_D = 0.81 ± 0.03 and $k_H/k_D \leq 0.78 \pm 0.03$ for the first and second methane elimination steps, respectively. The activation parameters for these two steps were also determined, both in C$_6$D$_6$ and d_8-toluene, and found to be almost identical, *viz.* $\Delta H^{\#}_{obs} = 35.0 \pm 1.1$ kcal mol^{-1}, $\Delta S^{\#}_{obs}$ 13 ± 3 e.u.

(1st elimination); $\Delta H^{\#}_{obs} = 34.0 \pm 1.0$ kcal mol^{-1}, $\Delta S^{\#}_{obs}$ 11 ± 3 e.u. (2nd elimination).[2]

The observation of H/D scrambling implicates the, now largely ubiquitous, intermediacy of a methane σ-complex in the methane-elimination step, thus offering two possible mechanisms for the C−H activation step, *viz. associative*—methane elimination is induced by the incoming ligand— or *dissociative*—the ligand occupies a vacant site afforded by methane loss. This was probed by thermolysis of **151** in MeCN/C$_6$F$_6$ to afford Tp*PtMe (NCMe) (**371**), which exhibits first-order kinetics with a rate constant of $k_{obs} = 5.1 \times 10^{-5}$ s^{-1} at 110 °C that is independent of [MeCN]. This is consistent with a dissociative mechanism, provided that formation of the σ-complex is not rate limiting. This was confirmed, given that the rate constant for H/D scrambling reaches this value at 60 °C ($k_{scr} = 7 \times 10^{-5}$ s^{-1}) and must thus far exceed k_{obs} at 110 °C. It should also be noted that the enthalpic activation barrier for formation of the methane σ-complex was experimentally derived as $\Delta H^{\#}_{scr} = 26$ kcal mol^{-1}, leaving an additional barrier of $\Delta\Delta H^{\#} = 9$ kcal mol^{-1} for the elimination step, contributing to the overall $\Delta H^{\#}_{RE}$.

Very recently, these data were supported by a theoretical reexamination using DFT calculations (B3LYP/BS1) to probe the reaction pathway and intermediate structures.[173] This study suggested that formation of the σ-complex from **151** involves a late transition state with an enthalpic barrier of 24.3 kcal mol^{-1}, giving rise to an unstable, essentially 4-coordinate square-planar complex, by a progressive lengthening of the axial N−Pt linkage, with concomitant shortening (by 0.2 Å) of the Pt−N$_{eq}$ *trans* to methyl. The shortening of this Pt−N$_e$ linkages continues during dissociation of the weakly bound methane ligand (to a limit of 1.98 Å) giving rise to the coordinately unsaturated κ^2-''Tp*PtMe'' via a transition state with $\Delta H^{\#} = 33.8$ kcal mol^{-1} relative to **151**. A slight shortening of the Pt−N$_{ax}$ separation was also noted, perhaps indicative of its complicity in ''stabilizing'' the 3-coordinate structure. Subsequent binding of benzene was determined to result in an η^2-C$_6$H$_6$ complex (consistent with that isolated upon protonation of **151** in benzene, *vide infra*), which is 4.91 kcal mol^{-1} more stable than its η^2-*C,H*-C$_6$H$_6$ analogue, though the two are linked by a transition state with $\Delta H^{\#} = 5.92$ kcal mol^{-1}. From this point, oxidative addition to afford **357** is facile ($\Delta H^{\#} = -24.52$ kcal mol^{-1}). A largely comparable reaction profile was established for the second methane-elimination/C−H activation sequence to afford **153**.

A propensity for H/D scrambling with solvent, in preference to methane elimination, has also been noted for the thermolysis (55−70 °C) of the related TpPtMe(H)$_2$ (**347**) in 1:1 C$_6$H$_6$/CH$_3$OD, which affords the fully deuterated **347**-*d*$_5$ over 6 h, with no evidence for loss of methane.[124]

---

[2] e.u. = 4.184 J K^{-1} mol^{-1}.

This reaction, which is completely reversible in CH_3OH, comprises a fast preequilibrium involving exchange of the hydridic positions with solvent, which is complete in <5 min. Allowing for this the kinetics were studied, revealing pseudo first-order behavior with calculated $k_{obs}{}^D = 24.2 \times 10^{-5}\,s^{-1}$ and $k_{obs}{}^H = 18.4 \times 10^{-5}\,s^{-1}$ for the forward and reverse reactions, respectively. In view of the lack of methane liberation, the resulting inverse kinetic isotope effect ($k_H/k_D = 0.76$) was considered to reflect the ΔG_{298} of the reductive coupling step, *not* the overall reductive elimination of methane.

Theoretical studies were undertaken to explain these observations,[125] and revealed a single viable σ-complex, *viz.* $TpPt(\eta^{2\text{-}C,H}\text{-}CH_4)H$ (**C**), with a relative energy of 24.1 kcal mol^{-1} with respect to **347** ($\Delta G_{298} = 19.1$ kcal mol^{-1}), accessed via a transition state with $\Delta E^{\#} = 28.5$ kcal mol^{-1} ($\Delta G_{298}{}^{\#} = 25.7$ kcal mol^{-1}) relative to **347** ($\Delta E^{\#} = 7.4$ kcal mol^{-1}, $\Delta G_{298}{}^{\#} = 6.6$ kcal mol^{-1} with respect to **C**). Coupled with a low barrier to rotation of the methane ligand ($\Delta E^{\#} = 2.9$ kcal mol^{-1}, $\Delta G_{298}{}^{\#} = 3.0$ kcal mol^{-1}), which renders each C−H linkage suitably oriented for oxidative addition, the facility of this addition relative to methane loss ($\Delta G_{298}{}^{\#} = 11.9$ kcal mol^{-1}) accounts for the overwhelming prevalence of scrambling. Nonetheless, heating at 130 °C does, over 8 days, enable methane loss with subsequent activation of solvent, ultimately affording $TpPtPh(H)_2$ (**514**).

2. Acid-assisted reductive elimination

The noted reluctance toward thermolytic reductive elimination is widely attributed to the necessity for coordinate unsaturation (i.e., a 5-coordinate species) and this being precluded by the flexible Tp^x ligand adopting the facially tridentate (κ^3) coordination mode. It was thus recognized that encouraging the κ^2 coordination mode, through protonation of one pyrazole donor, might facilitate elimination of RH under mild conditions. Thus, treatment of Tp^*PtMe_2H (**151**) with $[H(OEt_2)]BAr^f_4$ in dichloromethane at −78 °C results in loss of methane (observed by *in situ* NMR spectroscopy) with formation of the solvate cation $[\kappa^2\text{-}HTp^*PtMe(CH_2Cl_2)]^+$ (**362⁺**), which decomposes above 0 °C but can be trapped as adducts with other donors: $[\kappa^2\text{-}HTp^*PtMe(L)]^+$ (**363⁺−370⁺** Section III. C.3).[65] Similarly, Tp^*PtPh_2H (**153**) liberates benzene when protonated to give $[\kappa^2\text{-}HTp^*PtPh(CH_2Cl_2)]^+$ (**534⁺**),[65] while the dihydride Tp^*PtMeH_2 (**152**) loses methane to afford $[\kappa^2\text{-}HTp^*PtH(CH_2Cl_2)]^+$ (**535⁺**), isolable as the acetonitrile adduct, but unstable with respect to formation of the dimeric hydride complex $[\{\kappa^2\text{-}N,N'\text{-}HTp^*)Pt(\mu\text{-}H)\}_2]^{2+}$ (**380²⁺**) even at −30 °C.[66] Each of these solvate cations has been demonstrated to oxidatively add aryl and alkyl C−H functionalities (RH), to form initially $[\kappa^2\text{-}HTp^*PtRR'H]^+$ (R'= Ph, Me, H), which can then be deprotonated to the respective neutral species (Section III.C.1).

The mechanism and kinetics of aryl C−H activation in such systems has been investigated, commencing with the series of complexes Tp*Pt(Ar)(H)$_2$ (Ar = Ph **177**, Tol **182**, *p*-Xyl **183**) and Tp*PtPh$_2$H (**153**), which when protonated at −78 °C in dichloromethane form initially the isolable η^2-Ar complexes [κ^2-HTp*PtH(η^2-Ar)]$^+$ (Ar = Ph **178**$^+$,[70,72] Tol **179**$^+$, *p*-Xyl **180**$^+$)[72] and [κ^2-HTp*PtPh(η^2-Ar)]$^+$ (**181**$^+$),[72] both **178**$^+$ and **180**$^+$ having been crystallographically characterized. Below 250 K each of the η^2-arene species is kinetically inert with respect to C−H activation; however, above this temperature broadening of both aryl C−H and Pt−H resonances was observed for each of **178**$^+$–**180**$^+$, indicative of hydrogen exchange between the two sites and thus incidence of C−H activation. For **178**$^+$, $\Delta G^{\ddagger}$ for this process was calculated as 12.7 kcal mol^{-1}, initially from line-broadening of the hydridic resonance at the 252 K slow-exchange limit.[70] This was subsequently verified by spin saturation transfer NMR studies of the hydride, in the temperature range 199–251 K, activation parameters being calculated from the Eyring plot, *viz.* $\Delta H^{\ddagger} = 11.7 \pm 0.5$ kcal mol^{-1}, $\Delta S^{\ddagger} = -3.8 \pm 2$ cal mol^{-1} K^{-1} and $\Delta G^{\ddagger}_{241\ K} = 12.7 \pm 1$ kcal mol^{-1}.[72] Activation barriers for the tolyl and xylyl systems were similarly obtained, thus for **179**$^+$ $\Delta G^{\ddagger}_{230\ K} = 13.6$ kcal mol^{-1} (*meta activation*), 13.3 kcal mol^{-1} (*para activation*), and for **180**$^+$ $\Delta G^{\ddagger}_{272\ K} = 14.2$ kcal mol^{-1}, while for the phenyl complex **181**$^+$ hydrogen exchange between the η^2-C$_6$H$_6$ and phenyl ligands was utilized to derive $\Delta G^{\ddagger}_{241\ K} = 12.9$ kcal mol^{-1}. Finally, for both phenyl systems (**178**$^+$ and **181**$^+$), the kinetic isotope effect was evaluated, based on first-order rate constants calculated from spin saturation transfer NMR studies; thus, for **178**$^+$ $k_H/k_D = 3.0$ at 259 K, and for **177**$^+$ $k_H/k_D = 4.7$ at 241 K. These large values were considered consistent with an activation step in which the C−H(D) bond is cleaved in the transition state.

In concluding this section, it is noteworthy that the Lewis acid B(C$_6$F$_5$)$_3$ has also been demonstrated to facilitate reductive elimination from Pt(IV) species in similar fashion to the protonation reactions discussed thus far (i.e., assisted dechelation of a pyrazolyl donor); indeed, borane-induced methane elimination from Tp*PtMeH$_2$ (**152**) in the presence of arenes was employed in the synthesis of Tp*Pt(Ar)H$_2$ (Ar = Ph **177**, Tol **182**, *p*-Xyl **183** *o*-Xyl **360**, *m*-Xyl **361**).[122] Significantly, these reactions occur catalytically, substoichiometric borane affording the products directly, with no isolable Tp*-borane adducts; cf. protonation, which stoichiometrically affords isolable ''HTp*Pt'' cations. Both of these methodologies have been employed to effect dehydrogenation of cycloalkanes by Tp*PtMe$_2$H (**151**), affording the Pt(II) π-alkene complexes Tp*Pt(H)(η^2-olefin) (olefin = *c*-C$_5$H$_8$ **164**, *c*-C$_6$H$_{10}$ **165**, *c*-C$_8$H$_{14}$ **166**), via the respective, spectroscopically observable, Pt(IV) alkyls Tp*PtMe(R)H (R = *c*-Pn **169**, Cy **170**, *c*-Oct **171**),[69] as discussed in Section III.C.1. The insertion of ethylene into a Pt−Ph bond, and subsequent C−H activation of the resulting

ethylbenzene fragment to afford an ortho-metallated phenethyl complex has been similarly effected.[67] Detailed studies of the kinetics of these reactions have yet to be reported.

V. CONCLUDING REMARKS

It is apparent that the organometallic chemistry of group 10 poly(pyrazolyl)borate complexes has, in many respects, been comprehensively investigated. Indeed, there are no obvious areas of omission other than perhaps the relative dearth nitrosyl complexes, which is now beginning to be addressed. Typically, the deficits encountered are largely symptomatic of the chemistry itself, extensive attempts having been made to utilize nickel, palladium, and platinum systems in catalytic roles, for all but a handful of which the compounds have been found wanting. However, those few viable systems have been investigated in considerable detail, such that mechanistic and kinetic details are already well known, offering the scope for future application and refinement. Moreover, it is within the past decade that this work has begun to reach fruition, which perhaps points to the key impetus for the future. Alongside this, one might anticipate that the recent explosion of new generation scorpionates, based on larger, more flexible chelates and softer donors, might soon permeate the group 10 triad, for which such complexes remain relatively scarce. Indeed, given the intrinsic stability of many $Tp^x M(IV)$ and $Tp^x M(II)$ systems, this would seem essential if wide-ranging catalytic activity is to be developed. A further area that has yet to emerge involves metal-carbon multiple bonding) other than carbonyl and isonitrile chemistry. The absence of alkylidene and alkylidyne chemistry from this discussion is, however, a general feature of the organometallic chemistry of group 10, rather than a peculiarity of poly(pyrazolyl)borate chemistry per se.

ACKNOWLEDGMENTS

REFERENCES

(1) Byers, P. K.; Canty, A. J.; Honeyman, R. T. *Adv. Organomet. Chem.* **1992**, *34*, 1.
(2) Belderrain, T. R.; Paneque, M.; Carmona, E.; Gutierrez-Puebla, E.; Monge, M. A.; Ruiz-Valero, C. *Inorg. Chem.* **2002**, *41*, 425.
(3) Echols, H. M.; Dennis, D. *Acta Crystallogr. Sect. B* **1976**, *32*, 1627.
(4) Clemente, D. A.; Cingi-Biagini, M. *Inorg. Chem.* **1987**, *26*, 2350.

(5) Trofimenko, S. *J. Am. Chem. Soc.* **1967**, *89*, 6288.

(6) Echols, H. M.; Dennis, D. *Acta Crystallogr. Sect. B* **1974**, *30*, 2173.

(7) Cotton, F. A.; Murillo, C. A. *Inorg. Chim. Acta* **1976**, 17.

(8) Trofimenko, S.; Calabrese, J. C.; Thompson, J. S. *Inorg. Chem.* **1992**, *31*, 974.

(9) Trofimenko, S.; Calabrese, J. C.; Thompson, J. S. *Angew. Chem. Int. Ed. Engl.* **1989**, *28*, 205.

(10) Kitajima, N.; Hikichi, S.; Tanaka, M.; Morooka, Y. *J. Am. Chem. Soc.* **1993**, *115*, 5496.

(11) Uehara, K.; Hikichi, S.; Akita, M. *J. Chem. Soc. Dalton Trans.* **2002**, 3529.

(12) Uehara, K.; Hikichi, S.; Akita, M. *Organometallics* **2001**, *20*, 5002.

(13) Kunrath, F. A.; De Souza, R. F.; Casagrande, O. L., Jr.; Brooks, N. R.; Young, V. G., Jr. *Organometallics* **2003**, *22*, 4739.

(14) Furlan, L. G.; Kunrath, F. A.; Mauler, R. S.; De Souza, R. F.; Casagrande, O. L., Jr. *J. Mol. Catal. A* **2004**, *214*, 207.

(15) Santi, R.; Romano, A. M.; Sommazzi, A.; Grande, M.; Bianchini, C.; Mantovani, G. *J. Mol. Catal. A* **2005**, *229*, 191.

(16) Grande, M.; Romano, A. M.; Bianchini, C.; Mantovani, G.; Santi, R.; Sommazzi, A. WO 2003070737 **2003**, *Chem Abstr 139*, 206606.

(17) Uehara, K.; Hikichi, S.; Inagaki, A.; Akita, M. *Chem. Eur. J.* **2005**, *11*, 2788.

(18) Lehmkuhl, H.; Naeser, J.; Mehler, G.; Keil, T.; Danowski, F.; Benn, R.; Mynott, R.; Schroth, G.; Krueger, C.; Betz, P. *Chem. Ber.* **1991**, *124*, 441.

(19) Akita, M.; Shirasawa, N.; Hikichi, S.; Moro-oka, Y. *Chem. Commun.* **1998**, 973.

(20) Shirasawa, N.; Nguyet, T. T.; Hikichi, S.; Moro-oka, Y.; Akita, M. *Organometallics* **2001**, *20*, 3582.

(21) Johnson, L. K.; Bennett, A. M. A.; Ittel, S. D.; Wang, L.; Parthasarathy, A.; Hauptman, E.; Simpson, R. D.; Feldman, J.; Coughlin, E. B.; et al. WO 9830609 **1998**, *Chem. Abstr. 129*, 149362.

(22) Mealli, C.; Midollini, S.; Moneti, S.; Sacconi, L. *J. Organomet. Chem.* **1981**, *205*, 273.

(23) Brunker, T. J.; Cowley, A. R.; O'Hare, D. *Organometallics* **2002**, *21*, 3123.

(24) Brunker, T. J.; Green, J. C.; O'Hare, D. *Inorg. Chem.* **2003**, *42*, 4366.

(25) Shirasawa, N.; Akita, M.; Hikichi, S.; Moro-oka, Y. *Chem. Commun.* **1999**, 417.

(26) Trieu, T. N.; Vu, D. D.; Trinh, N. C.; Akita, M.; Morooka, Y. *Tap Chi Hoa Hoc* **1999**, *37*, 41.

(27) Gutierrez, E.; Hudson, S. A.; Monge, A.; Nicasio, M. C.; Paneque, M.; Ruiz, C. *J. Organomet. Chem.* **1998**, *551*, 215.

(28) Black, S. I.; Young, G. B. *Polyhedron* **1989**, *8*, 585.

(29) Gutierrez, E.; Hudson, S. A.; Monge, A.; Nicasio, M. C.; Paneque, M.; Carmona, E. *J. Chem. Soc. Dalton Trans.* **1992**, 2651.

(30) Domhover, B.; Klaui, W.; Kremer-Aach, A.; Mootz, D. *Angew. Chem. Int. Ed.* **1998**, *37*, 3050.

(31) Klaui, W.; Turkowski, B.; Rheinwald, G.; Lang, H. *Eur. J. Inorg. Chem.* **2002**, 205.

(32) Klaui, W.; Bongards, J.; Reiss, G. J. *Angew. Chem. Int. Ed.* **2000**, *39*, 3894.

(33) Yoshimitsu, S.-I.; Hikichi, S.; Akita, M. *Organometallics* **2002**, *21*, 3762.

(34) Belderrain, T. R.; Gutierrez, E.; Monge, A.; Nicasio, M. C.; Paneque, M.; Poveda, M. L.; Carmona, E. *Organometallics* **1993**, *12*, 4431.

(35) Uehara, K.; Hikichi, S.; Akita, M. *Chem. Lett.* **2002**, 1198.

(36) Li, D.; Ruschman, C.; Parkin, S.; Clerac, R.; Holmes, S. M. *Chem. Commun.* **2006**, 4036.

(37) Landry, V. K.; Pang, K.; Quan, S. M.; Parkin, G. *Dalton Trans.* **2007**, 820.

(38) Harding, D. J.; Harding, P.; Adams, H.; Tuntulani, T. *Inorg. Chim. Acta* **2007**, *360*, 3335.

(39) Schubert, D. M.; Knobler, C. B.; Trofimenko, S.; Hawthorne, M. F. *Inorg. Chem.* **1990**, *29*, 2364.

(40) Varadarajan, A.; Johnson, S. E.; Gomez, F. A.; Chakrabarti, S.; Knobler, C. B.; Hawthorne, M. F. *J. Am. Chem. Soc.* **1992**, *114*, 9003.

(41) Desrochers, P. J.; LeLievre, S.; Johnson, R. J.; Lamb, B. T.; Phelps, A. L.; Cordes, A. W.; Gu, W.; Cramer, S. P. *Inorg. Chem.* **2003**, *42*, 7945.

(42) Holah, D. G.; Hughes, A. N.; Hui, B. C.; Wright, K. *Can. J. Chem.* **1974**, *52*, 2990.

(43) Yan, L. Z.; Dawson, P. E. J. *Am. Chem. Soc.* **2001**, *123*, 526.

(44) Ma, H.; Chattopadhyay, S.; Petersen, J. L.; Jensen, M. P. *Inorg. Chem.* **2008**, *47*, 7966.

(45) Onishi, M.; Ohama, Y.; Sugimura, K.; Hiraki, K. *Chem. Lett.* **1976**, 955.

(46) Komorowski, L.; Meller, A.; Niedenzu, K. *Inorg. Chem.* **1990**, *29*, 538.

(47) Bortolin, M.; Bucher, U. E.; Ruegger, H.; Venanzi, L. M.; Albinati, A.; Lianza, F.; Trofimenko, S. *Organometallics* **1992**, *11*, 2514.

(48) Komorowski, L.; Maringgele, W.; Meller, A.; Niedenzu, K.; Serwatowski, J. *Inorg. Chem.* **1990**, *29*, 3845.

(49) Bielawski, J.; Hodgkins, T. G.; Layton, W. J.; Niedenzu, K.; Niedenzu, P. M.; Trofimenko, S. *Inorg. Chem.* **1986**, *25*, 87.

(50) Trofimenko, S. J. *Am. Chem. Soc.* **1967**, *89*, 4948.

(51) Trofimenko, S. J. *Am. Chem. Soc.* **1967**, *89*, 3165.

(52) Trofimenko, S. J. *Coord. Chem.* **1972**, *2*, 75.

(53) Clark, H. C.; Manzer, L. E. *J. Chem. Soc. Chem. Commun.* **1973**, 870.

(54) Clark, H. C.; Manzer, L. E. J. *Am. Chem. Soc.* **1973**, *95*, 3812.

(55) Clark, H. C.; Manzer, L. E. *Inorg. Chem.* **1974**, *13*, 1996.

(56) Clark, H. C.; Manzer, L. E. *Inorg. Chem.* **1974**, *13*, 1291.

(57) Davies, B. W.; Payne, N. C. *Inorg. Chem.* **1974**, *13*, 1843.

(58) Van Gaal, H. L. M.; Graef, M. W. M.; Van der Ent, A. *J. Organomet. Chem.* **1977**, *131*, 453.

(59) Rice, N. C.; Oliver, J. D. *Acta Crystallogr. Sect. B* **1978**, *B34*, 3748.

(60) Manzer, L. E. *Inorg. Chem.* **1976**, *15*, 2354.

(61) Clark, H. C.; Von Werner, K. *J. Organomet. Chem.* **1975**, *101*, 347.

(62) Davies, B. W.; Payne, N. C. *J. Organomet. Chem.* **1975**, *102*, 245.

(63) Nussbaum, S.; Storr, A. *Can. J. Chem.* **1985**, *63*, 2550.

(64) Haskel, A.; Keinan, E. *Tetrahedron Lett.* **1999**, *40*, 7861.

(65) Reinartz, S.; White, P. S.; Brookhart, M.; Templeton, J. L. *Organometallics* **2000**, *19*, 3854.

(66) Reinartz, S.; Baik, M.-H.; White, P. S.; Brookhart, M.; Templeton, J. L. *Inorg. Chem.* **2001**, *40*, 4726.

(67) MacDonald, M. G.; Kostelansky, C. N.; White, P. S.; Templeton, J. L. *Organometallics* **2006**, *25*, 4560.

(68) West, N. M.; Reinartz, S.; White, P. S.; Templeton, J. L. J. *Am. Chem. Soc.* **2006**, *128*, 2059.

(69) Kostelansky, C. N.; MacDonald, M. G.; White, P. S.; Templeton, J. L. *Organometallics* **2006**, *25*, 2993.

(70) Reinartz, S.; White, P. S.; Brookhart, M.; Templeton, J. L. J. *Am. Chem. Soc.* **2001**, *123*, 12724.

(71) Norris, C. M.; Templeton, J. L. *Organometallics* **2004**, *23*, 3101.

(72) Norris, C. M.; Reinartz, S.; White, P. S.; Templeton, J. L. *Organometallics* **2002**, *21*, 5649.

(73) Binotti, B.; Bellachioma, G.; Cardaci, G.; Macchioni, A.; Zuccaccia, C.; Foresti, E.; Sabatino, P. *Organometallics* **2002**, *21*, 346.

(74) Trofimenko, S. J. *Am. Chem. Soc.* **1969**, *91*, 588.

(75) Trofimenko, S.; Calabrese, J. C.; Thompson, J. S. *Inorg. Chem.* **1987**, *26*, 1507.

(76) Bai, J.; Niedenzu, K. *Inorg. Chem.* **1990**, *29*, 4693.

(77) Lalor, F. J.; Miller, S.; Garvey, N. J. *Organomet. Chem.* **1988**, *356*, C57.

(78) Rheingold, A. L.; Liable-Sands, L. M.; Incarvito, C. L.; Trofimenko, S. *J. Chem. Soc. Dalton Trans.* **2002**, 2297.

(79) Rheingold, A. L.; Ostrander, R. L.; Haggerty, B. S.; Trofimenko, S. *Inorg. Chem.* **1994**, *33*, 3666.

(80) Rheingold, A. L.; Liable-Sands, L. M.; Golan, J. A.; Trofimenko, S. *Eur. J. Inorg. Chem* **2003**, 2767.

(81) Rheingold, A. L.; Liable-Sands, L. M.; Golen, J. A.; Yap, G. P. A.; Trofimenko, S. *Dalton Trans.* **2004**, 598.

(82) Rheingold, A. L.; White, C. B.; Trofimenko, S. *Inorg. Chem.* **1993**, *32*, 3471.

(83) Canty, A. J.; Jin, H.; Roberts, A. S.; Traill, P. R.; Skelton, B. W.; White, A. H. *J. Organomet. Chem.* **1995**, *489*, 153.

(84) Onishi, M.; Yamaguchi, M.; Nishimoto, E.; Itoh, Y.; Nagaoka, J.; Umakoshi, K.; Kawano, H. *Inorg. Chim. Acta* **2003**, *343*, 111.

(85) Trofimenko, S. *J. Am. Chem. Soc.* **1969**, *91*, 3183.

(86) Niedenzu, K.; Serwatowski, J.; Trofimenko, S. *Inorg. Chem.* **1991**, *30*, 524.

(87) Ohkita, K.; Kurosawa, H.; Hasegawa, T.; Shirafuji, T.; Ikeda, I. *Inorg. Chim. Acta* **1992**, *198–200*, 275.

(88) Ruiz, J.; Florenciano, F.; Rodriguez, V.; de Haro, C.; Lopez, G.; Perez, J. *Eur. J. Inorg. Chem.* **2002**, 2736.

(89) Watanabe, S.; Kurosawa, H. *Organometallics* **1998**, *17*, 479.

(90) Brock, C. P.; Das, M. K.; Minton, R. P.; Niedenzu, K. *J. Am. Chem. Soc.* **1988**, *110*, 817.

(91) Clark, H. C.; Manzer, L. E. *Inorg. Chem.* **1972**, *11*, 2749.

(92) King, R. B.; Bond, A. *J. Am. Chem. Soc.* **1974**, *96*, 1338.

(93) Roth, S.; Ramamoorthy, V.; Sharp, P. R. *Inorg. Chem.* **1990**, *29*, 3345.

(94) Fekl, U.; van Eldik, R.; Lovell, S.; Goldberg, K. I. *Organometallics* **2000**, *19*, 3535.

(95) Canty, A. J.; Patel, J.; Pfeffer, M.; Skelton, B. W.; White, A. H. *Inorg. Chim. Acta* **2002**, *327*, 20.

(96) Canty, A. J.; Dedieu, A.; Jin, H.; Milet, A.; Skelton, B. W.; Trofimenko, S.; White, A. H. *Inorg. Chim. Acta* **1999**, *287*, 27.

(97) Khaskin, E.; Zavalij, P. Y.; Verdernikov, A. N. *Angew. Chem. Int. Ed.* **2007**, *46*, 6309.

(98) Canty, A. J.; Jin, H.; Roberts, A. S.; Skelton, B. W.; Traill, P. R.; White, A. H. *Organometallics* **1995**, *14*, 199.

(99) Canty, A. J.; Honeyman, R. T.; Roberts, A. S.; Traill, P. R.; Colton, R.; Skelton, B. W.; White, A. H. *J. Organomet. Chem.* **1994**, *471*, C8.

(100) Canty, A. J.; Jin, H.; Roberts, A. S.; Skelton, B. W.; White, A. H. *Organometallics* **1996**, *15*, 5713.

(101) Canty, A. J. *Acc. Chem. Res.* **1992**, *25*, 83.

(102) Markies, B. A.; Canty, A. J.; Janssen, M. D.; Spek, A. L.; Boersma, J.; Van Koten, G. *Recl. Trav. Chim. Pays-Bas* **1991**, *110*, 477.

(103) Canty, A. J.; Fritsche, S. D.; Jin, H.; Skelton, B. W.; White, A. H. *J. Organomet. Chem.* **1995**, *490*, C18.

(104) Canty, A. J.; Jin, H.; Skelton, B. W.; White, A. H. *J. Organomet. Chem.* **1995**, *503*, C16.

(105) Milet, A.; Dedieu, A.; Canty, A. J. *Organometallics* **1997**, *16*, 5331.

(106) Canty, A. J.; Traill, P. R. *J. Organomet. Chem.* **1992**, *435*, C8.

(107) Canty, A. J.; Fritsche, S. D.; Jin, H.; Patel, J.; Skelton, B. W.; White, A. H. *Organometallics* **1997**, *16*, 2175.

(108) O'Reilly, S. A.; White, P. S.; Templeton, J. L. *J. Am. Chem. Soc.* **1996**, *118*, 5684.

(109) Campora, J.; Palma, P.; del Rio, D.; Lopez, J. A.; Valerga, P. *Chem. Commun.* **2004**, 1490.

(110) Canty, A. J.; Hoare, J. L.; Patel, J.; Pfeffer, M.; Skelton, B. W.; White, A. H. *Organometallics* **1999**, *18*, 2660.

(111) Campora, J.; Palma, P.; del Rio, D.; Lopez, J. A.; Alvarez, E.; Connelly, N. G. *Organometallics* **2005**, *24*, 3624.

(112) Canty, A. J.; Jin, H. *J. Organomet. Chem.* **1998**, *565*, 135.

(113) Canty, A. J.; Jin, H.; Skelton, B. W.; White, A. H. *Aust. J. Chem.* **1999**, *52*, 417.

(114) Canty, A. J.; Dedieu, A.; Jin, H.; Milet, A.; Richmond, M. K. *Organometallics* **1996**, *15*, 2845.

(115) Wick, D. D.; Goldberg, K. I. *J. Am. Chem. Soc.* **1999**, *121*, 11900.

(116) Look, J. L.; Wick, D. D.; Mayer, J. M.; Goldberg, K. I. *Inorg. Chem.* **2009**, *48*, 1356.

(117) Haskel, A.; Keinan, E. *Organometallics* **1999**, *18*, 4677.

(118) Keinan, E.; Haskel, A. WO 2001005208 **2001**, *Chem Abstr. 134*, 101016.

(119) Lo, H. C.; Iron, M. A.; Martin, J. M. L.; Keinan, E. *Chem. Eur. J.* **2007**, *13*, 2812.
(120) Reinartz, S.; Brookhart, M.; Templeton, J. L. *Organometallics* **2002**, *21*, 247.
(121) Wick, D. D.; Goldberg, K. I. *J. Am. Chem. Soc.* **1997**, *119*, 10235.
(122) Reinartz, S.; White, P. S.; Brookhart, M.; Templeton, J. L. *Organometallics* **2001**, *20*, 1709.
(123) Jensen, M. P.; Wick, D. D.; Reinartz, S.; White, P. S.; Templeton, J. L.; Goldberg, K. I. *J. Am. Chem. Soc.* **2003**, *125*, 8614.
(124) Lo, H. C.; Haskel, A.; Kapon, M.; Keinan, E. *J. Am. Chem. Soc.* **2002**, *124*, 3226.
(125) Iron, M. A.; Lo, H. C.; Martin, J. M. L.; Keinan, E. *J. Am. Chem. Soc.* **2002**, *124*, 7041.
(126) Reinartz, S.; White, P. S.; Brookhart, M.; Templeton, J. L. *Organometallics* **2000**, *19*, 3748.
(127) Reinartz, S.; White, P. S.; Brookhart, M.; Templeton, J. L. *J. Am. Chem. Soc.* **2001**, *123*, 6425.
(128) Manzer, L. E.; Meakin, P. Z. *Inorg. Chem.* **1976**, *15*, 3117.
(129) Oliver, J. D.; Rush, P. E. *J. Organomet. Chem.* **1976**, *104*, 117.
(130) Rush, P. E.; Oliver, J. D. *J. Chem. Soc. Chem. Commun.* **1974**, 996.
(131) Oliver, J. D.; Rice, N. C. *Inorg. Chem.* **1976**, *15*, 2741.
(132) Thomas, C. M.; Peters, J. C. *Organometallics* **2005**, *24*, 5858.
(133) Campora, J.; Palma, P.; del Rio, D.; Carmona, E.; Graiff, C.; Tiripicchio, A. *Organometallics* **2003**, *22*, 3345.
(134) Clark, H. C.; Puddephatt, R. J. *Inorg. Chem.* **1970**, *9*, 2670.
(135) Diaz-Requejo, M. M.; Nicasio, M. C.; Belderrain, T. R.; Perez, P. J.; Puerta, M. C.; Valerga, P. *Eur. J. Inorg. Chem.* **2000**, 1359.
(136) Gutierrez, E.; Nicasio, M. C.; Paneque, M.; Ruiz, C.; Salazar, V. *J. Organomet. Chem.* **1997**, *549*, 167.
(137) Klaeui, W.; Turkowski, B.; Wunderlich, H. *Z. Anorg. Allg. Chem.* **2001**, *627*, 2397.
(138) Onishi, M.; Ito, T.; Hiraki, K. *J. Organomet. Chem.* **1981**, *209*, 123.
(139) Kujime, M.; Hikichi, S.; Akita, M. *Organometallics* **2001**, *20*, 4049.
(140) Kläui, W.; Turkowski, B.; Chenskaya, T. B. *Z. Anorg. Allg. Chem.* **2001**, *627*, 2609.
(141) Novikova, E. V.; Belov, G. P.; Klaui, W.; Solotnov, A. A. *Polym. Sci. A* **2003**, *45*, 941.
(142) Onishi, M.; Hiraki, K.; Itoh, T.; Ohama, Y. *J. Organomet. Chem.* **1983**, *254*, 381.
(143) Canty, A. J.; Hoare, J. L.; Skelton, B. W.; White, A. H.; van Koten, G. *J. Organomet. Chem.* **1998**, *552*, 23.
(144) Onishi, M.; Hiraki, K.; Shironita, M.; Yamaguchi, Y.; Nakagawa, S. *Bull. Chem. Soc. Jpn.* **1980**, *53*, 961.
(145) Onishi, M.; Sugimura, K.; Hiraki, K. *Bull. Chem. Soc. Jpn.* **1978**, *51*, 3209.
(146) Valk, J.-M.; Maassarani, F.; van der Sluis, P.; Spek, A. L.; Boersma, J.; van Koten, G. *Organometallics* **1994**, *13*, 2320.
(147) Valk, J.-M.; Belzen,, R.v.; Boersma, J.; Spek, A. L.; van Koten, G. *J. Chem. Soc. Dalton Trans.* **1994**, 2293.
(148) Ma, B.; Li, J.; Djurovich, P. I.; Yousufuddin, M.; Bau, R.; Thompson, M. E. *J. Am. Chem. Soc.* **2005**, *127*, 28.
(149) Niedermair, F.; Waich, K.; Kappaun, S.; Mayr, T.; Trimmel, G.; Mereiter, K.; Slugovc, C. *Inorg. Chim. Acta* **2007**, *360*, 2767.
(150) Sekine, N.; Oshiyama, T.; Nishizeki, M. JP 2006182921 **2006**, *Chem. Abstr. 145*, 155724.
(151) Oshiyama, T.; Otsu, S.; Yasukawa, N. WO 2006126389 **2006**, *Chem. Abstr. 146*, 36023.
(152) Oshiyama, T.; Nishizeki, M.; Sekine, N.; Kita, H. JP 2006060198 **2006**, *Chem. Abstr. 144*, 283335.
(153) Oshiyama, T.; Nishizeki, M. JP 2006120762 **2006**, *Chem. Abstr. 144*, 477928.
(154) Nishizeki, M.; Oshiyama, T. JP 2006103874 **2006**, *Chem. Abstr. 145*, 407141.
(155) Nishizeki, M.; Oshiyama, T. JP 2006098120, **2006**, *Chem Abstr. 145*, 366139.
(156) Oshiyama, T.; Nishizeki, M.; Katoh, E.; Kita, H. JP 2005123873 **2005**, *Chem. Abstr. 143*, 97393.
(157) Oshiyama, T.; Kita, H.; Inoue, Y.; Oi, S. JP 2005083033, **2005**, *Chem. Abstr. 143*, 295292.

(158) Oshiyama, T.; Katoh, E.; Kita, H.; Oi, S.; Inoue, Y. JP 2005097941, **2005**, *Chem. Abstr. 143*, 413280.

(159) Kita, H.; Suzuri, Y.; Oshiyama, T. JP 2005101912, **2005**, *Chem. Abstr. 143*, 429827.

(160) Onishi, M.; Yamamoto, H.; Hiraki, K. *Bull. Chem. Soc. Jpn.* **1980**, *53*, 2540.

(161) Canty, A. J.; Jin, H.; Penny, J. D. *J. Organomet. Chem.* **1999**, *573*, 30.

(162) Onishi, M.; Hiraki, K.; Konda, H.; Ishida, Y.; Ohama, Y.; Uchibori, Y. *Bull. Chem. Soc. Jpn.* **1986**, *59*, 201.

(163) Tanase, T.; Fukushima, T.; Nomura, T.; Yamamoto, Y.; Kobayashi, K. *Inorg. Chem.* **1994**, *33*, 32.

(164) Crossley, I. R.; Hill, A. F.; Willis, A. C. *Organometallics* **2005**, *24*, 4889.

(165) Aizenberg, M.; Milstein, D. *Angew. Chem. Int. Ed. Engl.* **1994**, *33*, 317.

(166) Tsukada, N.; Hartwig, J. F. J. *Am. Chem. Soc.* **2005**, *127*, 5022.

(167) Akita, M.; Miyaji, T.; Hikichi, S.; Morooka, Y. *Chem. Lett.* **1999**, 813.

(168) Reger, D. L.; Baxter, J. C.; Lebioda, L. *Inorg. Chim. Acta* **1989**, *165*, 201.

(169) Onishi, M.; Hiraki, K. *Inorg. Chim. Acta* **1994**, *224*, 131.

(170) Do, H. O.; Lee, J. H.; Kim, H.; Park, S. *J. Coord. Chem.* **2001**, *53*, 143.

(171) Britovsek, G. J. P.; Bruce, M.; Gibson, V. C.; Kimberley, B. S.; Maddox, P. J.; Mastroianni, S.; McTavish, S. J.; Redshaw, C.; Solan, G. A.; Stromberg, S.; White, A. J. P.; Williams, D. J. *J. Am. Chem. Soc.* **1999**, 8728.

(172) Johnson, L. K.; Killian, C. M.; Arthur, S.; Feldman, J.; Mc-Cord, E.; McLain, S.; Kreutzer, K.; Bennet, M.; Coughlin, E.; Ittel, S.; Parthasarathy, A.; Tempel, D.; Brookhart, M. WO 9623010 **1996**, *Chem. Abs. 125*, 222773.

(173) Vastine, B. A.; Webster, C. E.; Hall, M. B. *J. Chem. Theory Comput.* **2007**, *3*, 2268.

SUBJECT INDEX

CUMULATIVE LIST OF CONTRIBUTORS FOR VOLUMES 1–36